MODELLING OF MICRO-ENVIRONMENT INSIDE EVAPORATIVELY AND COOLBOT COOLED STORES USING COMPUTATIONAL FLUID DYNAMICS MODELS AND CHANGES IN QUALITY OF STORED TOMATOES

Getachew Neme Tolesa

Submitted in partial fulfilment of the academic requirements
for the degree of Doctor of Philosophy in Agricultural Engineering

School of Engineering
College of Agriculture, Engineering and Science
University of KwaZulu-Natal
Pietermaritzburg
South Africa

January 2018

DECLARATION

I, *Getachew Neme Tolesa*, declare that:

(i) The research reported in this thesis, except where otherwise indicated or acknowledged, is my original work;

(ii) This thesis has not been submitted in full or in part for any degree or examination to any other university;

(iii) This thesis does not contain other persons' data, pictures, graphs or other information, unless specifically acknowledged as being sourced from other persons;

(iv) This thesis does not contain other persons' writing, unless specifically acknowledged as being sourced from other researchers. Where other written sources have been quoted, then:

a) their words have been re-written but the general information attributed to them has been referenced;

b) where their exact words have been used, their writing has been placed inside quotation marks, and referenced;

(v) Where I have used material for which publications followed, I have indicated in detail my role in the work;

(vi) This thesis is primarily a collection of material, prepared by myself, published as journal articles or presented as a poster and oral presentations at conferences. In some cases, additional material has been included;

(vii) This thesis does not contain text, graphics or tables copied and pasted from the Internet, unless specifically acknowledged, and the source being detailed in the dissertation and in the References sections.

Signed Date

Student: Getachew Neme Tolesa: _____ _____

Supervisor: Prof. Tilahun Seyoum Workneh: _____ _____

ABSTRACT

The postharvest loss of fresh produce is a global problem, with the tomato fruit being subjected to a 30-50% loss of total production after harvest. The cost and the technicality of modern technology, including mechanical refrigeration, are not appropriate and sustainable for small-scale and middle-income fruit and vegetable farmers. Low-cost cooling technologies, such as evaporative cooling (EC), CoolBot-air-conditioning (CBAC) and a combination of the two (EC+CBAC), provide alternative solutions to minimize postharvest losses. However, there is insufficient information on the modelling of airflow, heat and mass transfer, using the computational fluid dynamics (CFD). The aims of this study were: i) to investigate the real-time airflow pattern, temperature, enthalpy, heat flux and relative humidity distribution inside the unloaded evaporative cooler and CoolBot-air-conditioner cooling systems, using CFD modelling techniques, ii) to evaluate the effect of inlet air characteristics on the airflow resistance inside the selected appropriate semi- and fully-loaded cold storage chambers, iii) to screen the best combinations of pre-storage disinfection treatments, combined with the low-cost cooling technologies, in terms of changes in quality of tomato fruit, and iv) to develop predictive models for the estimation of changes in quality and probability of marketability, using experimental data, obtained during the storage of tomatoes, after they have been subjected to different postharvest treatments and low-cost cooling technologies. The specific aim of this study was to investigate the real-time airflow pattern, temperature and heat flux inside EC, CBAC and EC+CBAC storage systems, using CFD models, to evaluate the changes in the quality of stored tomatoes and to develop predictive models for quality changes of tomatoes stored under EC and CBAC.

The experimental results showed that the indirect heat exchanger (IHE) and one evaporative cooling wet pad were sufficient to reduce the temperature of the hot ambient air from 34.1℃ to 22.82℃. However, using multi-layer evaporative cooling pads was proven to have significant importance in increasing the relative humidity of air leading to the storage chamber. The EC+CBAC combination was the best for maintaining an optimum temperature (8-15°C) and relative humidity (80-99%) of the micro-environment inside the cold storage chamber during the storage period. A computational fluid dynamics (CFD) model was used to investigate the airflow, temperature and heat flux across the IHE and psychrometric unit. The numerical results showed that the psychrometric unit was not sufficient for reducing the ambient air temperature

to at least near the wet-bulb temperature of the ambient air, hence, the modification of the airflow regulating fan is required. The steady state and transient CFD modelling of the micro-environment was performed in order to visualize the inside of the unloaded EC, CBAC and EC+CBAC storage chambers, the non-uniform distribution of air velocities, temperature and heat flux was found inside the storage chambers. Visual observations of velocity vector magnitude and temperature uniformity distribution inside unloaded stores were demonstrated in decreasing order, from EC+CBAC, CBAC and EC, respectively.

The modelling of the semi- and fully-loaded tomatoes stacked in the EC+CBAC cold storage chamber, using CFD models, was found to be crucial for determining the airflow resistance, which is the fundamental parameter for the engineering analysis of heat and mass transfer inside the cold storage chamber during the re-design process. The results showed that the long-side of the tomato stack, facing the direction of the airflow, had a lower airflow resistance, when compared to the short-side stack. Therefore, it was demonstrated that there was better airflow through the long-side stack. The CFD models that were developed were validated by comparing the air velocity and the reported RMSE was found to be acceptable, compared to literature. The information generated in this study has resulted in EC and CBAC cold store systems being used, for the first time, for the analysis of airflow characterisation and heat transfer that takes place inside a storage chamber.

The integrated approach, combining the application of low-cost evaporative cooling storage and pre-storage disinfection treatments (*i.e.* chlorinated water and anolyte water), was found to be the best method, for extending the shelf-life of the tomato fruit, by maintaining the better quality of fresh tomatoes for 28 days of storage. A combination of the green maturity stage and both chlorinated and anolyte water maintained better quality parameters, in terms of the colour, firmness and many other quality indices, when using the low-cost cooling technology during storage period.

Logistic regression, polynomial, fractional polynomial, multivariate and covariance models were developed for low-cost cold storage systems for the first time, to predict the quality of the stored tomatoes under integrated postharvest handling and treatment. These models were developed for the tomato quality indices subjected to low-cost cooling technologies and pre-storage disinfection treatments and they were found to follow curvilinear relationships. Utilizing the logistic regression model, the marketability of tomatoes was found to be higher

for tomatoes stored under an evaporative cooling environment than for those stored under ambient environment. The fractional polynomial, polynomial and multivariate models that were developed can be used by farmers to predict the changes in the quality of fresh tomatoes during storage, for the selective quality parameters such as tomato firmness, colour and many others. A study of model's development, as well as the use of low-cost cooling technologies and pre-storage disinfection treatments, should be conducted for other fresh produce.

AKNOWLEDGEMENT

The journey of my PhD studies at the University of KwaZulu-Natal, South Africa, began on September 2014. Over the past four years, I have not only gained academic knowledge, but, I have also learnt how to become responsible and independent. I am very grateful to have met and worked with so many people, who have guided me during this study period. Now, I have the opportunity to express my heartfelt appreciation, to them all.

First of all, I thank my Saviour, the Lord "Jesus Christ", for His mercy and grace, for the opportunity to study at PhD level, and for giving me the strength and time to complete this thesis. God is good ALL the time and He is faithful to His children. I would also like to gratefully acknowledge and record my heartfelt gratitude to the following people for their help, insight, support and encouragement.

I am extremely grateful to my academic supervisor, Prof. Dr. Tilahun Seyoum Workneh, in the discipline of Bioresources Engineering, at the School of Engineering of the University of KwaZulu-Natal, South Africa, for his unreserved advice, support and guidance throughout the study period. I enjoyed the freedom to explore all options during the various stages of my research work and this is all due to your experience and advice. I sincerely honour his insight into my study problems, his philosophy of supervision and his patience. Despite his busy schedule, and even during his precious holidays, he always made time for me, whether it was on or off campus. Whenever we met, he was always diligent in meeting the deadlines had encouraged me to complete my thesis work. Prof. Workneh has inspired me in many areas of my life; his commitment to work, his accomplishments, his academic and research excellence, his devotion and simplicity, as well as always being available are qualities that I will strive to emulate. Without his critical comments and useful suggestions, his commitment and prompt feedback, this work would not have been accomplished. Prof. Workneh is very family-oriented and treated me as his older son. Prof., you are not only my mentor, but also a good father and friend. May God bless you and give you a long life.

I am grateful to Dr. Tsion Tesfaye Kidane, Dr. Sileshi Fanta Melesse, Dr. Alemayehu Ambaw Tsige and Dr. Mulugeta Delele for all their suggestions and never-ending support throughout the study period. Furthermore, I would like to thank the anonymous reviewers for their helpful

suggestions in the articles presented in this thesis and in the thesis itself. Without the conducive study environment that was created by the employees of the Bioresources Engineering (Agricultural engineering) discipline, this work would not have been possible. I am particularly thankful to Mrs. Natasha Moneyvalu, Mr. David Clark, Mr. Merrvyn Hansen, Mr. Alan Hill, Mr. Kumalo, Mrs. Elsie Correia and Dr. Sharon Rees for their helpful assistance, friendship, motivation and hospitality during the field and laboratory work of my research.

I gratefully acknowledge the Ethiopian Federal Ministry of Education for its partial financial support for my stipend and research work in South Africa. The PhD research was partly financed by the National Research Fund of South Africa (NRF-TWAS: Grant Number SFH 150902141138). I gratefully acknowledge the ZZ2 Tomato Producer Organization and the Postharvest Innovation Program Tomato Project (Grant No. 7/2015) for their provision of sample tomatoes for my study. I acknowledge my host university, the University of KwaZulu-Natal is well acknowledged for its support of all aspects of my research work. This thesis work would be incomplete if I ignored the role played by my employer; the Haramaya University, Ethiopia, for granting me study leave in South Africa. Such a positive decision deserves my profound acknowledgement and gratitude.

It was not easy to live in a foreign country for such a long time. I thank my Ethiopian community Ebenezer Church elders, my fellow-students, Zerihun Asmelash, Yibrah Hagos, Kassahun Mengist and Melkamu Dedefo, Cherono Kipchumba, Dr. Sylver Milindi Sibomana, Dr. Macdex Mutema, and Sabelo Shezi, for being part of my life and in your prayers and for being such good friends.

I am thankful to my whole family back home for their constant support and encouragement. Most importantly, I am strongly indebted to my darling sweetheart, my wife Meseret Dawit Teweldebrihan, for her love, prayers, care and support, as well as for being patient and tolerant and taking on the dual responsibility of being a mum and a dad to our children. I will always love you; you are not only my wife, but, my mum, friend, sister and my blessing. My children Yoftahe Getachew and Ketim Getachew, your dad loves you too much. Thank you my wife's father, Dawit Teweldebrihan, my wife's mother, Atsede Yadeta, my wife's sister Mahilet Dawit and all of my families and relatives, for the unreserved love and care that you gave to Ketim and Yoftahe over all these days. Thank you, my mother, father, sisters and brothers, for all your prayers and support. For those who contributed in various ways, but whom I have not mentioned

here, because of my poor memory, as well as those who did not get the opportunity to contribute, I am still very grateful**.**

DEDICATED TO:

MY BELOVED WIFE, ***MESERET DAWIT***

MY WONDERFUL CHILDREN, ***YOFTAHE GETACHEW***

AND

KETIM GETACHEW

AND

ALL MY FAMILIES

"GOD IS GOOD ALWAYS AND HE IS FAITHFUL"

PREFACE

The thesis considers the “Modelling of micro-environment inside evaporatively and CoolBot cooled stores using computational fluid dynamics models and changes in quality of stored tomatoes”. The thesis is based on and contains the following papers for the evaluation the philosophy of doctor (PhD) in Engineering, discipline of Agricultural Engineering, University of KwaZulu-Natal, Pietermaritzburg, South Africa. Four papers published on peer reviewed journals, five papers prepared to be submitted, four papers presented on conferences and two papers submitted and accepted to be presented on a conference and proceedings (listed under list of contributions sub-section). The papers are here re-set in the present thesis format and some minor differences are present as compared to the published versions.

The thesis was outlined in the following order: general introduction (chapter one), literature review on the detailed study of computational fluid dynamics (CFD) model study for low-cost cooling technologies and for modelling quality of fruit and vegetables (Chapter Two). The following Chapters (Three, Four, Five, Six, Seven and Eight) are presented and analysed scientifically and sequentially for the air characteristics that cooled evaporatively and air conditioned across the psychrometric unit and inside cold rooms experimentally and using CFD models. Followed by the study of integration effects of pre-storage disinfection treatments and the low-cost cold stores on quality of tomato fruit. Moreover, models were developed for the quality of tomato fruit that affected by the low-cost cold storage and pre-storage disinfection treatments.

The main results of the papers are presented in the context of a general introduction to the field of engineering (agricultural engineering, which is relevant on postharvest technology and engineering), for modelling of airflow inside cold storage chambers and modelling of tomato quality attributes, which affected by the cold storages and postharvest disinfection treatments. Finally, chapter Nine concludes the results of this study and gives recommendations for future study prospective.

TABLE OF CONTENTS

LIST OF FIGURES

Page

LIST OF TABLES

Page

LIST OF CONTRIBUTIONS

Papers and posters published, submitted and under preparation for submission are listed below:

A. Published papers:

1. Tolesa, GN and Workneh, TS. 2017. Influence of storage environment, maturity stage and pre-storage disinfection treatments on tomato fruit quality during winter in KwaZulu-Natal, South Africa. Journal of Food Science and Technology, 54(10), 3230-3242. https://doi.org/10.1007/s13197-017-2766-6.
2. Tolesa, GN, Workneh, TS and Melesse, SF. 2018. Logistic regression analysis of marketability of tomato fruit harvested at different maturity stages and subjected to disinfection, storage condition and storage period treatments. Biological Agriculture & Horticulture, 34(1), 40-52. https://doi.org/10.1080/01448765.2017.1368414.
3. Tolesa, GN, Workneh, TS, and Melesse, SF. 2018. Modelling Effects of Pre-Storage Treatments, Maturity Stage, Low-Cost Storage Technology Environment and Storage Period on the Quality of Tomato Fruit. CyTA Journal of Food, 16(1), 271-280. https://doi.org/10.1080/19476337.2017.1392616.
4. Tolesa, GN and Workneh, TS. 2018. Effects Of Evaporative Cooling and CoolBot Air Conditioning on Changes in the Environmental Conditions inside The Cooling Chamber. Acta Horticulture (Accepted and *In Press*).

B. Papers under preparation for submission

1. Tolesa, GN and Workneh, TS. Low-Cost Fresh Produce Cold Storage Technologies and the Prospect of CFD Modelling of Microclimate Inside the Sellected Coolers: Areview (prepared for submission).
2. Tolesa, GN, Ambaw A, Workneh TS and Opara UL. Evaluation of airflow and temperature profile characteristics across the indirect heat exchanger and multi-pads evaporative cooler psychrometric unit (prepared for submission).
3. Tolesa, GN, Ambaw A, Workneh TS and Opara UL. CFD Modelling of Airflow inside Unloaded Evaporative Cooler, Coolbot-Air-Conditioner and Combined Operations (prepared for submission).

4. Tolesa, GN, Ambaw A, Workneh, TS and Opara, UL. CFD Modelling of Temperature and Enthalpy Distribution inside Unloaded store subjected to Evaporative Cooling and, CoolBot-Air-Conditioning (prepared for submission).Tolesa, GN, Ambaw A, Workneh, TS and Opara, UL. Investigating the airflow inside a semi-loaded and fully loaded cold store under combined evaporative cooling and CoolBot-air-conditioner cooling system using CFD method (prepared for submission).

C. Conference presentations and proceedings

1. Tolesa, GN and Workneh, TS. 2016. Effect of evaporative cooling environment, maturity stage and pre-storage treatments on tomato fruit quality. The college of Agriculture, Engineering and Science Research Day, University of KwaZulu-Natal, Durban, South Africa (Oral presentation). http://caes.ukzn.ac.za/news/16-12-09/Postgraduate_Students_Excel_at_Research_and_Innovation_Day.aspx.
2. Tolesa, GN, Workneh, TS and Melesse, SF. 2017. Logistic Regression Analysis of Marketability of Tomato Fruit Harvested at Different Maturity Stage and Subjected to Disinfection, Storage Conditions and Storage Period Treatments. The 2nd Ukulinga Howard Devis Memorial Symposium, University of KwaZulu-Natal, Pietermaritzburg, South Africa (Poster presentation). http://caes.ukzn.ac.za/news/17-06 08/Second_Ukulinga_Howard_Davis_Memorial_Symposium_Unites_Stakeholders_for_ Food_Security.aspx.
3. Tolesa GN and Wokneh TS. 2017. Comparison of the changes of microclimates inside the charcoal evaporative cooler and CoolBot-Air Conditioner cooled cold stores. SAAFoST 2017 Congress and Exhibition at Century City Convention Centre in Cape Town from the 3rd - 6th September 2017 (Poster presentation). http://www.saafost2017.org.za/registration.asp.
4. Tolesa, GN, Workneh, TS and Melesse, SF. 2017. Logistic Regression Analysis of Marketability of Tomato Fruit Harvested at Different Maturity Stage and Subjected to Disinfection, Storage Conditions and Storage Period Treatments. SAAFoST 2017 Congress and Exhibition at Century City Convention Centre in Cape Town from the 3-6 September 2017 (Poster presentation). http://www.saafost2017.org.za/registration.asp.
5. Tolesa, GN and Workneh, TS. 2018. A Comparison of the Influence of Different Low-Cost Cooling Technologies on Tomato Cooling Time (Conference paper submitted and

accepted for oral presentation by Acta Horiculture, June 11 – 15, 2018, Athens, Greece). https://www.ishs.org/symposium/645

6. Tolesa, GN, Ambaw A, Workneh, TS and Opara, UL. CFD modelling of airflow inside unloaded evaporative cooler, CoolBot-air-conditioner and combined operations (Conference paper submitted and accepted for oral presentation by Acta Horticulture, August 12 - 16, 2018, Istanbul, Turkey). https://www.ishs.org/symposium/674

1. GENERAL INTRODUCTION

1.1 Introduction

The postharvest losses (PHL) of fruit and vegetables can be as much as 30-50% of the production (van Gogh *et al.*, 2013). Tomatoes (*Solanum Lycopersicum L.*) are among the most widely consumed, perishable and economically important fresh produce, making up one-seventh of the total crop production (Nasrin *et al.*, 2008). Moreover, tomatoes are the second most important fresh produce after potatoes, contributing about 24% of total vegetables grown in South Africa (DAFF, 2010). Despite huge production figures, the PHL of tomatoes is reported to be 10-30% of the total production (Etebu *et al.*, 2013), resulting in a significant loss to the economy and lowering food security (Parfitt *et al.*, 2010a). For the above reasons, special attention should be given to reducing the PHL of tomatoes through the application of proper postharvest management and appropriate postharvest technologies, to maintain the quality of fresh produce (Ait-Oubahou, 2013).

The most important postharvest management practice for the cooling of fruit and vegetables are advanced cold storage technologies, which reduce respiration, ripening, transpiration and decay (Roy and Pal, 1994; Ambaw *et al.*, 2013a). These technologies reduce the temperature of the micro-environment between -1 and 13°C, as well as that of the fresh produce, thereby reducing the respiration and ethylene production rate (Paull and Duarte, 2011; Yahia, 2011). Cold chain mismanagement can lead to a PHL of between 10-40% for fruit (Parfitt *et al.*, 2010) and 15-30% for vegetables (Gustavsson *et al.*, 2011). Common cold storage technologies include mechanical refrigeration, evaporative cooling (EC), vacuum cooling and many others (ASHRAE, 2011; Ambaw *et al.*, 2013b). Among these technologies, forced air assisted cold storage is important for minimizing and uniformly distributing the storage climate composition, including ethylene, temperature, relative humidity (RH) and the heat generated through respiration (Kader, 2001). In spite of its popularity, the mechanical refrigerated storage is expensive, energy-intensive and requires high installation costs, making this technology unfeasible for small-scale farmers (Roy and Pal, 1994). Low-cost EC technology does save energy, is reliable, cheap and environmentally friendly. It is also appropriate for hot, arid and semi-arid climates (Bom *et al.*, 1999; Thompson *et al.*, 2002; Xuan *et al.*, 2012; Hao *et al.*, 2013). The evaporatively-cooled air forced through cooling pads to the storage room, cools the

storage environment and the produce (Thompson *et al.*, 2002). Unlike mechanical refrigeration, EC does not use chlorofluorocarbons, minimizes carbon dioxide release, maintains a good quality of cold air inside cold rooms, and has less dependency on public energy sources (Bom *et al.*, 1999). In addition, Workneh (2010) reported that the use of low-cost EC for fruit and vegetables is found to be a feasible technology, especially for arid and semi-arid areas in sub-Saharan African countries. Similarily, EC is recommended for the preservation of modest respiration fruit and vegetables (Jain, 2007). In spite of many studies in the use of EC for preserving fruit and vegetables, there is limited information on the dynamics of airflow, heat and mass transfer that takes place inside the evaporative cool chamber system.

The CoolBot-air-conditioner (CBAC), an electronic device, that overrides a room air conditioner (AC), was developed recently (Boyette and Rohrbach, 1993). It reduces the cooling temperature below the set point and allows the maintenance of near optimum conditions for the preservation of fresh produce, while it is also easy to handle, install and maintain (Saran *et al.*, 2013). The total cost of a CBAC cooling system is (90%) less than a of mechanical refrigeration system (Kitinoja, 2013). Saran *et al.* (2013) reported that, by using a CBAC, a 4-5°C temperature is attainable for low-cost insulated rooms. The CBAC has been used for the storage of cauliflower, cabbages, tomatoes and okra and has resulted in freshness, good quality and marketability for prolonged periods (Saran *et al.*, 2013). The installation costs, repair costs, and electricity usage are all low, together with the reduced operational cost, make the system feasible for small-scale producers (Kitinoja, 2013). However, no studies have been carried out on the CBAC in the area of the dynamics of the airflow pattern, or the heat and mass transfer.

1.2 Justification

The non-uniform airflow distribution, as well as heat and energy transfer, in cold storage may cause unevenly distributed cold spots within the storage unit (Ambaw *et al.*, 2013a). Therefore, understanding the airflow pattern, as well as heat and mass transfer distribution in a cold room, is crucial for the design of EC and CBAC cold storage systems. Once the airflow distribution, heat and mass transfer are well understood, appropriate designs can be developed to uniformly cool the produce that is stored inside.

Computational fluid dynamics (CFD) is a computer-aided numerical analysis method that is used to solve the fluid dynamics problems (Norton and Sun, 2006). The CFD model applies the

general transport equations (Navier-Stokes equations), which are comprised of the equations of continuity, momentum and enthalpy over the controlled volume (Nicolaï *et al.*, 2001; Verboven *et al.*, 2006; Versteeg and Malalasekera, 2007; Ambaw *et al.*, 2013a). Therefore, a CFD model is a valuable tool for solving the problem of airflow (fluid) patterns in cold storage and cold rooms, the liquid flow in food, and the transport phenomena in agricultural produce storage (Tijskens *et al.*, 2001; Verboven *et al.*, 2006; Chen *et al.*, 2010; Chen *et al.*, 2011). CFD models have become essential in solving the problem of transport phenomena of cold storage and stored produce, by simulating and predicting important parameters (Wang and Sun, 2003; Nahor *et al.*, 2005).

In addition, fruit quality is becoming an important marketing factor, which makes the management of fruit vital (Sloof *et al.*, 1996). There is limited literature on the modelling of quality data of fresh produce stored in EC and CBAC storage systems, resulting in limited predictions of produce quality under EC and CBAC storage systems (van Boekel, 2010). Therefore, models for quality data are important for experimental tomatoes stored inside EC and CBAC conditions.

In conclusion, cooling is essential for storage and transportation, in order to reduce the PHL (Singh *et al.*, 2014). Therefore, the implementation of low-cost, effective and environmentally-friendly postharvest technologies, is vital, particularly among poor farmers in developing countries (Gustavsson *et al.*, 2011). The EC and CBAC are among the most affordable cold storage systems for fruit and vegetables in arid and semi-arid countries, and the modelling of airflow patterns, heat and mass transfer within the storage chambers could provide the insight required for further improvements, in terms of the airflow velocity, temperature and relative humidity distribution, as well as heat and mass transfer. Modelling can provide for the further modification and improvement of the storage design, stacking patterns and storage life of stored tomatoes. Moreover, understanding the effect of storage systems, such as these, on the storage life and quality of fresh tomatoes is vital, as well as having an insight into the possibilities of modelling changes on the quality of stored tomatoes.

1.3 Aims of the Research

The general objectives of the project were to investigate the real-time airflow pattern and the heat and mass transfer inside an EC and CBAC storage system, using CFD models, to evaluate

the changes in the quality of stored tomatoes and to develop a predictive model for the quality data of fresh tomatoes.

1.4 Specific Objectives

The objectives of this study are listed below:

(i) To investigate the real-time airflow pattern, temperature, enthalpy, heat flux and relative humidity distribution inside the unloaded evaporative cooler and CoolBot-air-conditioner cooling systems, using CFD modelling techniques,

(ii) To evaluate the effect of inlet air characteristics on the airflow resistance inside the selected appropriate semi- and fully-loaded cold storage chambers,

(iii) To screen the best combinations of pre-storage disinfection treatments, combined with the low-cost cooling technologies, in terms of changes in quality of tomato fruit, and

(iv) To develop predictive models for the estimation of changes in quality and probability of marketability, using experimental data, obtained during the storage of tomatoes, after they have been subjected to different postharvest treatments and low-cost cooling technologies.

1.5 Thesis Outline

Chapter One gives the overall introduction, problem statements and objectives of the thesis.

Chapter Two presents the support literature on the research of interest to this research project. It reviews the detailed studies of low-cost cooling technologies (EC, CBAC and EC+CBAC) for fresh produce, CFD modelling studies for the low-cost cooling systems and the tomato fruit qualities affected by the postharvest pre-storage disinfection treatments and low-cost cooling technologies.

Chapter Three addresses the basic experiment on the effects of the evaporative cooler and CoolBot-air-conditioner on the air velocity, temperature and relative humidity. The hobo data loggers and hot-air anemometer were used for the temperature, relative humidity and air speed measurements. The research experiment led to the detailed CFD modelling for a detailed study air environment inside the coolers.

Chapter Four addresses the detailed CFD model analysis of the airflow, temperature and enthalpy distribution across the indirect heat exchanger (IHE) and evaporative cooling multi-pads, to characterize the air that passes through the psychrometric unit towards the cold storage chambers. Evaluation of airflow and temperature profile characteristics across the indirect heat exchanger and multi-pads evaporative cooler psychrometric unit. Experimental and numerical air velocity and temperature studies were carried out to validate the CFD models. The pressure drop across the IHE and pads were used from literature.

Chapter Five describes the detailed CFD model study of unloaded EC, CBAC and EC+CBAC cold storage chambers. Section 5.1 presents a detailed study on the spatial temporal air flow distribution and is entitled, "CFD Modelling of Airflow inside Unloaded Evaporative Cooler, CoolBot Air Conditioner and Combined Operation". Section 5.2 describes the detailed temperature and enthalpy distribution inside the low-cost cold technologies and is entitled, "CFD Modelling of Temperature and Enthalpy Distribution inside an Unloaded Storage Chamber subjected to Evaporative Cooling and CoolBot-air-conditioning". The experimental hobos and anemometers with data loggers were located at different locations inside the cool storage chambers, to measure the temperature, RH and air velocity distribution, for validation purposes.

Chapter Six describes the detailed CFD model study of semi- and fully loaded EC+CBAC cold stores and is entitled, "Investigating the Airflow inside a Semi-Loaded and Fully-Loaded Cold Storage Chamber of a Combined Evaporative Cooling and Coolbot-Air-Conditioner Cooling System, Using the CFD Method ". This chapter led to the detailed airflow characterization of the loaded low-cost storage chambers.

Chapter Seven addresses the effects of the cold storage chamber and other postharvest treatments on the quality of stored tomatoes. Different factors, such as the fruit maturity stage, the pre-storage disinfection treatments, the storage period and storage conditions studied is entitled, "Influence of storage environment, maturity stage and pre-storage treatments on tomato fruit quality during winter in KwaZulu-Natal, South Africa".

Chapter Eight describes the modelling possibilities of quality indices of tomatoes affected by EC storage, the maturity stage, pre-storage disinfection treatments and the storage period. It is comprised of two parts. Section 8.1 describes the modelling of the probability of marketability

of the tomato fruit, which affected by the treatments mentioned, and is entitled, "Logistic regression analysis of the marketability of the tomato fruit harvested at different maturity stages and subjected to disinfection, storage conditions and storage period treatments". The second part, Section 8.2, describes the detailed model development for the quality indices of tomatoes stored inside an evaporative cooler and is entitled, "Modelling effects of pre-storage treatments, maturity stage, low-cost storage technology environment and storage". Chapter Nine summarizes the concluding remarks, limitations and recommendations.

1.6 References

Ait-Oubahou, A. 2013. Postharvest technologies in sub-Saharan Africa: status, problems and recommendations for improvements. *In:* Abdullah, H and Latifah, MN, eds. Proc. 7th International Postharvest Symposium, 1273-1282. Acta Horticulture, International Society for Horticultural Science (ISHS), Leuven, Belgium.

Ambaw, A, Delele, MA, Defraeye, T, Ho, QT, Opara, LU, Nicolai, BM and Verboven, P. 2013a. The use of CFD to characterize and design post-harvest storage facilities: Past, present and future. *Computers and Electronics in Agriculture,* 93**,** 184-194.

Ambaw, A, Verboven, P, Defraeye, T, Tijskens, E, Schenk, A, Opara, UL and Nicolai, BM. 2013b. Effect of box materials on the distribution of 1-MCP gas during cold storage: A CFD study. *Journal of Food Engineering,* 119**,** 150-158.

Ashrae, A. 2011. ASHRAE/USGBC/IES standard 189.1-2011. Standard for the design of high-performance green buildings. *American Society of Heating, Refrigerating and Air-Conditioning Engineers.* Inc., Atlanta, GA.

Bom, GJ, Foster, R, Dijkstra, E and Tummers, M. 1999. *Evaporative air-conditioning: applications for environmentally friendly cooling.* World Bank Publishing., Washington DC, USA.

Boyette, MD and Rohrbach, RP. 1993. A low-cost, portable, forced-air pallet cooling system. *Applied engineering in agriculture,* 9**,** 97-104.

Chen, Q, Pan, N and Guo, Z-Y. 2011. A new approach to analysis and optimization of evaporative cooling system II: Applications. *Energy,* 36**,** 2890-2898.

Chen, Q, Yang, K, Wang, M, Pan, N and Guo, Z-Y. 2010. A new approach to analysis and optimization of evaporative cooling system I: Theory. *Energy,* 35**,** 2448-2454.

DAFF. 2010. Department of Agriculture, Forestry and Fisheries, Republic of South Africa, Directorate of Marketing: Production guideline of tomato. *Unpublished.* South Africa.

Etebu, E, Nwauzoma, A and Bawo, D. 2013. Postharvest Spoilage of Tomato (Lycopersicon esculentum Mill.) and Control Strategies in Nigeria. *Journal of Biology, Agriculture and Healthcare,* 3**,** 51-61.

Gustavsson, J, Cederberg, C, Sonesson, U, Van Otterdijk, R and Meybeck, A. 2011. Global food losses and food waste: extent, causes and prevention. Study conducted for the International Congress SAVE FOOD at Interpack201, 1-38. FAO, Düsseldorf, Germany.

Hao, XL, Zhu, CZ, Lin, YL, Wang, HQ, Zhang, GQ and Chen, YM. 2013. Optimizing the pad thickness of evaporative air-cooled chiller for maximum energy saving. *Energy and Buildings,* 61**,** 146-152.

Jain, D. 2007. Development and testing of two-stage evaporative cooler. *Building and Environment,* 42**,** 2549-2554.

Kader, AA. 2001. Recent advances and future research needs in postharvest technology of fruits. Bulletin of the International Institute of Refrigeration, 3-13. Acta Horticulture.

Kitinoja, L. 2013. Innovative Small-scale Postharvest Technologies for reducing losses in Horticultural Crops. *Ethiop .J. Appl. Sci. Technol. ,* Special Issue, 1**,** 9-15.

Nahor, HB, Hoang, ML, Verboven, P, Baelmans, M and Nicolai, BM. 2005. CFD model of the airflow, heat and mass transfer in cool stores. *International Journal of Refrigeration-Revue Internationale Du Froid,* 28**,** 368-380.

Nasrin, TaA, Molla, MM, Hossaen, MA, Alam, MS and Yasmin, L. 2008. Effect of postharvest treatments on shelf life and quality of tomato. *Bangladesh Journal of Agricultural Research,* 33**,** 579-585.

Nicolaï, BM, Verboven, P and Scheerlinck, N. 2001. The modelling of heat and mass transfer. *In:* Tijskens, I, Hartgot, M and Nicolaï, BM (eds.) *Food Process Modelling.* Ch. 4, 60-86. CRC Press and Woodhead Publishing Limited, Cambrige, England.

Norton, T and Sun, DW. 2006. Computational fluid dynamics (CFD): an Effective and efficient design and analysis tool for the food industry: a review. *Trends in Food Science & Technology,* 17**,** 600-620.

Parfitt, J, Barthel, M and Macnaughton, S. 2010. Food waste within food supply chains: quantification and potential for change to 2050. *Philosophical Transactions of the Royal Society B-Biological Sciences,* 365**,** 3065-3081.

Paull, RE and Duarte, O. 2011. *Tropical fruits.* CAB International, Reading, UK.

Roy, SK and Pal, RK. 1994. A low-cost cool chamber: an innovative technology for developing countries. *In:* Champ, BR, Highley, E and Johnson, GI, eds. Postharvest Handling of

Tropical Fruits: ACIAR Proceedings, 393-395. Australian Centre for International Agricultural Research, Australia.

Saran, S, Dubey, N, Mishra, V, Dwivedi, SK and Raman, NLM. 2013. Evaluation of coolbot cool room as a low cost storage system for marginal farmers. *Progressive Horticulture,* 45**,** 115-121.

Singh, V, Hedayetullah, M, Zaman, P and Meher, J. 2014. Postharvest Technology of Fruits and Vegetables: An Overview. *Journal of Post-Harvest Technology,* 2**,** 124-135.

Sloof, M, Tijskens, LMM and Wilkinson, EC. 1996. Concepts for modelling the quality of perishable products. *Trends in Food Science & Technology,* 7**,** 165-171.

Thompson, JF, Mitchell, FG and Kasmire, RF. 2002. Cooling horticultural commodities. *In:* Kader, AA (ed.) *Postharvest technology of horticultural crops.* 3rd ed, Cha. 11, 97- 112. Agriculture and Natural Resources, University of California, USA.

Tijskens, LMM, Hertog, MLaTM and Nicolaï, BM. 2001. *Food process modelling.* Woodhead Publishing Limited and CDC press, Cambrige, England.

Van Boekel, MaJS. 2010. *Kinetic modeling of reactions in foods.* CRC press, Tayplor & Francis Group, New York, USA.

Van Gogh, JB, Van Der Sluis, AA and Soethoudt, JM. 2013. *Feasibility of a network of excellence postharvest food losses: Combining knowledge and compepetences to reduce food losses in developing and emerging economies.* Wageningen UR Food & Biobased Research, Netherland.

Verboven, P, Flick, D, Nicolai, BM and Alvarez, G. 2006. Modelling transport phenomena in refrigerated food bulks, packages and stacks: basics and advances. *International Journal of Refrigeration-Revue Internationale Du Froid,* 29**,** 985-997.

Versteeg, HK and Malalasekera, W. 2007. *An introduction to computational fluid dynamics: the finite volume method.* Pearson Education Limited, UK.

Wang, L and Sun, DW. 2003. Recent developments in numerical modelling of heating and cooling processes in the food industry: a review. *Trends in Food Science & Technology,* 14**,** 408-423.

Workneh, TS. 2010. Feasibility and economic evaluation of low-cost evaporative cooling system in fruit and vegetables storage. *African Journal of Food, Agriculture, Nutrition and Development,* 10**,** 2984-2997.

Xuan, YM, Xiao, F, Niu, XF, Huang, X and Wang, SW. 2012. Research and application of evaporative cooling in China: A review (I) - Research. *Renewable & Sustainable Energy Reviews,* 16**,** 3535-3546.

Yahia, EM. 2011. *Postharvest Biology and Technology of Tropical and Subtropical Fruits: Fundamental Issues.* Woodhead Publishing Limited, UK.

2. LITERATURE REVIEW

This chapter consists of the relevant literature on fresh produce cold storage technologies and the prospects of CFD modelling of micro-environment inside the selected coolers. The CFD modelling review covered modelling of airflow micro-climatic dynamics, energy, and mass transfer properties in cold storage systems. In addition, it covered the review of modelling of quality characteristics of tomato fruit subjected to low-cost cold storage technologies and pre-storage disinfection treatments were explored from literature.

2.1 Introduction

Postharvest loss (PHL) of fresh produce has reached 30-50% of production (Xu *et al.*, 2002; van Gogh *et al.*, 2013). Thus, appropriate postharvest technologies are required to reduce PHL and to keep the quality of fresh produce longer (Ait-Oubahou, 2013). Cooling technologies reduce the temperature of microenvironment of the fresh produce storage, which can result in reduction of respiration, ripening, transpiration and decay rates (Ambaw *et al.*, 2013a). Cold chain mismanagement contributed to PHL of 10-40% of fresh produce (Parfitt *et al.*, 2010; Gustavsson *et al.*, 2011). Common cooling technologies include mechanical refrigeration, evaporative cooling (EC), vacuum cooling, CoolBot-air-conditioner (CBAC) and many others (ASHRAE, 2011; Saran *et al.*, 2013). Among these technologies, forced air assisted cold storages are important to uniformly distribute the storage microclimate compositions (Kader, 2001).

In addition to saving energy, low-cost EC technology is reliable, affordable, environmentally friendly and appropriate for arid and semi-arid climates (Bom *et al.*, 1999; Thompson *et al.*, 2002; Xuan *et al.*, 2012a; Hao *et al.*, 2013). The working fluid for EC is water, which minimizes the risk of greenhouse effect gasses on the environment. It also produce good quality of cold air inside the cold rooms (Bom *et al.*, 1999). In addition, Workneh (2010) reported that the use of low-cost EC for fruit and vegetables is found to be feasible technology especially for arid and semi-arid sub-Saharan African countries. Similarily, EC was recommended for preservation of modest respiration fruit and vegetables (Jain, 2007).

Moreover, recently, low-cost CoolBot-air-conditioner (CBAC), an electronic device that overrides domestic air conditioner (AC) temperature, was developed (Boyette and Rohrbach, 1993). It reduces cooling temperature below the AC set point and allows maintaining optimum conditions for the preservation of fresh produces. It is easy to handle, install, and maintain and make is feasible for small-scale producers (Saran *et al.*, 2013). The total cost is less by 90% than that of mechanical refrigeration system (Kitinoja, 2013a). Saran *et al.* (2013) reported that 4-5°C temperature is attainable for insulated rooms.

Both technologies, EC and CBAC cooling systems are not yet well understood with regard to performance improvement in terms of design and cooling. While the micro-climate optimisation for heat load, removal is very critical for efficient utilization of the technologies in food industries and stakeholders in food cold supply chain. There is limited research carried out on the dynamics of how the airflow, heat and mass transfer take place inside low-cost forced air EC chambers for fresh produce storage. With regard to CBAC cooling system there is no relevant study conducted thus far. Ambaw *et al.* (2013a) warned that non-uniform airflow distribution, heat and energy transfer in the cold storage might cause unevenly distributed cold spots inside the storage. Hence, an understanding of the dynamics of microclimate inside EC and CBAC is of paramount importance for the designing the enclosures and optimizing cooling processes. Several researchers reported that computational fluid dynamics (CFD) is powerful tool to solve air flow, heat and mass transfer dynamics problems inside cold storage (Norton and Sun, 2006). Hence, this review focuses on the state of the art of low-cost cold storage technologies airflow pattern, heat and mass transfer studies and finally provides direction for the future trend.

2.2 Low-cost Evaporative Cooling Technology

Eaporative cooler (EC) cools the storage room using cold air which has been cooled, by the removal of heat of evaporation through the wetted, and perforated cooling pad (Kitinoja, 2013b) (Figure 2.1). The cooling performance of EC relies on atmospheric air RH, pore size and surface characteristics of the cooling pad (Kitinoja and Thompson, 2010). The lower the RH, the lower the cold air temperature attained by EC (Paliyath and Murr, 2008; Yahia, 2010). It does save energy, which is required for fan and water pump. Moreover, it is reliable, cheap and environmentally friendly for arid and semi-arid climates (Bom *et al.*, 1999; Thompson *et al.*, 2002; Xuan *et al.*, 2012a; Hao *et al.*, 2013). In addition, water is the working fluid, the deficit

of both vapour pressure and temperature are the controlling mechanisms for mass and heat transfer (ASHRAE, 2011). Furthermore, the feasibility of EC technology to extend the shelf-life of fruit and vegetables under arid and semi-arid climate was reported by Workneh (2010). Therefore, this technology was recommended for preservation of modest respiration fruit and vegetables (Jain, 2007).

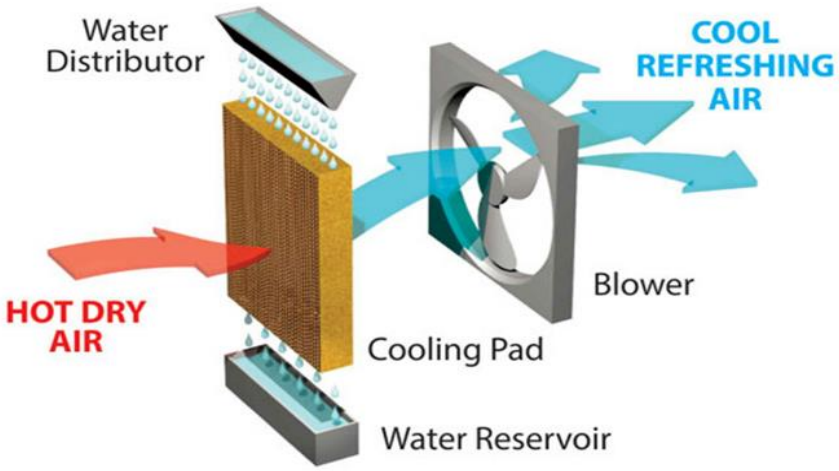

Figure 2.1 Direct evaporative cooling fundamental principles (Muñoz *et al.*, 2017)

The EC can reduce air temperature to 10 - 15°C approaching the air wet bulb, and increase the RH to about 90% (Thompson, 2002), and can be passive without the application of energy or the assisted with fan (Kitinoja, 2013b). Kitinoja (2013b) also reported that EC reduces the temperature of the produce 2 - 3°C higher than the dew point of air temperature used. Moreover, three basic types of evaporative coolers commonly used, including direct EC, indirect EC, and semi-indirect EC (ASHRAE, 2011; Xuan *et al.*, 2012a).

Different pads made of porous and water adsorbing materials have been used (Nenguwo, 2002; Olosunde *et al.*, 2009; Manuwa and Odey, 2012; Xuan *et al.*, 2012a). Several researchers have compared different cellulose cooling pads and their efficiency, and reported that slower air speed and the finer corrugation resulted in higher cooling (ASHRAE, 2001; Barzegar *et al.*, 2012). In addition to pads, storage rooms require fans with a total capacity of 0.3 $m^3.s^{-1}.ton^{-1}$ of product storage capacity that enables to adequately remove the field and the heat generation against a wide range of static pressures of fresh produce (Thompson *et al.*, 2002). The EC was reported to reduce the ambient air temperature from 38°C to about 12°C significantly (Anyanwu, 2004).

In Ethiopia, EC was used to preserve mangoes where the ambient temperature of 23 - 43°C, was reduced to 14.3 - 19.2°C, while the RH was increased from 16 - 79% to 70 - 82.4% (Tefera *et al.*, 2007). As a result, the shelf-life of the mangoes was doubled. Getinet *et al.* (2008) demonstrated in another multiple pad and single pad EC study in Ethiopia. The authors reported that the multiple pad reduced the ambient temperature by 5°C, and increased RH by 18% more than the single pad EC. Samira *et al.* (2013) reported that the shelf-life of different hot pepper varieties were increased under EC by more than 400% than ambient storage. In Nigeria, tomatoes and carrots preserved inside EC, the ambient air temperature dropped to 16-26°C from 26-32°C, and RH increased 33-88% from 18-31% that provided an increase in shelf-life by 14 days (Mogaji and Fapetu, 2011). In addition, a clay EC was developed in Nigeria (Chinenye, 2011) and it dropped the ambient temperature to 24-29°C from 32-40°C, while the RH rose from 40.3% to 90% preserved tomatoes for 19 days. Chinenye *et al.* (2013) also reported that an active EC reduced the temperature from 4-13°C, but RH increased to 96.8%. In India, Roy and Pal (1989) developed a low-cost zero energy EC chamber from locally available materials, resulting in the air temperature dropping to 10-15°C and RH increasing to 90%. Royston and Altman (1994) developed different EC chambers and stored bananas, mangoes, lime and guava that increased the shelf-life of the tropical fruit by 2-14 days more than ambient storage. In China, a variety of EC air conditioning equipment and systems were developed for different stake holders, including agricultural storage buildings (Xuan *et al.*, 2012b). Limited storage performance of the low-cost cold storage technologies might come from unevenly distributed moist air psychometrics properties. In spite of several studies on the application of EC for the preservation of fresh produce, there is inadequate research on the dynamics of airflow, heat, and mass transfer phenomena taking place inside forced air low-cost EC systems.

2.3 Low-cost CoolBot-air-conditioner

Recently, Boyette and Rohrbach (1993) developed the CoolBot-air-conditioner (CBAC) cooling system as a low-cost and forced-air by modification of the domestic air conditioner for fresh produce storage as shown in Figure 2.2 (CoolBot Installation Guide, 2015). CBAC is an electronic device that overrides room AC to reduce cooling temperature below the set point. According to Saran *et al.* (2013), it is a low-cost storage unit which can be transformed into a walk-in cooler with capability of reducing temperature to 4-5°C. Retention of freshness and marketability has been noted for cauliflower, cabbage, tomato and okra kept inside it (Saran *et al.*, 2013). In addition, it can reduced the temperature to 2°C and increases the shelf-life of the

fresh produce for 4-8 months (Kitinoja, 2013a). Several reports show that it is a promising technology to reduce the temperatures as low as 0°C (Kitinoja, 2013b; Adamczyk *et al.*, 2014). It has an overall cost of 90% less than the mechanical refrigerator system (Kitinoja, 2013a). In India, it has been used for potato storage at $1296/6MT and for onion in Ghana at $8790/6MT (Kitinoja, 2013a). Similar to EC, CBAC reported to be feasible in arid and semi-arid climates. However, no research conducted on the airflow pattern, heat, and mass transfer inside CBAC cold room.

Figure 2.2 CoolBot and the air conditioner installed inside the cold storage chamber

2.4 Rationale of CFD in Low-cost Cold Storage Micro-climate Dynamics Modelling

Recently, the computational fluid dynamics (CFD) has been progressively applied to the food processing industry (Norton and Sun, 2006; Ambaw *et al.*, 2013a). Norton and Sun (2006) reported that CFD modelling could replace expensive experimental runs and unit operations such as cooling, refrigeration, mixing and drying for the control and prediction of processing conditions. Hence, it could create a highly optimized platform for equipment design, storage design and cost effective production (Norton and Sun, 2006).

Heating and cooling are comprised of complex problem and process of fluid flow, heat and mass transfer occurring simultaneously that occur in food processing with 3-dimensions (Tijskens *et al.*, 2001). The real-time transfer of mass and energy challenges are solved through numerical modelling rather than the analytical approach (Nicolaï *et al.*, 2001b; Norton and Sun, 2006; de Baerdemaeker *et al.*, 2011; Ambaw *et al.*, 2013a). According to Nahor *et al.* (2005), understanding the air-velocity pattern, temperature, relative humidity and moisture distribution

in a cold room is very crucial for the designing of storage enclosures (Laguerre *et al.*, 2013). In forced air cold storages, heat transfer is by convection transfer (Laguerre *et al.*, 2013). The general transport equations (Navier Stokes) are principal to apply in the CFD application (Nicolaï *et al.*, 2001b; Verboven *et al.*, 2006; Versteeg and Malalasekera, 2007; Ambaw *et al.*, 2013a). In addition to Navier Stokes equation, diffusion and convective liquid particle transport models are important inside cold storage (Ambaw *et al.*, 2013a). The driving force for forced convection is pressure gradient (Tijskens *et al.*, 2001). As a consequence, the Navier Stokes equation to control volume *dx*dy*dz* on Cartesian Coordinates (i directions *i.e.* x (1), y (2) and z (3)) are applied for transport phenomena manipulation inside cold chambers (Versteeg and Malalasekera, 1995). The Navier Stokes equations, are designated by Equations 2.1 - 2.5:

General, Continuity equation:

$$\frac{\partial u}{\partial x} + \frac{\partial v}{\partial y} + \frac{\partial w}{\partial z} = 0 \tag{2.1}$$

General, Momentum Equation (for x, y and z directions, respectively):

$$\rho \frac{Du}{Dt} = -\frac{\partial p}{\partial x} + div(\mu\ grad\ u) + S_{Mx} \tag{2.2}$$

$$\rho \frac{Dv}{Dt} = -\frac{\partial p}{\partial y} + div(\mu\ grad\ v) + S_{My} \tag{2.3}$$

$$\rho \frac{Dw}{Dt} = -\frac{\partial p}{\partial z} + div(\mu\ grad\ w) + S_{Mz} \tag{2.4}$$

General, Energy equation:

$$\rho \frac{DE}{Dt} = -div(\rho U) + \left[\frac{\partial(u\tau_{xx})}{\partial x} + \frac{\partial(u\tau_{yx})}{\partial y} + \frac{\partial(u\tau_{zx})}{\partial z} + \frac{\partial(v\tau_{xy})}{\partial x} + \frac{\partial(v\tau_{yy})}{\partial y} + \frac{\partial(v\tau_{zy})}{\partial z} + \frac{\partial(w\tau_{xz})}{\partial x} + \frac{\partial(w\tau_{yz})}{\partial y} + \frac{\partial(w\tau_{zz})}{\partial z}\right] + div(k\ grad\ T) + S_E \tag{2.5}$$

Where:

u, *v* and *w* = the velocity vector of x, y and z Cartesian Coordinate, respectively ($m.s^{-1}$),

U = for average velocity vector as a function of (x, y, z, t) ($m.s^{-1}$),

T = the temperature of the fluid or product (ºC or ºK),

p = the atmospheric pressure (Pa),

ρ = the density of fluid or produce (kg.m^{-3}),

H = the enthalpy of the moving fluid or produce (J.kg^{-1}),

μ = the viscosity of fluid (kg.m^{-1}.s^{-1}),

S_{Mx}, S_{My}, S_{Mz} = the source terms in x, y and z coordinates, respectively (m^3.s^{-1}),

S_E = the energy source term (m^3.s^{-1}),

t = the flow time of fluid (s),

τ_{ij} = the stress component i (x, y, z) with j direction (Pa), and

k = the thermal conductivity of the produce or flowing fluid (W.m^{-1}.ºC^{-1}).

The above notions have five equations with different variables (*u*, *v*, *w*, *p*, *h*, *T, ρ)* and hence additional equations are required to solve the seven variable matrixes. Therefore, from thermodynamics equations the relation of density, temperature and pressure are required (Tijskens *et al.*, 2001). From the ideal gas equation, the following equations can be obtained (Equations 2.6 to 2.10):

$$\rho = \frac{pM}{RT} \tag{2.6}$$

$$C = \frac{\partial H}{\partial T} \tag{2.7}$$

$$H = C_{p,f}(T - T_0) \tag{2.8}$$

$$C_{p,f} = Y c_{p,w} + (1 - Y) C_{p,a} \tag{2.9}$$

$$\frac{\partial \rho Y}{\partial t} + \rho \frac{\partial (\rho u_i Y)}{\partial x_i} = \frac{\partial \rho}{\partial x_j} D \frac{\partial Y}{\partial x_i} \tag{2.10}$$

Where:

M = the molecular weight flowing fluid/gas (kg.mol^{-1}),

R = the universal gas constant (J.mol^{-1}.K^{-1}),

Y = the humidity ratio (kg$_{w.}$kg$_{air}^{-1}$),

$C_{p,w}$ = the specific heat capacity of water (J.kg^{-1}.°C^{-1}),

$C_{p,f}$ = the specific heat capacity of fluid (J.kg^{-1}.°C^{-1}),

$C_{p,a}$ = the specific heat capacity of air (J.kg^{-1}.°C^{-1}), and

D = the diffusivity (m^2.s^{-1}).

For constant specific heat capacity (C_p), changes in H and changes in T are linearly related. Since the velocity assumed to be of low magnitude in storage that the fluid is incompressible and the equations can be applied. The lumped model as indicated below can calculate the evaporation and/or condensation of moisture inside the experimental cold storage (Nahor *et al.*, 2005).

$$m = -\frac{\partial x}{\partial t} = h_m A_{spec}\left({\rho_p}^v - {\rho_a}^v\right) = \rho_a \frac{\partial r_a Y}{\partial t} + r_a \rho_a \frac{\partial (u_i Y)}{\partial x_i} - r_a \rho_a \frac{\partial}{\partial x_j} D \frac{\partial Y}{\partial x_i} \quad (2.11)$$

Where:

m = the moisture condensation or evaporation rate ($kg.m^{-3}.s^{-1}$),

x = the moisture content of product ($kg_w.m^{-1}$),

Y = the humidity ratio ($kg_w.kg_{air}^{-1}$),

h_m = the mass transfer coefficient ($m.s^{-1}$),

${\rho_a}^v$ = the density of water vapour in the air phase ($kg.m^{-3}$),

${\rho_p}^v$ = ther density of water vapour at equilibrium ($kg.m^{-3}$),

A_{spec} = the surface area of the particle ($m^2.m^{-3}$), and

r_a = the volume fraction of air (-).

Inside the cold store, the following model calculates the temperature of the stored fresh commodities (Nahor *et al.*, 2005):

$$\rho_p c_{p,p} \frac{\partial}{\partial t}\left(r_p T_p\right) = h_T A_{spec}\left(T_a - T_p\right) \frac{\partial (u_i Y)}{\partial x_i} - h_{fg} m + r_p q_p \quad (2.12)$$

Where:

r_p = the volume fraction of product (-),

T_p = the temperature of product (°C),

Ta = the temperature of air (°C),

h_T = the heat transfer coefficient ($W.m^{-2}.°C^{-1}$),

A_{spec} = the surface area of the particle ($m^2.m^{-3}$),

h_{fg} = the heat of evaporation/condensation ($J.kg^{-1}$),

q_p = the heat of respiration of the product ($W.m^{-1}$),

m = the moisture condensation or evaporation ($kg.m^{-3}.s^{-1}$), and

$C_{p,p}$ = the specific heat capacity of product ($J.kg^{-1}.°C^{-1}$).

Moreover, Nahor *et al.* (2005) reported that if variation in density could happen due to buoyancy, there would be two ways to solve the problem. The first, approach is Boussinesq approximation for small temperature differences. Where, β is thermal expansion coefficient ($°K^{-1}$), T and T_{ref} are instantaneous and reference temperature (°K), and ρ and ρ_{ref} are instantaneous and reference density, respectively. The second was when the temperature difference is very high and the fluid or cold air is treated as ideal gas, the density difference expressed by the following equation with the Wa is molecular weight of air ($kg.kmol^{-1}$).

$$\rho = \rho_{ref}\left[1 - \beta\left(T - T_{ref}\right)\right] \tag{2.13}$$

$$\rho = \frac{\rho_{ref} W_a}{RT} \tag{2.14}$$

Norton and Sun (2006) reported that to compromise the limitations of Navier Stokes equations in food processing, additional equations including models for porous media, eddy flow, non-Newtonian, and multiphase approaches used by several researchers. Forced airflow and water flow which are caused by baffles, fans, shelves and the food materials themselves are being considered as turbulent-flow (Norton and Sun, 2006). Therefore, the airflow in cold storage is characterized by turbulent, which is dependent on time and control volume (Nicolaï *et al.*, 2001b; Ambaw *et al.*, 2013a). Turbulence enhances the transfer rate, but pressure drop must be considered throughout food processing equipment designs, including those for fresh produce storage, handling and processing (Tijskens *et al.*, 2001). Hence, to incorporate the turbulence in the Navier Stokes equation, the popular approach of Reynolds Average Navier Stokes (RANS) equations are being used. According to Xu *et al.* (2002) and Nahor *et al.* (2005), standard *Kε* models are used for turbulent airflow modelling. The turbulent viscosity η_t is calculated based on eddy constant (C_η) in turbulent kinetic energy (*k)* through varying velocities, and eddy energy degeneracy rate (ε) (Nicolaï *et al.*, 2001b) as follows:

$$\eta_t = \rho C_\eta \frac{K^2}{\varepsilon} \tag{2.15}$$

Three different types of turbulent *K-ε* models including the Low Reynolds Number (LRN) *k-ε*, ordinary *K-ε*, and Renormalization Group (RNG) *k-ε* (Nicolaï *et al.*, 2001a; Tijskens *et al.*, 2001). According to Xu *et al.* (2002), the standard *K-ε* model is formulated as:

$$\frac{\partial(\rho k)}{\partial t} + \nabla(\rho u_i k) - \nabla\left[\left(\mu + \frac{\mu_T}{\delta_k}\right)\nabla k\right] = P + G - \rho\varepsilon \tag{2.16}$$

$$\frac{\partial(\rho\varepsilon)}{\partial t} + \nabla(\rho u_i \varepsilon) - \nabla\left[\left(\mu + \frac{\mu_T}{\delta_\varepsilon}\right)\nabla\varepsilon\right] = C_1 \frac{\varepsilon}{K}\left(P + C_3 max(G, 0)\right) - C_2 \rho \frac{\varepsilon^2}{K} \quad (2.17)$$

Where:

P = the shear production rate ($N.m^{-2}.s^{-1}$),

G = the turbulent generation rate ($N.m^{-2}.s^{-1}$),

k = the turbulent energy ($m^2.s^{-2}$),

ε = the turbulence dissipation rate ($m^2.s^{-3}$),

ρ = the density ($kg.m^{-3}$),

μ_T = the turbulent viscosity ($kg.m^{-1}.s^{-1}$),

μ = the air/fluid viscosity ($kg.m^{-1}.s^{-1}$),

C_1, C_2, C_3 = the standard k-ε model constants (dimensionless),

u_i = the air velocity of direction Xi ($m.s^{-1}$), and

t = the time (s).

For modelling the airflow of stored fruit and vegetables, attention will be given for multiple flow to be considered as separate phases (Tijskens *et al.*, 2001). In line with, diffusion equation used for water vapour mass fraction modelling in the wet-air (Nicolaï *et al.*, 2001b) and designated as follow:

$$\frac{\partial \rho X_a}{\partial t} + \frac{\partial}{\partial x_j}\rho u_j X_a = \frac{\partial}{\partial x_i}\rho D_a \frac{\partial}{\partial x_i} X_a + r'_a \quad (2.18)$$

Where:

Xa = the water vapour mass fraction, and

r'_a = the source/sink of water vapour (condensation, evaporation) ($kg.m^{-3}.s^{-1}$).

A mixed model approach is used in particle dispersions including water droplets, for drying moist particles, dispersion of disinfectants and solid liquid interactions (Nicolaï *et al.*, 2001b). The Lagrangian model which is derived from Newton's second law, is commonly used for modelling particle motion in fluids (Nicolaï *et al.*, 2001b; Tijskens *et al.*, 2001):

$$m_p \frac{du_{pi}}{dt} = Fi \quad (2.19)$$

Where:

m_p = stands for particle mass (kg),

u_{pi} = the velocity component of the particle (m.s^{-1}), and

Fi = the total force of the particle (N).

Nahor *et al.* (2005) summarized that the energy conservation equation of the cold stores consists of energy transfer from produce to fluid stream. Because of respiration heat, dissipated energy and heat of formation between the fresh produce and fluid interface determines the direction of heat and mass transfer (Nahor *et al.*, 2005) Moreover, Nahor *et al.* (2005) reported the importance of fans and the tube heat exchangers' modelling for a detailed insight into the transport phenomena.

In CFD simulation, the computational domain is divided into a number of grids (meshes) followed by solving the governing equations. Different types of discretization techniques applied, including finite difference, finite element and finite volume methods. Commonly, the finite volume approach used for postharvest studies (Tijskens *et al.*, 2001; Delele *et al.*, 2009; Ambaw *et al.*, 2013a). The more the number of grids of discrete points in the geometry, the more accurate the numerical analysis taking place (Ambaw *et al.*, 2013a; Defraeye *et al.*, 2014).

Initial and boundary conditions are very critical in modelling including CFD (Tijskens *et al.*, 2001; Ambaw *et al.*, 2013a). The initial values of the variables for CFD modelling should be provided, but particularly in biological systems, the difficulty is where the exact initials values are unknown. It could be estimated from the other parameters such as inlet air velocity and the geometry of the produce (Nicolaï *et al.*, 2001b). Effects of pressure resistance on the fan is always neglected, but should be considered for the air flow rate calculations (Nicolaï *et al.*, 2001b; Tijskens *et al.*, 2001).

2.5 Modelling of Airflow, Heat and Mass Transfer in Cold Stores

Low-cost EC and CBAC forced air cooling is used because of its efficiency, flexibility and low cost (Allais and Alvarez, 2001). Recently, several researchers used numerous models to simulate the real-time problem of airflow pattern, energy and mass movement through cold/refrigerated storage systems (Ambaw *et al.*, 2013a; Defraeye *et al.*, 2013b; Defraeye *et al.*, 2014). De Baerdemaeker *et al.* (2011), Ambaw *et al.* (2013a) and Defraeye *et al.* (2014) noted that there has been great interest in using mathematical modelling for the optimization of postharvest cooling system operations, design, processing, and food engineering with multi-

scale modelling approaches. Moreover, several studies demonstrated the use of CFD for the modelling of cold storage, refrigerated storage, drying, and building ventilation (Saneinejad *et al.*, 2011; Moonen *et al.*, 2012; Saneinejad *et al.*, 2012; Ambaw *et al.*, 2013a; Ambaw *et al.*, 2013b, 2013c; Defraeye *et al.*, 2013a; Ho *et al.*, 2013b; Defraeye, 2014; Defraeye *et al.*, 2014). According to Akdemir *et al.* (2013) two different cold storage models using the CFD tool, specifically temperature and RH distribution were captured by standard turbulent k-ε model approach. Chourasia and Goswami (2007b) simulated the effects of dimensions on potatoes packed in sacks, and positions of energy movement with the help of CFD tools. Transient temperature and the analytical temperature were used for validation and a difference of 1.4±0.98°C was found. Moreover, Xu *et al.* (2002) and Wang and Sun (2003) noted that foods including onion, potato and grain stored in cold stores had been considered as porous media for energy and mass transfer simulations. Additionally, for transport phenomena with porous media approach, the prediction of specific physical parameters and analysis with CFD modelling was described as possible by (Wang and Sun, 2003; Nahor *et al.*, 2005) for the simulation of porous, stored food material.

According to Andersson *et al.* (2012), multiphase heat and mass transfer modelling is based on Sherwood (Sh) and Nusselt dimensionless parameters (Nu). The interaction between the fluid flowing including cold air and the particles are heating, cooling, evaporation, and condensation. For the small net flow to or from solid particle, mass transfer between the solid and flowing fluid estimated by film model and described as follow:

$$N_n = k_{c,n}(C_{n,s} - C_{n,bulk}) \tag{2.20}$$

Where:

N_n = the mass flux (mol.m^{-2}.s^{-1}),

$C_{n,s}$ = the concentration of species n on the surface,

$C_{n,bulk}$ = the concentration in the fluid bulk surrounding the particle, and

$k_{c,i}$ = the convective mass-transfer coefficient (m.s^{-1}).

$$\mathrm{Sh} = \frac{\mathrm{K_{c,i}d_p}}{\mathrm{D_i}} = 2 + 0.6\mathrm{Re_d}^{1/2}\mathrm{Sc}^{1/3} \tag{2.21}$$

Where:

Sh = the Sherwood number (dimensionless),

Re_d = the local Reynolds number (dimensionless),

d_p = the characteristics length (m),

D_i = the diffusivity coefficient ($m^2.s^{-1}$), and

Sc = the Schmidt number (dimensionless).

Heat transfer described in a similar way using the Nusselt number, Nu:

$$Nu = \frac{hd_p}{\lambda} = 2 + 0.6Re_d^{1/2}Pr^{1/3} \quad (2.22)$$

Where:

Nu = the Nusselt number (dimensionless),

h = the local convection heat transfer coefficient ($W.m^{-2}.K$),

d_p = the characteristic length (m),

Pr = Prandtl number (dimensionless),

λ = the thermal conductivity coefficient ($W.m^{-1}.K$), and

Re_d = the local Reynolds number (dimensionless).

Heat balance of a particle is given as:

$$m_p C_p \frac{dT_p}{dt} = hA_p\left(T_{bulk} - T_p\right) + \frac{dm_p}{dt}h_{fg} + R\Delta H + A_p\varepsilon_p\sigma\left(T^4{}_{surr} - T^4{}_p\right) \quad (2.23)$$

$$\dot{m}_k = \frac{\partial(\alpha_k\rho_k)}{\partial t} + \frac{\partial(\alpha_k\rho_k u_{i,k})}{\partial x_i} \quad (2.24)$$

Where:

m_p = the mass of the particle (kg),

h_{fg} = the enthalpy of evaporation (kJ),

R = the reaction rate (s^{-1}),

h = the convection heat transfer coefficient ($W.m^{-2}.K$),

ΔH = the change in reaction enthalpy (kJ),

A_p = surface area of the particle (m^{-2}),

$\dot{m}_k$ = the mass transfer from/to phase k per unit volume and unit time,

α_k = the volume fraction of a fluid in multiphase flows (dimensionless),

ρ_k = the density of materials at the state of phase k ($kg.m^{-3}$),

k = the phase state of the material (dimensionless),

$u_{i,k}$ = the overall velocity of fluid particles for phase k ($m.s^{-1}$), and

t = the unit time (s).

To date, for a low Reynolds number and laminar flow, Lattice Boltzmann scheme model suggested being a substitute for CFD modelling (van der Sman, 2008; Ambaw *et al.*, 2013a). Advanced applied mathematics is used in the governing equations of CFD modelling (Norton and Sun, 2006; Versteeg and Malalasekera, 2007). The readiness of 3-D applications with CFD tools assist in the use of a multi scale modelling approach for postharvest cold chain management systems (Ambaw *et al.*, 2013a). Foster *et al.* (2005) and (Norton and Sun, 2006) demonstrated that large-scale modelling could probably take a longer time for computation, and for detailed solutions. Therefore, at the pre-processing and solving stage, reducing the modelling to several computational models is crucial for coping with a CFD package. Similarly, Ho *et al.* (2010) compared 2-D and 3-D models and recommended a proper 2-D as preferable for saving computing costs and time, while still producing useful results, which are accurate enough for a cold storage house modelling. While reduced models have been reasonably successful, the solution quality is under question for 1-D and 2-D approaches (Norton and Sun, 2006). As such, an appropriate selection of designs and variables is necessary for modelling in food storage systems (Lukasse *et al.*, 2007).

Several of the fundamental codes of CFD packages include FLUENT, CFX, PHONICS, FLOW3D, STAR-CD (Versteeg and Malalasekera, 1995, 2007). All CFD codes share three common crucial steps for computing CFD modelling analysis: namely pre-processors, solver, and post-processor (Versteeg and Malalasekera, 1995, 2007; Ambaw *et al.*, 2013a).

Pre-processing is a step whereby fundamental problems are recognized and defined (Ambaw *et al.*, 2013a). Moreover, the creation of the geometry of interest, and compilation of a grid or mesh creation, with fine divisions and without overlapping mesh cells, under the control volume are developed and generated to realize a specific point in space under the modelling boundary conditions (Versteeg and Malalasekera, 1995). In addition, settings of the physical and chemical phenomena, boundaries, solving techniques, physical parameters and governing equation selections made with pre-processor coding (Ambaw *et al.*, 2013a). According to Norton and Sun (2006), the grids deliver the discretization of the leading equation, and are therefore the 'road map' for precision forecasting of the transport phenomena in fluid flow. Furthermore, flow types, direction, geometry, and state of flow identification done at the pre-processing step (Versteeg and Malalasekera, 1995; Ambaw *et al.*, 2013a).

The Solver step is the iterative solving of different numerical solution techniques of the set of discretized equations (Delele *et al.*, 2012). For precise and accurate solutions, advanced degree computational equations are sufficient (Defraeye *et al.*, 2010; Ambaw *et al.*, 2013a). At this stage, the control volume is also decided (Versteeg and Malalasekera, 1995).

The post-processor step is the third element of CFD modelling where the solution output is solved, visualized and interpreted (Versteeg and Malalasekera, 1995). This stage permits simple, abstract and important parameters that have practical meaning to understand the question of the problem (Ambaw *et al.*, 2013a). Consequently, the output includes advanced graphics, isosurfaces, slices, vectors, streamlines, animations, contours, and many others (Versteeg and Malalasekera, 1995; Ambaw *et al.*, 2013a). Both the graphics and quantification analysis help to visualize and choose the solutions from the numerical modelling (Foster *et al.*, 2005; Ambaw *et al.*, 2013a), and hence solution interpretation is a vital aspect of CFD modelling. (Foster *et al.*, 2005); Norton and Sun (2006) reported that interpreting the solution of the CFD package includes visualization, contour vector, line plot, animated flow and other parameters.

For the model's quality and accuracy, validation is crucial. Hence, for successful CFD modelling, the accurate validation of numerical model outcomes with experimental results is crucial for the model's validity (Norton and Sun, 2006). Several researchers have mentioned that validation was achieved by manipulating specific experimental data, including temperature, air-velocity, and RH distribution, and indirectly by the measurement of energy change and pressure deficit (Ferrua and Singh, 2008). The covariance comparison of analytical errors is very important for validation of the models (Ambaw *et al.*, 2014), as are estimated parameters, including R^2 and mean percentage of errors (Ambaw *et al.*, 2014). Applications of different CFD models for fresh produce is summarized in Table 2.1.

Table 2.1 Applications of different Models and CFD tools for fresh produce storage modelling

	Software	Cold storage and descriptions	Boundary conditions	Validation and method	Author/s
CFD, Turbulence K-ε	ANSYS14.0	Simulated two cold storages spatial distribution of temperature and the RH	Fluid inlet-surface, outlet-Surface, and walls-solid, proof against flow of fluid	Descriptive statistics comparison of the two stores for T and RH	Akdemir *et al.* (2013)
CFD, RANS, SST k- ε model	ANSYS13.0	Super-vent and Ecopack packaging evaluated for cooling performance	Top, bottom, fruit, cardboard, and plastic containers surfaces, upstream-downstream of the containers	Temperature profiles	Defraeye *et al.* (2013a)
CFD, RANS, k– ε, k– ω, RSM	ANSYS12.0	CFD application in postharvest and food process engineering with spherical foods	Boundary layer modelling with wall functions Sphere surface	Fluid-flow and scalar exchanges evaluated for several physical variables	Defraeye *et al.* (2013c)
3-D CFD , RANS	ANSYS13.0	Air-flow, heat transfer, vented packaging, explicit geometries, and turbulence property distributions	$-17.8^{o}C \leq Ta \leq 37.8^{o}C$, Inlet and outlet boundary conditions of the cold air	Air velocity, pressure drop and temperature were monitored for citrus storage	Delele *et al.* (2013a)
3-D CFD, Forchheimer Equation	ANSYS13.0	Air-flow and heat transfer vented packaging system with vent % (1, 3, 5, 7, 9, 11, 20 and 100%)	Box and product surfaces as no slip wall boundary	-	Delele *et al.* (2013b)
3-D CFD model	ANSYS13.0	CFD study of packed table grapes transport phenomena characteristics (energy, momentum, mass)	Non-perforated plastic liner, porous jump boundary as fan boundary	Inside fruit Temperature and RH	Delele *et al.* (2013c)
CFD 3-D & 2-D	-	Velocity of air and temperature distribution in refrigerated storage	velocity at outlet, planes symmetry, solid surface; Temperature outlet, surfaces floor, wall, ceiling	2D and 3D velocity and temperature compared to each other	Ho *et al.* (2013a)
CFD, 3-D, standard k– ε	CFX4.4	Air-flow, heat and mass transfer in empty and loaded cold storages	Inner walls,	Velocity measurements, air and product temperature	Nahor *et al.* (2005)

RANS=Reynolds-Averaged-Stokes; SST=Shear Stress Transport; RSM= Reynolds-Stress- Model.

2.6 Limitations of CFD modelling for the Low-cost Cooling Technologies

Although CFD modelling has been used in refrigerated storage, few researchers have used it for EC of buildings and greenhouses (Adanez *et al.*, 2012). Accordingly, Montazeri *et al.* (2015) used it to study the performance of EC of buildings cooled with water spray. Adanez *et al.* (2012) applied CFD modelling for greenhouse fan system to simulate the micro-environment conditions, water consumption, fogging, energy consumption and airflow. Moreover, Cui *et al.* (2014) studied CFD modelling and the results of a dew point evaporative air conditioner. In addition, the Eulerian-Lagrangian CFD model was implemented for flows including several phases, such as microorganisms in the air, vapour, and powders (Norton and Sun, 2006; Cui *et al.*, 2014). The Eulerian concept is only valid for particle sizes present in the airflow of about 1µm, in the continuous phase, while the Lagrangian use of a random flight model of the particles (water droplets as discrete phase) near the boundary region (Cui *et al.*, 2014).

So far, airflow, heat and mass transfer modelling extensively studied for mechanical refrigerated storage, with the assistance of CFD models (Ambaw *et al.*, 2013a). However, there is limited research for modelling of the low-cost EC and CBAC cold storage systems, for airflow pattern, heat and mass transfer for fresh produce. The CFD tools reported to be powerful enough, to accurately simulate the transport phenomenon dynamics taking place inside the cold storage and be reproducible. The CFD tools are also arguably useful for the design of storages including EC and CBAC. Therefore, CFD tools could be appropriate, when studying the airflow pattern, heat and mass transfer dynamics of the forced air low-cost cooling technologies.

2.7 Instrumentation in Advancing Monitoring Micro-environment in Cold Stores

Studman (2001) reviewed that computer and electronics applications are highly essential and utilized by postharvest industry to monitor micro-climate, quality, grading, inventory, and postharvest management of the stored fresh produce. Grubben and Keesman (2015) reported that CFD simulation of agricultural fresh produce cold storage facilities (in particular) is very crucial for monitoring of the produce quality and storability. Well ventilated, designed and functional of postharvest handling facilities (*i.e.* cold store, refrigerated truck, packaging house) provides required fresh air and removes airborne contaminants; of which the real time properties at different spots can be recorded with the help of electronics and computer programs (Zong, 2013). Raghavan and Gariepy (1984) reported that application of several sensors and

instrumentations for storage system optimization leads to reduction of produce loss under cold storage systems for fresh produce.

2.8 Instrumentation in Fresh Produce Quality Prediction

Grubben and Keesman (2015) reported that CFD simulation is very crucial for prediction of the changes in produce quality and their shelf-life. The authors recommended that the parameters including CO_2, ethylene, sugar and many other should be covered by the spatial distribution CFD models too. It could have elaborated to have an insight of real time produce quality during storage or transportation and air dynamics inside stores. Moreover, Wang *et al.* (2006) reported that wireless sensors including for real time air dynamics monitoring and optimization for agricultural food industry are vital. In general, literature shows that there will be need for research focus on air dynamics and agricultural produce quality inside controlled storage chambers (Ugwuishiwu *et al.*, 2014). In this regard, new electronics and computer technologies including instrumentation and computer software should be applied to follow real time changes in micro-climate environment near fresh produce and their quality changes.

2.9 Instrumentation to Generate Realistic Empirical Data for Modelling Micro-environment and Quality Changes

Quality assurance of agricultural produce utilizes computer and electronics which was reported to be realistic enough to model the data acquisitioned by sensors (El Barbri *et al.*, 2008). Moreover, Martins *et al.* (2008) indicated that for monitoring diagnose and shelf-life and quality control of fresh produce, multivariate instrumentations, sensors, and complex data mining systems are crucial for fresh produce storage manipulations throughout the cold chain supply.

2.9.1 Modelling quality changes of fresh produce stored in cold storage systems

There is an increasing demand for fruit and vegetables to feed the ever increasing world population. According to Sloof *et al.* (1996), consumers are looking for good quality, fresh produce through the supply chain. Quality changes, including physiological, microbiological, physical and biochemical happen during postharvest cold storage (Laguerre *et al.*, 2013). Moreover, according to Laguerre *et al.* (2013), the quality of fresh produce can be lost if non-uniform temperature and relative humidity distribution occurs, in cold storage operations. Sloof

et al. (1996) emphasised that quality is becoming an increasingly important marketing factor, both for producers and for consumers, making the management of quality essential. Therefore, it is important to have tools to control, and to predict the quality of fruit and vegetables, as well as being able to cope with the ever changing consumer needs (van Boekel, 2010). To understand the postharvest physiological behaviour of fresh produce, Abbott (1999) and van Boekel (2010) believe that a knowledge of the physiological, physico-chemical and biochemical processes, and their interactions are crucial. Primarily, the development of a generic model and the selection of appropriate mathematical models is necessary to govern the physical process that occurs at their interface (Sloof *et al.*, 2001; Tijskens *et al.*, 2001). In addition, appropriate and valid mathematical models can be selected from thousands of models and applied for quality modelling (Tijskens *et al.*, 2001; van Boekel, 2010). Physical, chemical, and biochemical factors are intrinsic factors, however extrinsic factors caused by food supply chain unit operations and affecting food quality, can be modelled (van Boekel, 2010). The parameters of the models, and the relationships which come out of the modelling, could be used to envisage, plan, and improve the quality and excellence of foodstuffs, including fruit and vegetables (van Boekel, 2008). The models should not be over parameterized for the sake of simplicity (Tijskens *et al.*, 2001). For instance, the effects of temperature on the quality and length of the shelf-life of fruit and vegetables is critical and hence kinetic reactions that are affected by temperature might be modelled by the Arrhenius model (Tijskens *et al.*, 2001). Measuring and modelling multiple reactants and/or products' effects simultaneously is applicable in food systems, and can be referred to as multi-response modelling (Tijskens *et al.*, 2001; de Baerdemaeker *et al.*, 2011). This approach is effective for extracting information from data, but it needs special determinants with specific packages (Sablani *et al.*, 2007). Schouten *et al.* (2007) modelled the colour and firmness of stored tomato from green mature to the red ripe stage, with time.

General modelling to determine the maintenance of vegetables quality can be described as either in a static state or a dynamic state (Tijskens and Polderdijk, 1996). Quality modelling in a static form takes into account constant conditions, including temperature. On the other hand, dynamic quality modelling considers the non-constant conditions including variations in temperature, acceptance limits and initial quality of the produce (Tijskens and Polderdijk, 1996). The models take into consideration the fresh produce's keeping quality, including the physical, chemical, physic-chemical and biochemical properties (Tijskens and Polderdijk, 1996). The zero order linear kinetics models apply for the static category as described by Equation 2.25.

$$\frac{dQ}{dt} = -k \quad (2.25)$$

Where

Q = the quality (amount, intensity, level, a) (qua^2),

k = the quality reaction rate ( )^1, and

t = the time (time).

The static temperature linear equation shown below:

$$Q = Q_O - kt \quad (2.26)$$

Where

Q_0 = the initial quality value of Q

The keeping quality (KQ) determined when the Q> Q_{ml}, then the time taken is the shelf-life time, zero order reaction shown below:

$$KQ = \frac{Q_0 - Q_{ml}}{k} \quad (2.27)$$

Where

KQ = the keeping quality or shelf-life (time), and

Q_{lm} = the quality limit for the product (qua^2).

2.9.2 Exponential kinetics

Most common natural processes encounter first order reactions and the basic relevant differential equation are shown below:

$$\frac{dQ}{dt} = -KQ \quad (2.28)$$

At constant temperature:

$$Q = Q_0 e^{-kt} \quad (2.29)$$

The shelf-life could be derived for the Q reaches Q_{lm} as follow:

$$KQ = \frac{\log_e(\frac{Q_0}{Q_{lm}})}{k} \quad (2.30)$$

Temperature dependent quality parameters could be modelled by Arrhenius equation below:

$$K = K_{ref}.e^{\frac{E0}{R}(\frac{1}{T_{ref}}-\frac{1}{T_{abs}})} \quad (2.31)$$

Where:

K_{ref} = the quality reaction rate at reference temperature,

E_a = the activation energy (J.mol^{-1}),

R = the universal gas constant (J.mol^{-1}.k^{-1}),

T_{ref} = the reference temperature [K or °C), and

T_{abs} = the absolute temperature (K or °C).

Dynamic modelling with constant boundary conditions could be modelled as follows:

$$KQ_{st} = KQ_{ref} - \frac{\int_o^t k(T(t))dt}{k(T_{st})} \quad (2.32)$$

Where:

KQ_{st} = the quality keeping at standard temperature (qua^2), and

KQ_{ref} = the quality keeping at standard temperature (qua^2).

Dynamic modelling with changing variable boundary conditions modelled with the following model:

$$\mathrm{KQ_{dyn}} = \log_e \frac{(\mathrm{Q_{b0}} - \int_{t=0}^{t} \frac{-\log_e(\frac{\mathrm{Qmo}}{\mathrm{Qml}})\mathrm{k(T)(t)Qb(t)dt})}{\mathrm{Qbl}}}{\log_e(\frac{\mathrm{Qmo}}{\mathrm{Qml}})\mathrm{k(T_{st})}} \quad (2.33)$$

Where:

KQ_{dyn} = the quality keeping at changing temperature (qua^2),

Q_{mo} = Initial quality (qua^2),

Q_{ml} = the quality limit (qua^2), and

Qb = the quality of particular batch (qua^2).

Tomato texture and colour are the most important quality parameters for consumers buying fresh tomatoes (Batu, 2004). Tomato ripening stages include mature-green, breaker, pink-orange, orange-red, red table ripe and dark-red overripe, graded 1 to 6, respectively (Kasmire *et al.*, 1975; USDA, 1976; Cantwell and Kasmire, 2002). The tomato's skin colour was

measured by Minolta Chromometer L*a*b and the texture by the Instron Universal Testing Machine (Batu, 2004). Batu (2004) categorised the firmness and colour values of tomatoes, and the resulting quality. Accordingly, the firmness values 1.28 $N.mm^{-1}$ is good for marketing and salad processing, while a value above 1.46 $N.mm^{-1}$ is very firm and marketable. In addition, the Minolta a*/b* of 0.6-0.95 represented a highly marketable quality.

2.9.3 Integrated modelling of cold storage and postharvest treatments

Shumye *et al.* (2014) noted that the use of a combination of different treatments including chlorine solution, $CaCl_2$ and 2, 4- Dichlorophenoxyacetic acid, and polyethylene sheet packaging followed by storage under EC, improved the storability and marketability percentages of cactus fruit. Oke *et al.* (2013) suggested that to contribute to food security, research should focus on integrating pre- and postharvest treatments, for an environmentally friendly, and cost effective way to improve the quality and yield of fresh produce.

2.10 Conclusions and Future Challenges

Cooling is vital for food preservation, during fresh produce transportation and storage and, thereby, for reducing postharvest loss. Appropriate postharvest cooling technologies are important to overcome the challenge of heat and mass transfer facing the cold supply chain of fresh produce. Given the trends in agricultural sector development in the African continent, low-cost and environmentally friendly postharvest cooling technologies are vital to meet the current demand by the farmers in developing countries (*i.e.* Africa). The EC and CBAC are among the low-cost cold storage technologies identified and found to be affordable to fresh producer farmers. Some of these technologies are highly suitable and appropriate for application in arid and semi-arid sub-Saharan African regions in terms of capital cost, infrastructure, maintaining local climate conditions, and there significantly reducing postharvest loss. Non-uniform airflow, temperature and relative humidity distributions are important conditions for fresh produce inside low-cost cold stores. Hence, modelling of airflow pattern, heat, and mass transfer, taking place inside a typical cooler could and uniformity be a novel insight to understanding on what is happening in real-time. Modelling also contributes to further modify and improve store designs, stacking patterns, and shelf-life determination of a stored fresh produce. In addition, with the help of new computer programmes, data mining, monitoring, and processing, instrumentation and sensors for monitoring, diagnose and control

of low-cost cold storage is paramount for fresh produce quality and shelf-life extension. In summary, literature shows that understanding the effects of storage systems on the fresh produce shelf-life and quality is important. In addition, it is evident from literature that there is limited information available on CFD modelling of micro-environment in low-cost sustainable cooling technologies. Hence, understanding of airflow, temperature and moisture distribution inside the low-cost cold stores are important and further investigated to optimize the design of the existing EC, CBAC and EC+CBAC and, thereby, manage the maintenance of fresh produce quality. Consequently, the heat and mass transfer analysis inside EC, CBAC and EC+CBAC stores could be used to estimate the addition and/or removal of moisture and heat from stored fresh produce.

2.11 Acknowledgements

We would like to warmly acknowledge the Federal Ministry of Education, Ethiopia. South African National Research Foundation (NRF – TWAS) and the host institute, University of Kwa-Zulu Natal.

2.12 References

Abbott, JA. 1999. Quality measurement of fruits and vegetables. *Postharvest Biology and Technology,* 15**,** 207-225.

Adamczyk, WP, Klimanek, A, Białecki, RA, Węcel, G, Kozołub, P and Czakiert, T. 2014. Comparison of the standard Euler–Euler and hybrid Euler–Lagrange approaches for modeling particle transport in a pilot-scale circulating fluidized bed. *Particuology*, 15**,** 129-137.

Adanez, J, Abad, A, Garcia-Labiano, F, Gayan, P and De Diego, LF. 2012. Progress in Chemical-Looping Combustion and Reforming technologies. *Progress in Energy and Combustion Science,* 38**,** 215-282.

Ait-Oubahou, A. 2013. Postharvest technologies in sub-Saharan Africa: status, problems and recommendations for improvements. *In:* Abdullah, H and Latifah, MN, eds. Proc. 7th International Postharvest Symposium, 1273-1282. Acta Horticulture, International Society for Horticultural Science (ISHS), Leuven, Belgium.

Akdemir, S, Ozturk, S, Edis, FO and Bal, E. 2013. CFD Modelling of Two Different Cold Stores Ambient Factors. *IERI Procedia,* 5**,** 28-40.

Allais, I and Alvarez, G. 2001. Analysis of heat transfer during mist chilling of a packed bed of spheres simulating foodstuffs. *Journal of Food Engineering,* 49**,** 37-47.

Ambaw, A, Delele, MA, Defraeye, T, Ho, QT, Opara, LU, Nicolai, BM and Verboven, P. 2013a. The use of CFD to characterize and design post-harvest storage facilities: Past, present and future. *Computers and Electronics in Agriculture,* 93**,** 184-194.

Ambaw, A, Verboven, P, Defraeye, T, Tijskens, E, Schenk, A, Opara, UL and Nicolai, BM. 2013b. Effect of box materials on the distribution of 1-MCP gas during cold storage: A CFD study. *Journal of Food Engineering,* 119**,** 150-158.

Ambaw, A, Verboven, P, Defraeye, T, Tijskens, E, Schenk, A, Opara, UL and Nicolai, BM. 2013c. Porous medium modeling and parameter sensitivity analysis of 1-MCP distribution in boxes with apple fruit. *Journal of Food Engineering,* 119**,** 13-21.

Ambaw, A, Verboven, P, Delele, MA, Defraeye, T, Tijskens, E, Schenk, A, Verlinden, BE, Opara, UL and Nicolai, BM. 2014. CFD-Based Analysis of 1-MCP Distribution in Commercial Cool Store Rooms: Porous Medium Model Application. *Food and Bioprocess Technology,* 7**,** 1903-1916.

Andersson, B, Andersson, R, Håkansson, L, Mortensen, M, Sudiyo, R and Van Wachem, B. 2012. *Computational fluid dynamics for engineers.* Cambridge University Press, UK.

Anyanwu, EE. 2004. Design and measured performance of a porous evaporative cooler for preservation of fruits and vegetables. *Energy Conversion and Management,* 45**,** 2187-2195.

ASHRAE. 2001. Fundamentals. *American Society of Heating, Refrigerating and Air Conditioning Engineers, Atlanta.* Inc., Atlanta, GA.

ASHRAE. 2011. ASHRAE/USGBC/IES standard 189.1-2011. Standard for the design of high-performance green buildings. *American Society of Heating, Refrigerating and Air-Conditioning Engineers.* Inc., Atlanta, GA.

Barzegar, M, Layeghi, M, Ebrahimi, G, Hamzeh, Y and Khorasani, M. 2012. Experimental evaluation of the performances of cellulosic pads made out of Kraft and NSSC corrugated papers as evaporative media. *Energy Conversion and Management,* 54**,** 24-29.

Batu, A. 2004. Determination of acceptable firmness and colour values of tomatoes. *Journal of Food Engineering,* 61**,** 471-475.

Bom, GJ, Foster, R, Dijkstra, E and Tummers, M. 1999. *Evaporative air-conditioning: applications for environmentally friendly cooling.* World Bank Publishing., Washington DC, USA.

Boyette, MD and Rohrbach, RP. 1993. A low-cost, portable, forced-air pallet cooling system. *Applied engineering in agriculture,* 9**,** 97-104.

Cantwell, MI and Kasmire, RF. 2002. Postharvest handling systems: fruits and vegetables. *In:* Kader, AA (ed.) *Postharvest technology of horticultural crops.* Cha. 33, 407-422. University of California Agriculture and Natural Resources, University of California, USA.

Chinenye, NM. 2011. Development of clay evaporative cooler for fruits and vegetables preservation. *Agricultural Engineering International: CIGR Journal,* 13**,** 1-8.

Chinenye, NM, Manuwa, SI, Olukunle, OJ and Oluwalana, IB. 2013. Development of an active evaporative cooling system for short-term storage of fruits and vegetable in a tropical climate. *Agricultural Engineering International: CIGR Journal,* 15**,** 307-313.

Chourasia, MK and Goswami, TK. 2007. Steady state CFD modeling of airflow, heat transfer and moisture loss in a commercial potato cold store. *International Journal of Refrigeration-Revue Internationale Du Froid,* 30**,** 672-689.

Coolbot Installation Guide. 2015. *Build Your Own Walk In Cooler with CoolBot Installation.* Store It Cold LLC, USA.

Cui, X, Chua, KJ and Yang, WM. 2014. Numerical simulation of a novel energy-efficient dew-point evaporative air cooler. *Applied Energy,* 136**,** 979-988.

De Baerdemaeker, J, Nicolai, BM, Delele, MA and Verboven, P. 2011. Multiscale Modelling of Postharvest Storage of Fruit and Vegetables in a Plant Factory Context. Preprints of the 18th IFAC World Congress, 616-620. International Federation of Automatic Control (IFAC), Milano, Italy.

Defraeye, T. 2014. Advanced computational modelling for drying processes: a review. *Applied Energy,* 131**,** 323-344.

Defraeye, T, Blocken, B, Koninckx, E, Hespel, P and Carmeliet, J. 2010. Computational fluid dynamics analysis of cyclist aerodynamics: Performance of different turbulence-modelling and boundary-layer modelling approaches. *Journal of biomechanics,* 43**,** 2281-2287.

Defraeye, T, Lambrecht, R, Delele, MA, Tsige, AA, Opara, UL, Cronje, P, Verboven, P and Nicolai, B. 2014. Forced-convective cooling of citrus fruit: Cooling conditions and energy consumption in relation to package design. *Journal of Food Engineering,* 121**,** 118-127.

Defraeye, T, Lambrecht, R, Tsige, AA, Delele, MA, Opara, UL, Cronje, P, Verboven, P and Nicolai, B. 2013a. Forced-convective cooling of citrus fruit: Package design. *Journal of Food Engineering,* 118**,** 8-18.

Defraeye, T, Verboven, P, Ho, QT and Nicolai, B. 2013b. Convective heat and mass exchange predictions at leaf surfaces: Applications, methods and perspectives. *Computers and Electronics in Agriculture,* 96**,** 180-201.

Defraeye, T, Verboven, P and Nicolai, B. 2013c. CFD modelling of flow and scalar exchange of spherical food products: Turbulence and boundary-layer modelling. *Journal of Food Engineering,* 114**,** 495-504.

Delele, MA, Defraeye, T, Tijskens, E, Schenk, A, Nicolai, B, Ambaw, A and Verboven, P. 2012. CFD Based Analysis of the 3D Spatial and Temporal Distribution of 1-Methylcyclopropene in Apple Fruit Storage. 1st International Symposium on CFD Applications in Agriculture, 165-170.

Delele, MA, Ngcobo, MEK, Getahun, ST, Chen, L, Mellmann, J and Opara, UL. 2013a. Studying airflow and heat transfer characteristics of a horticultural produce packaging system using a 3-D CFD model. Part I: Model development and validation. *Postharvest Biology and Technology,* 86**,** 536-545.

Delele, MA, Ngcobo, MEK, Getahun, ST, Chen, L, Mellmann, J and Opara, UL. 2013b. Studying airflow and heat transfer characteristics of a horticultural produce packaging system using a 3-D CFD model. Part II: Effect of package design. *Postharvest Biology and Technology,* 86**,** 546-555.

Delele, MA, Ngcobo, MEK, Opara, UL and Meyer, CJ. 2013c. Investigating the Effects of Table Grape Package Components and Stacking on Airflow, Heat and Mass Transfer Using 3-D CFD Modelling. *Food and Bioprocess Technology,* 6**,** 2571-2585.

Delele, MA, Schenk, A, Tijskens, E, Ramon, H, Nicolai, BM and Verboven, P. 2009. Optimization of the humidification of cold stores by pressurized water atomizers based on a multiscale CFD model. *Journal of Food Engineering,* 91**,** 228-239.

El Barbri, N, Llobet, E, El Bari, N, Correig, X and Bouchikhi, B. 2008. Application of a portable electronic nose system to assess the freshness of Moroccan sardines. *Materials Science and Engineering,* C-28**,** 666-670.

Ferrua, MJ and Singh, RP. 2008. A nonintrusive flow measurement technique to validate the simulated laminar fluid flow in a packed container with vented walls. *International Journal of Refrigeration-Revue Internationale Du Froid,* 31**,** 242-255.

Foster, AM, Madge, M and Evans, JA. 2005. The use of CFD to improve the performance of a chilled multi-deck retail display cabinet. *International Journal of Refrigeration-Revue Internationale Du Froid,* 28**,** 698-705.

Getinet, H, Seyoum, T and Woldetsadik, K. 2008. The effect of cultivar, maturity stage and storage environment on quality of tomatoes. *Journal of Food Engineering,* 87**,** 467-478.

Grubben, NLM and Keesman, KJ. 2015. Modelling ventilated bulk storage of agromaterials: A review. *Computers and Electronics in Agriculture,* 114**,** 285-295.

Gustavsson, J, Cederberg, C, Sonesson, U, Van Otterdijk, R and Meybeck, A. 2011. Global food losses and food waste: extent, causes and prevention. Study conducted for the International Congress SAVE FOOD at Interpack201, 1-38. FAO, Düsseldorf, Germany.

Hao, XL, Zhu, CZ, Lin, YL, Wang, HQ, Zhang, GQ and Chen, YM. 2013. Optimizing the pad thickness of evaporative air-cooled chiller for maximum energy saving. *Energy and Buildings,* 61**,** 146-152.

Ho, QT, Carmeliet, J, Datta, AK, Defraeye, T, Delele, MA, Herremans, E, Opara, L, Ramon, H, Tijskens, E, Van Der Sman, R, Van Liedekerke, P, Verboven, P and Nicolai, BM. 2013a. Multiscale modeling in food engineering. *Journal of Food Engineering,* 114**,** 279-291.

Ho, QT, Carmeliet, J, Datta, AK, Defraeye, T, Delele, MA, Herremans, E, Opara, L, Ramon, H, Tijskens, E, Van Der Sman, R, Van Liedekerke, P, Verboven, P and Nicolaï, BM. 2013b. Multiscale modeling in food engineering. *Journal of Food Engineering,* 114**,** 279-291.

Ho, QT, Verboven, P, Delele, M, Verlinden, B, Schenk, A, Vercammen, J and Nicolai, B. 2010. Evaluation of optimal storage conditions for apple fruit using a gas exchange model. *FOODSIM 2010.* CIMO Research Centre, Braganca, Portugal.

Jain, D. 2007. Development and testing of two-stage evaporative cooler. *Building and Environment,* 42**,** 2549-2554.

Kader, AA. 2001. Recent advances and future research needs in postharvest technology of fruits. Bulletin of the International Institute of Refrigeration, 3-13. Acta Horticulture.

Kasmire, RF, Kader, AA and Morris, LL. 1975. Maturity, ripening and transit temperaatures: a suggested guide for shipping and buyers. *In:* Tomato, TC and Board, eds. Ripening stages for tomatoes. USDA visual aid. UCDAVIS.

Kitinoja, L. 2013a. Innovative Small-scale Postharvest Technologies for reducing losses in Horticultural Crops. *Ethiop .J. Appl. Sci. Technol. ,* Special Issue, 1**,** 9-15.

Kitinoja, L. 2013b. *Use of cold chains for reducing food losses in developing countries.* The Postharvest Education Foundation, University of California, La Pine, Oregon, USA.

Kitinoja, L and Thompson, JF. 2010. Pre-cooling systems for small-scale producers. *Stewart Postharvest Review,* 6**,** 1-14.

Laguerre, O, Hoang, HM and Flick, D. 2013. Experimental investigation and modelling in the food cold chain: Thermal and quality evolution. *Trends in Food Science & Technology,* 29**,** 87-97.

Lukasse, LJS, De Kramer-Cuppen, JE and Van Der Wort, AJ. 2007. A physical model to predict climate dynamics in ventilated bulk-storage of agricultural produce. *International Journal of Refrigeration-Revue Internationale Du Froid,* 30**,** 195-204.

Manuwa, SI and Odey, SO. 2012. Evaluation of pads and geometrical shapes for constructing evaporative cooling system. *Modern Applied Science,* 6**,** 38-45.

Martins, RC, Lopes, VV, Vicente, AA and Teixeira, JA. 2008. Computational shelf-life dating: complex systems approaches to food quality and safety. *Food and Bioprocess Technology,* 1**,** 207-222.

Mogaji, TS and Fapetu, O. 2011. Development of an evaporative cooling system for the preservation of fresh vegetables. *African Journal of Food Science,* 5**,** 255-266.

Montazeri, H, Blocken, B and Hensen, JLM. 2015. Evaporative cooling by water spray systems: CFD simulation, experimental validation and sensitivity analysis. *Building and Environment,* 83**,** 129-141.

Moonen, P, Defraeye, T, Dorer, V, Blocken, B and Carmeliet, J. 2012. Urban Physics: Effect of the micro-climate on comfort, health and energy demand. *Frontiers of Architectural Research,* 1**,** 197-228.

Muñoz, RC, Diuco, LT, Martinez, SMS, Oliveria, IKA, Quiroz, NA and Maria, DJR. 2017. Automated electronic evaporative cooler for fruits and vegetables preservation. *International Journal of Engineering Sciences & Research Technology,* 6**,** 352-364.

Nahor, HB, Hoang, ML, Verboven, P, Baelmans, M and Nicolai, BM. 2005. CFD model of the airflow, heat and mass transfer in cool stores. *International Journal of Refrigeration-Revue Internationale Du Froid,* 28**,** 368-380.

Nenguwo, N. 2002. *Appropriate technology cold store construction and review of post-harvest transport and handling practices for export of fresh produce from Rwanda.* Chemonics International Inc., Washington, DC, USA.

Nicolaï, BM, Verboven, P and Scheerlinck, N. 2001a. Modelling and simulation of thermal processes *In:* Richardson, P (ed.) *Thermal technologies in food processing.* Cha. 6, 91-112. CRC Press and Woodhead Publishing Limited, USA.

Nicolaï, BM, Verboven, P and Scheerlinck, N. 2001b. The modelling of heat and mass transfer. *In:* Tijskens, I, Hartgot, M and Nicolaï, BM (eds.) *Food Process Modelling.* Ch. 4, 60-86. CRC Press and Woodhead Publishing Limited, Cambrige, England.

Norton, T and Sun, DW. 2006. Computational fluid dynamics (CFD): an Effective and efficient design and analysis tool for the food industry: a review. *Trends in Food Science & Technology,* 17**,** 600-620.

Oke, MO, Sobratee, N and Workneh, TS. 2013. Integrated pre-and postharvest management processes affecting fruit and vegetable quality. *Stewart Postharvest Review,* 9**,** 1-8.

Olosunde, WA, Igbeka, JC and Olurin, TO. 2009. Performance Evaluation of Absorbent Materials in Evaporative Cooling System for the Storage of Fruits and Vegetables. *International Journal of Food Engineering,* 5**,** 1-15.

Paliyath, G and Murr, DP. 2008. Postharvest Biology and Technology of Fruits, Vegetables, and Flowers. *In:* Paliyath, G, Murr, DP, Handa, AK and Lurie, S (eds.) *Common Fruits, Vegetables, Flowers, and Their Quality Characteristics.* Cha. 2, 8-18. Blackwell Publishing Ltd, USA.

Parfitt, J, Barthel, M and Macnaughton, S. 2010. Food waste within food supply chains: quantification and potential for change to 2050. *Philosophical Transactions of the Royal Society B: Biological Sciences,* 365**,** 3065-3081.

Raghavan, GSV and Gariepy, Y. 1984. Structure and instrumentation aspects of storage systems. *Postharvest Handling of Vegetables 157***,** 5-30.

Roy, SK and Pal, RK. 1989. A low cost zero energy cool chamber for short term storage of mango. III International Mango Symposium 291, 519-524.

Royston, P and Altman, DG. 1994. Regression using fractional polynomials of continuous covariates: parsimonious parametric modelling. *Applied statistics,* 43**,** 429-467.

Sablani, SS, Datta, AK, Rahman, MS and Mujumdar, AS. 2007. *Handbook of food and bioprocess modeling techniques.* CRC Press Taylor and Francis Group, New York, USA.

Samira, A, Woldetsadik, K and Workneh, TS. 2013. Postharvest quality and shelf life of some hot pepper varieties. *Journal of food science and technology,* 50**,** 842-855.

Saneinejad, S, Moonen, P, Defraeye, T and Carmeliet, J. 2011. Analysis of convective heat and mass transfer at the vertical walls of a street canyon. *Journal of Wind Engineering and Industrial Aerodynamics,* 99**,** 424-433.

Saneinejad, S, Moonen, P, Defraeye, T, Derome, D and Carmeliet, J. 2012. Coupled CFD, radiation and porous media transport model for evaluating evaporative cooling in an urban environment. *Journal of Wind Engineering and Industrial Aerodynamics,* 104**,** 455-463.

Saran, S, Dubey, N, Mishra, V, Dwivedi, SK and Raman, NLM. 2013. Evaluation of coolbot cool room as a low cost storage system for marginal farmers. *Progressive Horticulture,* 45**,** 115-121.

Schouten, RE, Huijben, TPM, Tijskens, LMM and Van Kooten, O. 2007. Modelling quality attributes of truss tomatoes: Linking colour and firmness maturity. *Postharvest Biology and Technology,* 45**,** 298-306.

Shumye, G, Woldetsadik, K and Fitiwi, I. 2014. Effect of integrated postharvest handling practices on quality characteristics and shelf life of cactus pear [Opuntia ficus-indica (L.) Mill.] fruit. *Journal of Post-Harvest Technology,* 2**,** 68-79.

Sloof, M, Everest, BV and 'S-Hertogenbosch. 2001. Problem decomposition. In: Tijskens, I., Hertog, M. & Nicolai, B. M. (Edt.) (2001). Food process modelling. *Woodhead Publishing,* 59**,** 510.

Sloof, M, Tijskens, LMM and Wilkinson, EC. 1996. Concepts for modelling the quality of perishable products. *Trends in Food Science & Technology,* 7**,** 165-171.

Studman, CJ. 2001. Computers and electronics in postharvest technology: a review. *Computers and electronics in Agriculture,* 30**,** 109-124.

Tefera, A, Seyoum, T and Woldetsadik, K. 2007. Effect of disinfection, packaging, and storage environment on the shelf life of mango. *Biosystems Engineering,* 96**,** 201-212.

Thompson, JF. 2002. Storage systems. *In:* Kader, AA (ed.) *Postharvest Technology of Horticulture Crops.* Cha. 12, 113-128. Agriculture and Natural Resources, University of California, USA.

Thompson, JF, Mitchell, FG and Kasmire, RF. 2002. Cooling horticultural commodities. *In:* Kader, AA (ed.) *Postharvest technology of horticultural crops.* 3rd ed, Cha. 11, 97- 112. Agriculture and Natural Resources, University of California, USA.

Tijskens, LMM, Hertog, MLaTM and Nicolaï, BM. 2001. *Food process modelling.* Woodhead Publishing Limited and CDC press, Cambrige, England.

Tijskens, LMM and Polderdijk, JJ. 1996. A generic model for keeping quality of vegetable produce during storage and distribution. *Agricultural Systems,* 51**,** 431-452.

Ugwuishiwu, BO, Ugwu, SN and Ohagwu, CJ. 2014. Analysis of thermal control in animal buildings: a review. *African Journal of Agricultural Science and Technology (AJAST),* 2**,** 84-96.

USDA. 1976. *United States standards for grade of fresh tomatoes.* US Dept. Agric., Mktg., Serv., Washington DC.

Van Boekel, MaJS. 2008. Kinetic modeling of food quality: a critical review. *Comprehensive Reviews in Food Science and Food Safety,* 7**,** 144-158.

Van Boekel, MaJS. 2010. *Kinetic modeling of reactions in foods.* CRC press, Tayplor & Francis Group, New York, USA.

Van Der Sman, RGM. 2008. Scale analysis and integral approximation applied to heat and mass transfer in packed beds. *Journal of Food Engineering,* 85**,** 243-251.

Van Gogh, JB, Van Der Sluis, AA and Soethoudt, JM. 2013. *Feasibility of a network of excellence postharvest food losses: Combining knowledge and compepetences to reduce food losses in developing and emerging economies.* Wageningen UR Food & Biobased Research, Netherland.

Verboven, P, Flick, D, Nicolai, BM and Alvarez, G. 2006. Modelling transport phenomena in refrigerated food bulks, packages and stacks: basics and advances. *International Journal of Refrigeration-Revue Internationale Du Froid,* 29**,** 985-997.

Versteeg, HK and Malalasekera, W. 1995. *An introduction to computational fluid dynamics* Essex, Longman Scientific & Technical and John Wiley & Sons Inc., USA.

Versteeg, HK and Malalasekera, W. 2007. *An introduction to computational fluid dynamics: the finite volume method.* Pearson Education Limited, UK.

Wang, CX, Pritchard, J and Thomas, CR. 2006. Investigation of the mechanics of single tomato fruit cells. *Journal of texture studies,* 37**,** 597-606.

Wang, L and Sun, DW. 2003. Recent developments in numerical modelling of heating and cooling processes in the food industry: a review. *Trends in Food Science & Technology,* 14**,** 408-423.

Workneh, TS. 2010. Feasibility and economic evaluation of low-cost evaporative cooling system in fruit and vegetables storage. *African Journal of Food, Agriculture, Nutrition and Development,* 10**,** 2984-2997.

Xu, YF, Burfoot, D and Huxtable, P. 2002. Improving the quality of stored potatoes using computer modelling. *Computers and Electronics in Agriculture,* 34**,** 159-171.

Xuan, YM, Xiao, F, Niu, XF, Huang, X and Wang, SW. 2012a. Research and application of evaporative cooling in China: A review (I) - Research. *Renewable & Sustainable Energy Reviews,* 16**,** 3535-3546.

Xuan, YM, Xiao, F, Niu, XF, Huang, X and Wang, SW. 2012b. Research and applications of evaporative cooling in China: A review (II)—Systems and equipment. *Renewable and Sustainable Energy Reviews,* 16**,** 3523-3534.

Yahia, EM. 2010. *Modified and controlled atmospheres for the storage, transportation, and packaging of horticultural commodities.* CRC press Taylor and Francis Group, New York, USA.

Zong, C. 2013. *Mid-term report: Precision zone ventilation design and control in pig housing.* Aarhus University, Department of Engineering, Denmark.

3. EFFECTS OF EVAPORATIVE COOLING AND COOLBOT AIR CONDITIONING ON CHANGES IN THE ENVIRONMENTAL CONDITIONS INSIDE THE COOLING CHAMBER

Abstract

The main purpose of this study was to compare the effectiveness of a low-cost evaporative cooler (EC) and a CoolBot-Air-Conditioner (CBAC) and the combination (EC+CBAC), in terms of the changes in temperature and relative humidity. The temperature and relative humidity (RH) distribution, as well as the cooling efficiency of cooling pads were evaluated. A comparison of the changes in temperature and RH was also performed. The results indicate that the CBAC cooler can maintain the required temperature of the air inside the empty store room by reducing the temperature to 6.3°C, compared to the maximum ambient air temperature of 34.1°C. A 28.1ºC temperature reduction was achieved by the CBAC cooling system. The RH was about 75%, which is not within the optimum range of the relative humidity air requirements for the storage of fruit and vegetables. On the other hand, the temperature and RH maintained by EC+CBAC, when operated together, were found to maintain the temperature of 8 - 15ºC and a RH of 80 - 99% within the optimum recommended range for fresh produce. The temperature maintained by EC (17 - 22ºC) was not within the optimum range for many fruit and vegetables, while the RH (95 - 98.6%) was found to be in the optimum range that is required by some of the fresh produce during storage. In conclusion, the EC maintained only the RH, but did not achieve the required temperature for short-term storage, while the EC+CBAC maintained both the optimum temperature and the RH required for fresh produce. On the other hand, the CBAC system alone can maintain the temperature, while the RH is required to be slightly higher in a fruit and vegetable storage room and is sufficient for the short-term storage of fruit and vegetables, without a significant deterioration in the produce. Although, these technologies demonstrated a promising alternatives for fresh produces shelf-life extension, further investigation in terms of detailed fluid dynamics study of the micro-environment inside the cooler with load taking in to account the heat of generation from respiring plant materials is required for the optimization of the cooling technologies.

Keywords: Air velocity distribution, CoolBot-air-conditioner, evaporative cooler, temperature distribution, relative humidity distribution

3.1 Introduction

Temperature and relative humidity management is one of the most important factors for the maintenance of the freshness and quality of fruit, thereby improving and extending its shelf-life (Thompson and Spinoglio, 1996; Kitinoja *et al.*, 2010). Affordable cooling technologies are of paramount importance for low-income farmers and small-scale fruit and vegetable processors, especially in arid and semi-arid climate regions (Kitinoja *et al.*, 2010; Workneh, 2010). Therefore, small-scale and low-cost cold storage options, including the evaporative cooler (EC) and CoolBot-Air-Conditioners (CBAC), are now becoming available for small-scale farmers (Kitinoja and Thompson, 2010; Saran *et al.*, 2010). An evaporative cooler may include an evaporative cooler pad made of porous materials, such as charcoal, rice husks, wood sawdust and many other materials, which are covered within a cooler box or duct (Gerlach, 2015). During the evaporative cooler (EC) process, the water is directed to wet the cooler pad and the ambient hot air is passed through the same pad. The water may evaporate into the air as the air passes through the cooler pad. Heat energy from the air is absorbed by the heat of the vaporization of the water, thereby cooling the air passing through the outlet pad (Gerlach, 2015). Thereafter, using a forced ventilation case, the air blown through a wet pad by a fan to the storage chamber. The EC has proved itself to be feasible in arid- and semi-arid climate areas essentially for the pre-cooling fruit and vegetables (Workneh, 2010).

Evaporative cooler was reported to perform best during the dry season, the time when cooling is the most important for fresh produce (Roy, 2007). However, it seems that the EC is less effective during times when there is high humidity. EC is dependent on the conditions of the outside air. The EC costs less and is mechanically simple to construct, to understand and to maintain (Kitinoja and Thompson, 2010; Workneh, 2010).

The CBAC is also reported to cost less (*i.e.* 90% less than a new commercial refrigeration cold storage unit) (Boyette and Rohrbach, 1993; Saran *et al.*, 2013). It has been successfully implemented in Ghana, Kenya, India and many other countries (Kitinoja and Cantwell, 2010; Saran *et al.*, 2010; Kitinoja, 2013). Depending on the insulation level and the performance of the air conditioner, it was reported that temperatures as low as zero to 2°C can be maintained by the CBAC system (Saran *et al.*, 2010).

The summer weather in South Africa, including that of the Pietermaritzburg area is characterized by a predominantly high global surface temperature, a high humidity and UV-radiation, as well as extremely intense and variable weather (Clark, 2006). Such environmental conditions influence the freshness and storability of fruit and vegetables. About 30-50% of fruit and vegetables are reported to be lost during the postharvest handling, storage and transportation of fresh produce. Many attempts have been made to reduce postharvest losses during the hot season, however most of the technologies require a high initial investment cost. This is therefore a challenge for small- and medium-scale farmers and processors, especially in tropical, sub-tropical arid and semi-arid climate regions, as high postharvest technologies are not affordable. Therefore, low-cost cooling technologies are recommended for low-income farmers to extend the shelf-life of fresh produce during the harvest period (Roy and Pal, 1994; Saran *et al.*, 2010; Workneh, 2010).

Although they are cheap, studies of the uniformity of the environment for all EC, CBAC and EC+CBAC cooled rooms is limited in the literature. The objective of this study, therefore, was to evaluate the influence of three low-cost cold storage systems on the micro-climate of non-loaded insulates that were stored in different locations, namely, inside the cold chambers, and outside, under ambient air conditions. Therefore, the cooling performance study, in terms of maintaining an optimum temperature and RH, is limited. Understanding the cooling performance ability of the low-cost cooling technologies can help to utilize the technologies to their full capacity. Hence, this study was devoted to studying the performance EC and CBAC in terms of temperature, RH and air velocity.

3.2 Materials and Methods

3.2.1 Study site

The study was conducted at the Ukulinga Research Farm (24°24′E, 30°24′S) of the University of KwaZulu-Natal, Pietermaritzburg, South Africa, where the 6 m × 2.4 m × 4 m low-cost insulated cooling chamber was constructed and installed. The walls of the storage chamber were constructed by using three layers, namely, 1 mm inner and outer sheet, made of mild steel carbon, and a 58 mm middle layer, made of polyurethane plastic insulation. The chamber was fitted with one indirect heat exchanger, followed by three direct evaporative cooling pads (charcoal granules), as well as two fans that were fitted to force air through the pads and into

the storage chamber. The first axial fan (Fan1 with a diameter of 240 mm) pushes atmospheric air (2 $m.s^{-1}$) through the heat exchanger and the pads, while the second fan (Fan2 with a diameter of 350 mm) pushes the cooled air into the store at a constant speed of 3.2 $m.s^{-1}$. In addition, the thermostat controller (CoolBot) and Air Conditioner (CBAC) were fitted to the same insulated store. An empty room was cooled batch-by-batch, either by an EC or a CBAC system, while simultaneously operating for five hot days each.

To evaluate the effectiveness of the cooler systems, the air temperature, relative humidity and air speed were monitored. The average daytime (from 8 am to 6 pm) temperature, the relative humidity and air velocity were measured, using Hobo data loggers (Hobo Prov2 Part No. U23-001 series) placed at different fixed locations inside the storage chamber, and one on the outside, to gather the ambient climate data for five hot dry days.

3.2.2 Data collection and analysis

The experiment was designed to consist of three types of cooling approaches, namely EC, CBAC and EC+CBAC. A comparison of the inside and outside temperatures and relative humidity was performed. The experiment work involved the hourly measurement of environmental parameters, the temperature and relative humidity throughout the hot days, from 8 am to 6 pm. The experiment was mainly concerned with evaluating the cooling performance, in terms of the temperature reduction, RH change and air speed achievements of the three cooling operations.

3.2.3 Temperature and relative humidity sensors locations

The experiment was carried out for five hot days with an average ambient temperature of 28.1 °C and RH of 64% of daytime during the month of February 2017, from 8:00 am to 6:00 pm (hourly). The time periods that were selected were very important and critical for the cooling of fruit and vegetables. The Hobo data logger was set at the inlets of both the EC and CBAC. The psychrometric unit of the evaporatively cooled room is shown in Figure 3.1. Fan 1 blows the ambient air through indirect heat exchanger (IHE) and three pads i.e. pad 1, 2 and 3. Fan 2 forces the air through the room. The hobo data logger were set at the inlets (Fan 2 and CBAC-inlets), the right and left corners of the wall (P2 and P3), the 2 m, 4 m, and 6 m hang at the center of the symmetry line of the storage chamber (P4, P5 and P6). The dimeters of the air exit

vents were 100 mm (P7 and P8). The hobo data loggers also put at the centre top of the right and left walls (P9 and P10, respectively). The speed of Fan 2 (3.2 $m.s^{-1}$) and after the CBAC-inlet (4.2 $m.s^{-1}$) were kept constant.

The same cold store chamber with three different settings i.e. EC, CBAC and EC+CBAC were evaluated for air temperature and relative humidity at different inside locations. Moreover, the temperature and the relative humidity of the air outside were measured for use as a control. The statistical design used the Completely Randomized Design (CRD) and the Duncan's multiple range tests were used for the means separation evaluation. GenStat Version 18 was used for the statistical analysis. Moreover, the efficiencies of the heat exchanger and charcoal cooling pads were calculated in terms of temperature ratios.

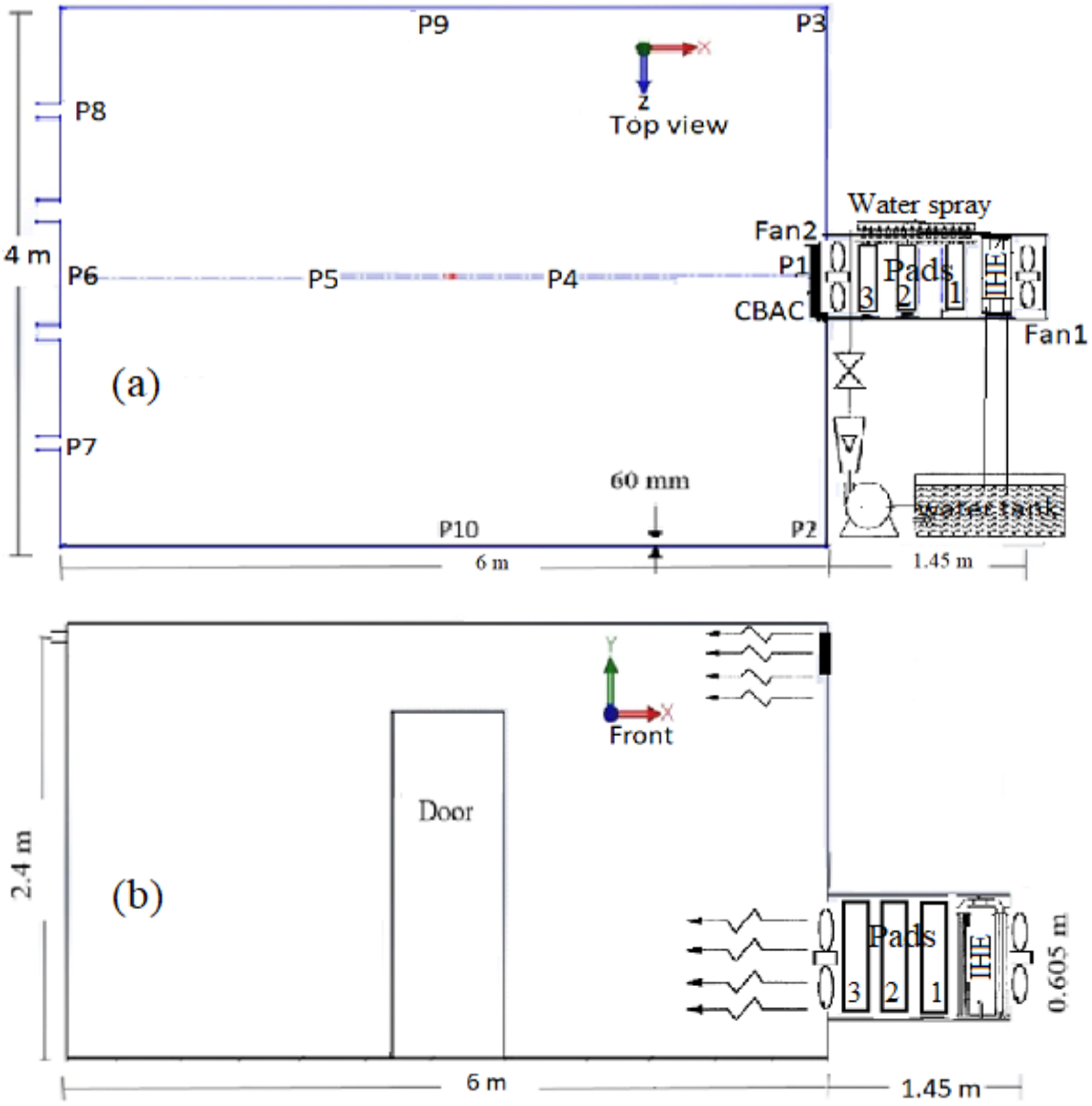

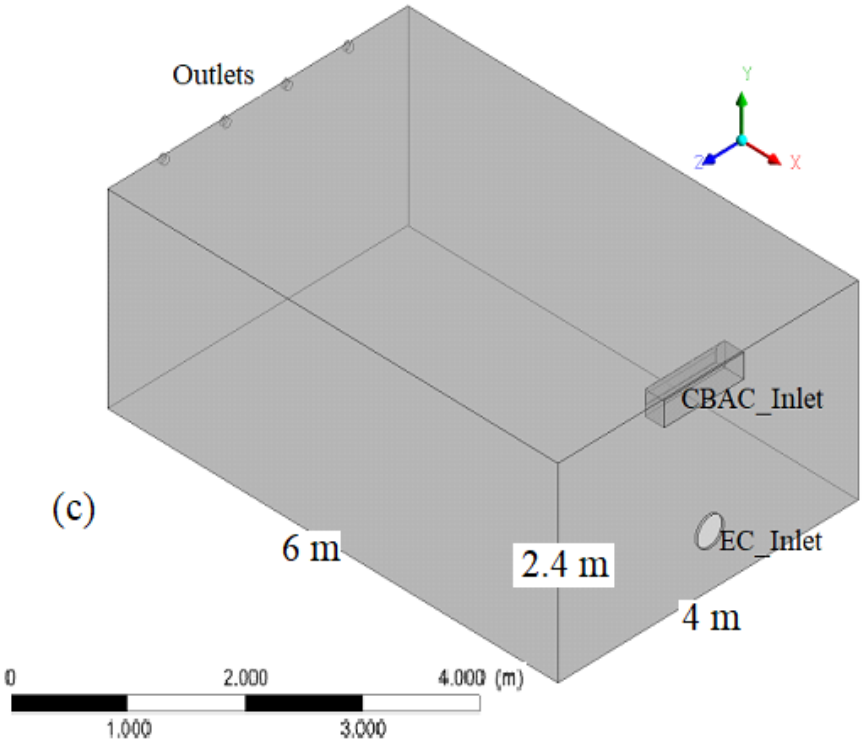

Figure 3.1 The hybrid of evaporative cooler (EC) and the CoolBot air conditioner (CBAC) cold storage chamber; top view (a), front view (b) and the overall 3-D of the combined EC+CBAC cold room (c). Temperature-RH sensors position-1 (P1), position-2 (P2), position-3 (P3), position-4 (P4), position-5 (P5), position-6 (P6), position-7 (P7), position-8 (P8), position-9 (P9), and position-10 (P10); and IHE is indirect heat exchanger

3.3 Results and Discussion

Table 3.1 illustrates the variations in air temperature, the RH and the air speed recorded inside three cooling operations (EC, CBAC and EC+CBAC). The recommended air speed for fruit and vegetables pre-cooling is 1 - 2 $m.s^{-1}$ and a high air velocity can affect the produce quality by removing more moisture (Dermesonlouoglou *et al.*, 2016). It is, therefore, important to understand the airflow characteristics and air properties, which affect the complex heat and mass transfer that influence the product quality (Smale *et al.*, 2006). The heat and mass transfer and airflow in cold storage chamber is a complex phenomenon (Smale *et al.*, 2006). Accordingly, the average air speed at the EC inlet was 3.2 $m.s^{-1}$, while at the inlet of the CBAC, it was recorded to be 4.2 $m.s^{-1}$. The air speed at the exit of non-loaded EC was 3.3 $m.s^{-1}$. On the other hand, the averaged air speed at the exit of non-loaded CBAC was 0.6 $m.s^{-1}$. Moreover,

the air speed at the exit of the non-loaded combination operation (EC+CBAC) cooling system was 3.1 $m.s^{-1}$.The moisture and quality loss of the stored produce inside the cold storage chamber were highly significant at the warm and high air velocity zone, due to the high respiration rate (Dermesonlouoglou *et al.*, 2016).

Table 3.1 The average temperature and relative humidity (RH) comparison table for evaporative cooler (EC), CoolBot-Air-Conditioner cold store and the combination of the two as an EC+CBAC cold storage chamber

Cooler	Temperature (°C)				Relative humidity (RH) (%)				Air speed ($m.s^{-1}$)	
	P1	P4	P5	Exit	P1	P4	P5	Exit	Inlet	Exit
EC	19.1	21.4	21.1	22.0	97.3	98.7	98.1	92.9	3.2	3.3
CBAC	6.3	10.3	10.6	10.6	95.2	82.1	80.2	79.4	4.2	0.6
EC+CBAC	18.7*	14.9	15.2	14.6	99.8*	82.1	79.2	97.9	3.0*	3.1
	8.4 **				99.7**				3.1**	

For the EC+CBAC operation, * indicates that at the inlet of EC and ** at the inlet of CBAC.

Cooling involves heat transfer from the produce to the medium that removes heat, such as cold air (Kitinoja and Thompson, 2010). The heat transfer of the cooling pad and a cold room is dependent on the magnitude of the temperature difference between the storage temperature, the stored produce and the outside environment air condition. The determinant parameters of the storage environment, primarily the temperature and relative humidity (RH), are critical for extending the shelf-life of the fresh produce (Thompson *et al.*, 2002). Several studies have shown that temperature, RH or moisture and airflow heterogeneity inside the cold rooms can affect the quality of the produce stored (Chourasia and Goswami, 2007). In addition, variations in heat transfer coefficients inside the cold storage chamber at different positions were determined, which lead to dynamic product cooling rates (Mirade, 2007). Therefore, the management of the temperature and RH inside the low-cost evaporative cooler (EC), CoolBot-air-conditioner and the combination is critical (Saran *et al.*, 2010; Saran *et al.*, 2013).

The average maximum and minimum ambient temperature obtained from the Ukulinga weather station was 34.1°C and 20.5°C (an averaged to 28.1°C), respectively. Moreover, the average maximum and minimum ambient relative humidity (RH) recorded was 91% and 49% (an averaged to 64%), respectively. Coolers' inlet temperatures changed between 15-20°C, 6-10°C and 6-7°C for EC, EC+CBAC and CBAC, respectively. Moreover, the relative humidity of the

ambient air varied between 52.62-99.9%, while it varied between 86-97.5% and 78-95%, for the EC and CBAC, respectively. The RH of the air was found to be higher inside the storage chamber, when compared to the RH of the outside ambient air. Nimje and Shyam (1993) reported that controlling the RH inside the controlled rooms, such as the greenhouse, and cold storage, such as the EC, would be difficult.

The mixing effect of the air during the simultaneous EC+CBAC operation (*i.e.* the EC blows air horizontally and the CBAC blows air at 45º in a –y direction) could contribute to the temperature and RH variation inside at the different positions of the cold storage chamber. The low RH at the middle positions shows that the center of the store, exposed to highly turbulent and hot spot area, might be caused by the effects of both the EC fan and air conditioner airflow direction at the inlet.

The average minimum and maximum temperatures recorded at the inlet of the room after Fan 2 of the EC were 17°C and 21°C, respectively, and thereafter increased to about 23°C and kept constant from the inside to the exit vents locations (Figure 3.2). Compared to the ambient temperature, the EC reduced the ambient temperature by 18.1% at the inlet and 17.2% at the exit vent of the cold storage chamber, while the average maximum and minimum-recorded RH was 98.6% and 94.8%, respectively, at the inlet of EC (Fan 2), and the RH was maintained inside the room at different sensor locations.

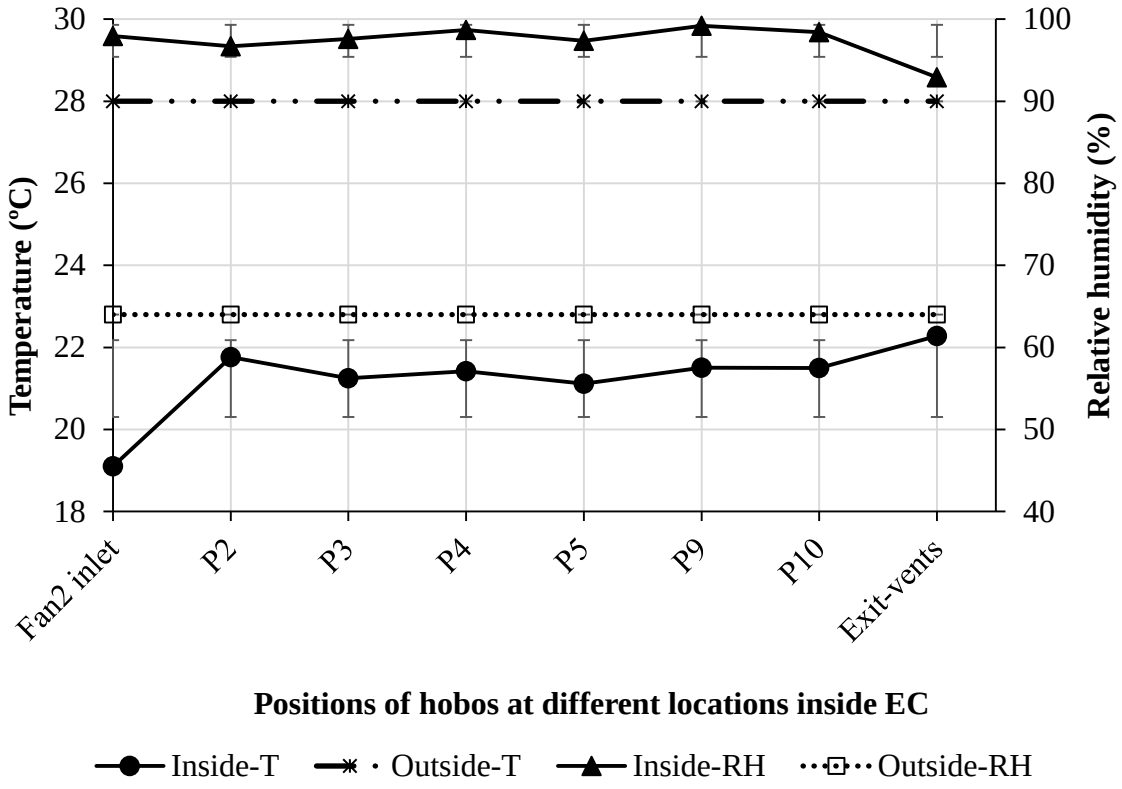

Figure 3.2 Temperature and RH distributions inside the evaporative cooler (EC) at different locations, such as after the inlet of the evaporative cooler and at different locations inside the cool chamber

Figure 3.3 shows the CoolBot air conditioner (CBAC) inlet temperature. The temperature at the inlet varied from 3 - 8°C, while the temperature varied between 8 - 13°C inside the room at different positions. The average ambient temperature and RH were 22.3°C and 82.9%, respectively. The results show that there were no significant variations in temperature changes inside the cool storage chamber. The air-conditioner inlet air speed varied from 5.3 to 6.0 m s^{-1}. The CBAC temperature was set at 3°C. The inlet temperature was found to be from 6 - 7°C. The reason for not achieving the temperature might be attributed to the open-air circulation vents at the outlets of the cold room. Compared to the ambient atmospheric temperature, the CBAC reduced the ambient temperature by 77.7% at the inlet and 63.3% at the exit vent of the cold storage chamber. On the other hand, the maximum and minimum inlet relative humidity (RH) at the CBAC, which was found to be 90.7% and 73.8% increased, when compared to the ambient RH, respectively. The RH value was the highest at the inlet of the air-conditioner and decreased to about 75% across the room to the exit vents. This variation in the RH could affect the freshness of the fruit and vegetables stored inside, in the long run *i.e.* surface shriveling could occur because of the removal of the moisture from the produce.

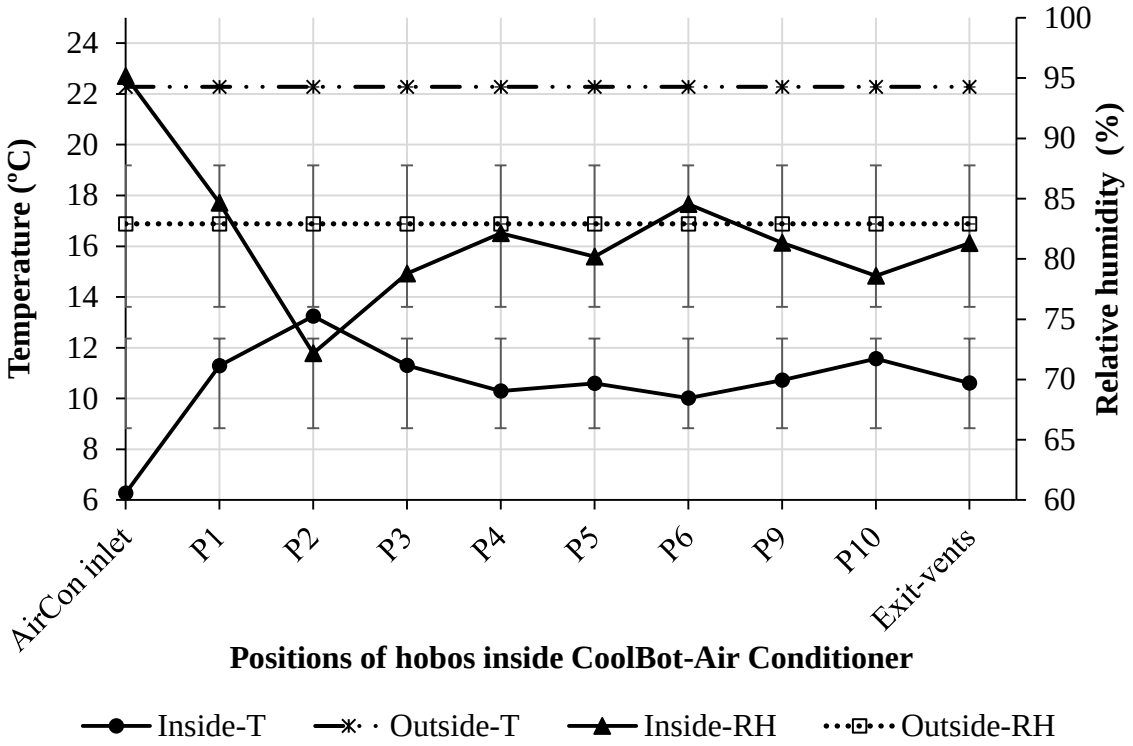

Figure 3.3 Temperature and relative humidity distribution inside the CoolBot air conditioner (CBAC) at different positions *i.e.* at the inlet of the CBAC and at different locations inside the chamber

Figure 3.4 displays the average temperature of the air inside the cooler, while both the EC psychrometric unit and the EC+CBAC were operating. The results showed that the temperature at the EC fan inlet was about 18.7°C, while at the air conditioner inlet was about 8.4°C. Moreover, the average temperature distribution inside the cooler varied from 13 - 15°C, which was good enough for the storage of most of the tropical and sub-tropical fruit and vegetables. Compared to the ambient atmospheric temperature, the EC+CBAC reduced the ambient temperature by 43.2% at the inlet and 38.9% at the exit vent of the cold store. The mixing effect of the air at the inlets (the EC inlet is horizontal and the CBAC was at 45° in a –y direction) might contribute to the temperature and RH variation inside at the transient positions of the combined operating room.

The average inside RH of both systems, when operated simultaneously, is displayed in Figure 3.4. As a result, the RH at both the inlet after fan and the air-conditioner was 99.9%, while at the center of the store the value decreased to about 80% and rose to a steady 98% towards the exit vents of the storage chamber. This shows that the center of the cooled chamber was exposed to a highly turbulent and hot spot area and this might be caused by the effects of both the EC

Fan 2 and air conditioner inlet blowing direction. All the experiments for EC, CBAC and EC+CBAC were performed at different ambient air conditions. Hence, the comparisons between the experimental inside and outside air temperature and RH might affected to some errors. Hence, the comparison among the EC, CBAC and EC+CBAC might be influenced.

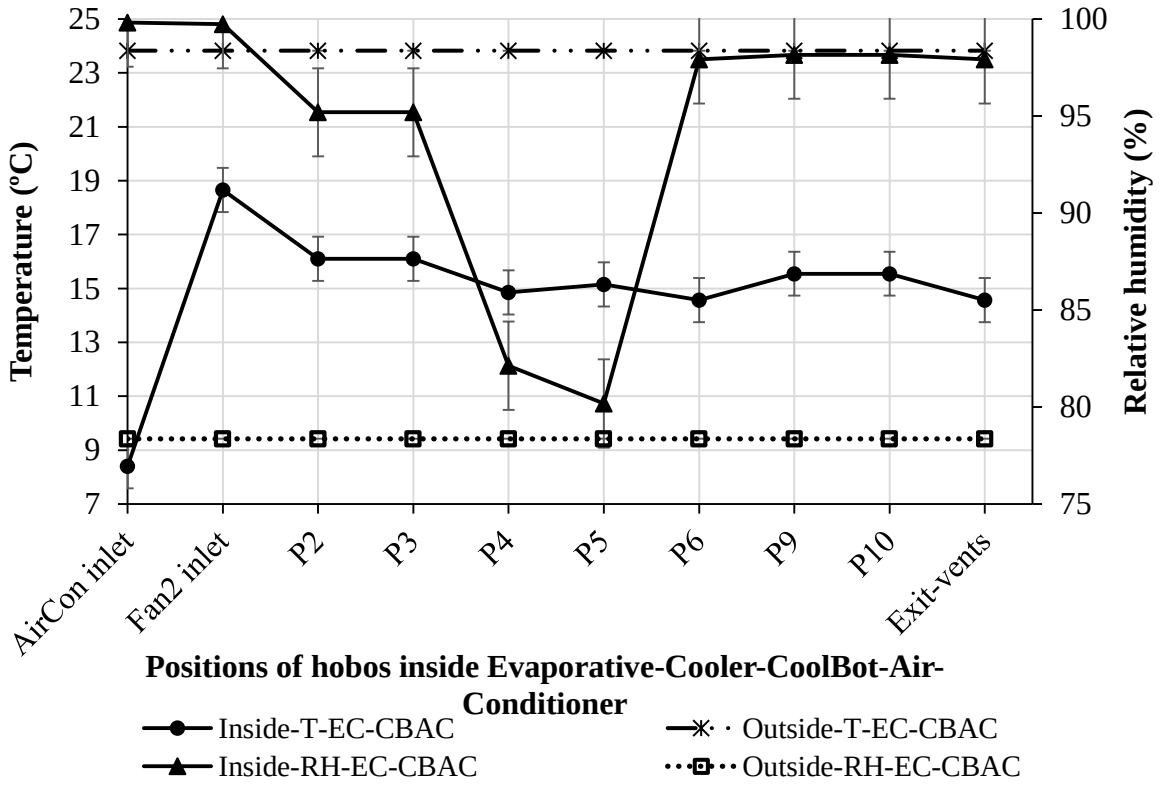

Figure 3.4 Temperature and relative humidity distribution inside the cooler when both the evaporative cooler and CoolBot air conditioner (EC+CBAC) were operating. Where AirCon inlet is at the inlet of air conditioner, the fan inlet is at the inlet of EC (Fan 2), P2 to Pn are different sensor locations (Figure 3.1) of both EC and CBAC cold storage chamber

The psychrometric moist air properties are displayed in Figure 3.5. The three cooling operations were performed independently and the average inlet temperature and the RH at Fan 2 and AirCon (air conditioner) were considered for the psychrometric chart display. The EC cooling process follows the adiabatic path (El-Dessouky *et al.*, 2004). Based on temperature reduction that is achieved, the cooling ability of CBAC, EC+CBAC and EC are in descending order, respectively.

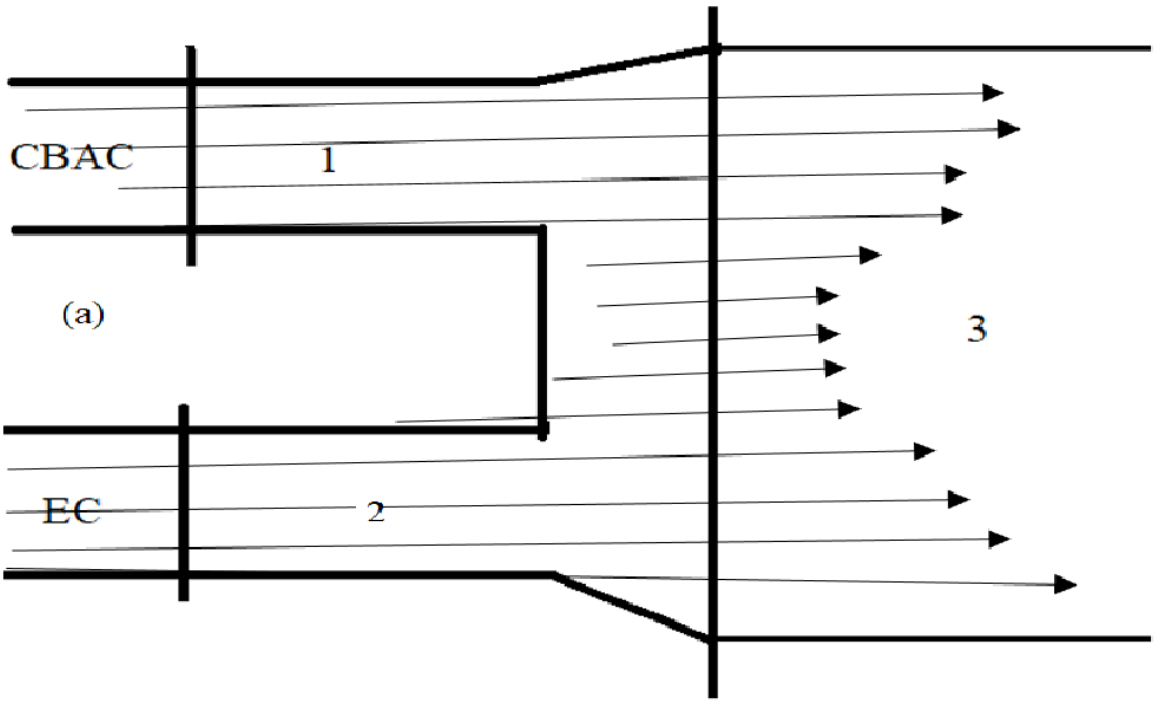
CBAC
1
(a)
3
EC
2

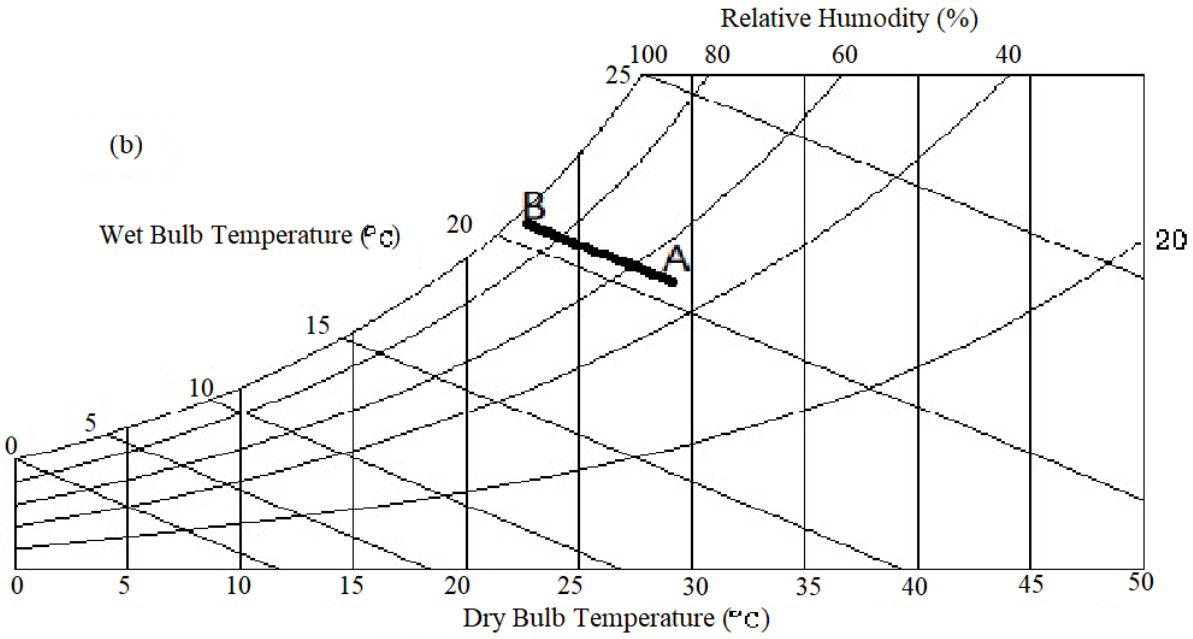
Relative Humodity (%)
100
80
60
40
25
(b)
Wet Bulb Temperature (°C)
20
B
A
20
15
10
5
0
0
5
10
15
20
25
30
35
40
45
50
Dry Bulb Temperature (°C)

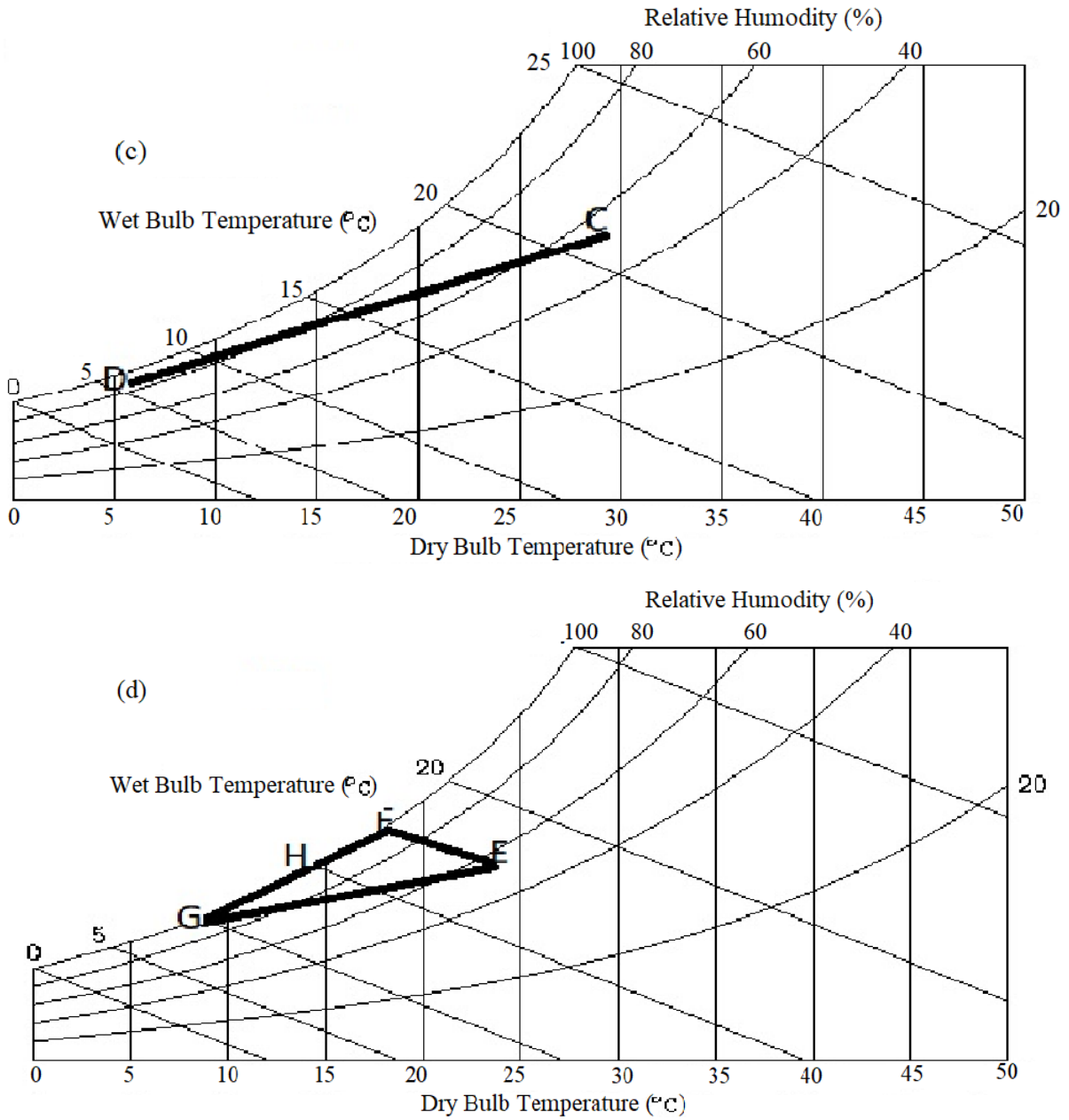

Figure 3.5 Block diagram and the psychrometric air properties of the EC, CBAC and EC+CBAC cooling operations where AB shows the adiabatic cooling of EC, CD shows the sensible cooling process of CBAC, and GH and FH are the mixing segment when EC+CBAC is operational

3.3.1 Pooled data

Figure 3.6 displays a comparison of the average temperature distribution inside the cooler. Each system operated separately. The average temperature (28.1°C) was considered for the comparison. The CBAC maintained the temperature at 8 - 10°C. The combined effect of both systems running together enabled the temperature to be maintained between 13 - 15°C inside

the chamber, while the evaporative cooling alone enabled the temperature of 22°C to be maintained.

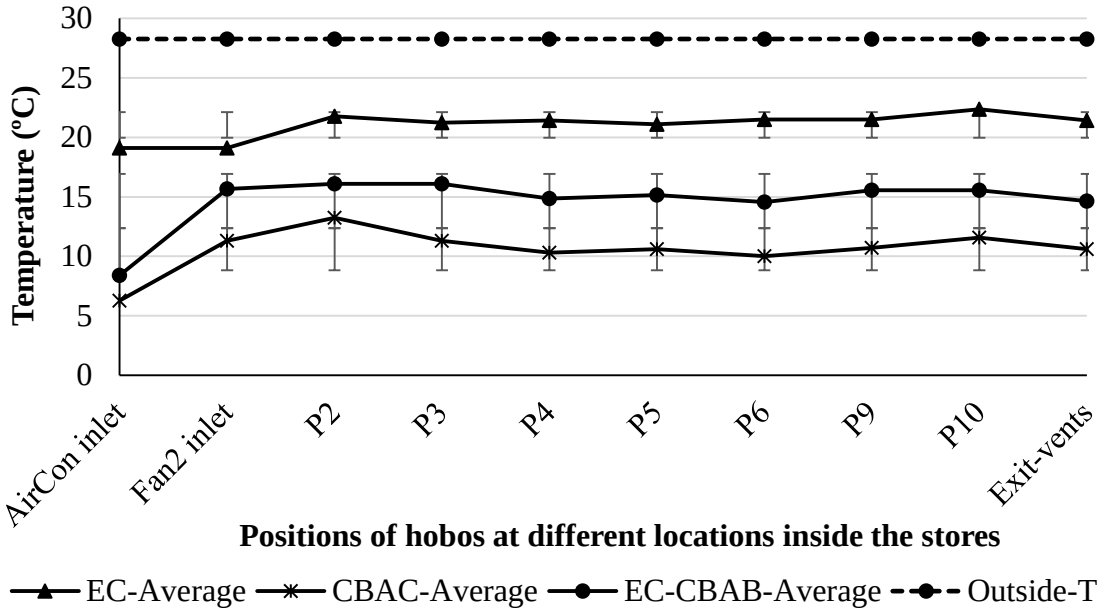

Figure 3.6 Averaged temperature distributions inside the evaporative cooler (EC), CoolBot-Air-Conditioner (CBAC) and combination of EC+CBAC storage chamber at different positions: the inlet of the stores and at different inside locations of the chamber

Figure 3.7 shows the average air RH of the pooled data of the three cooling systems. The EC maintained the highest RH throughout the storage locations, while the CBAC showed the lowest RH inside the cold room at different locations. The EC+CBAC cooling system showed high variations at different positions inside the storage chambers. The average ambient RH was 50.6%.

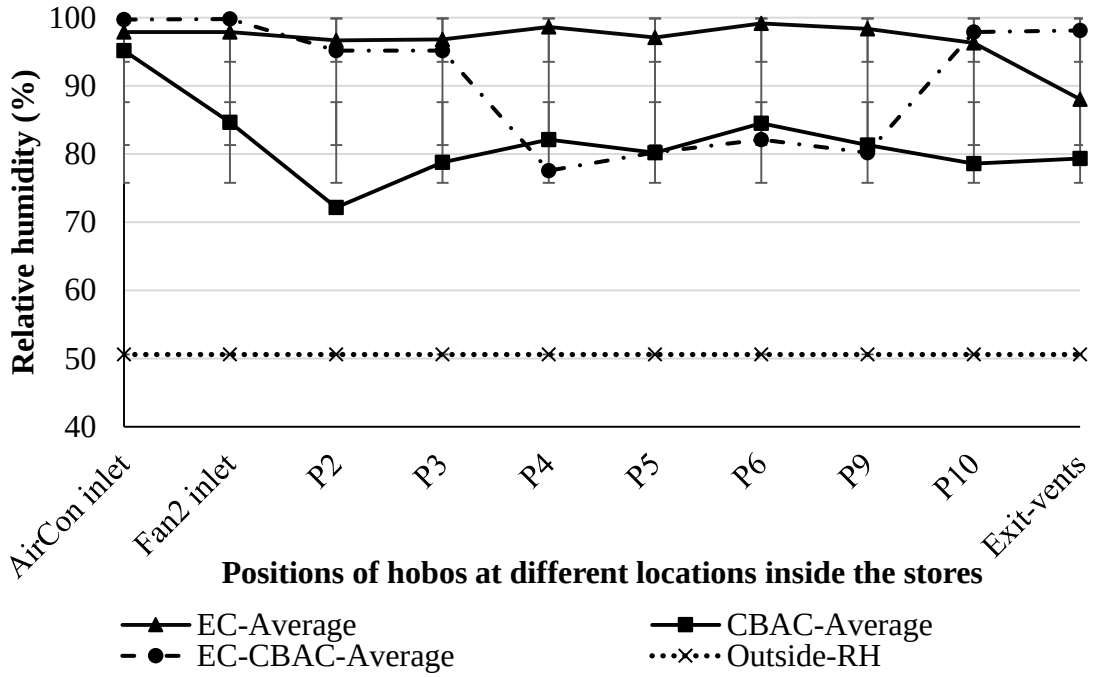

Figure 3.7 Averaged relative humidity (RH) distribution inside the evaporative cooler (EC), CoolBot air conditioner (CBAC) and the combination of EC+CBAC storage chamber at different positions: the inlet of the chamber at different inside locations of the chamber

The mean differences in the temperature of the storage inlets were 6.27, 13.53, 20.09 and 28.12°C, for CBAC, EC+CBAC, EC and ambient, respectively. All the means temperatures were significantly ($P \leq 0.001$) different for all storage conditions. On the other hand, the RH of all the three individual cold storage chambers was not significantly ($P \geq 0.001$) different, but the ambient temperature was significantly different from the storage chambers.

Table 3.2 shows the optimum environmental storage conditions for some selected tropical and sub-tropical fruit and vegetables. A deviation from the optimum temperature and RH might cause either chilling injuries or physiological disorders for fruit and vegetables stored in cold storage (Ahumada and Cantwell, 1996; Rodríguez *et al.*, 2015). For instance, tomatoes are sensitive to chilling injury when stored more than two weeks at a temperature below 10ºC (Cantwell and Kader, 1992; Cantwell and Kasmire, 2002). In this study, the management of the optimum temperature and RH is a very critical operation, which is similar to the report of Sargent *et al.* (1988) and Paull (1999). The low-cost cooling technologies (*i.e.* EC, CBAC and

EC+CBAC) have shown that they have the potential to achieve the optimum conditions that are required for extending the shelf-life of fresh produce (Table 3.2).

Table 3.2 Optimum storage environmental conditions for some selected tropical and sub-tropical fruit and vegetables from literature

Fresh produce	Storage temperature (ºC)	Storage RH (%)	Shelf-life (days)	References
Avocado	8-12	85-90	14-28	Bill et al. (2014)
Banana (green)	13–14	90-95	7-28	Nunes (2008)
Bell paper	7-13	90-95	14-21	Nunes (2008)
Cucumbers	10-13	95	10-14	Nunes (2008)
Grape	10–15	90-95	3-7	Paull and Duarte (2011)
Guava	5-10	90	7-14	Barman et al. (2015)
Lemon	10-14.5	85-90	30-120	Thompson (2003)
Mandarin	5-8	90-95	21-60	Thompson (2003)
Mango	5-13	85-90	14-21	Paull and Duarte (2011)
Orange	0-8	85-90	21-56	Thompson (2003)
Papaya	7–13	85-90	7-21	Nunes (2008)
Pepper (Bell)	7-13	90-95	14-21	Barman et al. (2015)
Pineapple	7-13	85-90	14-28	Paull and Duarte (2011)
Potato	4-16	90-95	120-300	Barman et al. (2015)
Pumpkin	10-15	50-70	60-90	Barman et al. (2015)
Sweet potato	13-16	85-90	120-210	Sargent et al. (1988)
Tomato (Green)	12.5-15	90-95	7-21	Cantwell et al. (1992)
Tomato (Pink)(USDA stage 5)	10-12.5	90-95	8-10	Cantwell et al. (1992)
Tomato (Red) (USDA stage 6)	7-10	90-95	4-7	Cantwell et al. (1992)
Watermelon	10–15	90	14-21	Nunes (2008)

3.3.2 Cooling efficiency of the heat exchanger and the cooling pads

The efficiencies of the indirect evaporative cooler and direct evaporative cooler were calculated in the El-Dessouky *et al.* (2004), using Equation 3.1 below:

$$\varepsilon = \frac{T_{db,inlet} - T_{db,outlet}}{T_{db,inlet} - T_{wb,inlet}} \; x \; 100\% \qquad (3.1)$$

Where:

$T_{db,inlet}$ = dry-bulb temperature at the inlet of the pad or heat exchanger (ºC),

$T_{db,inlet}$ = dry-bulb temperature leaving (ºC), and

$T_{wb,inlet}$ = wet-bulb temperature of the air at the inlet (ºC).

The efficiency of the cooling systems was shown in Table 3.3. The same ambient air passes through all IHE, Pad 1, 2 and 3. The results indicate that the IHE alone was 93.8% efficient in reducing the ambient temperature and combination of IHE and Pad 1 can perform 97.27% efficient. The result gives a direction that combination of IHE and Pad 1 or Pad 2 can produce reasonable reduction in temperature of ambient air to a minimum temperature approaching wet bulb temperature of the ambient air. The relative efficiencies after Pad 2 and 3 might be due to the use of the same ambient wet-bulb temperature to see how efficiencies changed from IHE to Pad 3.

Table 3.3 Cumulative cooling efficiencies of the indirect heat exchanger (IHE) and three charcoal cooling pads (Pads 1, 2 and 3)

Cooling method	$T_{db,inlet}$ (°C)	$T_{db,outlet}$ (°C)	$T_{wb,inlet}$ (°C)	Efficiency (%)
IHE	34.10	23.22	22.50	93.80
Pad 1	23.22	22.82	22.50	97.27
Pad 2	22.82	22.37	22.50	101.12
Pad 3	22.37	21.86	22.50	105.52

The dry-bulb temperature and relative humidity of the indirect heat exchanger (IHE) and cooling pads (Pads 1, 2 and 3) is demonstrated in Figure 3.8. It can be seen from Figure 3.8 that a decrease in temperature was observed, while an increase in RH from IHE to Pad 3 was observed.

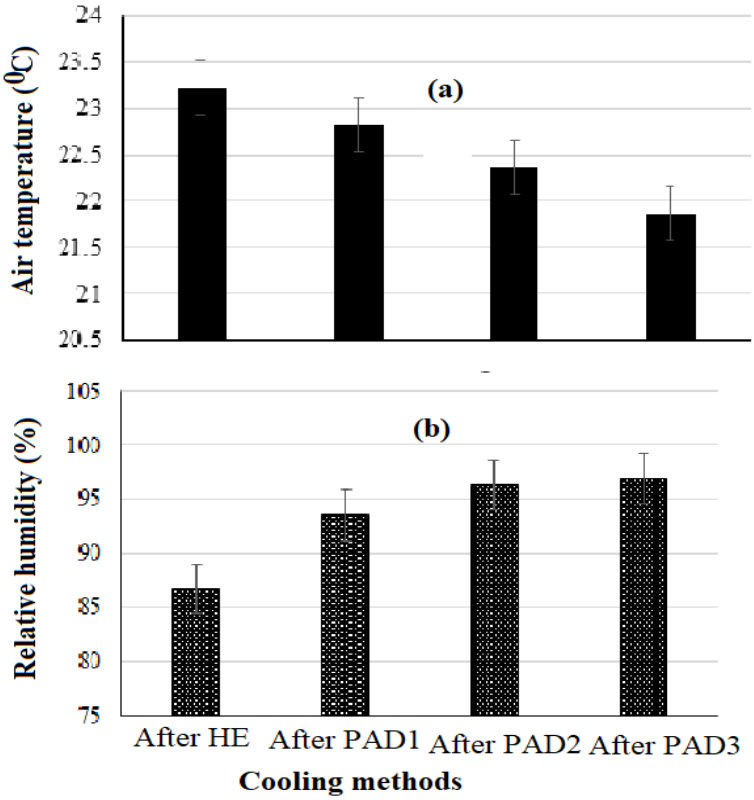

Figure 3.8 Dry-bulb temperature (a) and relative humidity (b) of the indirect heat exchanger (HE) and the cooling pads (Pads 1, 2 and 3) of the evaporative cooling pad tunnel

3.4 Conclusions

Compared to the ambient air conditions, the EC reduced the temperature by 10 ±1°C, while the CoolBot air conditioner reduced the ambient air by 28±1°C. The simultaneous operation of both the EC and CBAC systems reduced the air temperature to a range of 8 to 13°C. The results indicate that the CBAC reduced the inside air temperature by 17 ±1°C, when compared to the EC storage system. Therefore, the CBAC alone had the capacity to reduce the storage temperature to as low as 6°C, which is a favorable air temperature for the storage of most of the tropical fruit and vegetables. Moreover, the CBAC cooling enables to control of temperature for the specific storage requirements of fruit and vegetable, since it has an in-built control system. However, the air RH removed by the EC was to be higher, compared to that of the RH of air achieved by CBAC operation system, which is recommended for fresh produce storage. The RH of the combined EC+CBAC system operation was maintained within the optimum required for fresh produce storage, but there was a slight fluctuation inside. The fluctuations in RH was due to the mixing effects of air by the fan and air conditioner inside the storage chamber. The simultaneous cooling operation might not be feasible, due to the energy

consumption implications. The results indicate that the CBAC cooling system alone can maintain the lower temperature of the empty room, by reducing it to 6°C from an ambient maximum temperature of 34.1°C. The RH was decreased to about 75%, which is not recommended for fruit and vegetable storage. Therefore, the CBAC, EC+CBAC and EC cooling operations can be recommended in decreasing order of their performance to reduce the temperature of the empty storage to an optimum temperature for most tropical and sub-tropical fruit and vegetables. This study was performed for using unloaded cold store subjected to three different cooling approaches. Thus, further study using fully load stores subjected to cooling, using different techniques, is critical to determine the optimum cooling capacity for different fresh produces. In addition, it is recommended that further study on the use of computational fluid dynamics modelling and simulation of air temperature, RH, airflow, heat and mass transfer associated with psychrometric unit and inside the store are required, at micro - level, for the optimisation of the air flow inside the proposed low-cost cooling technologies and their combinations.

3.5 Acknowledgements

We gratefully acknowledge the Federal Ministry of Education of Ethiopia for its research grant support and the South African National Research Fund (NRF-TWAS) for its scholarship grant (Reference Number: SFH150902141138). The host institute, University of KwaZulu-Natal, is warmly acknowledged for its support.

3.6 References

Ahumada, M and Cantwell, M. 1996. Postharvest studies on pepino dulce (Solanum muricatum Ait.): maturity at harvest and storage behavior. *Postharvest Biology and Technology,* 7**,** 129-136.

Barman, K, Ahmad, MDS and Siddiqui, MW. 2015. Factors affecting the quality of fruits and vegetables: Recent understandings. *In:* Siddiqui, MW (ed.) *Postharvest Biology and Technology of Horticultural Crops: Principles and Practices for Quality Maintenance.* Ch. 1, 1-49. Apple Academic Press and CRC Press Taylor and Francis Group, Canada.

Bill, M, Sivakumar, D, Korsten, L and Thompson, AK. 2014. The efficacy of combined application of edible coatings and thyme oil in inducing resistance components in

avocado (Persea americana Mill.) against anthracnose during post-harvest storage. *Crop Protection,* 64**,** 159-167.

Boyette, MD and Rohrbach, RP. 1993. A low-cost, portable, forced-air pallet cooling system. *Applied engineering in agriculture,* 9**,** 97-104.

Cantwell, M, Flores-Minutti, J and Trejo-González, A. 1992. Developmental changes and postharvest physiology of tomatillo fruits (Physalis ixocarpa Brot.). *Scientia Horticulturae,* 50**,** 59-70.

Cantwell, M and Kader, AA. 1992. Postharvest technology of horticultural crops. *Postharvest technology of horticultural crops*.

Cantwell, MI and Kasmire, RF. 2002. Postharvest handling systems: fruits and vegetables. *In:* Kader, AA (ed.) *Postharvest technology of horticultural crops.* Cha. 33, 407-422. University of California Agriculture and Natural Resources, University of California, USA.

Chourasia, MK and Goswami, TK. 2007. CFD simulation of effects of operating parameters and product on heat transfer and moisture loss in the stack of bagged potatoes. *Journal of Food Engineering,* 80**,** 947-960.

Clark, BM. 2006. Climate change: A looming challenge for fisheries management in southern Africa. *Marine Policy,* 30**,** 84-95.

Dermesonlouoglou, E, Giannou, V and Tzia, C. 2016. Chilling. *In:* Vadiee, A and Tzia, C (eds.) *Handbook of Food Processing: Food Preservation.* Ch. 6, 223-258. CRC Press, Taylor and Francis Group, New York, USA.

El-Dessouky, H, Ettouney, H and Al-Zeefari, A. 2004. Performance analysis of two-stage evaporative coolers. *Chemical Engineering Journal,* 102**,** 255-266.

Gerlach, DW. 2015. Evaporative cooler including one or more rotating cooler louvers. USA, US 8,943,851 B2.

Kitinoja, L. 2013. *Use of cold chains for reducing food losses in developing countries.* The Postharvest Education Foundation, University of California, La Pine, Oregon, USA.

Kitinoja, L, Alhassan, HA, Saran, S and Roy, SK. 2010. Identification of appropriate postharvest technologies for improving market access and incomes for small horticultural farmers in Sub-Saharan Africa and South Asia. XXVIII International Horticultural Congress on Science and Horticulture for People (IHC2010): International Symposium, 31-40. Acta Horticulture.

Kitinoja, L and Cantwell, M. 2010. *Identification of Appropriate Postharvest Technologies for Improving Market Access and Incomes for Small Horticultural Farmers in Sub-Saharan Africa and South Asia, BMGF Grant Number-52198.* University California, USA.

Kitinoja, L and Thompson, JF. 2010. Pre-cooling systems for small-scale producers. *Stewart Postharvest Review,* 6**,** 1-14.

Mirade, PS. 2007. CFD modeling of indoor atmosphere and water exchanges during the cheese ripening process. *In:* Sun, DWE (ed.) *Computational fluid dynamics in food processing.* CHa. 28, 697-726. CRC Press and Woodhead Publishing Ltd, Cambridge.

Nimje, PM and Shyam, M. 1993. Effect of plastic greenhouse on plant microclimate and vegetable production. *Farming Systems* 9**,** 13–19.

Nunes, MCDN. 2008. *Color atlas of postharvest quality of fruits and vegetables.* Blackwell publishing, USA.

Paull, RE. 1999. Effect of temperature and relative humidity on fresh commodity quality. *Postharvest Biology and Technology,* 15**,** 263-277.

Paull, RE and Duarte, O. 2011. *Tropical fruits.* CAB International, Reading, UK.

Rodríguez, GRV, Salmerón-Ruiz, ML, Aguilar, GaG, Siddiqui, MW and Zavala, JFA. 2015. Advances in Storage of Fruits and Vegetables for Quality Maintenance. *In:* Siddiqui, MW (ed.) *Postharvest Biology and Technology of Horticultural Crops: Principles and Practices for Quality Maintenance.* Cha. 5, 193-216. Apple Academic Press and CRC Taylor and Francis Group, Canada.

Roy, SK. 2007. *Low or no-cost cool chambers for fruits and vegetables.* National Horticulture Mission, India.

Roy, SK and Pal, RK. 1994. A low-cost cool chamber: an innovative technology for developing countries. *In:* Champ, BR, Highley, E and Johnson, GI, eds. Postharvest Handling of Tropical Fruits: ACIAR Proceedings, 393-395. Australian Centre for International Agricultural Research, Australia.

Saran, S, Dubey, N, Mishra, V, Dwivedi, SK and Raman, NLM. 2013. Evaluation of coolbot cool room as a low cost storage system for marginal farmers. *Progressive Horticulture,* 45**,** 115-121.

Saran, S, Roy, SK and Kitinoja, L. 2010. Appropriate postharvest technologies for small scale horticultural farmers and marketers in Sub-Saharan Africa and South Asia-Part 2. Field trial results and identification of research needs for selected crops. *In:* Cantwell, MI and Almeida, DPF, eds. XXVIII International Horticultural Congress on Science and

Horticulture for People (IHC2010): International Symposium 41-52. Acta Horticulture, Lisbon, Portugal.

Sargent, SA, Talbot, MT and Brecht, JK. 1988. Evaluating precooling methods for vegetable packinghouse operations. *Eng. Sci*, 23**,** 1147-1155.

Smale, NJ, Moureh, J and Cortella, G. 2006. A review of numerical models of airflow in refrigerated food applications. *International Journal of Refrigeration-Revue Internationale Du Froid,* 29**,** 911-930.

Thompson, AK. 2003. Postharvest technology of fruits and vegetables. *In:* Thompson, AK (ed.) *Fruits and vegetables: harvesting handling and storage. Blackwell Publishing Ltd, Oxford.* 2nd ed, Cha. 12, 115-369. Blackwell Publishing Ltd, UK.

Thompson, JF, Mitchell, FG and Kasmire, RF. 2002. Cooling horticultural commodities. *In:* Kader, AA (ed.) *Postharvest technology of horticultural crops.* 3rd ed, Cha. 11, 97- 112. Agriculture and Natural Resources, University of California, USA.

Thompson, JF and Spinoglio, M. 1996. *Small-scale cold rooms for perishable commodities.* University of California, Division of Agriculture and Natural Resources, USA.

Workneh, TS. 2010. Feasibility and economic evaluation of low-cost evaporative cooling system in fruit and vegetables storage. *African Journal of Food, Agriculture, Nutrition and Development,* 10**,** 2984-2997.

4. EVALUATION OF AIRFLOW AND TEMPERATURE PROFILE CHARACTERISTICS ACROSS THE INDIRECT HEAT EXCHANGER AND MULTI-PAD EVAPORATIVE COOLER PSYCHROMETRIC UNITS

Abstract

A combination of a multi-pad and an indirect heat exchanger evaporative cooler was recommended for small-scale and immerging farmers to tackle the postharvest losses of fresh produce. The purpose of this study was to analyse the air flow and temperature profile through the psychrometric unit that was comprised of indirect heat and cooling wet pad heat exchangers. A computational fluid dynamics (CFD) model was applied to study the qualitative and quantitative air characteristics across the psychrometric unit. The air velocity vector was found to be 1 $m.s^{-1}$ at the exit of the unit (*i.e.* after Pad 1), small temperature change between inlet and outlet was achieved (0.6 ºC) and the static enthalpy of the air at the exit of the psychrometric unit was found to be 86.$kJ.kg^{-1}$. The result indicated that optimising air velocity at the inlet is critically important for reducing the temperature of the air to at least the wet-bulb temperature of the ambient air. The CFD model clearly shows how to solve the problem of the psychrometric unit to optimise the airflow, and, hence the temperature distribution, across the psychrometric unit.

Keywords: Air temperature, air velocity distribution, charcoal pad, enthalpy, indirect heat exchanger

4.1 Introduction

Mechanical refrigeration is reported to increase global warming and requires a high investment cost (Kapilan *et al.*, 2016). On the other hand, evaporative cooling is a low-cost cooling technology. It is also environmentally friendly and applicable in arid and semi-arid, hot and dry climate regions for the extension of the shelf-life of fruit and vegetables (Workneh, 2010). As a result, air with a high temperature and a low relative humidity evaporates more water than cold and moist air, hence reducing the air temperature after the evaporation of the moisture. The direct evaporative cooler gives an added advantage over the air environment conditioning, by increasing the relative humidity, which is an advantage for extending the shelf-life of fresh produce (Kapilan *et al.*, 2016). In non-arid climate regions, indirect evaporative cooling is advantageous, because it keeps the RH constant (Kapilan *et al.*, 2016). The wet pad surface and the dry and unsaturated air blown through the pad release the heat of vaporization which is scattered into the air as water vapor, and finally the air temperature is reduced and the RH is increased after passing through the pads (Vala *et al.*, 2014; Kapilan *et al.*, 2016). This is cooled by evaporation of water, which removes the heat of vaporization and the sensible heat from air consumes less energy than mechanical refrigeration cooling (Kapilan *et al.*, 2016).The evaporative cooling system is efficient during the summer, when cooling is important for the pre-cooling of fresh produce (Thompson *et al.*, 2002; Kapilan *et al.*, 2016). This cooling method is reported to be an alternative to the expensive and unaffordable mechanical refrigeration cooling system in arid and semi-arid regions, especially for cooling in summer (Gunhan *et al.*, 2007; Kapilan *et al.*, 2016). A multiple consecutive cooling pad arrangement was assumed to reduce the temperature of the blown air more (Kapilan *et al.*, 2016). Different cheap and easily-available pad materials, including charcoal, were used as water adsorbents to keep the surface wet for a longer period during the evaporative cooling of the air (Liberty *et al.*, 2013). The cooling efficiency and effectiveness of evaporative cooling pads is dependent on the environmental climatic conditions (Chaudhari *et al.*, 2015). A fast evaporation rate of the water from the wet pads and the maximum cooling effect of the cold air can be achieved (Chaudhari *et al.*, 2015).

The recent availability of computers has made the computation and simulation of time-consuming and complex fluid dynamics problems easy (Norton and Sun, 2006). Computational fluid dynamics (CFD) models require a high performance computer for modelling and to solve fluid flow problems (Norton and Sun, 2006). Franco *et al.* (2011) recommended that CFD

models are appropriate tools for the simulation and modelling of cooling processes of cooling pads for green houses. Kapilan *et al.* (2016) modelled two evaporative cooler pads and verified that the computation of the temperature and relative humidity was accurate. A charcoal pad was assumed to be a porous medium. The porous media approach was applied by several researchers to characterize the fluid dynamics, using CFD models (Nield and Bejan, 2013). The fine charcoal pack was characterized and the physical properties were determined by Venu *et al.* (2014). A charcoal of a 2-3 cm bulk-like structure was used and the properties were determined. Accordingly, the water-holding capacity, the bulk density, the true density and the porosity of the charcoal were reported to be 69.1%, 85.66 $kg.m^{-3}$, 217.66 $kg.m^{-3}$, and 60.66%, respectively (Venu *et al.*, 2014).

The cooling rate of the heat exchanger and cooling pads can be affected by the airflow resistance (pressure drop) characteristics of the heat exchanger and charcoal pack. The pressure drop (air flow resistance) across the wet pads increased with the increase of the cooling pad thickness and the air speed can affect the cooling process (Yadav *et al.*, 2002). In the case of the indirect heat exchanger, the air and the cooling medium (cold water) have no contact, hence, there is no change in the absolute humidity of the cooling air (Tripathi and Lawande, 2010). On the other hand, for direct evaporative cooling pads, the water and the pads have direct contact. As a result, there is an increase in the relative humidity and absolute humidity of the final cooled air. The temperature is reduced to approach the wet bulb temperature (Tripathi and Lawande, 2010; Xuan *et al.*, 2012). The cooling process is accounted for by the removal of the latent heat of vaporization from the surface of the wet pads to the environment.

Kovačević and Sourbron (2017) produced a numerical model for a single metallic and compact direct evaporative cooler for outlet air characterization and water consumption by the pad. However, the combination of an indirect heat exchanger and multi-stage direct cooling pads was suggested, for the more effective cooling of the air (Yadav *et al.*, 2002). The air cooling process was accounted for by the removal of latent heat of vaporization from the surface of the wet pads to the environment. The heat loss from the heat exchanger is ideally equal to the heat gained by the cooled air. Moreover, the heat of vaporization from the water was assumed to be lost from the wet air passing through the charcoal wet pads. The rate of heat transfer for a well-insulated indirect heat exchanger can be calculated by the following Equation 4.1 (Çengel, 1998).

$$\dot{Q} = \dot{m}_a C_a \Delta T_a \quad (4.1)$$

To calculate the heat transfer rate of the cooling pads, the mass of water evaporated was considered and multiplied by the heat of vaporization, as indicated in Bergman *et al.* (2011) (Equation 4.2):

$$\dot{Q} = \dot{m}_v h_v \quad (4.2)$$

Where:

$\dot{Q}$ = the heat transfer rate ($W.m^{-2}$),

$\dot{m}_a$ = the rate of mass transfer ($kg.m^{-2}.s^{-1}$),

$\dot{m}_v$ = the rate of mass transfer of water vapor ($kg.m^{-2}.s^{-1}$),

h_v = the heat vaporization of water ($kJ.kg^{-1}$),

C_a = the specific heat capacity of air ($J.kg^{-1}.K^{-1}$), and

ΔT = the change in temperature (K).

The cooling capacity of wet pads is dependent on the ambient air temperature, relative humidity, surface area, evaporative media and air velocity (Gunhan *et al.*, 2007; Fabiya, 2010). Literature shows that there are not too many studies on the airflow characteristics across the fan-indirect heat exchanger and charcoal pads (Gunhan *et al.*, 2007; Fabiya, 2010). This study, therefore, aims to explore the capacity of the fan to blow the air through the indirect heat exchanger and the pad psychrometric unit tunnel, using CFD model.

4.2 Materials and Methods

4.2.1 Cooling pad and heat exchanger arrangements

A cooling tunnel was comprised of one indirect heat exchanger (IHE), with model number M14-120SB1 and three direct cooling pads (Pad 1, 2 and 3), as shown in Figure 4.1. Cold water from buried underground water tank circulates through IHE. The purpose of the heat exchanger was to maintain the level of moisture of the air, while reducing the air temperature. The IHE was constructed from copper tube with a diameter of 12.7 mm, and a height of 336 mm, which was coiled to produce a length of 356 mm and a thickness of 51 mm enclosed inside the fins of aluminum and covered by stainless steel. The dimensions (L × W × H) of the cooling pads are 160 mm × 380 mm × 380 mm, respectively. The psychrometric unit was established at the

Ukulinga Research Station of the University of KwaZulu-Natal, South Africa (24°24′E, 30°24′S) (Tolesa *et al.*, 2018). The pads were filled with coarse charcoal (2 to 3 mm) in a mesh of 5 mm x 5 mm wire and they were continuously wetted by water flowing through, to ensure the evaporative cooling process at the charcoal-water-interface, hence, the wet charcoal pad is treated as a porous medium for the simulation.

An axial exhaust fan (Fan 1) at the inlet of the IHE, with a capacity for blowing the air through the tunnel, was 0.218 $m^3.s^{-1}$, where the air changes took place (Workneh *et al.*, 2012). The reservoir was a 250 L plastic tank buried underground, to keep the temperature of the reservoir water low. The continuous water pump with a capacity of 0.115 $m^3.s^{-1}$ was used (Workneh *et al.*, 2012). The outlet of the psychrometric unit was fitted with a fan (Fan 2), and the axial fan that pushed the cold air into the cold room (inlet of the room) had an external diameter of 350 mm, with the capacity of 0.218 $m^3.s^{-1}$ air changes per second. To achieve the lowest temperature in the cooling pad, the following parameters were set, as reported by Thompson and Spinoglio (1996). The parameters includes fan capacity i.e. 4.25 $m^3.min^{-1}$ for 0.09 m^2 pad, the fan should have ability to remove the air completely from the storage room every 2 minutes. The water pump to circulate water to wet the pads should have the capacity to pump 0.0004 $m^3.min^{-1}.m^{-1}$ of pad length. The water thank should have the capacity of 0.016 $m^3.m^{-1}$ of pad length. The constant water flow was maintained by a float valve. Small amount of water should be drained continuously to prevent salt blockage to wet the pads.

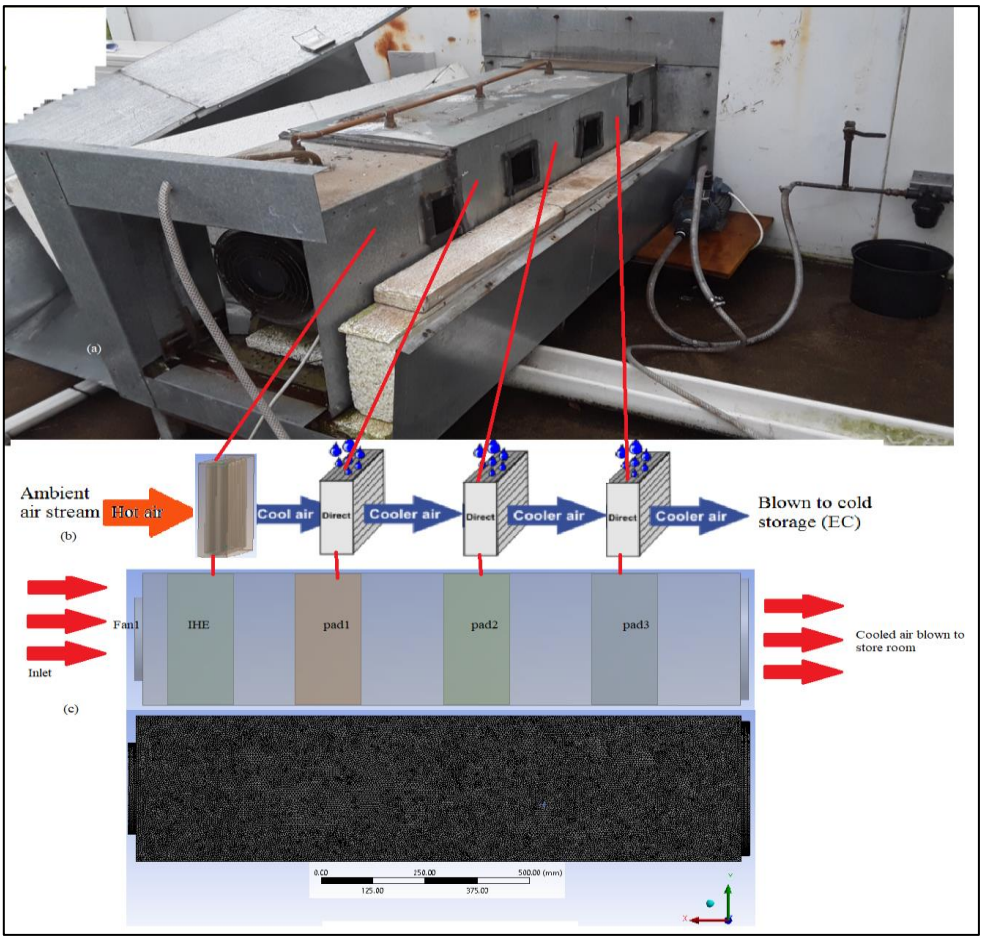

Figure 4.1 The skeleton of the psychometrics unit tunnel constructed from one indirect heat exchanger (IHE) and three direct cooling pads (Pad 1, 2 and 3) (a) structural schematic, (b) arrangements and (c) the geometry and mesh arrangements

4.2.2 Computational parameters for the psychrometric units

The input values of CFD models for the charcoal pads and indirect heat exchanger were sourced from literature and used in this analysis. Pressure drop across the charcoal pad-related geometries of different materials, as well as the porosity, water adsorption and density for the charcoal pads were characterized by several researchers (Gunhan *et al.*, 2007; Venu *et al.*, 2014). The experimental data of temperature, RH and air velocity were used for the model boundary and validation process. To represent the cooling pad, the porous medium approach was used to simulate the charcoal-filled rectangular box pads and the heat exchangers (Zhao *et al.*, 2016). Since there is no pressure drop test for charcoal in literature, the pressure drops for similar geometry materials (volcanic tuff and pumice stones) was used to estimate the quadratic and linear terms of the pressure drop coefficients at different air velocities (Gunhan *et al.*, 2007).

The porous media model parameters were considered, by taking into account the indirect heat exchanger, the charcoal and the entrained air inside the packs and by using the average material properties of the porous domain (Dehghannya *et al.*, 2010; Zhao *et al.*, 2016). The parameters of the air resistance characteristics from literature were used for the analysis

4.2.3 Numerical modelling

Mathematical models

The evaporation pad materials were considered as a porous medium through which a cross flow of water and air takes place. The energy and mass balance between the air flow and wet charcoal pads can be calculated by Equations 4.3 to 4.5 (Liao and Chiu, 2002; Franco *et al.*, 2014; Kovačević and Sourbron, 2017). Most of the physical air parameters that are determined form the psychrometric moist air properties of moist air at the inlet and outlet of the IHE and pads.

$$q = m_a C_{pa}(T_1 - T_2) + m_a(W_1(h_{va} - h_{wb}) - W_2(h_{v2} - h_{wb}) \quad (4.3)$$

$$\Delta \dot{m}_e = \dot{m}_a(W_2 - W_1) \quad (4.4)$$

$$w = \frac{m_v}{m_a} \quad (4.5)$$

Where:

q = the heat transfer flow (W),

m_a = the mass of inlet air to the pads (kg h^{-1}), which can be expressed by $m_a = \rho_a \times q_a$,

ρ_a = the density of dry air (kg.m^{-3}),

m_a = the air flow rate through the cooling pad ($m^3.h^{-1}$),

m_e = the mass of water evaporated (kg.h^{-1}),

C_{pa} = the specific heat of dry air (kJ.$Kg^{-1}.K^{-1}$),

T_1 = the dry bulb temperature of the inlet ambient air (°C),

T_2 = the dry bulb temperature of the exit air from the pads and HE (°C),

h_{v1} and h_{v2} = the enthalpy of saturated water vapour at the inlet and outlet of the pads, respectively (kJ.Kg^{-1}),

h_{wb} = the enthalpy of saturated water vapor at the wet-bulb temperature (T_{wb}) (kJ.Kg^{-1}),

W = the absolute humidity ratio ($kg_w.kg_a^{-1}$), and

W_1 and W_2 = the absolute humidity ratios of the air at the inlet and outlet of the cooling pads, respectively ($kg_w.kg_a^{-1}$).

The latent heat of evaporation (q_{ev}) from cooling pad can be approximated as the product of evaporative water mass flux and latent heat of vaporization (h_{fg} = 2257 $kJ.kg^{-1}$) (Bergman *et al.*, 2011):

$$q_{ev} = m_e h_{fg} \tag{4.6}$$

Alternatively, heat transfer rate (q) through the pads can be expressed as:

$$q = h_H A_S \Delta T \tag{4.7}$$

$$m_e = h_M A_S \Delta \rho_v \tag{4.8}$$

Where:

h_H = the heat transfer coefficient ($W.m^{-2}.K^{-1}$),

h_M = the mass transfer coefficient ($m.s^{-1}$),

A_S = the contact surface area of the material (m^2), and

ΔT = the mean logarithmic temperature difference (K)

To estimate the pressure drop across the porous media (IHE and cooling pads), a combined Darcy-Forchhheimer equation can be used, from which the quadratic and linear coefficients are estimated (van der Sman, 2003; Verboven *et al.*, 2006; Rawangkul *et al.*, 2008):

$$\Delta P = -\frac{\mu}{k}\vec{u} - \beta\rho|u|\vec{u} \tag{4.9}$$

Where:

ΔP = the pressure drop across the thickness of the obstacle ($Pa.m^{-1}$),

μ = the dynamics viscosity of air (fluid) ($kg.m^{-1}.s^{-1}$),

κ = the permeability of the porous medium (IHE and pads) (m^2),

u = the superficial velocity ($m.s^{-1}$), and

β = the Forchheimer coefficient (m^{-1}).

Governing equations

The current study describes the porous medium approach, as indicated by Zhao *et al.* (2016). The cooling pads were comprised of the indirect heat exchanger zone, the pads zone and the air zones, which created the heterogeneous and continuous porous medium. The porous medium approach is advantageous in avoiding the small details of stack geometry and applies the averaged Reynolds Average Navier-Stokes equation (Equations 2.1 to 2.5) to solve the fluid flow problems (Sapounas *et al.*, 2016; Zhao *et al.*, 2016; Getahun *et al.*, 2017). The porous media approach solves the difficulty in the precision geometry design (Ambaw *et al.*, 2013).

4.2.4 Model parameters

The porous medium model parameters were considered, by taking into account the indirect heat exchanger, the charcoal and the entrained air inside the packs and by using the average material properties of the porous domain (Dehghannya *et al.*, 2010; Zhao *et al.*, 2016). The parameters of the air resistance characteristics from literature were used for the analysis.

4.2.5 Boundary and initial conditions set-up

Though the walls of the psychrometric unit (indirect heat exchanger and pad-evaporative cooler) was insulated, it was in contact with the ambient atmospheric air of the walls as its boundary condition. Inside the psychrometric unit boundaries were the porous domains, which included the indirect heat exchanger, the charcoal pad and the remaining free air zones considered as a fluid domain (air). The cooling unit was represented by the temperature and velocity boundaries at the inlet of the cooling system. The internal walls of the psychrometric tunnel were set as no slip walls and it was assumed that there would be no heat exchange with environment, due to the insulation.

4.2.6 Simulation set-up

From the experimental set-up, the second and third pads contributed only a small temperature change. Hence, Pads 2 and 3 were avoided in the simulation. Only the effects of indirect heat exchanger and Pad 1, on the temperature distribution along the tunnel towards the cold room, were simulated. The domains of all models were discretised by tetrahedral elements meshing.

The level of grid independency was evaluated by using the Richardson extrapolation method (Roache, 1994; Franke, 2007).The commercial Academic ANSYS CFX 17.0 (ANSYS, Canonsburg, PA, USA) was used for the simulation, together with finite volume method, to solve the numerical problem of the indirect heat exchanger and the cooling pad. The CFX is available within the ANSYS Workbench, uses advanced technologies with algebraic multigrid solvers and has effective parallelization that could assist with quick simulation (Kapilan *et al.*, 2016). Turbulence was considered by applying the SST (k-ε) model. The time step size of 0.025 s, with total time of 5 s, was used to evaluate the transient temperature profile across the IHE and Pad 1. The SIMPLE discretization approach was used for the coupling of the porous media pressure velocity and second order upwind discretization was applied for the momentum, specific dissipation rate and energy computation (Roache, 1994). Steady state simulation was performed to evaluate the airflow. The steady state solutions were used as an initial value for the subsequent transient simulation in order to study the temperature profile. The full simulation took between 30 minutes and two hours to come to convergence on a 64-bit, Dell Precision Tower 5810, Intel Xeon CPU E5-16600v4 @ 3.20 GHz 3.20GHz and 32GB RAM, Windows 10 Pro PC.

4.2.7 Simulations

The airflow and temperature distributions inside the psychrometric tunnel were simulated. A validation of the airflow and temperature distribution models was performed by comparing the experimental air velocity at the exit of Pad 1. Since, the air velocity at the inlet of the psychrometric unit was constant and was set at 2 $m.s^{-1}$. Assumptions for the heat exchanger and Pad 1 were made, so that both were insulated and there was no heat exchange from and to the environment.

4.3 Results and Discussion

The heat flux for the indirect heat exchanger and cooling pads were calculated from the psychrometric chart of the moist air and thermodynamic constants (Table 4.1). The calculated heat fluxes were used for input during the simulation of heat transfer. The heat gain or loss was estimated using Equations 4.2 and 4.3. Since there were small changes in the temperature after Pads 2 and 3 (Table 4.2), only the indirect heat exchanger and Pad 1 were simulated for the air and temperature distribution study.

Table 4.1 Heat fluxes of indirect heat exchanger and the charcoal cooling pads, which were estimated from the thermodynamic and psychrometric properties

Item	Heat flux ($W.m^{-2}$)	Heat flux ($W.m^{-3}$)
Indirect heat exchanger	25.4490	318.1121
Pad 1	16.8205	105.1282
Pad 2	8.4689	52.93081
Pad 3	2.8230	17.6436

Table 4.2 Cooling Pad and indirect heat exchanger data collected from the experimental set-up

Expression	Expression definition	Detailed information
Ambient air	Maximum T = 34.1 (ºC), Minimum RH = 40 %	Average temperature = 28.14ºC
Heat Exchanger (IHE)	Heat exchanger used for air cooling after fan 1 T_{Inlet} =34.1ºC, T_{Outlet} = 23.22ºC RH_{Inlet} = 40.7%, RH_{Outlet} = 86.73% Airflow rate = 0.108 $kg.s^{-1}$ Heat flux gained = 25.4490 $W.m^{-2}$ $V_{AfterHE}$ = 1.43 $m.s^{-1}$	Continuous cooling of the outside air cooled by the heat exchanger to prevent more RH addition to the air from the cooling water
Pad 1	T_{Inlet} = 23.22ºC, T_{Outlet} = 22.82ºC RH_{Inlet} = 86.73%, RH out = 93.6% Mass Flow = 0.007452595 $kg.m^{-2}.s^{-1}$ Heat flux (latent heat of vaporization) = 16.82051 $W.m^{-2}$	Temperature and RH of air at the outlet of Pad 1
Pad 2	T_{Inlet} = 22.8164ºC, T_{Outlet} = 22.3707ºC RH_{Inlet} = 93.6 %, RH out = 96.3 % Mass Flow = 0.003752 $kg.m^{-2}.s^{-1}$ Heat flux (latent heat of vaporization) = 8.4689 $W.m^{-2}$	Temperature and RH of air at the outlet of Pad 2
Pad 3	T_{Inlet} = 22.3707 ºC, T_{Outlet} = 21.8598 ºC RH_{Inlet} = 96.3 %, RH out = 96.9 % Mass Flow = 0.001251 $kg.m^{-2}.s^{-1}$ Heat flux (latent heat of vaporization) = 2.822977 $W.m^{-2}$	Temperature and RH of air at the outlet of Pad 3
T_{Tol}	1 K	Temperature tolerance
TStep	10 s	Time step size
TTotal	300 s	Total time
VInlet	2 $m.s^{-1}$	Air speed at the inlet (Fan1) was used for simulation validation

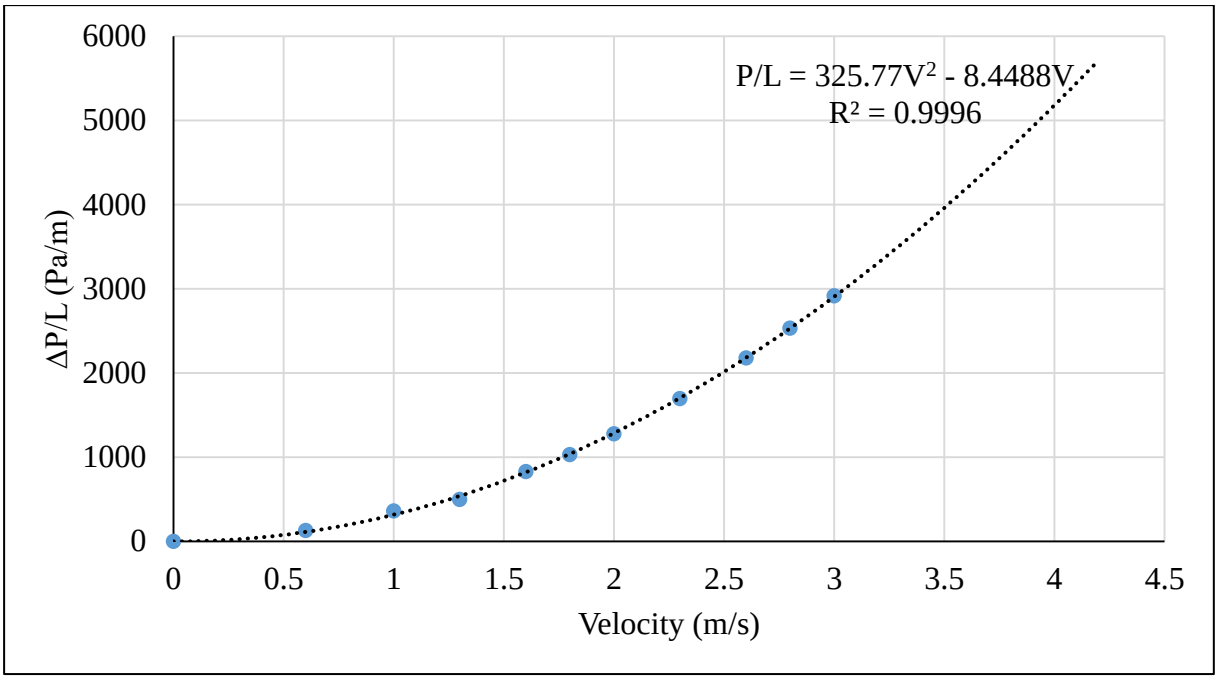

Figure 4.2 Pressure drop across the coarse pumice stones, which is similar geometry to a charcoal pad, at 2 $m.s^{-1}$ of inlet air velocity (V)

The coefficients of Darcy-Forchhmeir for the indirect heat exchanger and pads were estimated from pressure drop equation and are displayed in Table 4.3.

Table 4.3 The pressure drop and the coefficients of Darcy-Forchhmeir

Item	K (m^{-2})	β (m^{-1})
Indirect heat exchanger	5.07 x 10^6	1.30184
Pad1	4.26 x 10^5	0.2996
Pad2	5.15 x 10^5	0.0259
Pad3	6.21 x 10^6	0.0264

Figure 3.8b in section 3.3.2 shows that there were no significant changes in temperature after Pads 1 and 2, but a small increase in the RH was found i.e. from Pad 1 to Pad 2 about 3%, between Pad2 and Pad 3 about 0.6% increase in RH observed. Therefore, the combination of one heat exchanger and one charcoal cooling Pad 1 was analyzed for air temperature distribution. The experiment was validated, based on the airflow of 2 $m.s^{-1}$. Hence, we can recommend that only one indirect heat exchanger and one charcoal cooling pad will be enough to achieve the required optimum temperature reduction. The streamlines and contours displayed in Figure 4.3 (a - b) show that the air velocity across the IHE and Pad 1 was decreasing and that

approximately 1 m.s^{-1} air velocity dominated at the exit of the pad, which clearly demonstrated that there was an insufficient air velocity at the exit of Pad 1 (Thompson, 2016). CFD modelling is reported to be a powerful tool for understanding the air movement and distribution across the cooling pads and inside the green house (Rui *et al.*, 2011). Therefore, the results show that Fan 1 is not sufficient to blow the air through the psychrometric unit arrangement. It was shown that the CFD model can also help to improve the design of the rooms, to ensure a uniform air distribution, thus improving the system's efficiency (Rui *et al.*, 2011). Therefore, the further simulation and screening of air speed values is required.

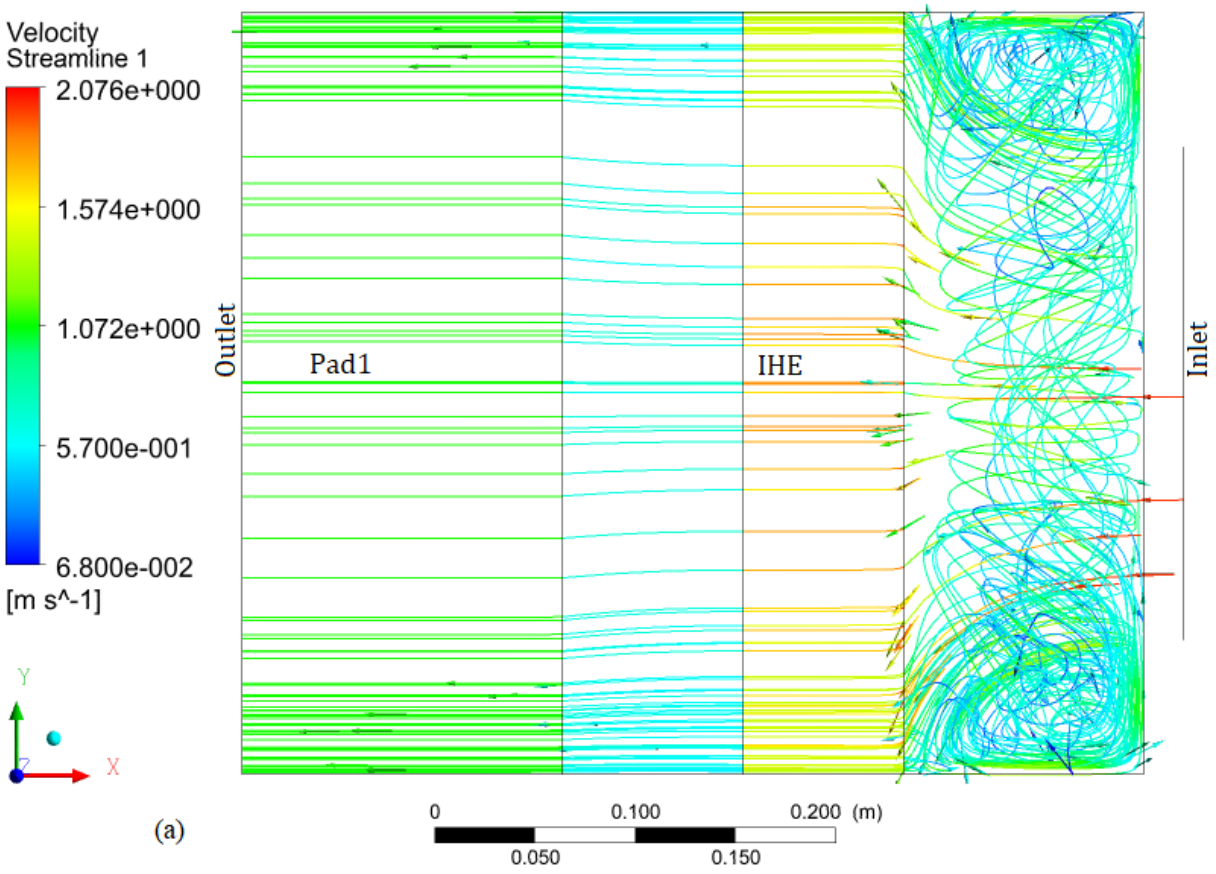

(a)

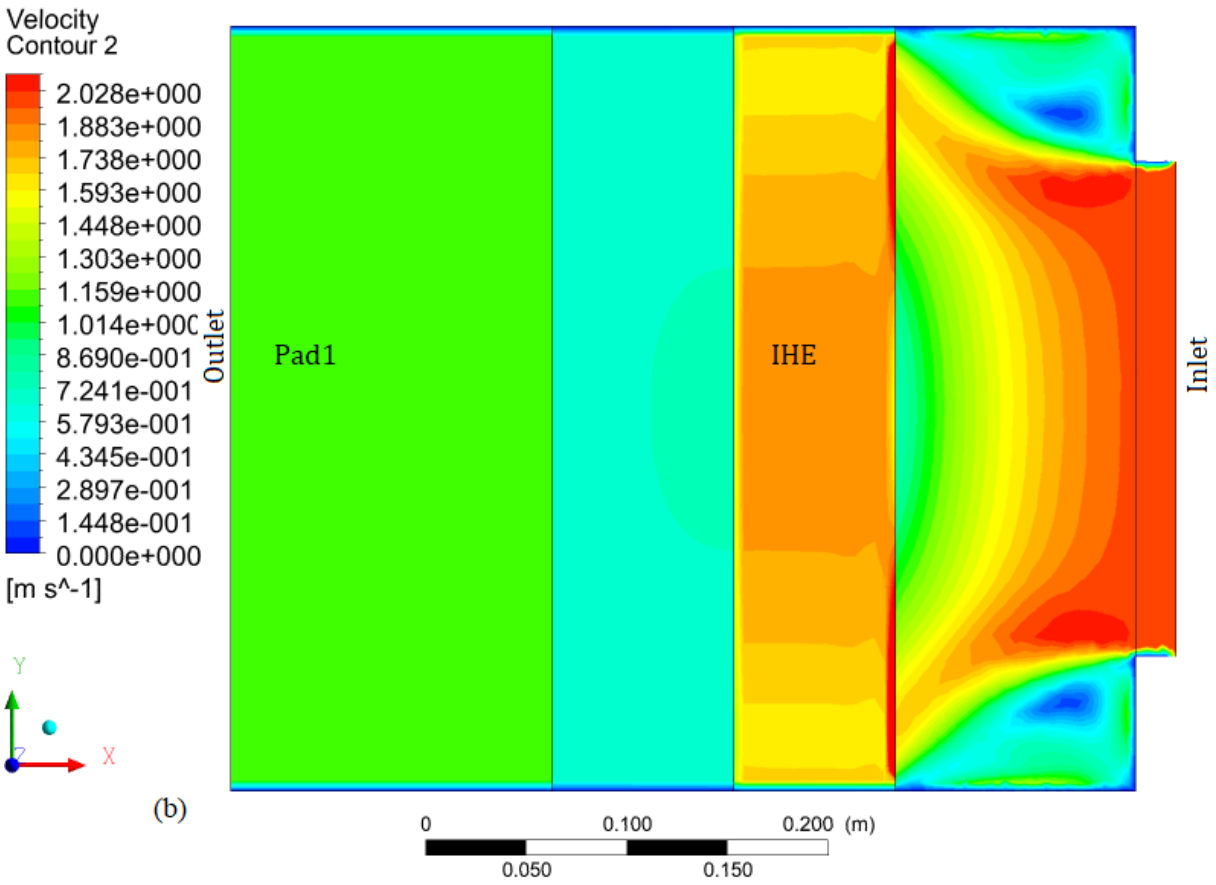

Figure 4.3 Air velocity streamline (a) and contours (b) across the indirect heat exchanger (IHE) and Pad 1 at 2 m.s^{-1} of inlet air velocity

The transient temperature and enthalpy at a 0.025 s step and a total time of 5 s, are displayed in Figure 4.4 (a - b) and help to understand the temperature and energy evolution. The results showed that the air temperature from the indirect heat exchanger side to the outlet (Pad 1) varied between 34.1ºC and 33.5ºC, which is a very small temperature change. On the other hand, the enthalpy across the tunnel, from the inlet to the exit, varied from 86 to 92 kJ.kg^{-1}. The result clearly shows that there is a need for more cooling to achieve a lower temperature at the exit of the tunnel (Pad 1). The cooling efficiency of evaporative cooling is fundamentally dependent on the airflow. The higher the air velocity, the more latent heat is removed from the pads through vaporization, which lowers the temperature of the air that passes through. Therefore, an air velocity higher than 2 m.s^{-1} is required to achieve more efficient cooling of the air blown through the tunnel. Hence, the optimization of air velocity is required to improve the pre-installed psychrometric unit investigated by this experiment.

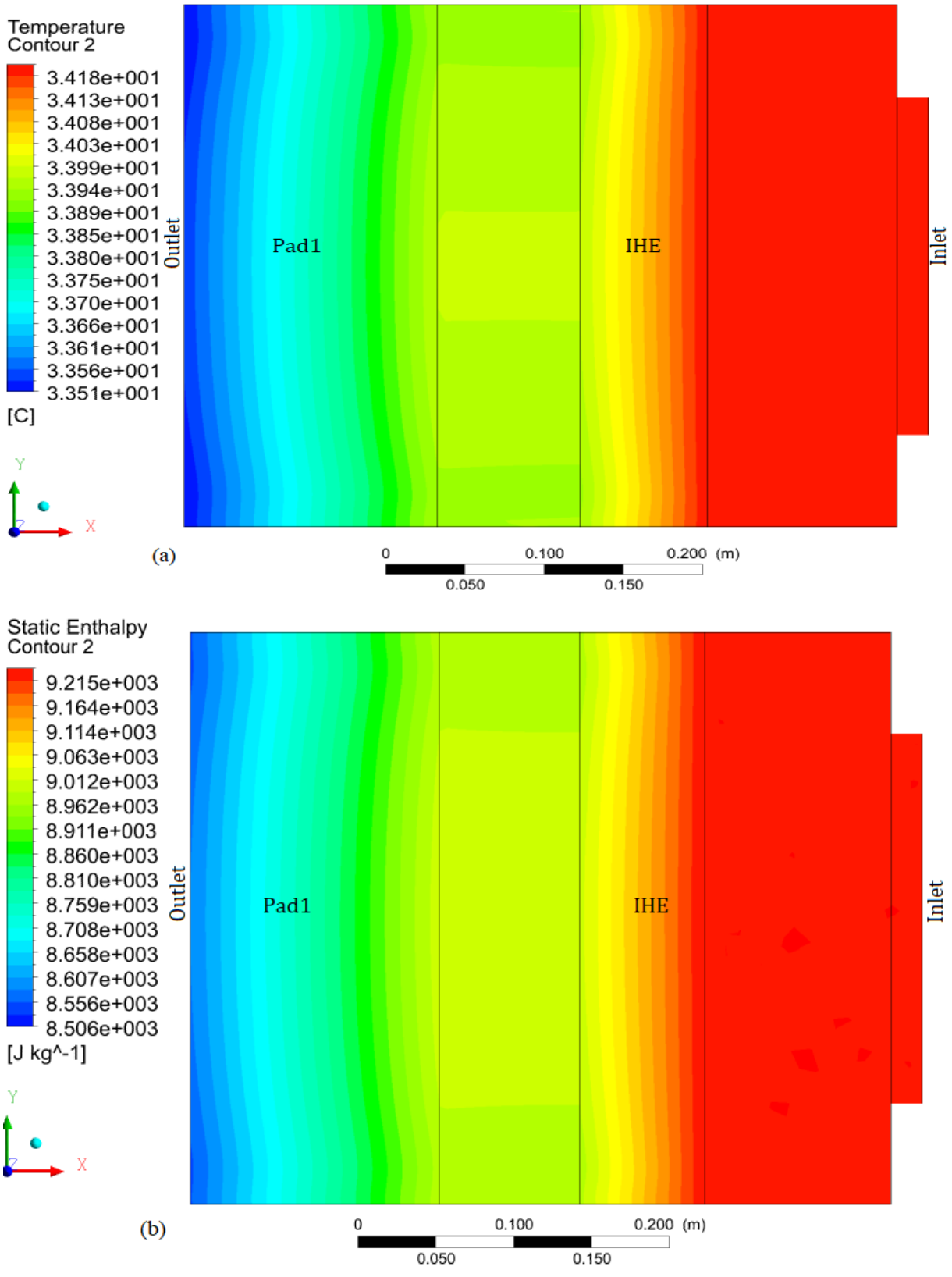

Figure 4.4 Transient state temperature contour (a) and static enthalpy contour (b) across the indirect heat exchanger (IHE) and wet Pad 1

4.3.1 Model validation

The model was validated by comparing the air speed at the outlet of Pad 1. The experimental air speed was found to be 0.8 $m.s^{-1}$, while an air velocity of 1.0 $m.s^{-1}$ was found from the simulation.

4.4 Conclusions

In conclusion, the psychrometric unit, with one indirect heat exchanger (IHE) and one charcoal pad (Pad 1), was investigated for an airflow and temperature profile across the cooler tunnel. The fan blowing air at 2 $m.s^{-1}$ was found to be not strong enough to push the air through the psychometric unit and to maintain the required optimum air properties at the outlet of the cooling unit. The air velocity achieved after pad1 was found to be 1 $m.s^{-1}$. On the other hand, the change in air temperature and enthalpy across the psychrometric unit were found to be 3.5ºC and 86 $kJ.kg^{-1}$, respectively. The temperature change was found to be very small, which demonstrates that the air flow through the psychrometric unit was good enough to cool the air temperature and near enough to the ambient air wet-bulb temperature. The study demonstrated the importance of CFD modelling for identifying the capacity of the psychrometric unit in conditioning the air before it enters the effective storage chamber. The results reported in this study demonstrated that further study is required to determine the optimization of airflow and heat transfer, with the help of a hybrid indirect and direct wet pad heat exchanger.

4.5 Acknowledgements

We would like to warmly acknowledge the Federal Ministry of Education, Ethiopia. South African National Research Foundation (NRF – TWAS) and the host institute, University of Kwa-Zulu Natal.

4.6 References

Ambaw, A, Verboven, P, Defraeye, T, Tijskens, E, Schenk, A, Opara, UL and Nicolai, BM. 2013. Porous medium modeling and parameter sensitivity analysis of 1-MCP distribution in boxes with apple fruit. *Journal of Food Engineering,* 119**,** 13-21.

Bergman, TL, Lavine, AS, Incropera, FP and Dewitt, DP. 2011. *Fundamentals of heat and mass transfer.* John Wiley & Sons, USA.

Çengel, YA. 1998. *Heat transfer: Apractial approach.* The McGraw-Hill Companies, Inc., USA.

Chaudhari, BD, Sonawane, TR, Patil, SM and Dube, A. 2015. A Review on Evaporative Cooling Technology. *International Journal of Research in Advent Technology,* 3**,** 88-96.

Dehghannya, J, Ngadi, M and Vigneault, C. 2010. Mathematical Modeling Procedures for Airflow, Heat and Mass Transfer During Forced Convection Cooling of Produce: A Review. *Food Engineering Reviews,* 2**,** 227-243.

Fabiya, AO. 2010. *Design, construction and testing of an evaporative cooling facility for storing Vegetables.* University of Agriculture, Abeokuta, Ogun state, Nigeria.

Franco, A, Valera, DL and Peña, A. 2014. Energy efficiency in greenhouse evaporative cooling techniques: cooling boxes versus cellulose pads. *Energies,* 7**,** 1427-1447.

Franco, A, Valera, DL, Pena, A and Perez, AM. 2011. Aerodynamic analysis and CFD simulation of several cellulose evaporative cooling pads used in Mediterranean greenhouses. *Computers and Electronics in Agriculture,* 76**,** 218-230.

Franke, J. 2007. *Best practice guideline for the CFD simulation of flows in the urban environment.* COST Office, ISBN 3-00-018312-4, Brussels, Belgium.

Getahun, S, Ambaw, A, Delele, M, Meyer, CJ and Opara, UL. 2017. Analysis of airflow and heat transfer inside fruit packed refrigerated shipping container: Part II e Evaluation of apple packaging design and vertical flow resistance. *Journal of Food Engineering,* 203**,** 83-94.

Gunhan, T, Demir, V and Yagcioglu, AK. 2007. Evaluation of the suitability of some local materials as cooling pads. *Biosystems engineering,* 96**,** 369-377.

Kapilan, N, Manjunath, GM and Manjunath, HN. 2016. Computational Fluid Dynamics Analysis of an Evaporative Cooling System. *Strojnícky casopis–Journal of Mechanical Engineering,* 66**,** 117-124.

Kovačević, I and Sourbron, M. 2017. The numerical model for direct evaporative cooler. *Applied Thermal Engineering,* 113**,** 8-19.

Liao, CM and Chiu, KH. 2002. Wind tunnel modeling the system performance of alternative evaporative cooling pads in Taiwan region. *Building and Environment,* 37**,** 177-187.

Liberty, JT, Ugwuishiwua, BO, Pukumab, SA and Odo, CE. 2013. Principles and Application of Evaporative Cooling Systems for Fruits and Vegetables Preservation. *International Journal of Current Engineering and Technology,* 3**,** 1000-1006.

Nield, DA and Bejan, A. 2013. *Convection in porous media.* Springer Science & Business Media, New York, USA.

Norton, T and Sun, DW. 2006. Computational fluid dynamics (CFD): an Effective and efficient design and analysis tool for the food industry: a review. *Trends in Food Science & Technology,* 17**,** 600-620.

Rawangkul, R, Khedari, J, Hirunlabh, J and Zeghmati, B. 2008. Performance analysis of a new sustainable evaporative cooling pad made from coconut coir. *International Journal of Sustainable Engineering,* 1**,** 117-131.

Roache, PJ. 1994. Perspective: a method for uniform reporting of grid refinement studies. *Transactions-American Society of Mechanical Engineers Journal of Fluids Engineering,* 116**,** 405-405.

Rui, W, Hui, X, Jian, M, Tianlia, L and Jia, Q. 2011. CFD analysis of airflow distribution in greenhouse with pad and fan cooling system. *Transactions of the CSAE,* 27**,** 250-255.

Sapounas, AA, Bartzanas, T, Nikita-Martzopoulou, C and Kittas, C. 2016. Aspects of CFD Modelling of a Fan and Pad Evaporative Cooling System in Greenhouses. *International Journal of Ventilation,* 6**,** 379-388.

Thompson, JF. 2016. Pre-cooling and storage facilities. *The Commercial Storage of Fruits, Vegetables, and Florist and Nursery Stocks: Agriculture handbook, No. 66.* Cha. 2, 11-18. USDA, ARS, Beltsville, USA.

Thompson, JF, Mitchell, FG and Kasmire, RF. 2002. Cooling horticultural commodities. *In:* Kader, AA (ed.) *Postharvest technology of horticultural crops.* 3rd ed, Cha. 11, 97- 112. Agriculture and Natural Resources, University of California, USA.

Thompson, JF and Spinoglio, M. 1996. *Small-scale cold rooms for perishable commodities.* University of California, Division of Agriculture and Natural Resources, USA.

Tolesa, GN, Workneh, TS and Melesse, SF. 2018. Logistic regression analysis of marketability of tomato fruit harvested at different maturity stages and subjected to disinfection, storage condition and storage period treatments. *Biological Agriculture & Horticulture,* 34**,** 40-52.

Tripathi, PC and Lawande, KE. 2010. Temperature-related changes in respiration and Q10 coefficient in different varieties of onion. *Progressive Horticulture,* 42**,** 88-90.

Vala, KV, Saiyed, F and Joshi, DC. 2014. Evaporative Cooled Storage Structures: An Indian Scenario. *Trends in Post HArvest Technology,* 2**,** 22-32.

Van Der Sman, RGM. 2003. Simple model for estimating heat and mass transfer in regular-shaped foods. *Journal of food engineering,* 60**,** 383-390.

Venu, SA, Kumaran, GS and Bali, V. 2014. Determination of some physical properties of insulation materials and for selected vegetables to design a low cost evaporative cooling system. *Plant Archives,* 14**,** 507-510.

Verboven, P, Flick, D, Nicolai, BM and Alvarez, G. 2006. Modelling transport phenomena in refrigerated food bulks, packages and stacks: basics and advances. *International Journal of Refrigeration-Revue Internationale Du Froid,* 29**,** 985-997.

Workneh, TS. 2010. Feasibility and economic evaluation of low-cost evaporative cooling system in fruit and vegetables storage. *African Journal of Food, Agriculture, Nutrition and Development,* 10**,** 2984-2997.

Workneh, TS, Ngejane, M, Thipe, EL, Larange, L and Smithers, JC. Nov. 25-28, 2012 2012. Design, construction and performance evaluation of a multistage pad evaporative cooler for extending the shelf life of fruit and vegetables. The 7th CIGR Section VI International Technical Symposium "Innovating the Food Value Chain" Postharvest Technology and AgriFood Processing, 1-20. CIGR, Stellenbosch, South Africa.

Xuan, YM, Xiao, F, Niu, XF, Huang, X and Wang, SW. 2012. Research and application of evaporative cooling in China: A review (I) - Research. *Renewable & Sustainable Energy Reviews,* 16**,** 3535-3546.

Yadav, VK, Singh, A and Chandra, P. 2002. Experimental Evaluation of the effect of Fan Pad Evaporative Cooling System parameters on Greenhouse Cooling. *Journal of Agricultural Engineering,* 39**,** 49-53.

Zhao, CJ, Han, JW, Yang, XT, Qian, JP and Fan, BL. 2016. A review of computational fluid dynamics for forced-air cooling process. *Applied Energy,* 168**,** 314-331.

5. CFD MODELLING OF AIRFLOW, TEMPERATURE AND ENTHALPY INSIDE UNLOADED EVAPORATIVE COOLER, COOLBOT-AIR-CONDITIONER AND COMBINED OPERATIONS

5.1 CFD Modelling of Airflow inside Unloaded Evaporative Cooler, CoolBot-Air-Conditioner and Combined Operation

Abstract

The cooling of unloaded storage rooms is critical to determine the heat and mass transfer that takes place inside the storage chamber that is later loaded with fresh produce, in order to establish the theoretical background in the design process. The Computational Fluid Dynamics (CFD) models can provide a good display of the qualitative visualization of the airflow distribution inside storage chamber. The purpose of this study was to simulate the air velocity and air distribution inside unloaded low-cost cold storage chamber. Therefore, the airflow inside the empty low-cost evaporative cooler (EC), the CoolBot-air-conditioner (CBAC) and the combined operation EC+CBAC was simulated, using CFD models. The steady state with the isothermal model was used to study the airflow inside the storage chambers subjected to EC, CBAC and EC+CBAC cooling. The results showed that airflow distribution was not uniform inside the storage chamber under all the three cooling methods. However, relatively-speaking, the EC+CBAC was found to be the best in its uniformity of the air velocity and distribution, which was followed by the CBAC and EC, respectively. A validation of the models was performed by comparing the experimental air velocity with that of the computed air velocity at different positions inside the storage chambers. The models fitted well to the experimental velocity values and also enabled them to clearly characterize airflow patterns in the storage chamber. This study clearly showed that CFD modelling application is a good way of identifying the airflow inside cold storage and it was hence found to be an appropriate tool, not only for advanced design technology, but also for low-cost technology design. Based on the results obtained in this study, the optimal design of cold storage chambers is required to ensure the uniformity of air distribution and air velocity, using computational fluid dynamics modelling.

Keywords: Airflow distribution, CoolBot-air-conditioner, computational fluid dynamics models, combined evaporative cooling and CoolBot-air-conditioner, evaporative cooler.

5.1.1 Introduction

Modelling the airflow, mass and heat transfer that takes place inside a cold storage chambers using CFD tools, is the recent trend in food engineering (Ambaw *et al.*, 2013a; Defraeye, 2014). Maintaining the even and rapid cooling of fresh produce after harvest is the major challenge for postharvest handling (Duan *et al.*, 2016; Getahun *et al.*, 2017b). The unevenly distributed micro-climate inside cold storage chambers might be due to the heterogeneous airflow distribution inside the cold storage rooms (Zou *et al.*, 2006a; Zou *et al.*, 2006b; Delele *et al.*, 2013). Only limited number of researchers have analyzed the performance of evaporative cooling technologies for fresh produce pre-cooling and green house cooling, using CFD (Sapounas *et al.*, 2007). Sapounas *et al.* (2016) performed a CFD model simulation and reported that the ventilation rate of the green house is the most important factor for improving the efficiency of the evaporative cooling system. Nahor *et al.* (2005) modeled the basics of airflow, heat and mass transfer inside an existing unloaded and loaded refrigerated room and characterized the cold air distribution. The authors validated the models by comparing the air velocity, temperature and weight loss of the pear fruit, which were measured experimentally, with the computation values.

The heat and mass transfer inside the cold storage chamber is mainly affected by the airflow dynamics (air velocity, air flow rate, temperature and relative humidity), the fresh produce properties (*i.e.* geometry, thermo-physical and physiological), the packaging and stacking pattern of the produce and the packaging material arrangements (Castro *et al.*, 2005; Ambaw *et al.*, 2013; Zhao *et al.*, 2016). Hence, a detailed study of the airflow characteristics inside the cold stores is fundamental for the further characterization of the storage performance determinations, in terms of air velocity optimization, structural design modification and the maintenance of the cold store.

Several pre-cooling low-cost technologies have been identified by several researchers that can be helpful for disadvantaged farmers, small-scale producers and emerging farmers. These cooling technologies include the evaporative cooler (EC), the CoolBot-air-conditioner (CBAC) and the combination (EC+CBAC) (Workneh, 2010; Saran *et al.*, 2013).

5.1.1.1 Theory of evaporative cooler

A combination of the direct and indirect evaporative cooler (EC) is recommended for arid and semi-arid climate regions, for the efficient pre-cooling of fruit and vegetables after harvest (Roy and Khardi, 1985; Roy and Pal, 1989, 1994; Yadav *et al.*, 2002; Roy, 2007; Tripathi and Lawande, 2010; Workneh, 2010). The temperature is reduced to approach the wet bulb temperature, while the relative humidity and absolute humidity increases after passing through the pads (Tripathi and Lawande, 2010; Xuan *et al.*, 2012). The cooling process was accounted for by the removal of the latent heat of vaporization from the surface of the wet pads to the environment (Pal *et al.*, 1997). Even though it is cheaper, there is limited research on the airflow pattern, the heat, and the mass transfer inside the evaporative cooler conditioned cold room.

5.1.1.2 CoolBot-air-conditioner cooling

Boyette and Rohrbach (1993) developed the CoolBot-Air-Conditioner (CBAC) cooling system as a low-cost, forced-air, portable modification of the domestic air conditioner, for fresh produce storage. The CBAC is an electronic device that overrides the room air conditioner to reduce cooling temperature below the set point for the preservation of fresh produce. It is easy to handle, install and maintain (Kitinoja, 2013; Saran *et al.*, 2013). However, there is limited research on the airflow pattern, the heat, and the mass transfer inside the CBAC cold room.

Computational fluid dynamics (CFD) simulations of the airflow, mass and heat transfer process in cold storage chambers shows it to be a promising alternative for analysing the micro-climate environmental conditions and postharvest equipment design optimization processes (Ambaw *et al.*, 2013; Kolodziejczyk *et al.*, 2016). The physical parameters, such as air velocity, airflow patterns and temperature inside the cold storage chamber are the determinant fundamental factors for heat and mass transfer modelling (Kolodziejczyk *et al.*, 2016). Therefore, airflow characteristics inside the empty storage chambers is a critical aspect that needs to be studied. Airflow inside the unloaded stores can be the basic to be characteristic before the pre-cooling of loaded fresh produce. Hence, the unloaded cold room airflow might indirectly determine the shelf-life and quality of stored fresh produce. In spite of low-cost, in the case of EC, CBAC and the combined operations (EC+CBAC), there is no detailed study of airflow inside the empty storage chambers. Hence, this study focuses on the study of the air velocity and distribution inside unloaded EC, CBAC and EC+CBAC cold rooms, with the help of CFD models.

5.1.2 Materials and methods

5.1.2.1 Cold room set-up

An insulated experimental cold room was installed at the Ukulinga Research Farm, Pietermaritzburg, South Africa. The cold room consisted of an indirect heat exchanger, wet charcoal cooling pads and a CoolBot-air-conditioner system (CBAC) (Figure 3.1). In the case of the evaporative cooler, the air was blown into the room by axial fan through the heat exchanger. All walls of the rooms were insulated with polyurethane foam in between 1 mm thick casted steel metal sheet. The floor of the store was made of concrete. The following assumptions were made for CFD modelling: (1) the charcoal was kept wet all the time, (2) the whole operation was run under normal atmospheric conditions (101.325 kPa), (3) it was assumed that there was no radiation effect, and (4) the condition was performed at steady state. The reservoir volume was a 250 l plastic tank buried underground, to keep the water reservoir cold during the day and night. The water pump capacity was 5 m x 2 $l.min^{-1}$. The axial fan (Fan 2) was used to push the cold air into the cold room, which had an external diameter of 350 mm and an air ventilation rate capacity of 0.218 $m^3.s^{-1}$ (Workneh *et al.*, 2012).

5.1.2.2 Cold store experiment

The experimental airflow was measured with a DS-2 sonic anemometer (Company, Decagon Devices, Inc., USA) at Fan 1 (0.6 m), air conditioner inlet (Y = 2.2 m), 2 m from the inlet along symmetry line at 1.3 m height, 4 m from the inlet along symmetry line at 1.3 m height, 6 m from the inlet along symmetry line at 1.3 m high (Y = 1.3 m) and at the exit holes (Y = 2.2 m). The temperature and relative humidity were measured at different positions by Hobo data loggers (Figure 3.1).

5.1.2.3 Numerical modelling

Governing equations

A steady state, with an isothermal and incompressible set-up option, was used to simulate the empty rooms to study the airflow distribution inside the storage chambers (Hoang *et al.*, 2000; Praneeth and Gowda, 2015). This study presents the exploration of the airflow velocity

distribution inside the three different cooling systems (*i.e.* the evaporative cooler (EC), the CoolBot-Air-Conditioner (CBAC) and the combined operation of EC and CBAC (EC+CBAC). The CFD model applied the Navier–Stokes equations (Hoang *et al.*, 2000; Nahor *et al.*, 2005; Ambaw *et al.*, 2013), which is designated by Equations 2.1 to 2.5 (see Chapter 2, section 2.4).

5.1.2.4 Model parameters

A steady state, with isothermal models, were used for the empty cold rooms (Hoang *et al.*, 2000; Nahor *et al.*, 2005). This state was chosen since it provided a better understanding of airflow and it reduced the simulation time. Heat transfer models were not considered. The simulation was performed based on unloaded (empty) rooms, and no resistance was considered for the simulations.

5.1.2.5 Boundary and initial conditions set-up

All the walls and the roof of the storage chambers and the psychrometric unit (EC, CBAC and EC+CBAC) were insulated by a layer of polyurethane foam that was 15 mm thick. The experimental air velocities were set at 3.2 $m.s^{-1}$ and 4.2 $m.s^{-1}$, at the inlet of the EC and CBAC air conditioner, respectively. Moreover, the air velocities were set at 3.1 $m.s^{-1}$ and 3.0 $m.s^{-1}$ at the inlets of the EC+CBAC combination fan inlet and air conditioner inlet, respectively. The exit vents were set as the boundary conditions (ANSYS, 2016). Inside the storage chamber, remain the free air zones remained as a fluid domain (Getahun *et al.*, 2017a). The cooling unit was represented by a velocity boundary at the inlet of the cooling system and by average static pressure (0 Pa). All walls, floors and ceilings of the cold rooms were set to no slip walls, and the invisible heat exchange between ambient environments was assumed to be negligible, since all the systems were insulated with polyurethane foam of 15 mm thick. The thermal conductivity of the insulator was 0.023–0.026 $W.m^{-1}.K^{-1}$ (Tseng *et al.*, 1997; Wu *et al.*, 1999) and, hence, the heat loss was assumed to be negligible.

5.1.2.6 Simulation setup

The domains of all models were discretized by meshing of tetrahedral elements and gave better coverage for the internal fluid domain zone, while the triangular elements were found to be better for surface meshing (Khodak *et al.*, 2015). ANSYS CFX 17.0 (ANSYS, Canonsburg,

PA, USA) was used for the simulation with the finite volume method and was used to solve the numerical problem (ANSYS, 2016; Getahun *et al.*, 2017a). Turbulence was considered by the k-ε SST model, to accommodate the fluid flow on the wall (Hoang *et al.*, 2000; Versteeg and Malalasekera, 2007; Ambaw *et al.*, 2013). A steady state calculation was performed to obtain the convergence state of the residuals and momentum parameters of airflow. The full simulation took 4-6 hours on a 64-bit, Dell Precision T3600, Intel Xeon CPU E5-16600 @ 3.30 GHz 3.30GHz and 32GB RAM, Windows 10 PC. The total iteration was 3000.

5.1.2.7 Simulations of unloaded cold stores

The airflow inside the unloaded EC, CBAC and EC+CBAC cold storage chambers were simulated. The airflow velocity, at horizontal (Y-plane at different locations) and vertical (Z-plane at different locations) locations, were analyzed by using ANSYS (CFX Solver Version 17.0). The validation of the models was performed by comparing the simulated airflow and the measured air velocity with that of the numerically computed values (Hoang *et al.*, 2000; Nahor *et al.*, 2005). Three separate simulations were executed for the empty EC, CBAC and EC+CBAC cooler systems.

5.1.3 Results and discussion

5.1.3.1 Airflow characteristics inside the evaporative cooler

Several researchers recommended that the suction fan be used for forced air cooling, to facilitate the airflow of cold air through the storage chamber, to enhance the airflow distribution uniformity and, hence, to cool effectively. Figure 5.1 displays the CFX simulation outputs of the 3D horizontal visualization of air velocity streamlines inside the evaporative cooler (EC). As can be seen from the Figure 5.1, the air velocity varied between 0.4 to 0.8 $m.s^{-1}$ at the top 2.2 m plane from the storage chamber floor surface, which is hardly sufficient to cool the room at this position. At the middle Y-plane (1.3 m high from floor), the air velocity varied between 0 to 1.0 $m.s^{-1}$. At the Y-plane, which was perpendicular to the fan (0.6 m high from floor), the air velocity varied between 0 to 3.2 $m.s^{-1}$. At this point, the air is barely distributed. At the bottom Y-plane (0.1 m high from floor), the air velocity varied between 0 to 1.5 $m.s^{-1}$. The air velocity streamlines indicated that there was no uniform airflow and air distribution vertically at different positions, which is similar to the results reported by Ho *et al.* (2010b). Moreover,

the data presented in Figure 5.1 showed that there was air circulation, particularly at the horizontal plane Y = 1.3 m high and parallel to fan (Y = 0.6 m), which might facilitate the turbulence and mixing of the air that optimizes heat and mass transfer (Ma *et al.*, 2011; Praneeth and Gowda, 2015). Similarly, Ho *et al.* (2010) recommended that the uniformity of air velocities inside the cold storage chamber can be achieved by increasing the blowing air velocity and/or locating the cooling units lower and closer to the products stored inside. Moreover, Praneeth and Gowda (2015) reported that the uniformity of airflow and temperature distribution inside cold storage chambers is affected by the position of the inlet fans, the numbers of inlets, and the stacking orientation inside the cold storage chambers. Hence, the unloaded EC store demonstrated that further modifications, in terms of the inlet airflow, the inlet positions and in numbers of inlets optimize the airflow and temperature inside the store.

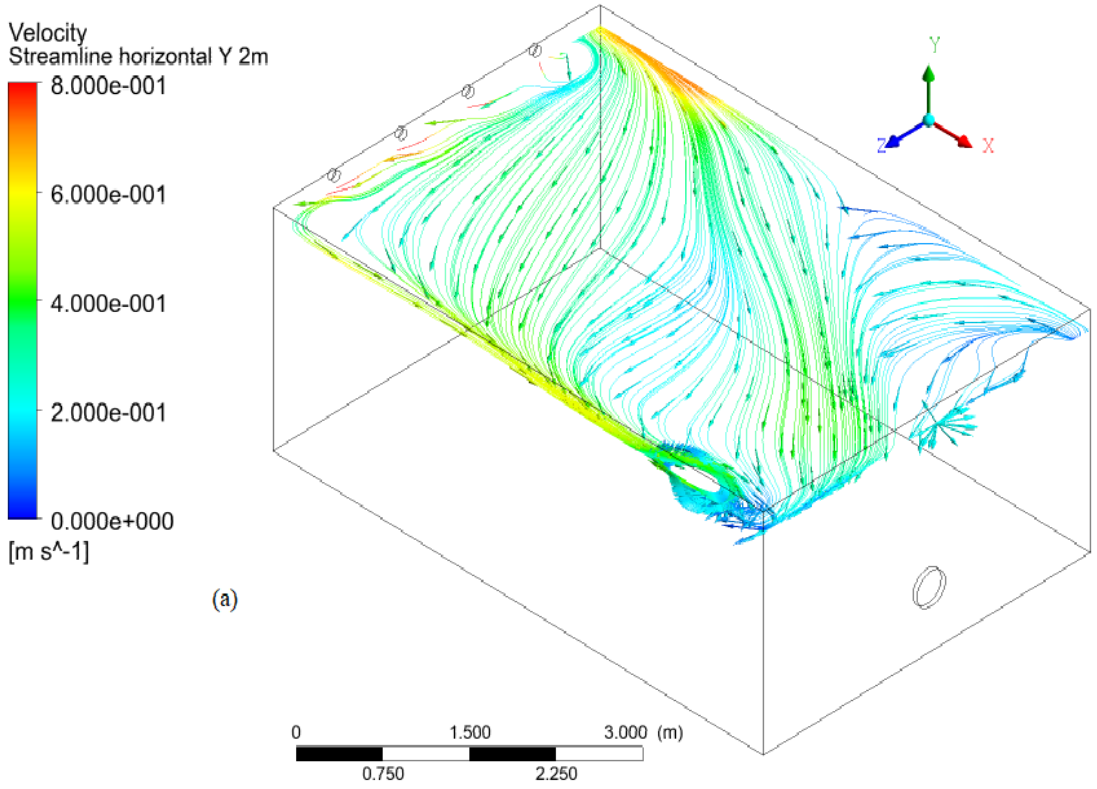

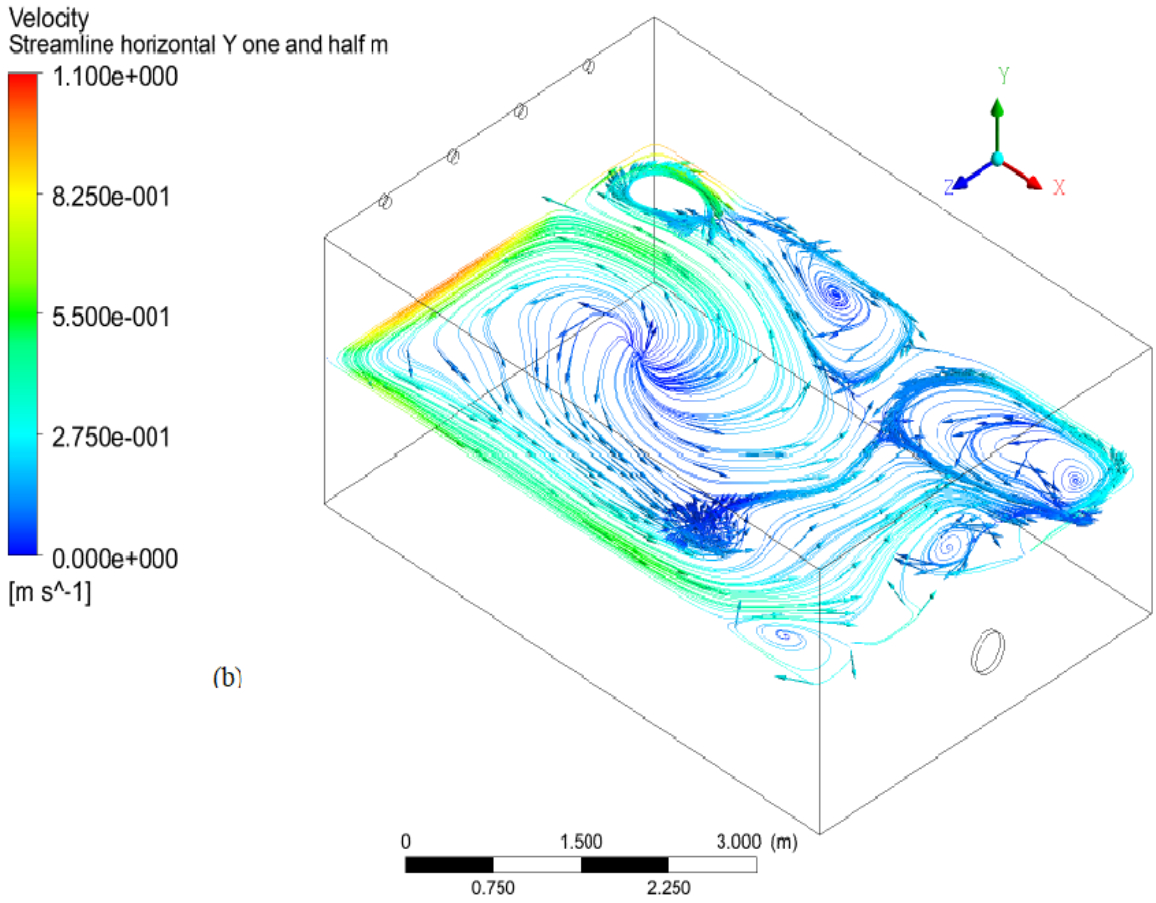
Velocity
Streamline horizontal Y one and half m
1.100e+000
8.250e-001
5.500e-001
2.750e-001
0.000e+000
[m s^-1]
Y
Z
X
0
1.500
3.000 (m)
0.750
2.250

(b)

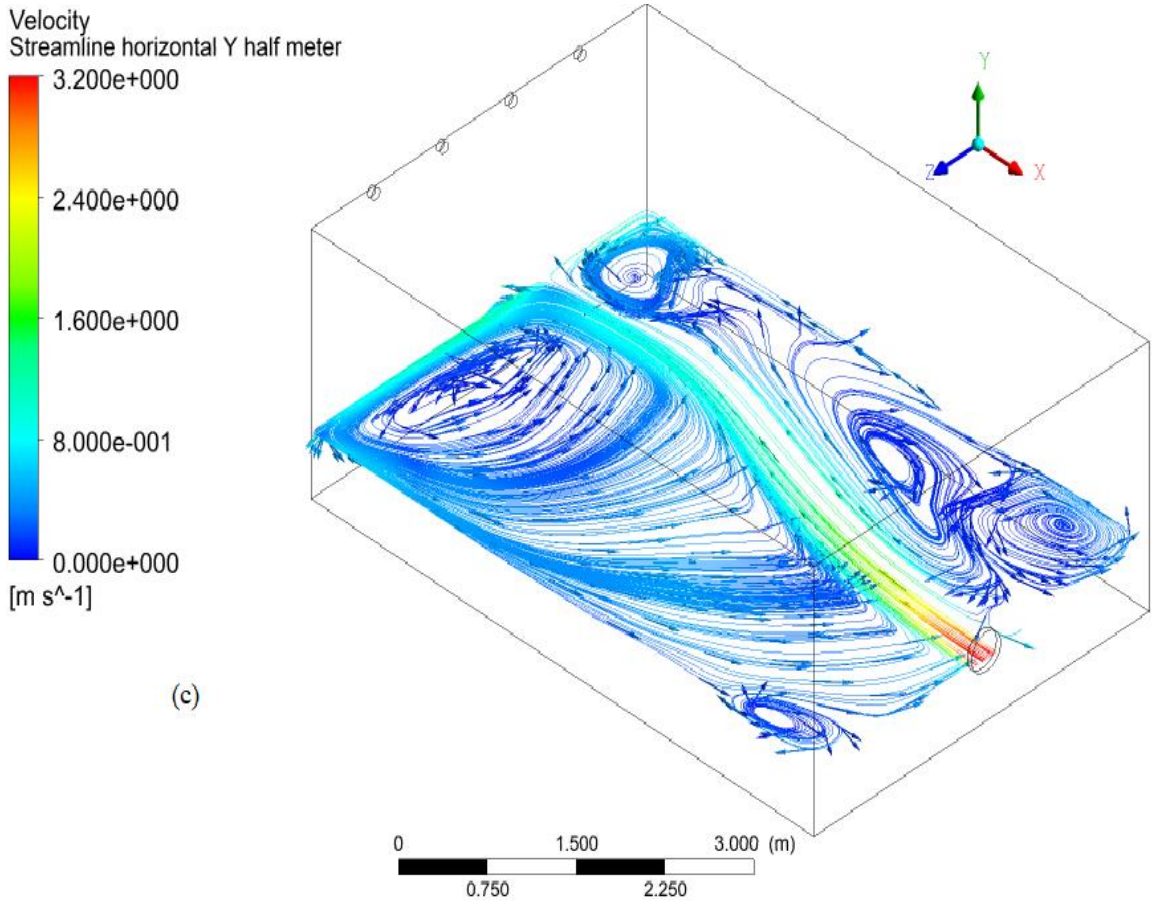
Velocity
Streamline horizontal Y half meter
3.200e+000
2.400e+000
1.600e+000
8.000e-001
0.000e+000
[m s^-1]
Y
Z
X
0
1.500
3.000 (m)
0.750
2.250

(c)

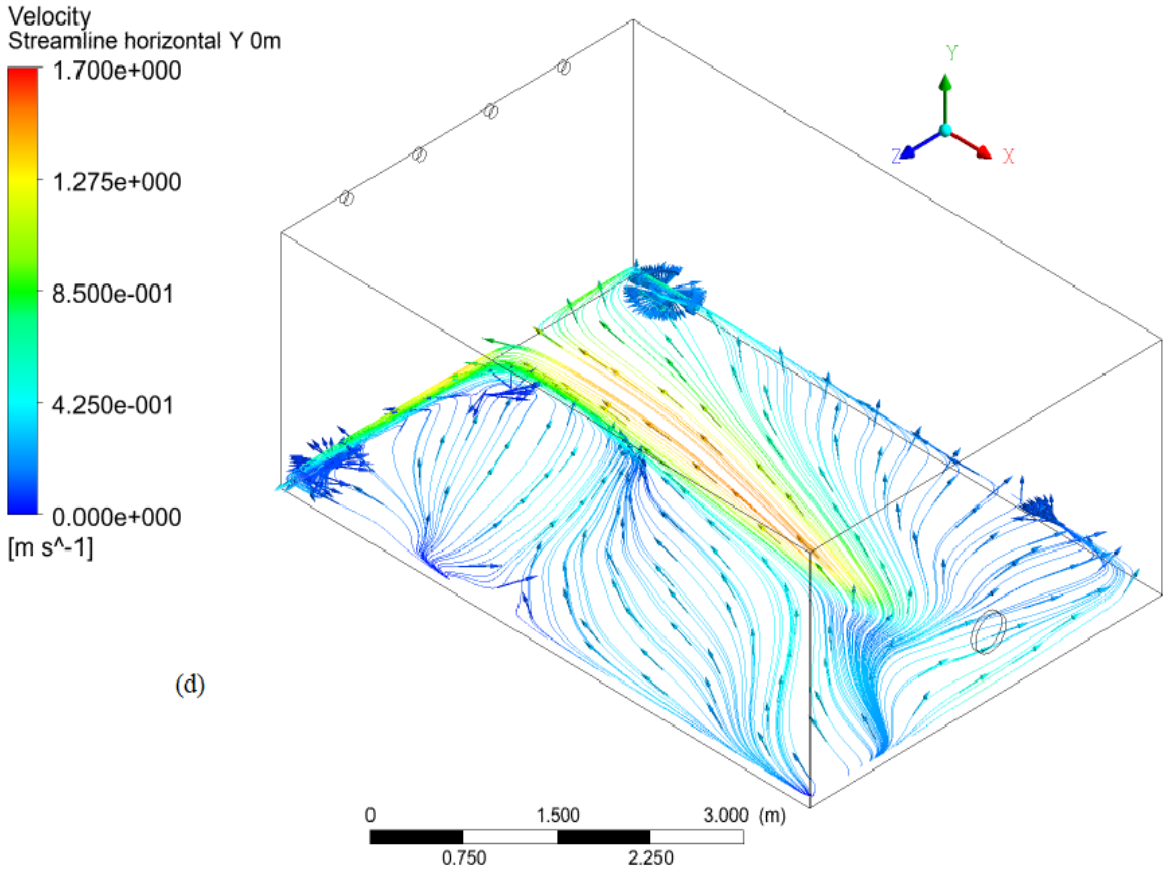

Figure 5.1 The air streamlines inside the evaporative cooler at imaginary horizontal planes located at different heights along the Y-direction from the ground cooler surface: (a) is air velocity at Y = 2.2 m high, (b) is air velocity at Y = 1.3 m high, (c) is air velocity at Y = 0.6 m high and (d) is air velocity at Y = 0.1 m high from the floor of the room

Figure 5.2 displays a 3D horizontal visualization of an air velocity contour. The air velocity varied between 0.0 m s^{-1} and 1.0 m.s^{-1} at the top Y = 2.2 m high plane. This shows that the airflow at this height surface hardly cools the room to the desired temperature at this position. At the middle horizontal Y-plane (1.3 m high), the air velocity varied from 0.0 to 1.0 m.s^{-1}. At the horizontal plane parallel to the fan direction (0.6 m high), the air velocity varied between 0.0 m.s^{-1} and 3.2 m.s^{-1} and the air was not well-distributed. The air velocity varied between 0.0 m.s^{-1} to 1.0 m.s^{-1} at the bottom horizontal plane, which was 0.1 m above the cooler ground surface. Airflow was reported to be affected by the numbers of inlets and locations of the inlet fans (Praneeth and Gowda, 2015) and the fan position of the EC was changed, to investigate the effects of the fan position.

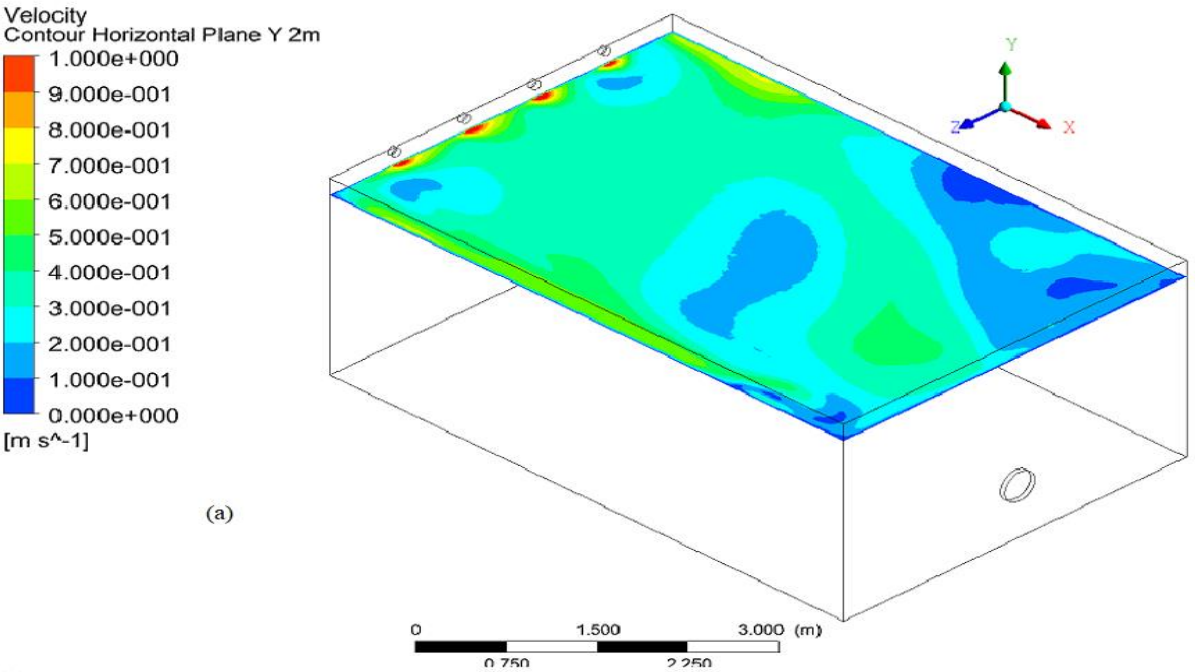
Velocity
Contour Horizontal Plane Y 2m
1.000e+000
9.000e-001
8.000e-001
7.000e-001
6.000e-001
5.000e-001
4.000e-001
3.000e-001
2.000e-001
1.000e-001
0.000e+000
[m s^-1]
Y
Z
X
0
1.500
3.000 (m)
0.750
2.250

(a)

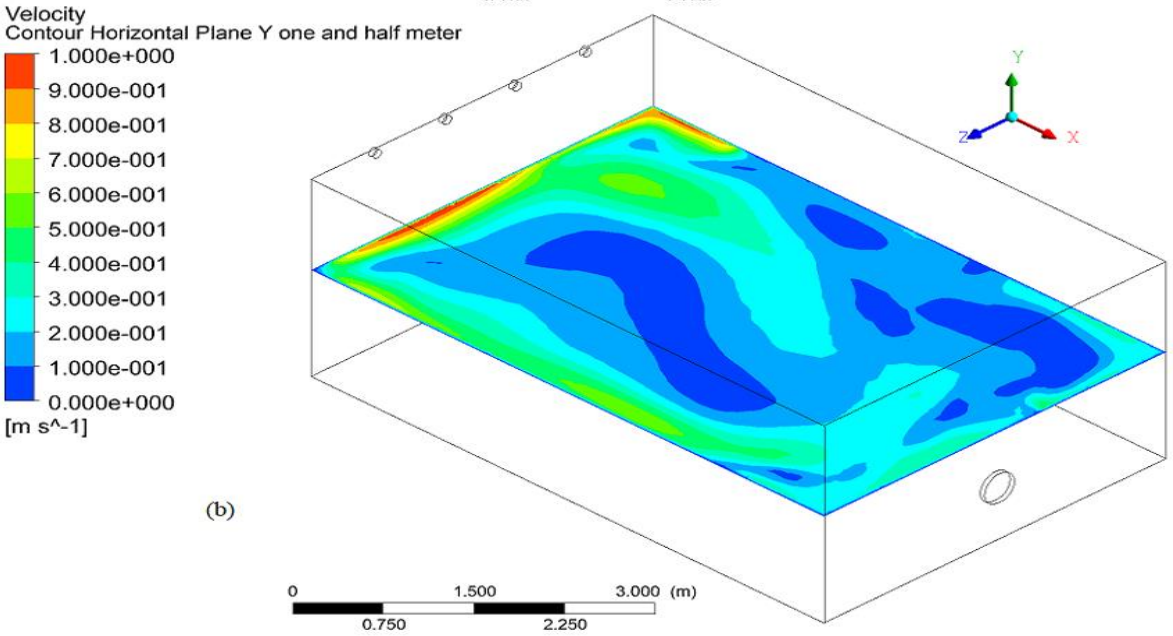
Velocity
Contour Horizontal Plane Y one and half meter
1.000e+000
9.000e-001
8.000e-001
7.000e-001
6.000e-001
5.000e-001
4.000e-001
3.000e-001
2.000e-001
1.000e-001
0.000e+000
[m s^-1]
Y
Z
X
0
1.500
3.000 (m)
0.750
2.250

(b)

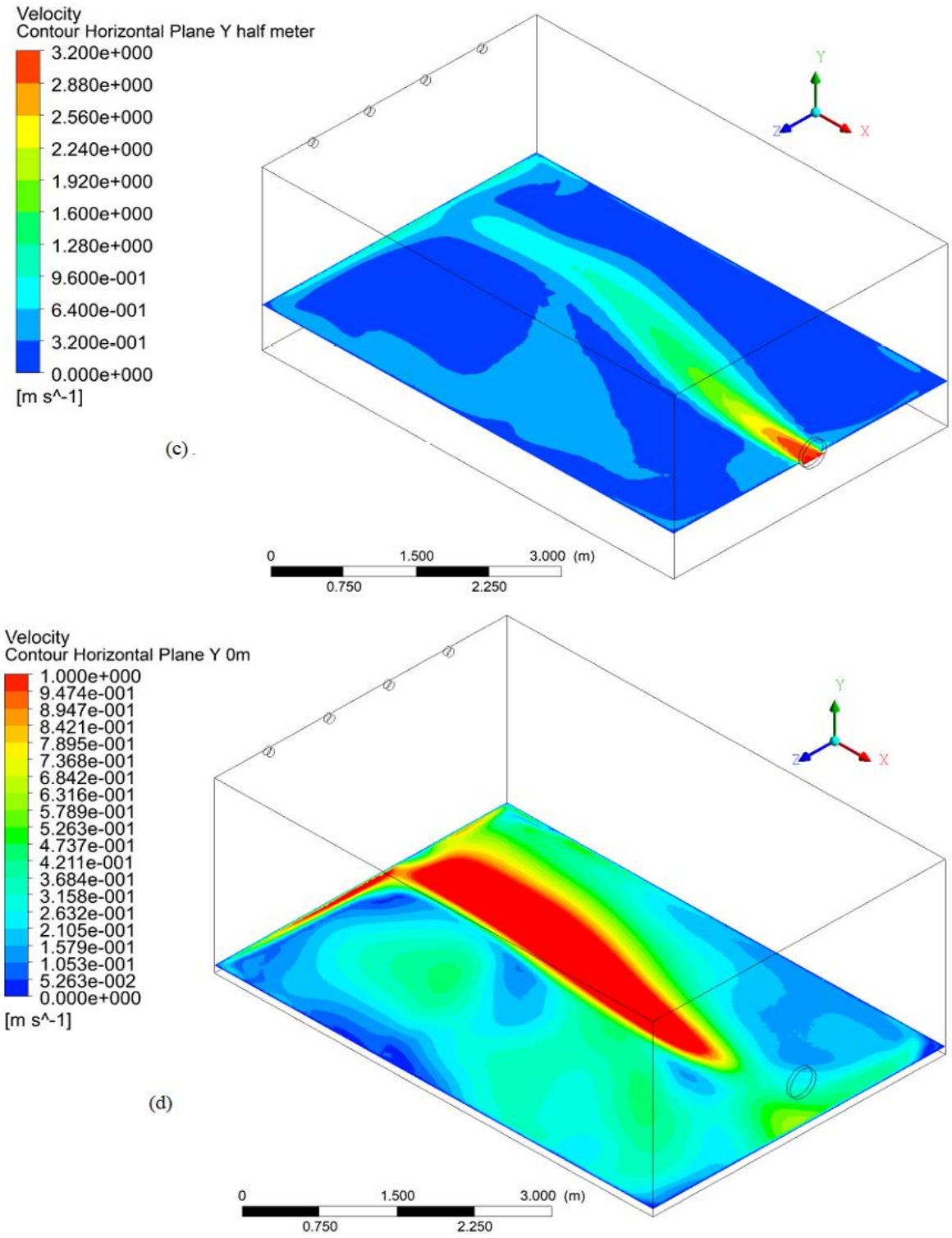

Figure 5.2 The 3-D air horizontal plane section showing the air velocity contour inside the evaporative cooler (EC) at different heights above cooler surface along the Y-direction: a) is air velocity at Y = 2.2 m high, b) is air velocity at Y = 1.3 m high, c) is air velocity at Y = 0.6 m high and d) is air velocity at Y = 0.1 m high from the floor of the room

Figure 5.3 shows the CFX simulation output of the air velocity streamlines inside the evaporatively cooled room (EC). The results display that the air velocity varied between 0.25 $m.s^{-1}$ and 0.8 $m.s^{-1}$ at the 0.1 m from the wall (Z = 0.1 m). The airflow was turbulent and low speed with circulation. At 1 m from the right wall, the air velocity varied between 0.0 $m.s^{-1}$ and 0.7 $m.s^{-1}$. The airflow showed turbulent recirculation near the top middle of the vertical plane, 1 m from the wall. On the symmetry line, 2 m from the wall (Z = 2 m), the air distribution varied from 0.0 $m.s^{-1}$ to 3.2 $m.s^{-1}$, with a very high circulation and turbulence along this vertical plane. The air rotation can enhance the rapid cooling of the room and the enclosed produce (Ma *et al.*, 2011). As the distance from the fan increases, the air velocity hardly enables the distribution of the air towards the center and to the outlets of the cooler.

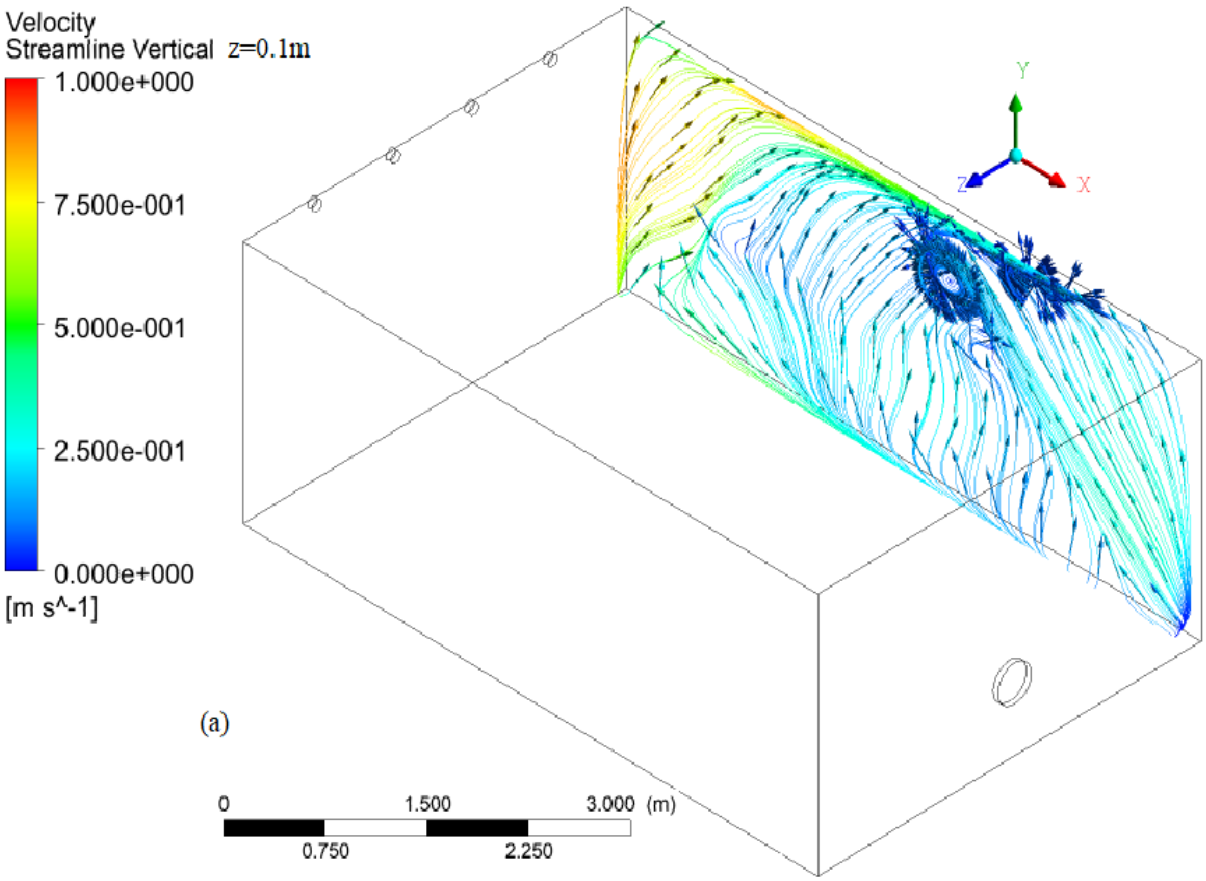

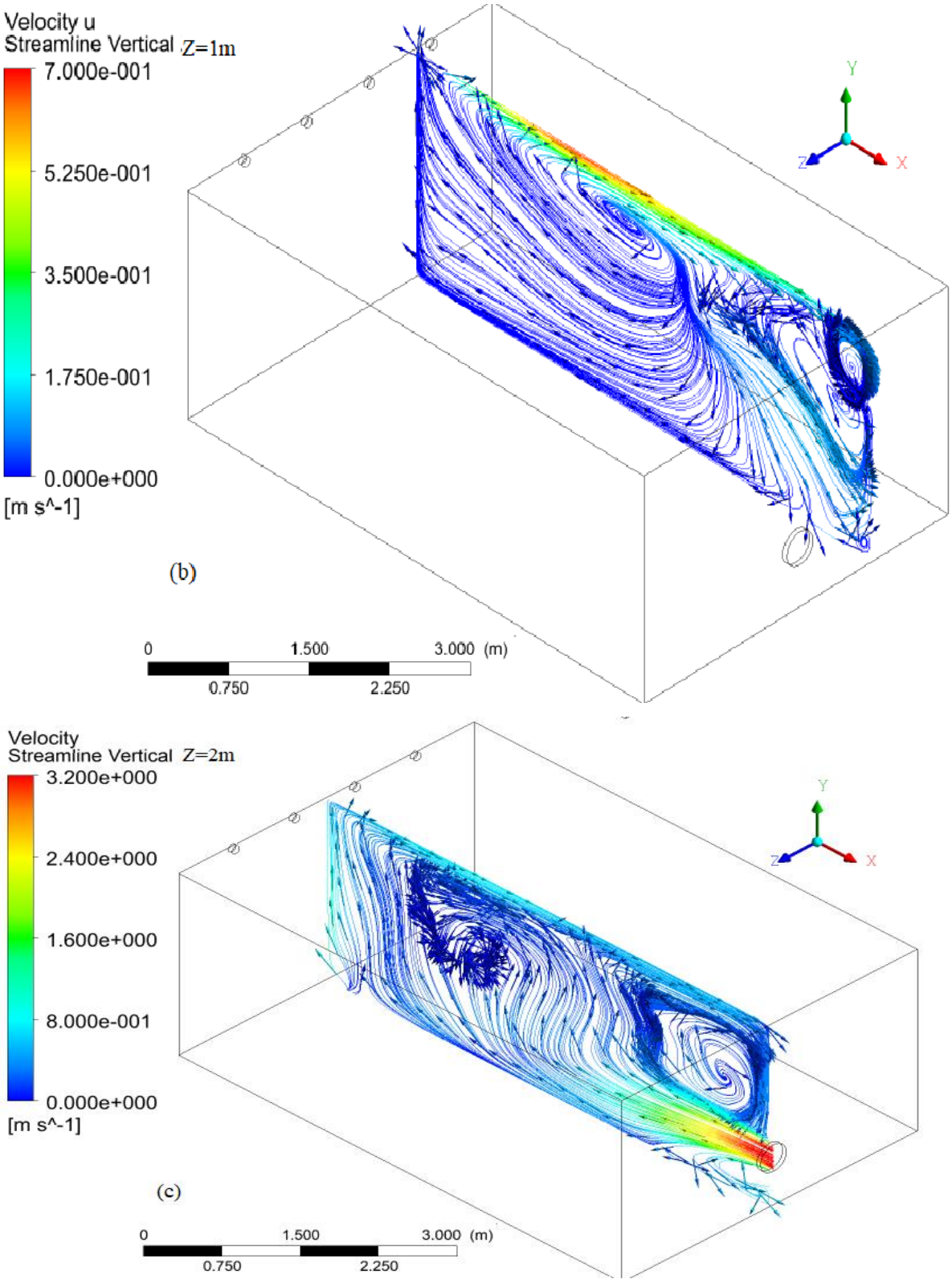

Figure 5.3 The air streamlines inside the evaporative cooler at an imaginary vertical planes located at different lengths along the Z-direction from the right wall surface of the evaporative cooler (a) is air velocity at Z = 0.1 m away from the wall, (b) is air velocity at Z = 1.0 m away from the wall, and (c) is air velocity along the vertical symmetry line (Z = 2 m) from the wall of the room

Figure 5.4 shows the contour visual display of the air velocity along the vertical imaginary plane at different locations from wall surface, towards vertical symmetry line inside the evaporative cooler. The air velocity varied between 0.0 $m.s^{-1}$ and 0.8 $m.s^{-1}$ at 0.1 m away from right wall (Z = 0.1 m) and was not uniformly distributed (Figure 5.4). At Z = 1 m from the right wall, the air velocity varied between 0.0 $m.s^{-1}$ and 1.3 $m.s^{-1}$ and the higher velocity was displayed at the bottom end of the horizontal plane towards the outlet. At 2 m from the right wall, along the symmetry line, the air distribution varied from 0.0 m s^{-1} to 3.2 $m.s^{-1}$, with the majority of the air velocities very low along the plane. As the distance from the fan increased, the air velocity appeared to hardly be distributed towards the center and outlets of the cooler. Overall, the air velocity created by the fan hardly pushed the air through the room along the symmetry line. Hence, the redesign of a more appropriate fan size or suction fan is required for the same insulated EC room for this experiment at the farm. This results clearly demonstrated that computational fluid dynamics modelling in the design of air conditioning (*i.e.* the determination of an appropriate ventilation rate) is in positive agreement with Praneeth and Gowda (2015).

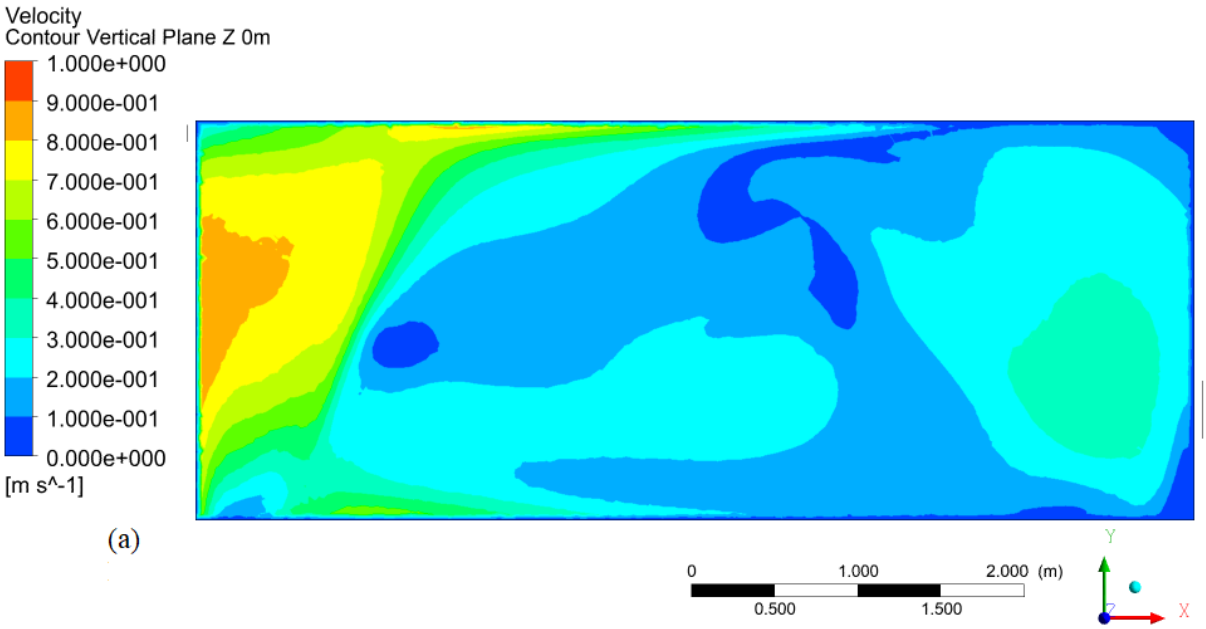

(a)

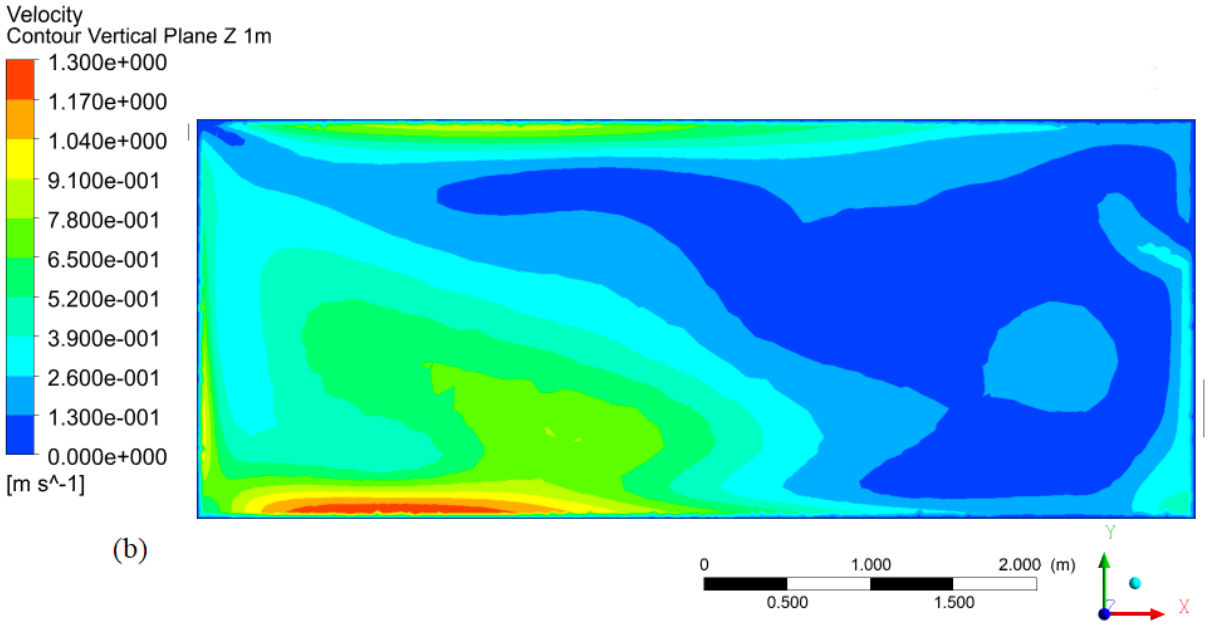

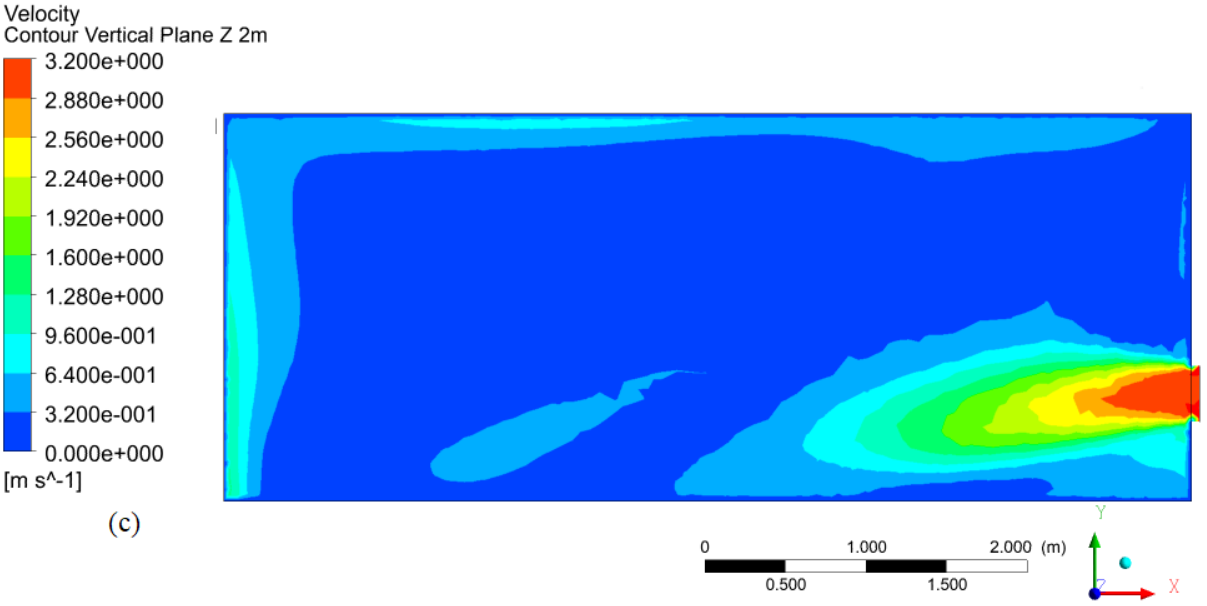

Figure 5.4 The air velocity contour inside the evaporative cooler at imaginary vertical planes located at different lengths along the Z-direction from the right wall surface of the evaporative cooler (a) is air velocity at Z = 0.1 m away from the wall, (b) is air velocity at Z = 1.0 m away from the wall, and (c) is air velocity along the vertical symmetry line (Z = 2 m) from the wall of the room

5.1.3.2 CoolBot-air-conditioner airflow characteristics

The CFX output of air streamlines inside the CoolBot-air-conditioner (CBAC) store room is shown in Figure 5.5 (a - d). The results show that the air velocity varied between 0.0 $m.s^{-1}$ and 1.0 $m.s^{-1}$ at the top surface 2.2 m high (parallel to the air conditioner inlet) (Figure 5.5 (a)). The

air velocity appeared to be non-uniform and there was good circulation along this plane. At the middle 1.3 m high along the horizontal imaginary plane, the air velocity varied between 0.0 $m.s^{-1}$ and 1.6 $m.s^{-1}$ with a high circulation, which might have occurred, due to the air below at –Y axis at 45 degrees (Figure 5.5 (b)). Moreover, the air circulation was displayed along the plane, which was reported to be good for airflow and temperature distribution (Ma *et al.*, 2011). At the horizontal Y = 0.6 m high, the air velocity varied from 0.0 $m.s^{-1}$ and 1.0 $m.s^{-1}$ and the air distribution was uniform, which indicated that cooling at this location was appropriate (Figure 5.5 (c)). At the bottom of the horizontal plane, which was situated at Y = 0.1 m high from the cooler bottom surface, the air velocity changed from 0.0 $m.s^{-1}$ to 0.7 $m.s^{-1}$ (Figure 5.6 (d)). The air streamlines indicated that there was uniformity in the air velocity. Moreover, Figure 5.5 (a - d) shows that air circulation at all the horizontal Y-planes were found to be relatively evenly distributed (Ma *et al.*, 2011).

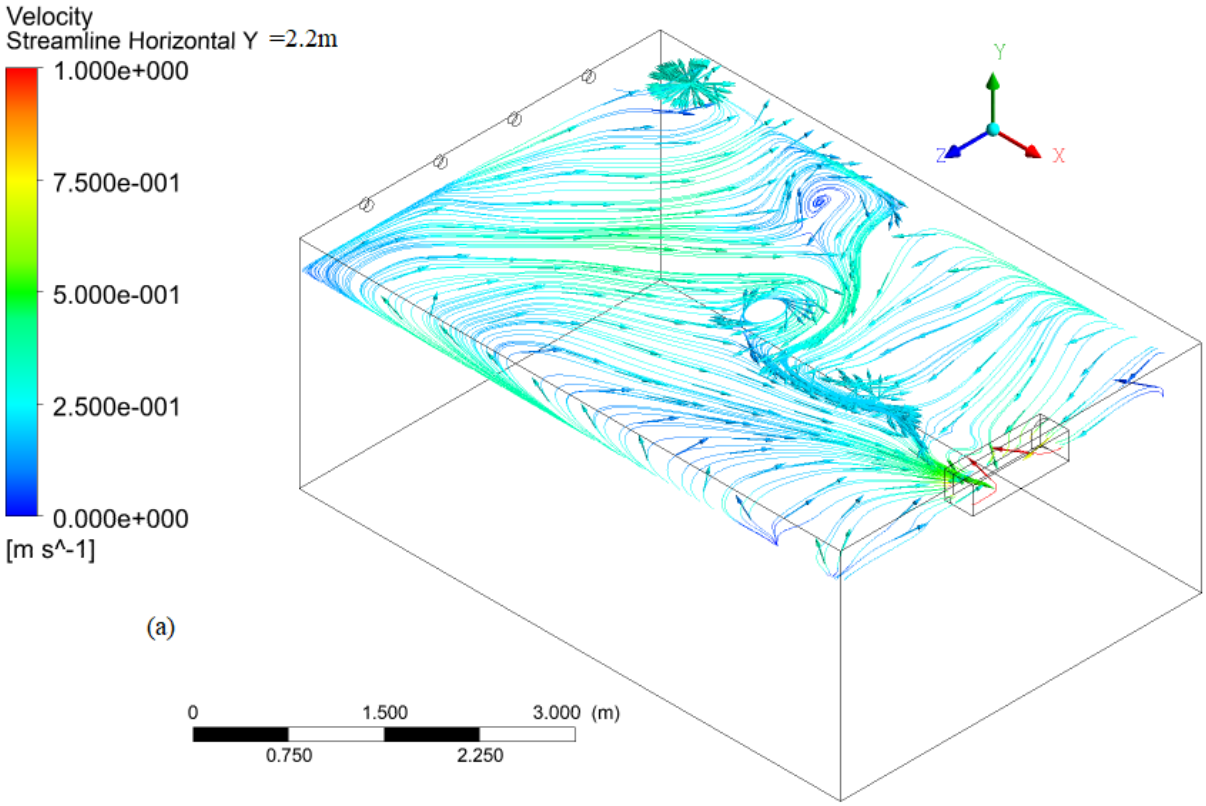

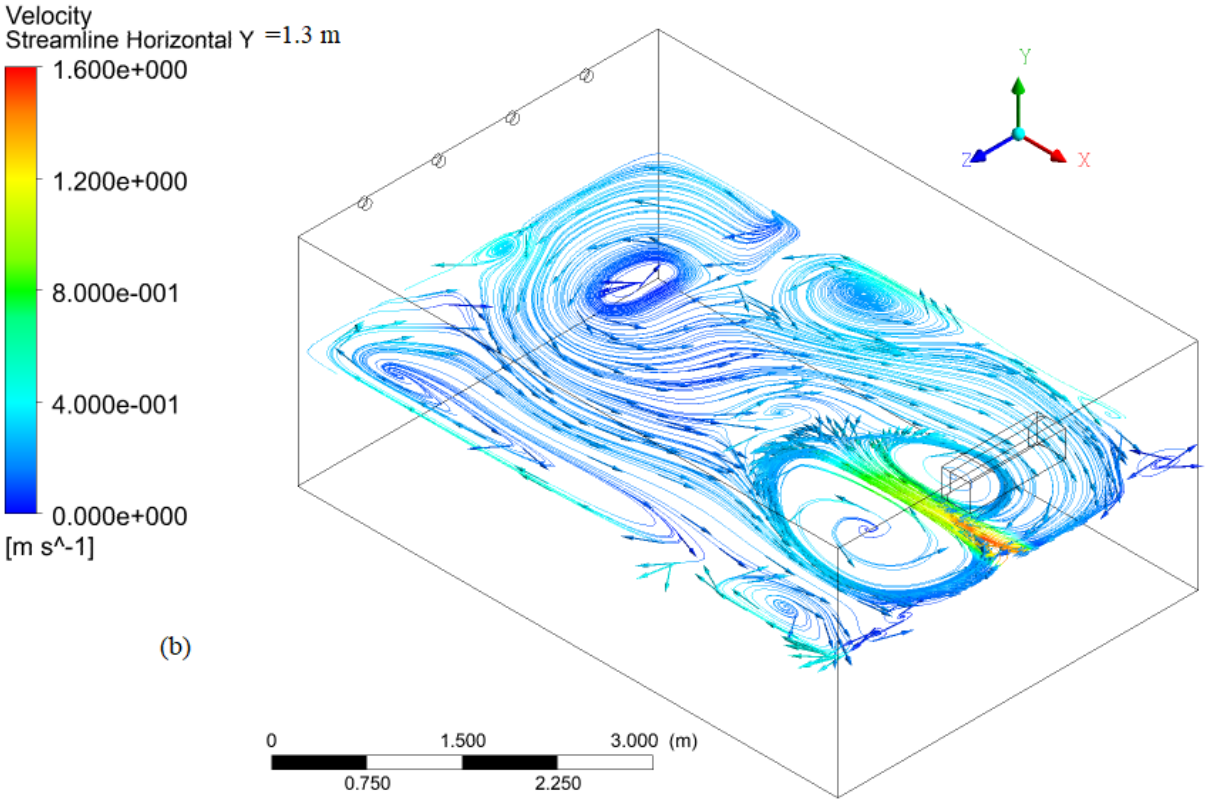
Velocity
Streamline Horizontal Y =1.3 m
1.600e+000
1.200e+000
8.000e-001
4.000e-001
0.000e+000
[m s^-1]
Y
Z
X
0
1.500
3.000 (m)
0.750
2.250

(b)

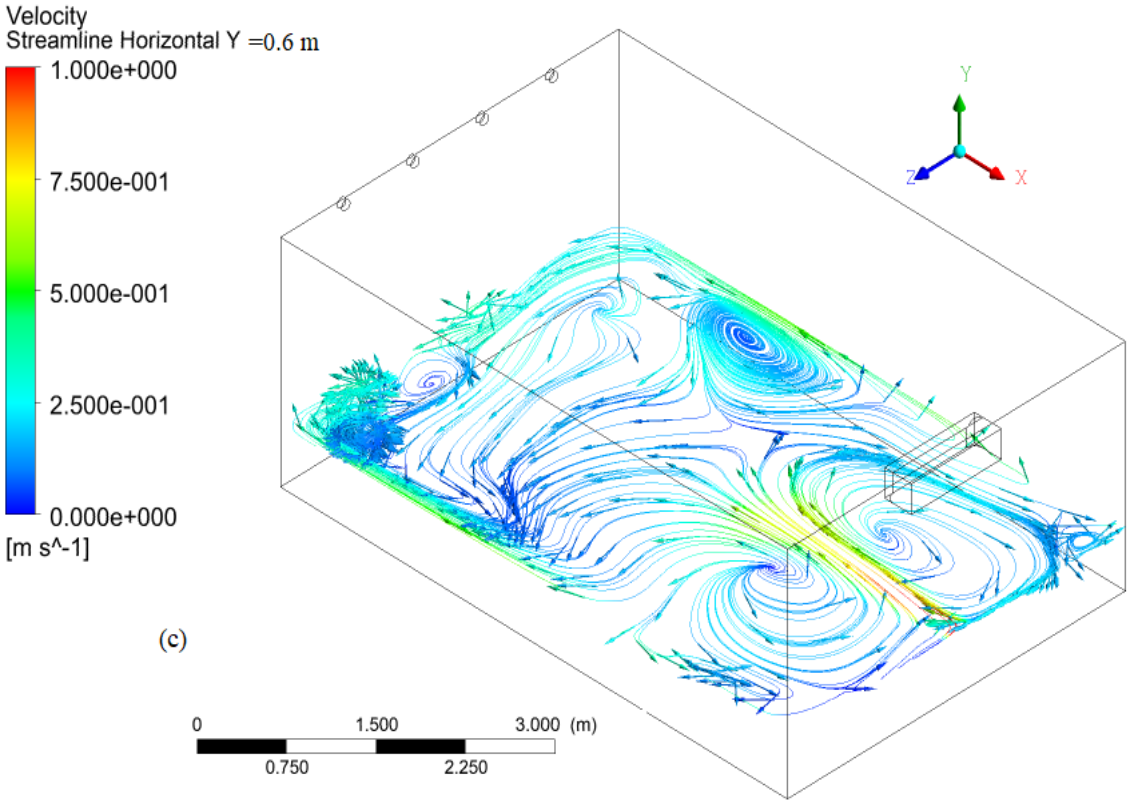
Velocity
Streamline Horizontal Y =0.6 m
1.000e+000
7.500e-001
5.000e-001
2.500e-001
0.000e+000
[m s^-1]
Y
Z
X
0
1.500
3.000 (m)
0.750
2.250

(c)

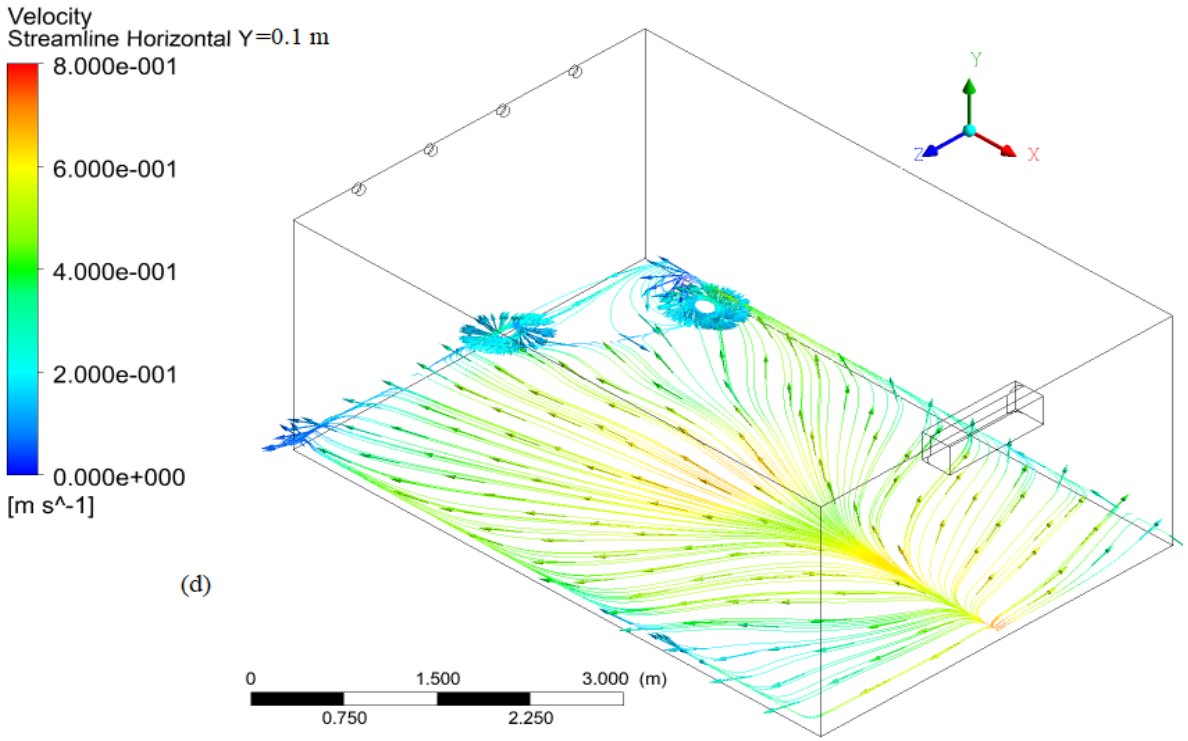

Figure 5.5 The air streamlines inside the CoolBot conditioned storage chamber at horizontal plane section simulated at different heights from bottom cooler surface along the Y-direction (a) is air velocity at Y = 2.2 m high, (b) is air velocity at Y = 1.3 m high, (c) is air velocity at Y = 0.6 m high and (d) is air velocity at Y = 0.1 m high from the floor of the room

Figure 5.6 (a - d) displays the CFX output of a 3-D horizontal, visualized and air velocity contours simulated under CBAC operation. The simulation displays that the air velocity ranged between 0.0 $m.s^{-1}$ and 4.2 $m.s^{-1}$ at the top horizontal plane, which was at Y = 2.2 m high from the bottom of the cooler surface (Figure 5.6 (a)). It was shown that that the air velocity distribution was not uniform and the flow was very slow, as the distance is far from the air conditioner inlet. The literature shows that air flow turbulence can cause the discontinuity of air flow, which further cools the air (Ma *et al.*, 2011), but it was not demonstrated at this plane position. At the middle plane, which was set at Y = 1.3 m high from the ground surface, the air velocity varied between 0.0 $m.s^{-1}$ and 1.5 $m.s^{-1}$ (Figure 5.6 (b)). As can be seen from the results, the air distribution in this section was good. At the Y = 0.6 m from the ground surface, the air velocity varied between 0.0 and 1.5 $m.s^{-1}$ and the air distribution was uniform (Figure 5.6 (c)). At the bottom horizontal plane section, which was set at Y = 0.1 m from the cooler ground surface, the air velocity was found to vary between 0.0 $m.s^{-1}$ and 0.8 $m.s^{-1}$. The variation in air velocity at the immediate bottom surface of the front wall was found to be high, while it

remained lower near the bottom of the outlet wall, compared to the front immediate section plane. Similar to the streamline flow, the air velocity contour indicated that there was less uniform movement and distribution vertically (*i.e.* from the top of the roof to floor) at different horizontal positions.

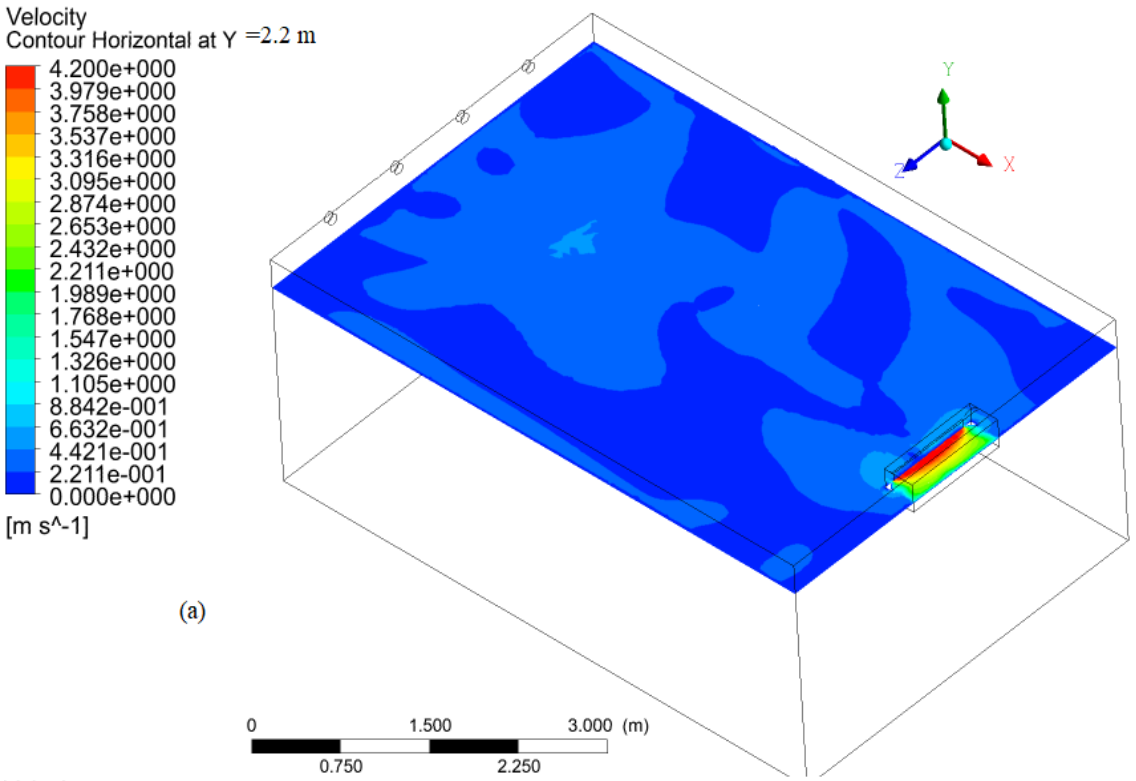

(a)

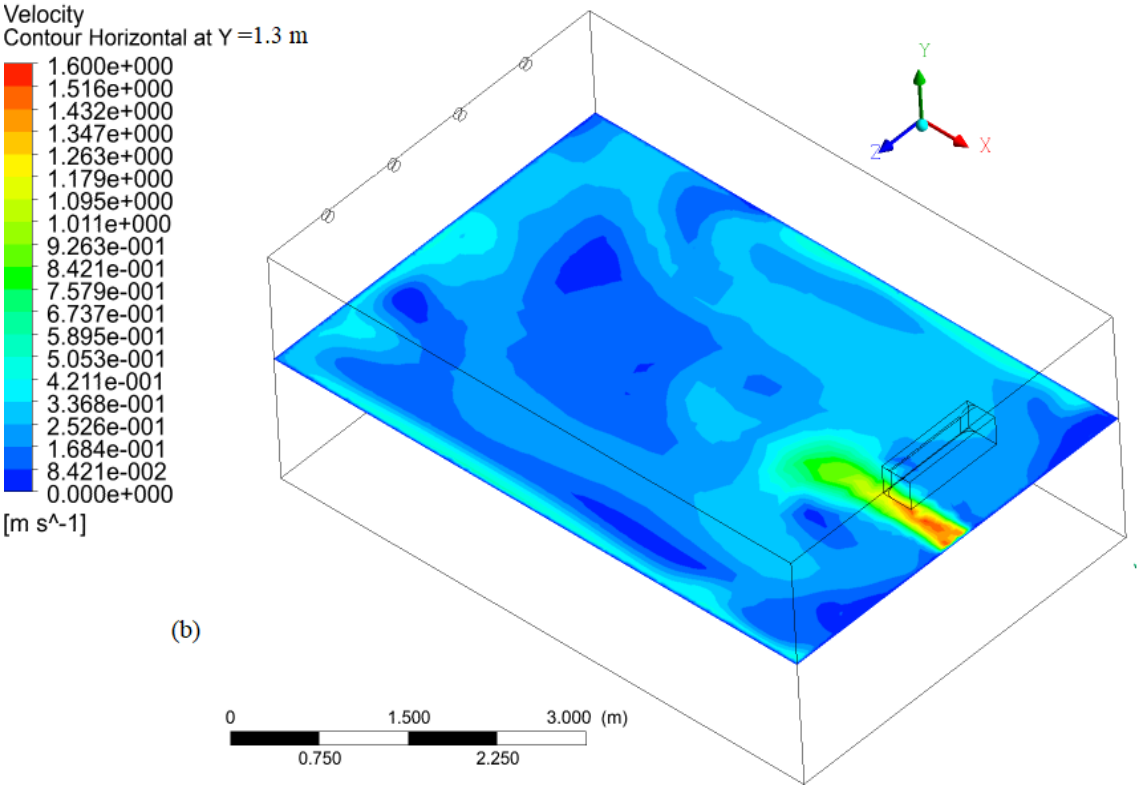

(b)

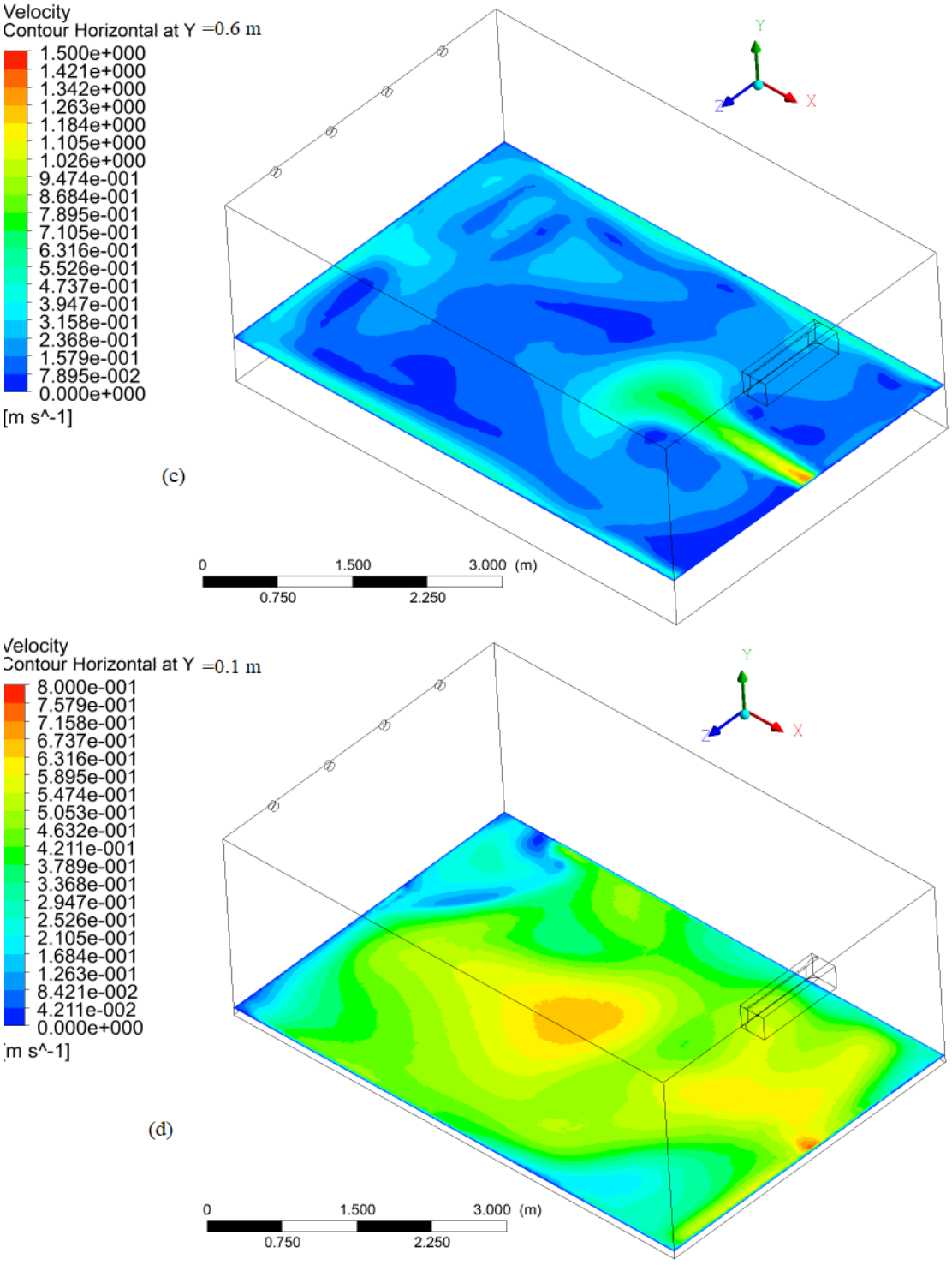

Figure 5.6 The 3-D air velocities contour inside the store room subjected to CoolBot air conditioning simulated at a horizontal imaginary plane at different heights above the cooler surface along the Y-direction (a) is air velocity at Y = 2.2 m high, (b) is air velocity at Y = 1.3 m high, (c) is air velocity at Y = 0.6 m high and (d) is air velocity at Y = 0.1 m high from the floor of the room

A 3-D vertical visualization using the CFX modelling of air streamlines inside the cooler that was subjected to the CoolBot-air-conditioning is displayed by Figure 5.7 (a - c). The results displayed that the air velocity varied between 0 $m.s^{-1}$ and 0.5 $m.s^{-1}$ at an imaginary vertical plane Z = 0.1 m from the right wall and the air exhibited a high circulation (Figure 5.7 (a)). At the vertical plane Z = 1 m from the right wall, the air velocity ranged from 0.0 $m.s^{-1}$ to 0.7 $m.s^{-1}$ and there was air circulation near the bottom of the plane at the exit wall (Figure 5.7 (b)). Along the symmetry line of vertical plane Z = 2 m, the air velocity varied between 0.0 $m.s^{-1}$ and 4.2 $m.s^{-1}$ (Figure 5.7 (c)). The air well circulated near the center of vertical plane at a low speed, which is important, to enhance cooling (Ma *et al.*, 2011). The air velocity demonstrated a decreasing trend from top to bottom along the vertical symmetry line.

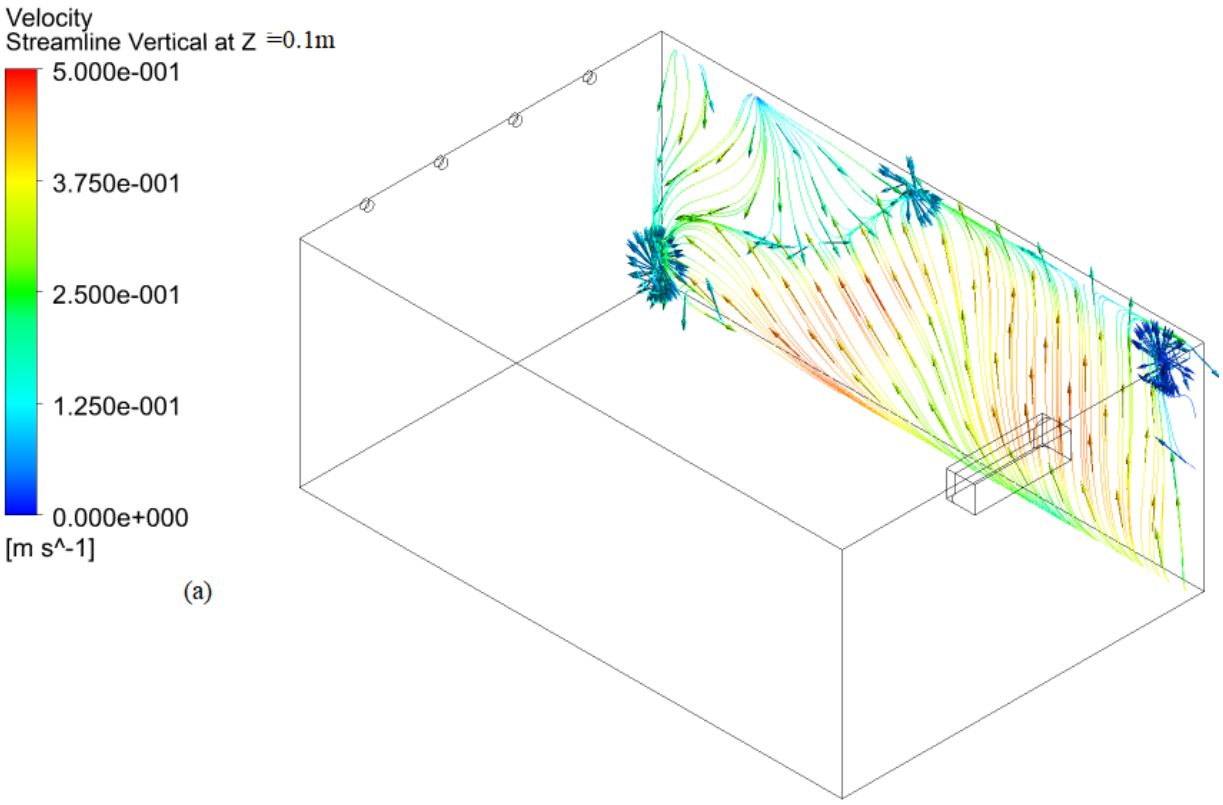

(a)

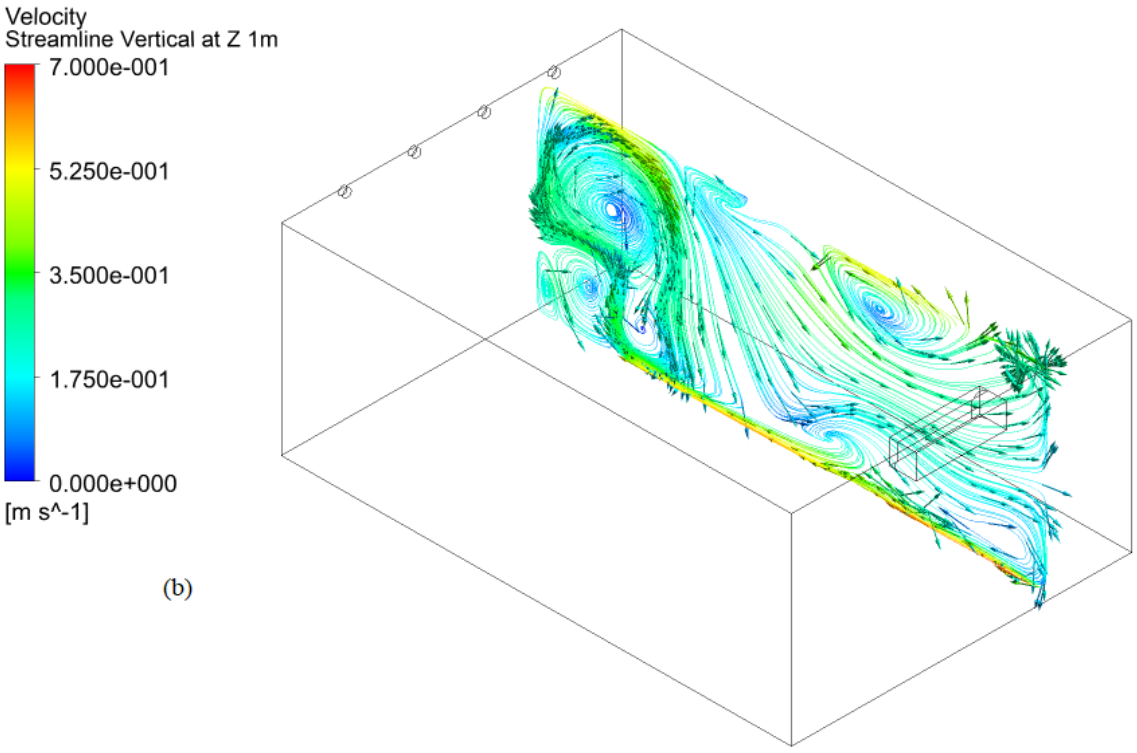

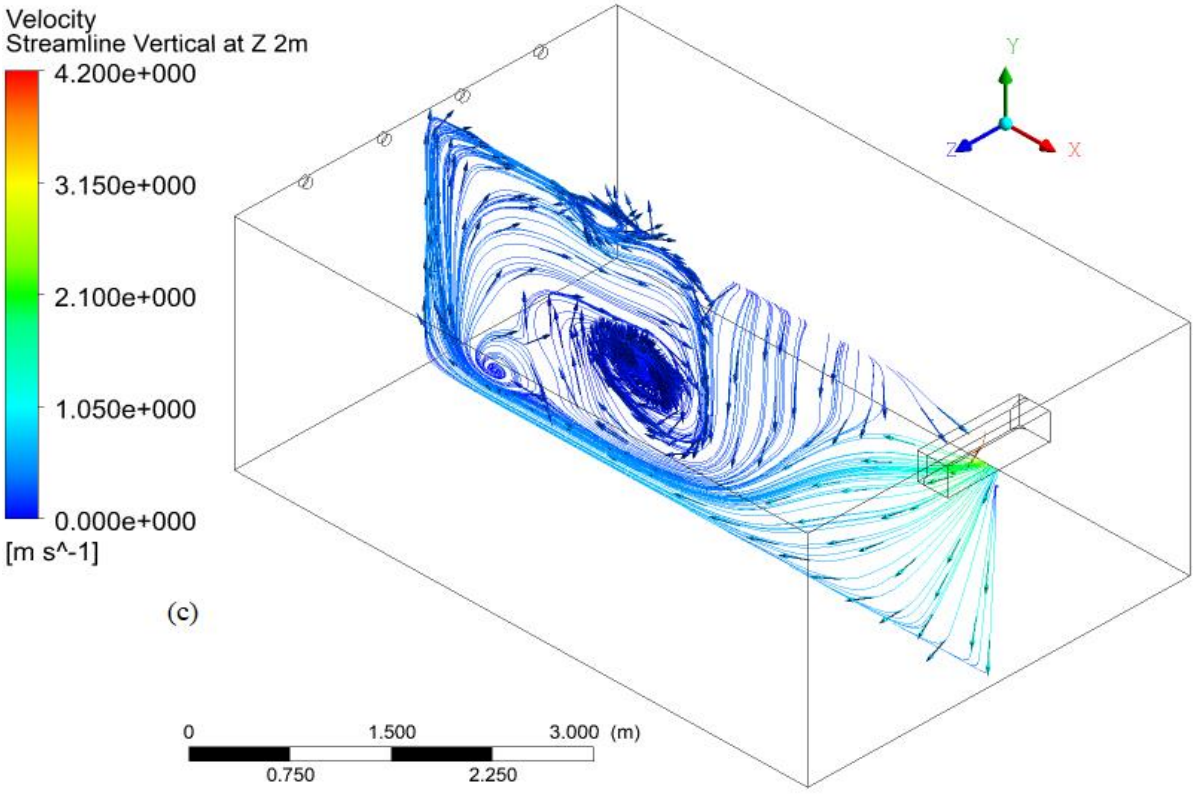

Figure 5.7 A 3-D air velocity streamline simulation inside the cooler subjected to the CoolBot air conditioner (CBAC) at a vertical section plane, which was positioned along a Z-direction (a) is air velocity at Z = 0.1 m away from the wall, (b) is air velocity at Z = 1.0 m away from the wall, and (c) is air velocity along the vertical symmetry line (Z = 2 m) from the wall of the room

Figure 5.8 (a - c) displays the CFX simulation output of a 3-D vertical visualization of air velocity contour subjected to the CoolBot-air-conditioning cold room. The contour showed that the air velocity varied between 0.0 $m.s^{-1}$ and 0.6 $m.s^{-1}$ at a vertical plane Z = 0.1 m from the right wall (Figure 5.8 (a)), which was slow. A uniform air velocity was observed at the top middle, while a relatively high velocity was displayed near the middle wall surface at the center of the wall plane section. The air velocity at the vertical plane Z = 1 m from the right wall was found to vary between 0.0 $m.s^{-1}$ and 0.8 $m.s^{-1}$ (Figure 5.8 (b)). A non-uniform air velocity and distribution were visually observed at Z = 1 m from the wall. At a vertical symmetry plane position Z = 2 m away from a side wall was found to vary from 0.0 $m.s^{-1}$ to 4.2 $m.s^{-1}$ and the majority of the air velocities were high near to the inlet wall and downward to the floor of the plane (Figure 5.8 (c)). However, a slow velocity was observed near the exit wall and at the center of the floor surface.

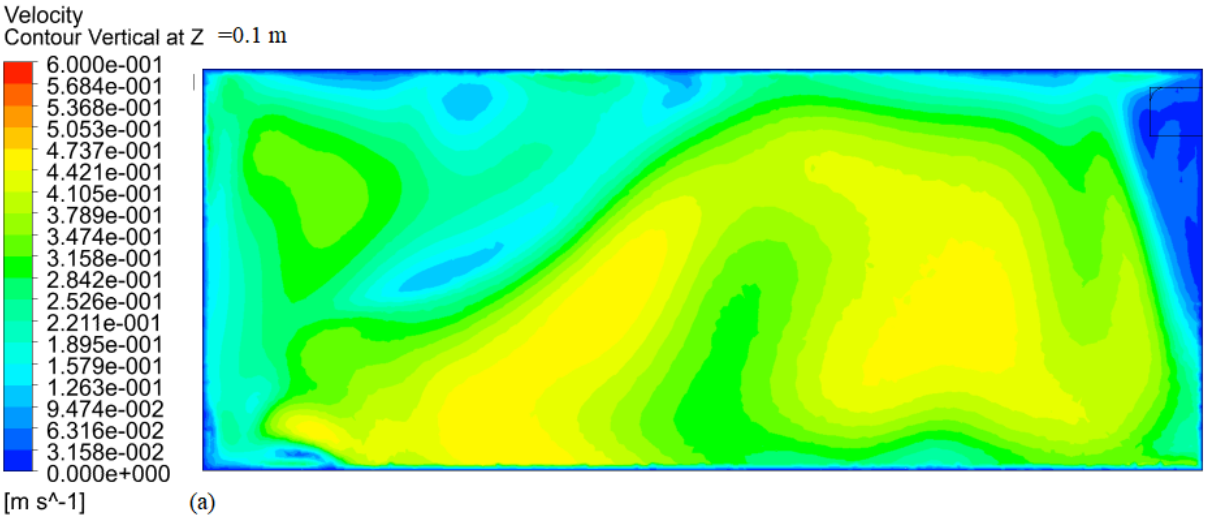

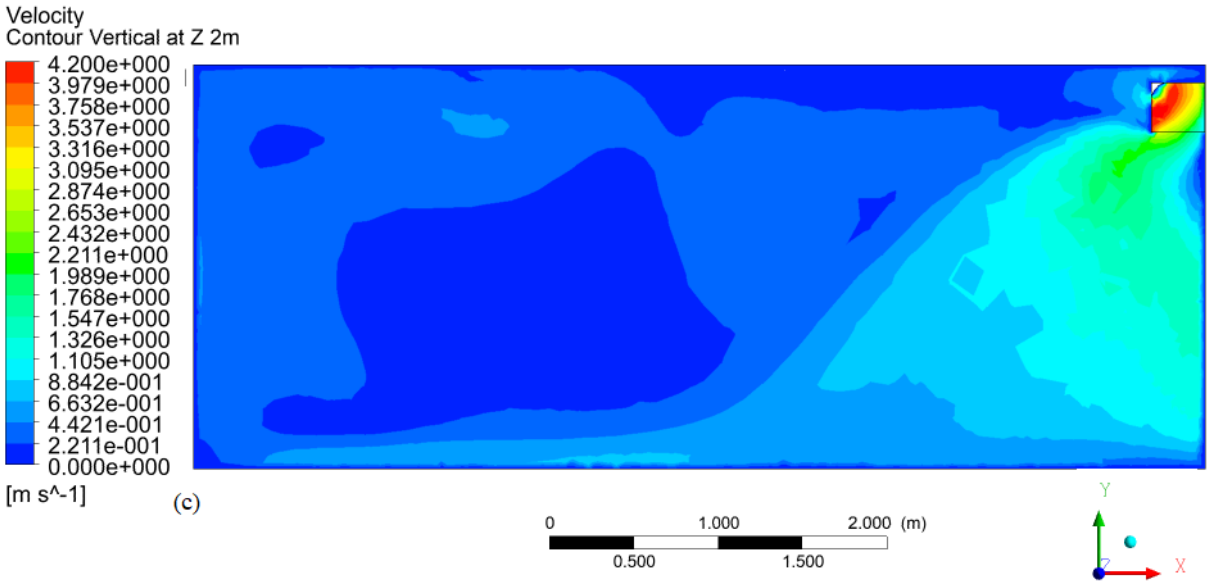

Figure 5.8 Air velocity contour captured inside the CoolBot air conditioned cold store at a vertical imaginary section plane at different positions along a vertical plane at different Z-positions) (a) is air velocity at Z = 0.1 m away from the wall, (b) is air velocity at Z = 1.0 m away from the wall, and (c) is air velocity along the vertical symmetry line (Z = 2 m) from the wall of the room

5.1.3.3 Effect of combined evaporative cooler and CoolBot-air-conditioner airflow characteristics

The air velocity streamline inside the coolers that were conditioned using EC and CBAC, when operated simultaneously together, is shown in Figure 5.9 (a - d). The results showed that the air velocity varied between 0.0 $m.s^{-1}$ and 2.0 $m.s^{-1}$ at a horizontal plane of Y = 2.2 m, parallel to the air conditioner inlet. Air velocity was found to be uniform and well circulated along the plane surface (Figure 5.9 (a)). At the middle of the horizontal plane Y = 1.3 m (Figure 5.9 (b)), the air velocity varied between 0.0 $m.s^{-1}$ and 1.6 $m.s^{-1}$. Very good air circulation along the plane was observed. The horizontal imaginary plane of Y = 0.6 m high displayed that the air velocity ranged between 0.0 $m.s^{-1}$ and 2.2 $m.s^{-1}$ (Figure 5.9 (c)). Air circulation and velocity distribution was sound along the plane parallel to the EC inlet. The bottom surface of a horizontal pale Y = 0.1 m from the floor demonstrated a slow velocity, but there was a uniform distribution that varied between 0.0 $m.s^{-1}$ and 1.5 $m.s^{-1}$ (Figure 5.9 (d)). The results (Figure 5.9 (a - d)) demonstrated that the best uniformity of air velocity and distribution was along the horizontal planes at different horizontal plane sections. Moreover, Figure 5.10 demonstrated the best uniform air circulation along the horizontal cross sections at different imaginary Y-planes, due

to the mixing scenarios by the fan and air conditioner. The cumulative effects of the combined EC + CBAC on the air velocity and airflow distribution were found to be the best, when compared to the EC and CBAC alone.

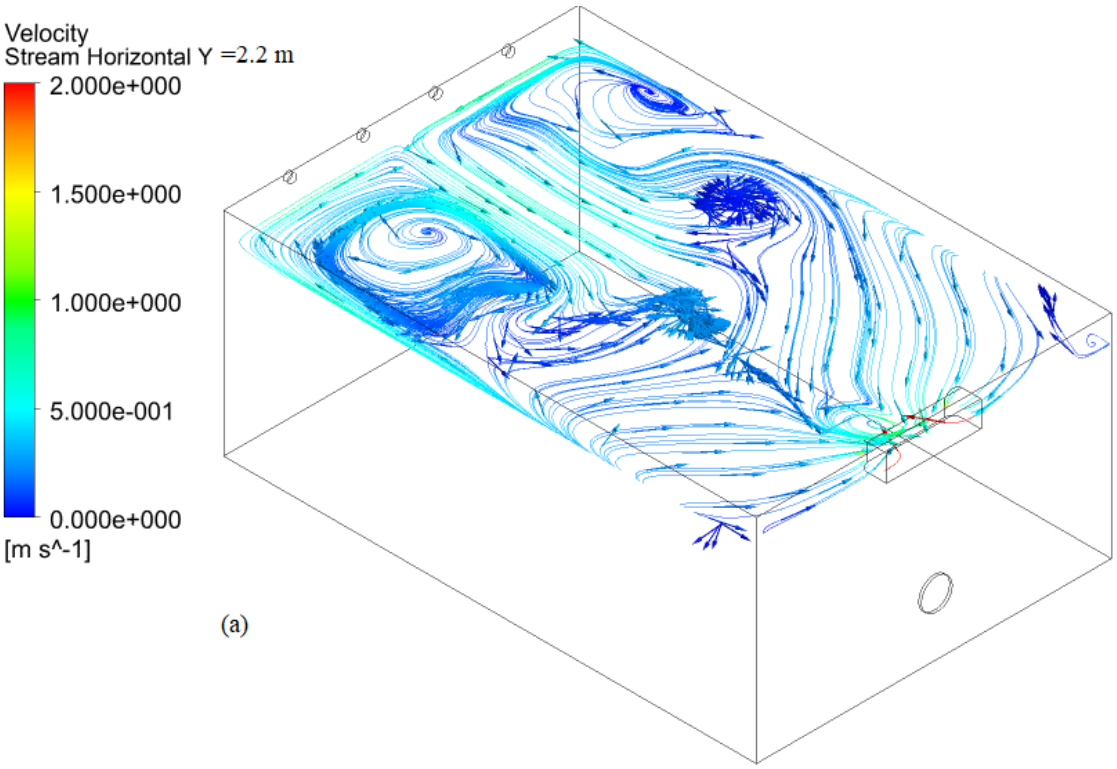

(a)

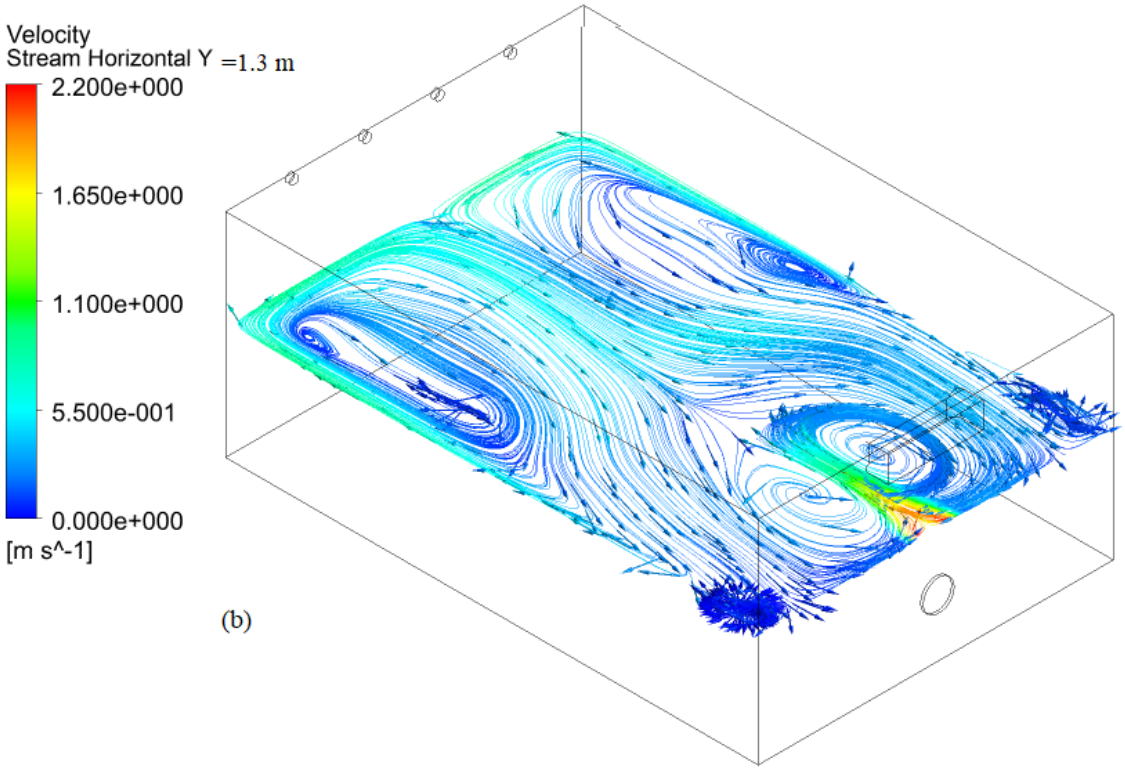

(b)

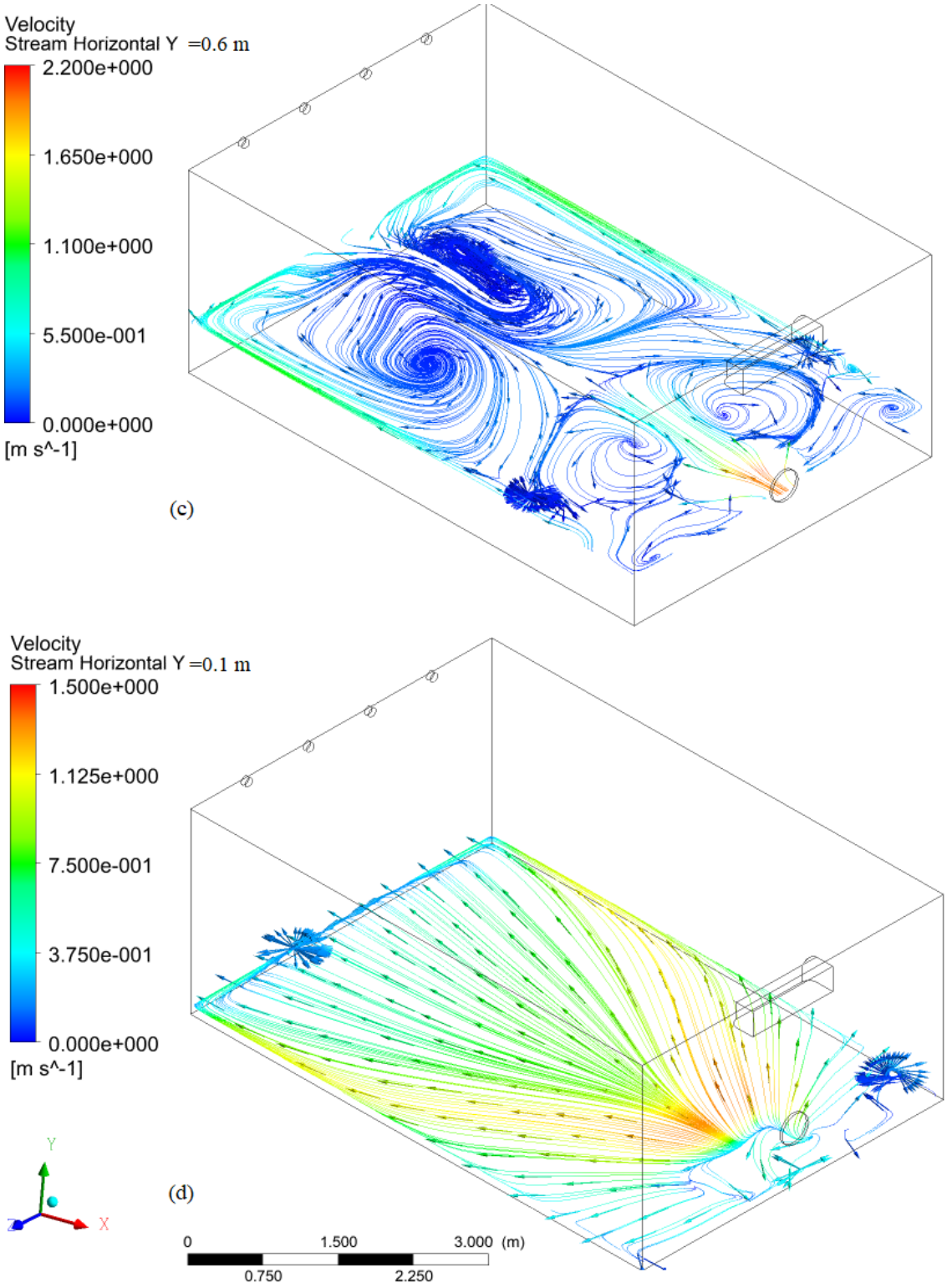

Figure 5.9 The air streamlines inside the combined evaporative cooler and the CoolBot conditioned storage chamber at horizontal plane section simulated at different heights from bottom cooler surface along the Y-direction (a) is air velocity at Y = 2.2 m high, (b) is air velocity at Y = 1.3 m high, (c) is air velocity at Y = 0.6 m high and (d) is air velocity at Y = 0.1 m high from the floor of the room

Figure 5.10 (a - d) displayed the CFX simulation contour of velocity output along the imaginary horizontal planes of the evaporatively cooled and ColBot air conditioner cooled storage chambers. The results displayed that air velocity varied between 0.0 $m.s^{-1}$ and 3.2 $m.s^{-1}$ at the top surface of the cooler Y = 2.2 m (Figure 5.10 (a)) and the air velocity and distribution were not found to be uniform. At the horizontal middle plane Y = 1.3 m, the air velocity was found to vary between 0.0 $m.s^{-1}$ and 2.0 $m.s^{-1}$ (Figure 5.10 (b)). At the horizontal plane (Y = 0.6 m), parallel to the evaporative cooler fan, the air velocity was found to range from 0.0 $m.s^{-1}$ to 2.5 $m.s^{-1}$ and variations in air velocity were observed (Figure 5.10 (c)). At the horizontal floor surface (Y = 0.1 m) ((Figure 5.10 (d)), the air velocity was found varied between 0.0 $m.s^{-1}$ and 1.6 $m.s^{-1}$ and uniformity along the plane was observed. Overall, the air velocity contour displayed that there was less uniform air velocity and air distribution vertically at different horizontal plane positions. The vertical non-uniformity of the air velocity and air distribution can affect the ideal air flow along the vertical directional airflow during storage of fresh produce, if it is ideally stacked (Nahor *et al.*, 2005).

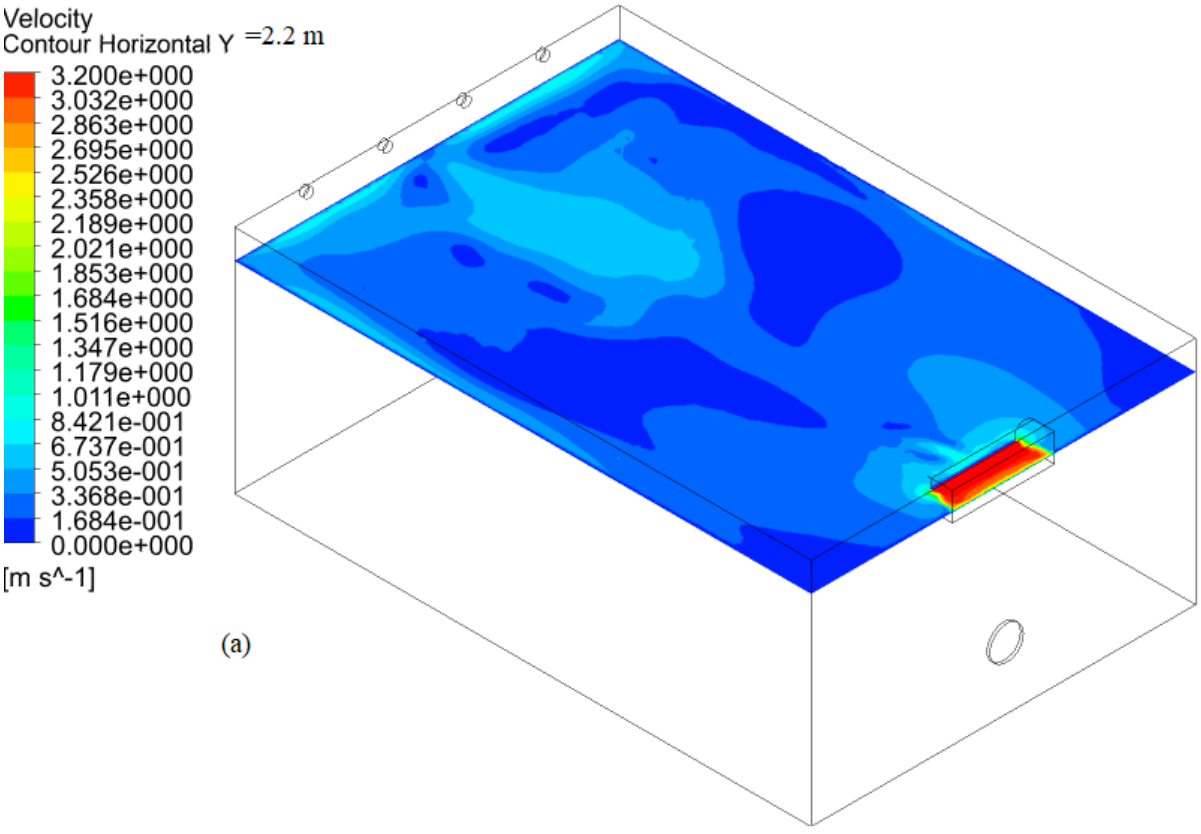

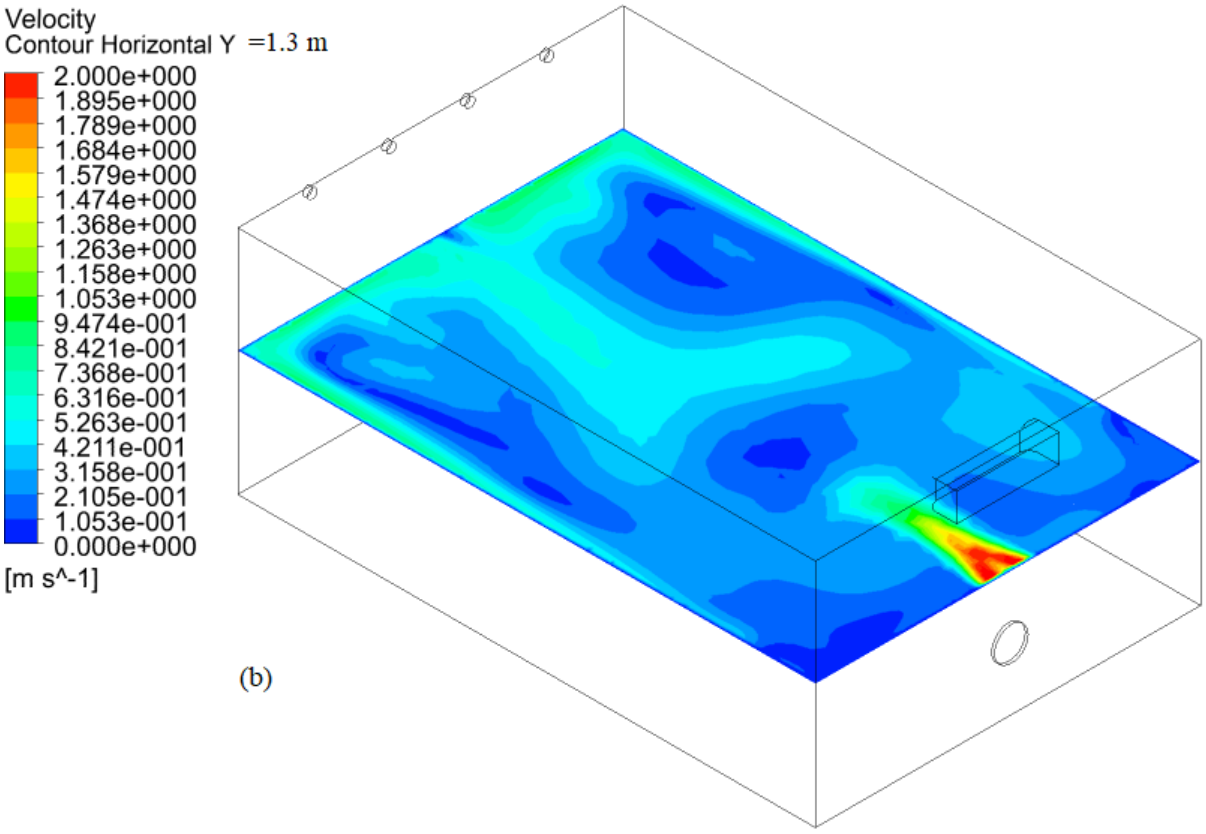
Velocity
Contour Horizontal Y =1.3 m
2.000e+000
1.895e+000
1.789e+000
1.684e+000
1.579e+000
1.474e+000
1.368e+000
1.263e+000
1.158e+000
1.053e+000
9.474e-001
8.421e-001
7.368e-001
6.316e-001
5.263e-001
4.211e-001
3.158e-001
2.105e-001
1.053e-001
0.000e+000
[m s^-1]

(b)

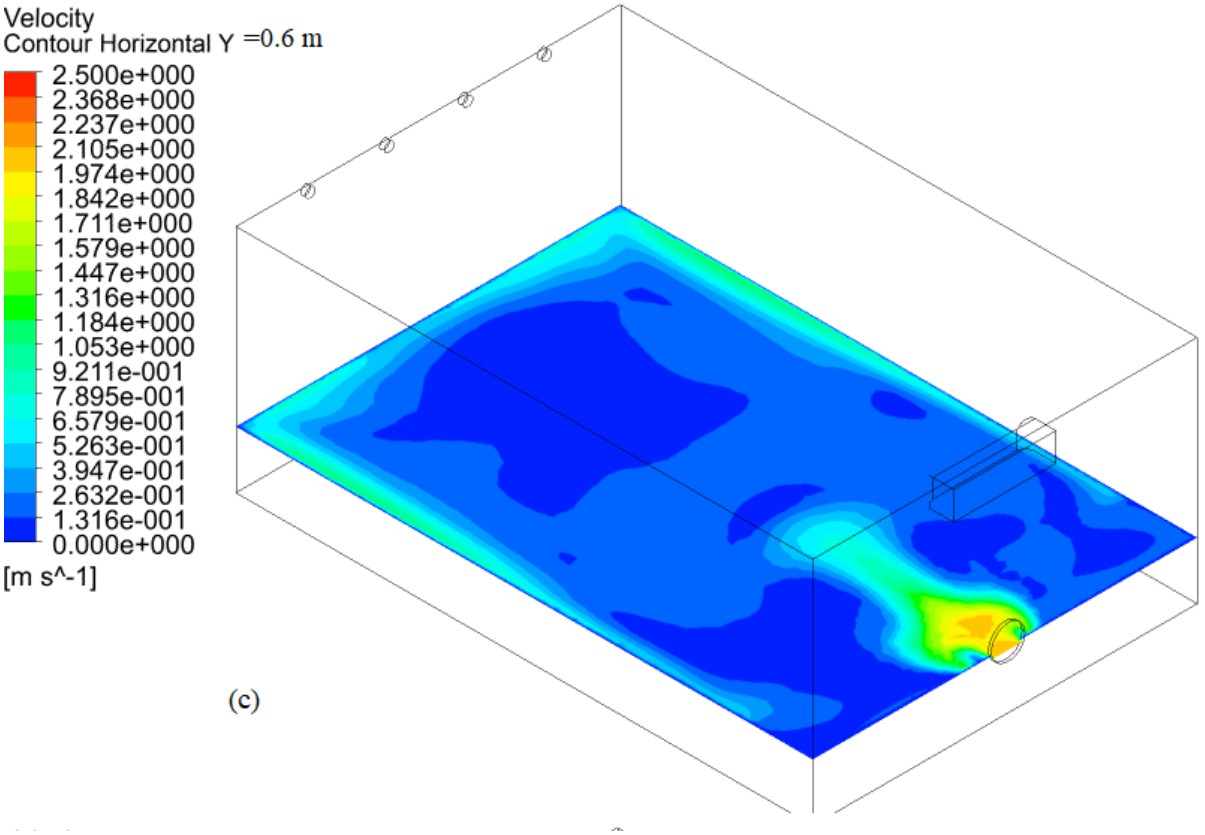
Velocity
Contour Horizontal Y =0.6 m
2.500e+000
2.368e+000
2.237e+000
2.105e+000
1.974e+000
1.842e+000
1.711e+000
1.579e+000
1.447e+000
1.316e+000
1.184e+000
1.053e+000
9.211e-001
7.895e-001
6.579e-001
5.263e-001
3.947e-001
2.632e-001
1.316e-001
0.000e+000
[m s^-1]

(c)

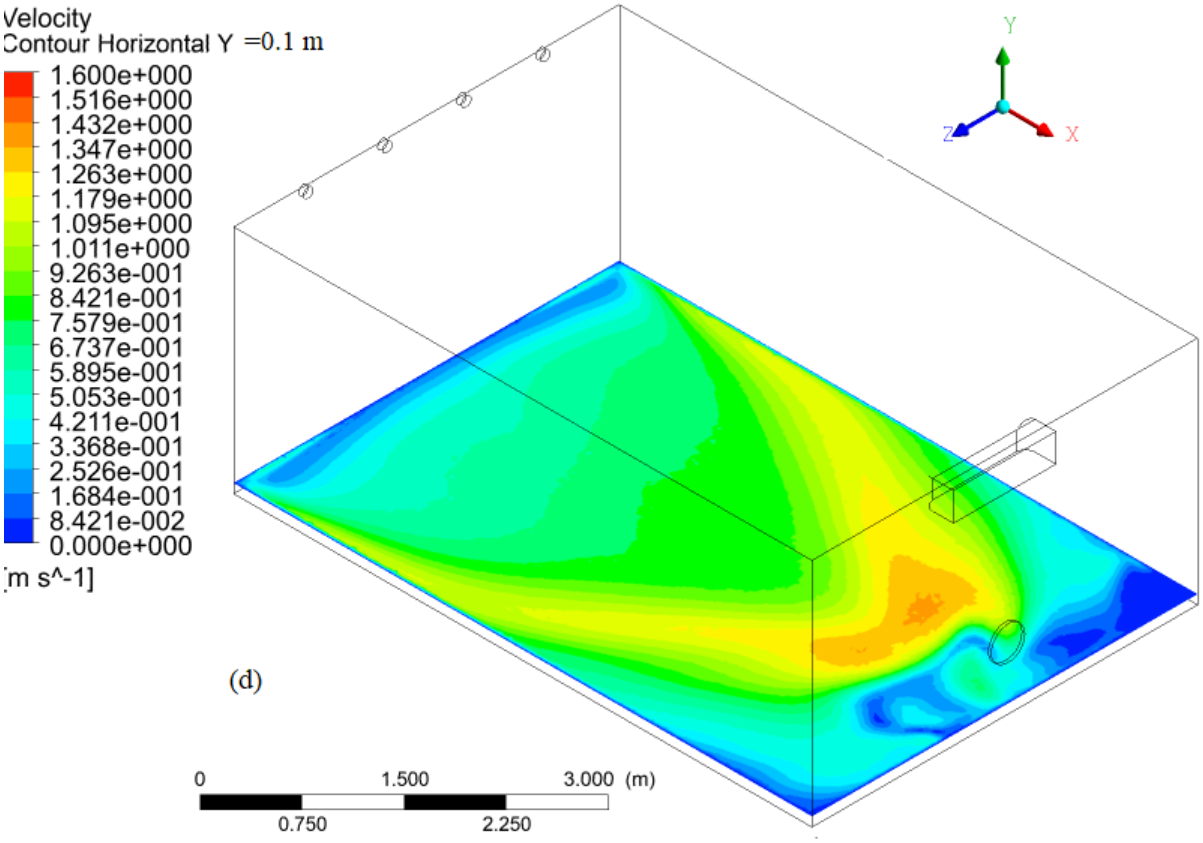

Figure 5.10 Air velocity contours inside the combined evaporatively cooled and CoolBot-air-conditioned cooled rooms (EC+CBAC) along different horizontal section planes Y-direction (a) is air velocity at Y = 2.2 m high, (b) is air velocity at Y = 1.3 m high, (c) is air velocity at Y = 0.6 m high and (d) is air velocity at Y = 0.1 m high from the floor of the room

The air velocity streamlines along the vertical plane at different Z-locations for the unloaded room cooled by combined operation of EC and CBAC storage chamber (Figure 5.11 (a - c)). The results showed that air velocity ranged from 0.0 $m.s^{-1}$ to 0.7 $m.s^{-1}$ at a vertical plane Z = 0.1 m from the right wall and showed good recirculation vertically (Figure 5.11 (a)). Along a vertical plane Z = 1 m from the right wall, the air velocity was found to vary between 0.0 $m.s^{-1}$ and 1.5 $m.s^{-1}$ and a good agitation of the air near the wall can enhance the cooling and more re-circulation (Figure 5.11 (b)) (Ma *et al.*, 2011). Along the vertical symmetry line Z = 2 m, the air velocity and air distribution was found to range from 0.0 $m.s^{-1}$ to 3.0 $m.s^{-1}$ (Figure 5.11 (c)). Moreover, a high air circulation was observed at the outlet wall and a low air velocity was observed along the vertical symmetry line (Figure 5.11 (c)).The air velocity and air distribution were found to be uniform, as well as air circulation from the top surface towards the bottom surface along the symmetry line.

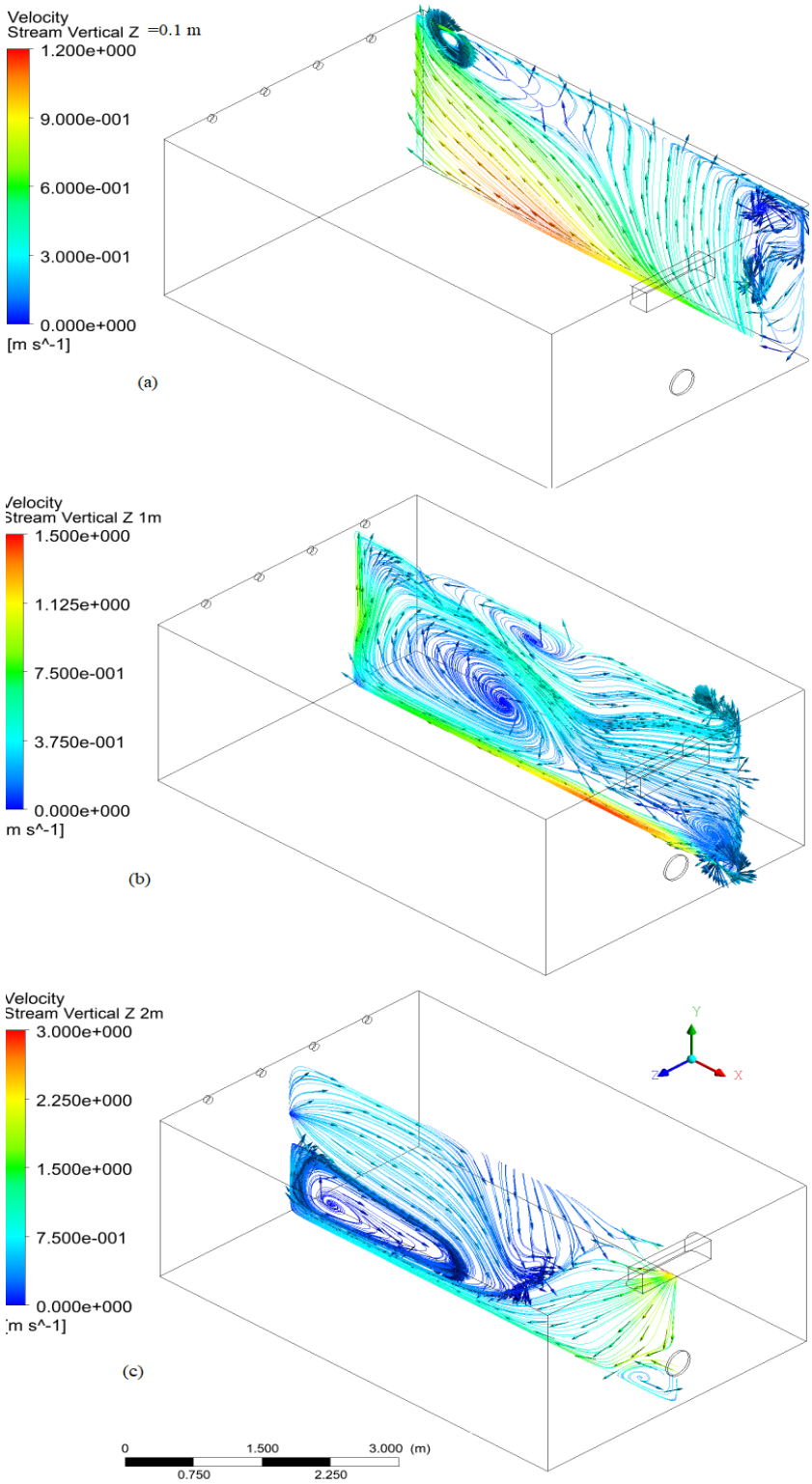

Figure 5.11 The 3-D air streamlines inside the evaporatively cooled and CoolBot-air-conditioned room (EC+CBAC) along different vertical section planes at different positions along Z-direction (a) is air velocity at Z = 0.1 m away from the wall, (b) is air velocity at Z = 1.0 m away from the wall, and (c) is air velocity along the vertical symmetry line (Z = 2 m) from the wall of the room

Figure 5.12 (a - c) displayed the CFX simulation output of the vertical air velocity contour of the combined EC+CBAC storage chamber. The contour showed that the air velocity ranged from 0.0 $m.s^{-1}$ to 1.2 $m.s^{-1}$ at a vertical imaginary plane, which was set at Z = 0.1 m from the right cooler near wall. A uniform air velocity and distribution were found along the plane near the middle and exit walls (Figure 5.12 (a)). The air velocity varied between 0.0 $m.s^{-1}$ and 1.0 $m.s^{-1}$ along the vertical plane section, which was set at Z = 1 m from the right cooler vertical wall (Figure 5.12 (b)). Moreover, a mixed air velocity and distribution was observed along the section plane, which is in agreement with the findings of Ma *et al.* (2011). Along the vertical symmetry line, which was set at Z = 2 m from the right cooler vertical wall, the air velocity and distribution was found to be between 0.0 $m.s^{-1}$ and 3.2 $m.s^{-1}$. The air velocity was high at the middle of the vertical symmetry plane section and along the vertical plane downward or/and upward, while near the outlet cooler vertical wall, a small air movement with lower velocity was observed (Figure 5.12 (c)). The air circulation, due to the mixing characteristics from the two inlets *i.e.* air conditioner inlet and the fan caused the air to circulate and distribute well.

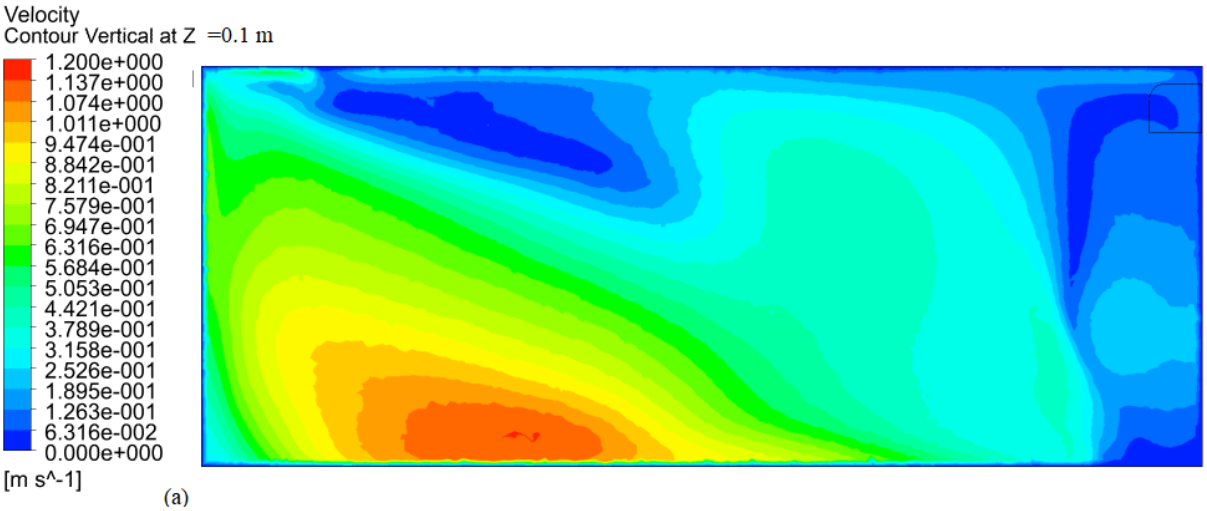

(a)

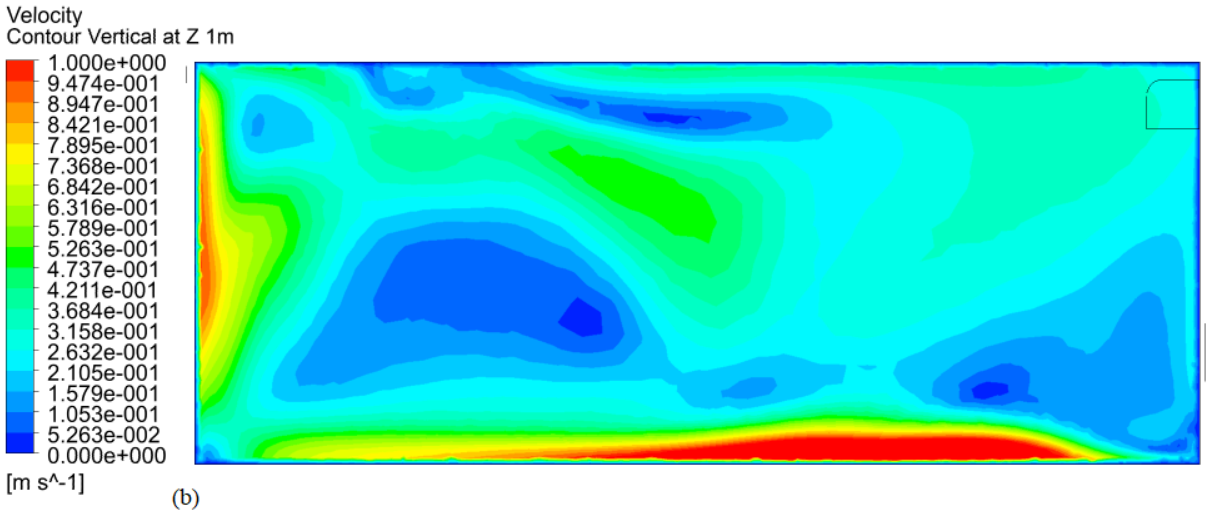

(b)

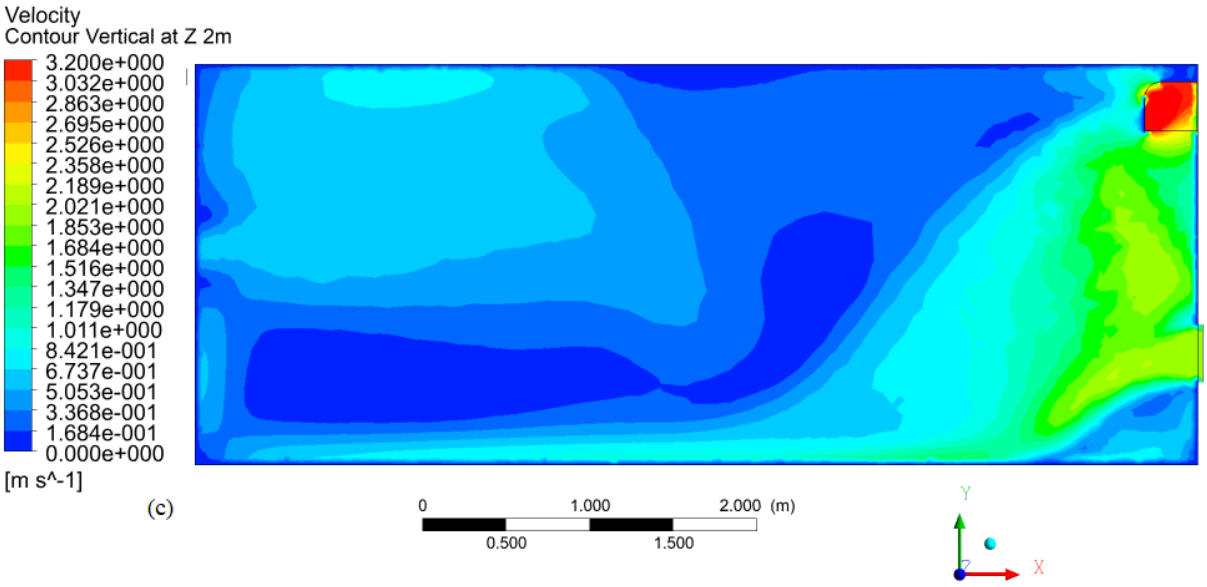

Figure 5.12 Air velocity contours inside the evaporatively cooled and CoolBot-air-conditioned (EC+CBAC) cooler at an imaginary vertical section plane at different positions along Z-direction (a) is air velocity at Z = 0.1 m away from the wall, (b) is air velocity at Z = 1.0 m away from the wall, and (c) is air velocity along the vertical symmetry line (Z = 2 m) from the wall of the room

Compared to the evaporatively cooled and CoolBot-air-conditioned cold rooms, the combined operation of both cooling systems led to more uniform air velocity and air flow distribution inside the room. More air circulation was also found in the combined operation. The uniformity of the airflow inside the cold rooms can affect the heat and mass transfer for the loaded produce (Nahor *et al.*, 2005; Xie *et al.*, 2006; Norton *et al.*, 2009, 2010).

5.1.3.4 Validation

The validation of the numerical model was done by comparing it with the measured air velocities inside pear cold store (Nahor *et al.*, 2005). The models validation were found to have a good agreement between the measured and predicted values i.e. the RMSE of air velocities were found to be 1.42 $m.s^{-1}$, 0.27 $m.s^{-1}$, 0.38 $m.s^{-1}$, for EC, CBAC and EC+CBAC, respectively. Several researchers reported that, the RMSE value 0.15 $m.s^{-1}$ for apple stacks inside cold store (Ambaw *et al.*, 2017). Nahor *et al.* (2005) reported that 20% of the air velocity magnitude accuracy was achieved inside loaded cold store, and a similar result was achieved in the current study.

5.1.4 Conclusions

The simulation of unloaded low-cost cold storage chambers is the basic principle for studying the heat and mass transfer phenomenon inside a loaded cold storage chambers. Steady state, incompressible, turbulent, isothermal CFD models were used to study the airflow computationally, by applying the Navier-Stokes models. The validation of the models was performed by comparing the experimental air velocity measurements inside the cooler with that of the computed air velocity at different positions inside the cold store. The visual CFD model airflow distribution study displayed that there was non-uniform airflow inside the storage chamber that was subjected to EC, CBAC or EC+CBAC. The vertical and horizontal airflow streamline and contour displayed that the airflow distribution was not totally uniform, when subjected to evaporative cooling and CoolBot-air-conditioning. On the other hand, the combined operation of evaporatively and CoolBot-Air-Conditioned cold rooms resulted in a good air distribution, both vertically and horizontally, throughout the cold room. The combined operation was the best for maintaining airflow distribution, which was followed by CBAC and EC, respectively. Therefore, the evaporative cooler psychrometric unit, the CoolBot-air-conditioner and the combination of the evaporative cooler and CoolBot-air-conditioning should be re-designed, with the aim of improving the uniformity of airflow distribution and airflow rate sufficiently, to ventilate the inside of the storage area. The airflow near the right, left and outlet walls locations receives air travels at very slow airflow velocities, which are not sufficient to ventilate the storage chamber with loads. Based on the results obtained in this study, the cold storage chamber requires a high speed fan to suck the inside air through each storage chamber. The detailed airflow, heat and mass transfer with loaded bulk/stacked fresh produce is critically important to optimize the airflow, in terms of air velocity and distribution, inside the cold storage chambers and to use the best of these technologies.

5.1.5 Acknowledgements

We would like to warmly acknowledge the Federal Ministry of Education, Ethiopia. South African National Research Foundation (NRF – TWAS) and the host institute, University of Kwa-Zulu Natal.

5.1.6 References

Ambaw, A, Delele, MA, Defraeye, T, Ho, QT, Opara, LU, Nicolai, BM and Verboven, P. 2013. The use of CFD to characterize and design post-harvest storage facilities: Past, present and future. *Computers and Electronics in Agriculture,* 93**,** 184-194.

Ansys. 2016. ANSYS CFX-Pre User's Guide. *ANSYS.* Canonsburg, PA, USA.

Boyette, MD and Rohrbach, RP. 1993. A low-cost, portable, forced-air pallet cooling system. *Applied engineering in agriculture,* 9**,** 97-104.

Castro, LR, Vigneault, C and Cortez, LaB. 2005. Cooling performance of horticultural produce in containers with peripheral openings. *Postharvest biology and technology,* 38**,** 254-261.

Defraeye, T. 2014. Advanced computational modelling for drying processes: a review. *Applied Energy,* 131**,** 323-344.

Delele, MA, Ngcobo, MEK, Getahun, ST, Chen, L, Mellmann, J and Opara, UL. 2013. Studying airflow and heat transfer characteristics of a horticultural produce packaging system using a 3-D CFD model. Part II: Effect of package design. *Postharvest Biology and Technology,* 86**,** 546-555.

Duan, Z, Zhan, C, Zhao, X and Dong, X. 2016. Experimental study of a counter-flow regenerative evaporative cooler. *Building and Environment,* 104**,** 47-58.

Getahun, S, Ambaw, A, Delele, M, Meyer, CJ and Opara, UL. 2017a. Analysis of airflow and heat transfer inside fruit packed refrigerated shipping container: Part I–Model development and validation. *Journal of Food Engineering,* 203**,** 58-68.

Getahun, S, Ambaw, A, Delele, M, Meyer, CJ and Opara, UL. 2017b. Analysis of airflow and heat transfer inside fruit packed refrigerated shipping container: Part II e Evaluation of apple packaging design and vertical flow resistance. *Journal of Food Engineering,* 203**,** 83-94.

Ho, SH, Rosario, L and Rahman, MM. 2010. Numerical simulation of temperature and velocity in a refrigerated warehouse. *International Journal of Refrigeration-Revue Internationale Du Froid,* 33**,** 1015-1025.

Hoang, ML, Verboven, P, De Baerdemaeker, J and Nicolai, BM. 2000. Analysis of the air flow in a cold store by means of computational fluid dynamics. *International Journal of Refrigeration-Revue Internationale Du Froid,* 23**,** 127-140.

Khodak, A, Loesser, G, Zhai, Y, Udintsev, V, Klabacha, J, Wang, W, Johnson, D and Feder, R. 2015. Numerical Analysis of Coolant Flow and Heat Transfer in ITER Diagnostic First Wall. *Fusion Science and Technology,* 68**,** 521-525.

Kitinoja, L. 2013. Innovative Small-scale Postharvest Technologies for reducing losses in Horticultural Crops. *Ethiop .J. Appl. Sci. Technol. ,* Special Issue, 1**,** 9-15.

Kolodziejczyk, M, Butrymowicz, D, Smierciew, K and Gagan, J. July 11-14, 2016 2016. Numerical Modelling of Heat And Mass Transfer Processes In Chinese Cabbage Cold Storage Chamber. 16th International Refrigeration and Air Conditioning Conference 1-9. Purdue e-Pubs, Purdue University, USA.

Ma, J, Mathúna, SC, Hayes, M and Provan, G. 11 May 2016 2011. Model and visualise the relationship between energy consumption and temperature distribution in cold rooms. *In:* Carr, H and Grimstead, I, eds. 29th conference of theory and practice of computer graphics, 1-2. The Eurographics Association, EG, UK

Nahor, HB, Hoang, ML, Verboven, P, Baelmans, M and Nicolai, BM. 2005. CFD model of the airflow, heat and mass transfer in cool stores. *International Journal of Refrigeration-Revue Internationale Du Froid,* 28**,** 368-380.

Norton, T, Grant, J, Fallon, R and Sun, DW. 2009. Assessing the ventilation effectiveness of naturally ventilated livestock buildings under wind dominated conditions using computational fluid dynamics. *Biosystems Engineering,* 103**,** 78-99.

Norton, T, Grant, J, Fallon, R and Sun, DW. 2010. Optimising the ventilation configuration of naturally ventilated livestock buildings for improved indoor environmental homogeneity. *Building and Environment,* 45**,** 983-995.

Pal, RK, Roy, SK and Srivastava, S. 1997. Storage performance of kinnow mandarins in evaporative cool chamber and ambient condition. *Journal of food science and technology,* 34**,** 200-203.

Praneeth, HR and Gowda, BS. 2015. An analysis of cold store by CFD simulation. *International Journal of Innovations in Engineering Research and Technology,* 2**,** 1-14.

Roy, SK. 2007. *Low or no-cost cool chambers for fruits and vegetables.* National Horticulture Mission, India.

Roy, SK and Khardi, DS. 1985. Zero Energy Cool Chamber. *India Agricultural Research Institute: New Delhi, India. ,* Research Bulletin No.43: 23-30.

Roy, SK and Pal, RK. 1989. A low cost zero energy cool chamber for short term storage of mango. III International Mango Symposium 291, 519-524.

Roy, SK and Pal, RK. 1994. A low-cost cool chamber: an innovative technology for developing countries. *In:* Champ, BR, Highley, E and Johnson, GI, eds. Postharvest Handling of Tropical Fruits: ACIAR Proceedings, 393-395. Australian Centre for International Agricultural Research, Australia.

Sapounas, AA, Bartzanas, T, Nikita-Martzopoulou, C and Kittas, C. 2016. Aspects of CFD Modelling of a Fan and Pad Evaporative Cooling System in Greenhouses. *International Journal of Ventilation,* 6**,** 379-388.

Sapounas, AA, Nikita-Martzopoulou, C and Martzopoulos, G. 2007. Numerical and Experimental Study of Fan and Pad Evaporative Cooling System in a Greenhouse with Tomato Crop. International Symposium on High Technology for Greenhouse System Management: Greensys2007 801, 987-994.

Saran, S, Dubey, N, Mishra, V, Dwivedi, SK and Raman, NLM. 2013. Evaluation of coolbot cool room as a low cost storage system for marginal farmers. *Progressive Horticulture,* 45**,** 115-121.

Tripathi, PC and Lawande, KE. 2010. Temperature-related changes in respiration and Q10 coefficient in different varieties of onion. *Progressive Horticulture,* 42**,** 88-90.

Tseng, CJ, Yamaguchi, M and Ohmori, T. 1997. Thermal conductivity of polyurethane foams from room temperature to 20 K. *Cryogenics,* 37**,** 305-312.

Versteeg, HK and Malalasekera, W. 2007. *An introduction to computational fluid dynamics: the finite volume method.* Pearson Education Limited, UK.

Workneh, TS. 2010. Feasibility and economic evaluation of low-cost evaporative cooling system in fruit and vegetables storage. *African Journal of Food, Agriculture, Nutrition and Development,* 10**,** 2984-2997.

Workneh, TS, Ngejane, M, Thipe, EL, Larange, L and Smithers, JC. Nov. 25-28, 2012 2012. Design, construction and performance evaluation of a multistage pad evaporative cooler for extending the shelf life of fruit and vegetables. The 7th CIGR Section VI International Technical Symposium "Innovating the Food Value Chain" Postharvest Technology and AgriFood Processing, 1-20. CIGR, Stellenbosch, South Africa.

Wu, JW, Sung, WF and Chu, HF. 1999. Thermal conductivity of polyurethane foams. *International Journal of Heat and Mass Transfer,* 42**,** 2211-2217.

Xie, J, Qu, XH, Shi, JY and Sun, DW. 2006. Effects of design parameters on flow and temperature fields of a cold store by CFD simulation. *Journal of Food Engineering,* 77**,** 355-363.

Xuan, YM, Xiao, F, Niu, XF, Huang, X and Wang, SW. 2012. Research and application of evaporative cooling in China: A review (I) - Research. *Renewable & Sustainable Energy Reviews,* 16**,** 3535-3546.

Yadav, VK, Singh, A and Chandra, P. 2002. Experimental Evaluation of the effect of Fan Pad Evaporative Cooling System parameters on Greenhouse Cooling. *Journal of Agricultural Engineering,* 39**,** 49-53.

Zhao, CJ, Han, JW, Yang, XT, Qian, JP and Fan, BL. 2016. A review of computational fluid dynamics for forced-air cooling process. *Applied Energy,* 168**,** 314-331.

Zou, Q, Opara, LU and Mckibbin, R. 2006a. A CFD modeling system for airflow and heat transfer in ventilated packaging for fresh foods: I Initial analysis and development of mathematical models. *Journal of Food Engineering,* 77**,** 1037-1047.

Zou, QA, Opara, LU and Mckibbin, R. 2006b. A CFD modeling system for airflow and heat transfer in ventilated packaging for fresh foods: II Computational solution, software development, and model testing. *Journal of Food Engineering,* 77**,** 1048-1058.

5.2 CFD Modelling of Temperature and Enthalpy Distribution inside an Unloaded Storage Chamber subjected to Evaporative Cooling and CoolBot Air Conditioning

Abstract

Temperature management is the key and most important factor that is to determine the cooling of fresh produce in cold storage. A hybrid 4-ton tomato evaporative cooler (EC) and a CoolBot-air-conditioner (CBAC) were pre-installed. The purpose of this paper was to study the temperature and heat distribution inside an unloaded storage chamber. The storage chamber was simulated using CFD model to evaluate the temperature and enthalpy of the storage chamber micro-environment. The ambient temperature (34.1ºC) was used as wall boundary. The inlet air velocities and static pressure at the outlets were used as a boundary set-up. A transient simulation, using the CFD model, was performed. The results were obtained for a single transient time, for all the simulation scenarios. The experimental temperatures measured at different locations inside the stores, were compared with the simulated values, in order to validate and good agreement between the two temperatures achieved. The result of this experiment showed that the EC room achieved a temperature of 25 - 27ºC, an enthalpy of 1.65 $kJ.kg^{-1}$, with heat flux of 2.7 - 40.0 $W.m^{-2}$ inside the room, while the CBAC reduced the temperature down to 10 - 11ºC, the enthalpy to -468.8 $J.kg^{-1}$ and with heat flux to 11.0 - 177.0 $W.m^{-2}$. On the other hand, the EC+CBAC attained a temperature of 12 - 13 ºC, an enthalpy of-8.91 to -9.83 $kJ.kg^{-1}$ and with the heat flux to 10 $W.m^{-2}$. However, in most cases the experiment showed that there was no uniform air temperature and enthalpy inside the storage chambers under different scenarios. Since the experiment was performed inside an unloaded storage chambers, the detailed analysis of heat and mass transfer in a loaded storages is critically important, to optimise micro-environment inside the storage chamber and to improve the cooling efficiency by ensuring the airflow.

Keywords: CoolBot-air-conditioner, CFD models, combined evaporative cooling and CoolBot-air-conditioner, enthalpy distribution, evaporative cooler, heat flux, temperature distributions

5.2.1 Introduction

The safety and quality of perishable commodities is mainly dependent on the temperature control during transportation, handling and storage. Removing the field heat, as well as heat of respiration and transpiration, is the key to the extension of the shelf-life of fresh produce. Modelling the temperature and heat transfer that takes place inside a cold storage, using computational fluid dynamics (CFD) models, is the recent trend in food engineering (Ambaw *et al.*, 2013; Defraeye, 2014). Maintaining the even and rapid cooling of fresh produce after harvest is a major challenge for postharvest handling (Duan *et al.*, 2016; Getahun *et al.*, 2017). Non-uniform cold storage conditions could contribute to the qualitative and quantitative postharvest losses of fresh produce (Kolodziejczyk *et al.*, 2016b). The unevenly distributed micro-climate inside cold storage chambers might be due to the heterogeneous air temperature and airflow distribution inside the cold storage rooms (Zou *et al.*, 2006a; Zou *et al.*, 2006b; Delele *et al.*, 2013). Nahor *et al.* (2005) modelled the basics of airflow, heat and mass transfer inside an existing empty and loaded refrigerated room and characterized the cold air distribution. The authors validated the simulation by comparing the air temperature, temperature and weight loss of the pear fruit that were measured experimentally, with that of the computation. It was reported that temperature pattern inside the cold store is the most important factor that affects the cooling uniformity of the micro-climate of cold storage facilities (Kolodziejczyk *et al.*, 2016b). CFD was reported to save energy, time and resources and can be applied for temperature and energy field analysis, both qualitatively and quantitatively (Han *et al.*, 2016).

The temperature field is a critical factor for determination of the cooling rate and quality of fresh produce stored inside cold storage chambers (Xie et al., 2006). The cooling rate and quality of foodstuffs are highly dependent on the temperature field inside the cold storage chambers. CFD model application is widely used for the simulation of the precooling temperature of storage facilities (Han *et al.*, 2016). Sapounas *et al.* (2016) performed a CFD simulation and reported that the ventilation rate of the green house is the most important factor for improving the efficiency of the evaporative cooling system. The physical air temperature and heat transfer distribution scenarios inside unloaded storage chambers can be the determining basic factor for the design optimization of cold storage chambers (Kolodziejczyk *et al.*, 2016a). Therefore, air flow characteristics inside the empty storage chambers is a critical aspect for the design optimization of cold stores.

Low-cost cooling technologies, such as evaporative cooled (EC) storage, CoolBot-air-conditioner (CBAC) storage and the combined operation of (EC+CBAC) storage, are recommended for small-scale and emerging farmers by several researchers (Workneh, 2010; Saran *et al.*, 2013). The shelf-life of tomatoes was improved four-fold, by using these technologies (Tolesa and Workneh, 2017). Although it is cheaper, the uniformity of the micro-environment climate, in terms of temperature and heat flux inside the unloaded storage, has not been well-researched. Hence, this study focused on the temperature and heat transfer distribution inside the unloaded EC, CBAC and EC+CBAC storage chambers, using CFD models.

5.2.2 Materials and methods

5.2.2.1 Cold room set-up

An experimental cold room was installed at the Ukulinga Research Farm, Pietermaritzburg, South Africa, which has been described, in detail, in sub-section 5.1.2.1 (Figure 3.1).

5.2.2.2 Cold store experiment

The experimental air velocity and temperature were measured with a DS-2 sonic anemometer (Company, Decagon Devices, Inc., USA). The detail, has been explained, in sub-section 5.1.2.2 (Figure 3.1).

5.2.2.3 Numerical modelling

Governing equations

This study presents the exploration of the air temperature and enthalpy distribution inside the three different cooling systems (*i.e.* the evaporative cooler (EC), the CoolBot-air-conditioner (CBAC) and the combined operation of EC and CBAC (EC+CBAC)). The CFD model applied the Raynolds-Average Navier–Stokes equations (Equations 2.1 to 2.5), which were expressed, to solve the free airflow zone and the energy conservation mode given in Equation 2.5.

5.2.2.4 Model parameters

Transient state models were used for the empty cold rooms, to model the temperature and thermal energy inside the unloaded rooms. The simulation was performed, based on the unloaded rooms, and no resistance was considered.

5.2.2.5 Boundary and initial conditions set-up

A similar experimental set-up was used to that described in sub-section 5.1.2.5. The experimental air velocity was set at 3.2 $m.s^{-1}$ and 4.2 $m.s^{-1}$ at the inlet of the evaporative cooler and CBAC air conditioner, respectively. Moreover, the measured air velocities were 3.1 $m.s^{-1}$ and 3.0 $m.s^{-1}$ at the inlets of the EC+CBAC combination fan and air conditioner inlets, respectively. The average air temperatures were set at 19.1ºC and 6.3ºC at the inlets of each evaporative cooler and CBAC air conditioner, respectively, while the actual values were 18.7ºC and 8.4ºC at the inlet of the combined operated evaporative cooler and CoolBot-air-conditioner (EC+CBAC), respectively.

5.2.2.6 Simulation set-up

The steady state simulation, performed in sub-section 5.1.2.6, was used as an initial condition for the transient simulation of the temperature and energy. Turbulence was considered by the SST (k-ε) model, to accommodate for the errors on the wall (Versteeg and Malalasekera, 2007). The transient state of the total time of 1200 s and 5 s time step was performed for each of the unloaded storage scenarios. The geometry was discretized to the 852942 mesh cells. The transient simulation was computed, using a time of 1200 s per 15 iterations was used with time. The second-order upwind for the convection parameters describe the turbulence and flow. The convergence criteria were considered as 10^{-4} and 10^{-6} for the mass and momentum transfer and the energy transfer models, respectively. The full simulation took 15-20 hours on a 64-bit, Dell Precision T3600, Intel Xeon CPU E5-16600 @ 3.30 GHz 3.30GHz and 32GB RAM, Windows 10 PC. The total iteration was 3000.

5.2.3 Results and discussion

5.2.3.1 Air temperature characteristics inside the evaporative cooler

Figure 5.14 displays a horizontal visualization of the air temperature contours. The air temperature varied between 19ºC and 26ºC along the parallel horizontal plane to the evaporative cooler fan inlet Y = 0.6 m high from the ground surface (Figure 5.1 (a)). On the other hand, the enthalpy changed from -5.94 kJ.kg^{-1} to 9.24 kJ.kg^{-1} across the EC room, which indicates a higher thermal energy toward the exit wall of the room. The wall near the inlet of the EC room showed small thermal energy in terms of static enthalpy. The negative enthalpy shows that the air loses more energy and may have more capacity to remove heat from the produce to be stored (Arora, 2010). High air velocity resulted in reducing temperature at specific position (Nahor *et al.*, 2005). Hence, better removal of heat generation can be achieved at near the inlet wall for the agricultural produce to be stored.

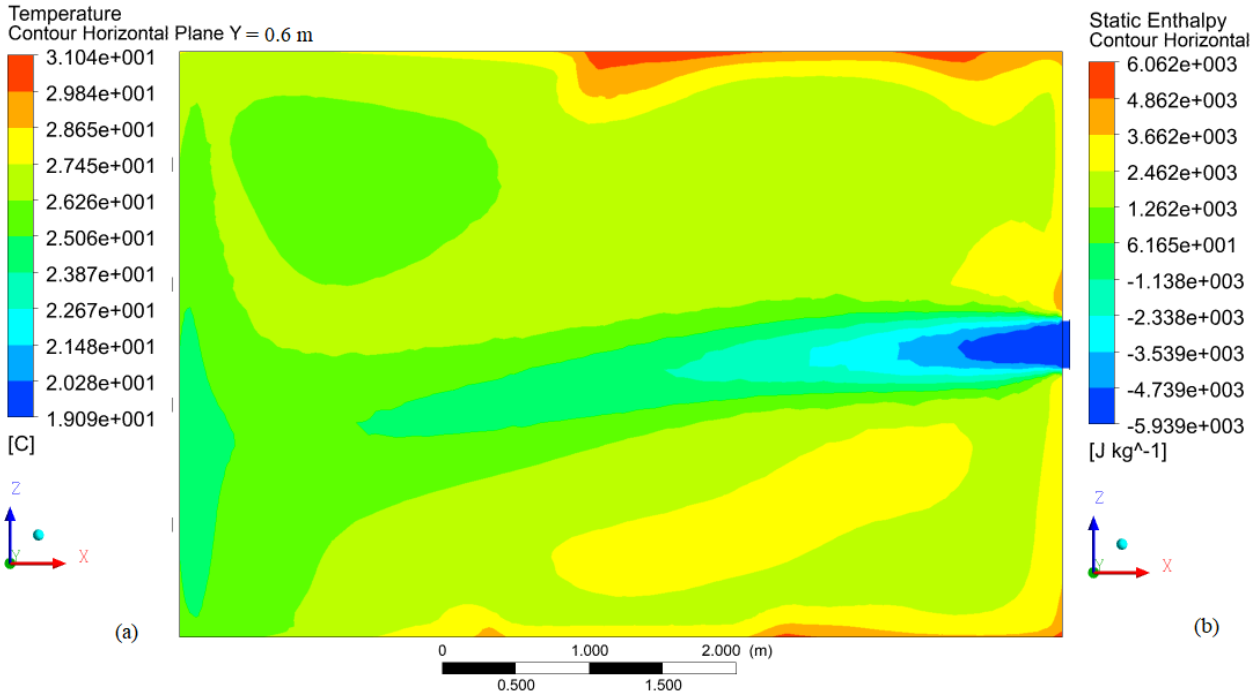

Figure 5.13 Horizontal air temperature (a) and static enthalpy contour (b) of the micro-environment inside evaporative cooler (EC) at a horizontal section plane Y = 0.6 m high from floor

The CFX modelling of the vertical visualization of air temperature and enthalpy contour, along the vertical symmetry plane Z = 2 m inside the EC, are shown in Figure 5.15. The temperature varied from 17.0ºC to 30ºC along the plane towards the wall edges (Figure 5.15 (a)), which revealed that the EC fan was not enough to blow the colder air at the inlet fan through the cold storage chamber. A temperature magnitude of 27ºC dominated across the vertical cross-section of the plane. The temperature across the plane, from the inlet into the outlet wall, varied a lot and hardly cooled the room toward the outlet wall. On the other hand, high thermal energy indicators were found near the walls and near the middle to the exit walls (*i.e.* the static enthalpy varied from -5.94 $kJ.kg^{-1}$ to 9.24 $kJ.kg^{-1}$) (Figure 5.15 (b)). The static enthalpy is the thermodynamic enthalpy of the air and it is directly related to the magnitude of the air temperature (Foster *et al.*, 2002). The lower temperature gives a low thermodynamic enthalpy (Fang *et al.*, 1998; Evans *et al.*, 2014). Inside the EC room, both the temperature and enthalpy were found to be low near the inlet wall and gradually increased towards the outlet and side walls, were no uniform distribution was achieved. Moreover, the overall heat flux achieved by the EC was found to be varied dominantly between 2.7 $W.m^{-2}$ and 40.0 $W.m^{-2}$ (Figure 5.15 (c)) and it shows that low heat there was a flow rate intensity EC store. The magnitude of heat flux indicates how much heat can be removed per unit area at specific location (Ho *et al.*, 2010), which has an implication on cooling performance of a cold room. In this study, the heat flux was found to be not uniform across the storage room and, hence, that can affects its cooling performance. The results obtained in this study showed that design modification is critical for achieving a uniform temperature, enthalpy and heat flux throughout the storage room area.

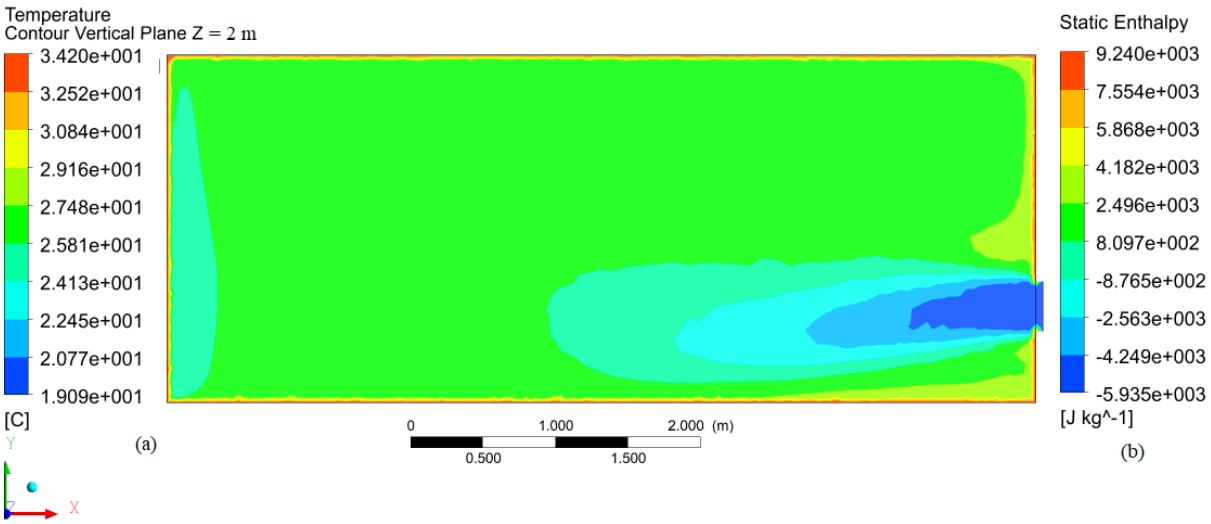

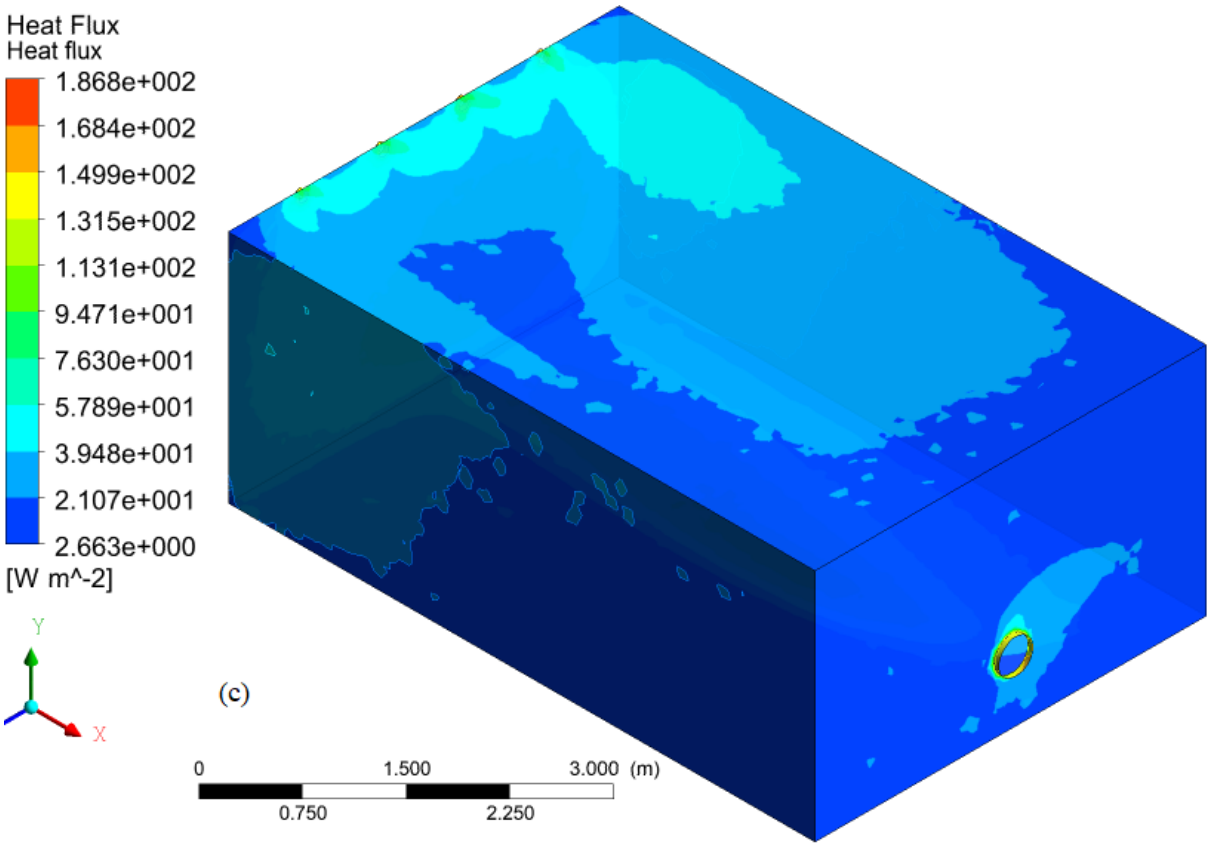

Figure 5.14 Vertical air temperature contour of evaporative cooler (EC) at horizontal section plane of different height positions along the Z-direction: (a) is air temperature at Z = 2 m (vertical symmetry plane section) and (b) is air static enthalpy and heat flux (c) inside evaporative cooler

5.2.3.2 The CoolBot-air-conditioner air temperature characteristics

Figure 5.16 describes the CFX result of a horizontal temperature and enthalpy contour along the imaginary horizontal plane at Y = 0.6 m high from the ground inside the CoolBot-air-conditioner (CBAC) cooler. Good air temperature distribution was found across this plane (*i.e.* the temperature values varied from 10 ºC to 22 ºC) (Figure 5.16 (a)). Similar temperature magnitude was reported by Peoun *et al.* (2015) and Seng *et al.* (2015). The results also showed that there was a uniform air enthalpy distribution (-468.8 $J.kg^{-1}$) inside CBAC. The negative enthalpy shows that the air is losing more energy and may have more capacity to remove more heat from the produce that is stored (Arora, 2010). The enthalpy value was small and could be ideal for the cooling of heat generated from produce to be stored inside the storage chamber with a low enthalpy distribution.

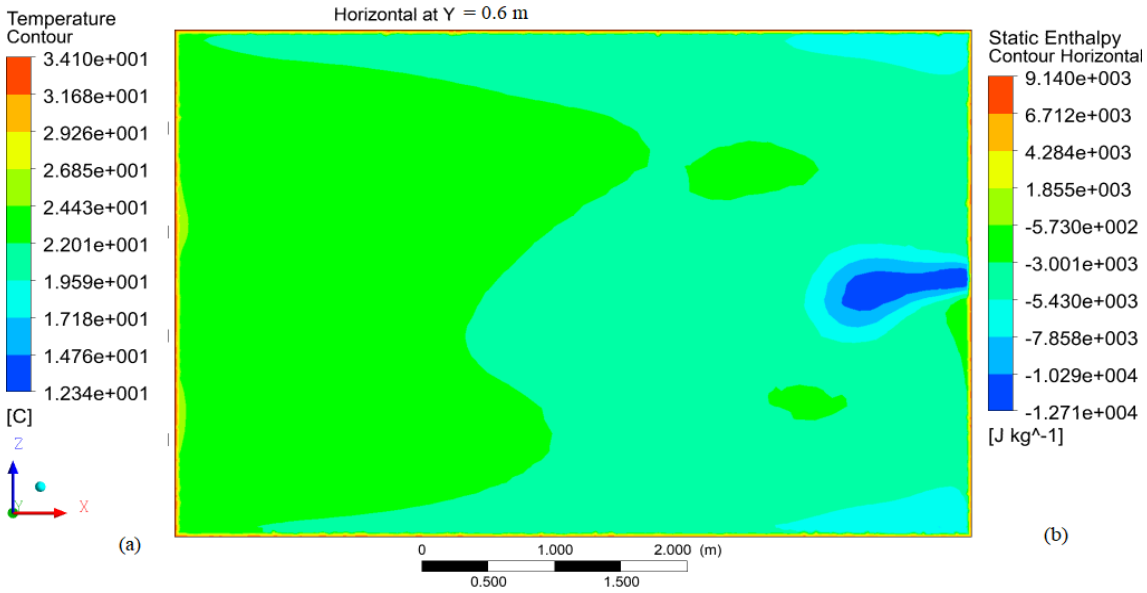

Figure 5.15 Horizontal air temperature contours inside the store room subjected to CoolBot air conditioning simulated at Y = 0.1 m high from the floor a) air temperature contour and b) static enthalpy contours

Figure 5.17 shows the CFX simulation results of the vertical visualization of air temperature and enthalpy contours inside the CBAC along the symmetry line of Z = 2 m from the wall. Both the temperature and enthalpy along the symmetry line were found to be uniformly distributed on a vertical plan (Figure 5.17 (a - b)). Near the wall to the inlet side and downward to the floor, both the temperature and enthalpy were found to be low at 11-15ºC and -11.44 kJ.kg^{-1}, respectively (Peoun *et al.*, 2015). Moreover the heat flux inside the store subjected to CBAC was found to be between 11 W.m^{-2} and 177 W.m^{-2} (Figure 5.17 (c). The results show that cooling was effective near the inlet wall to middle of the plane section.

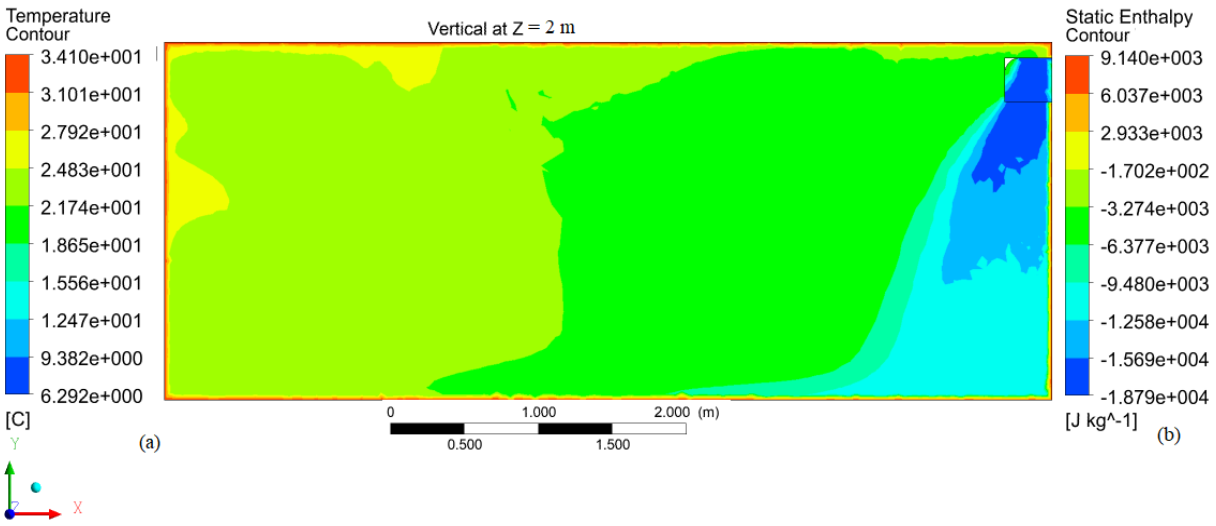

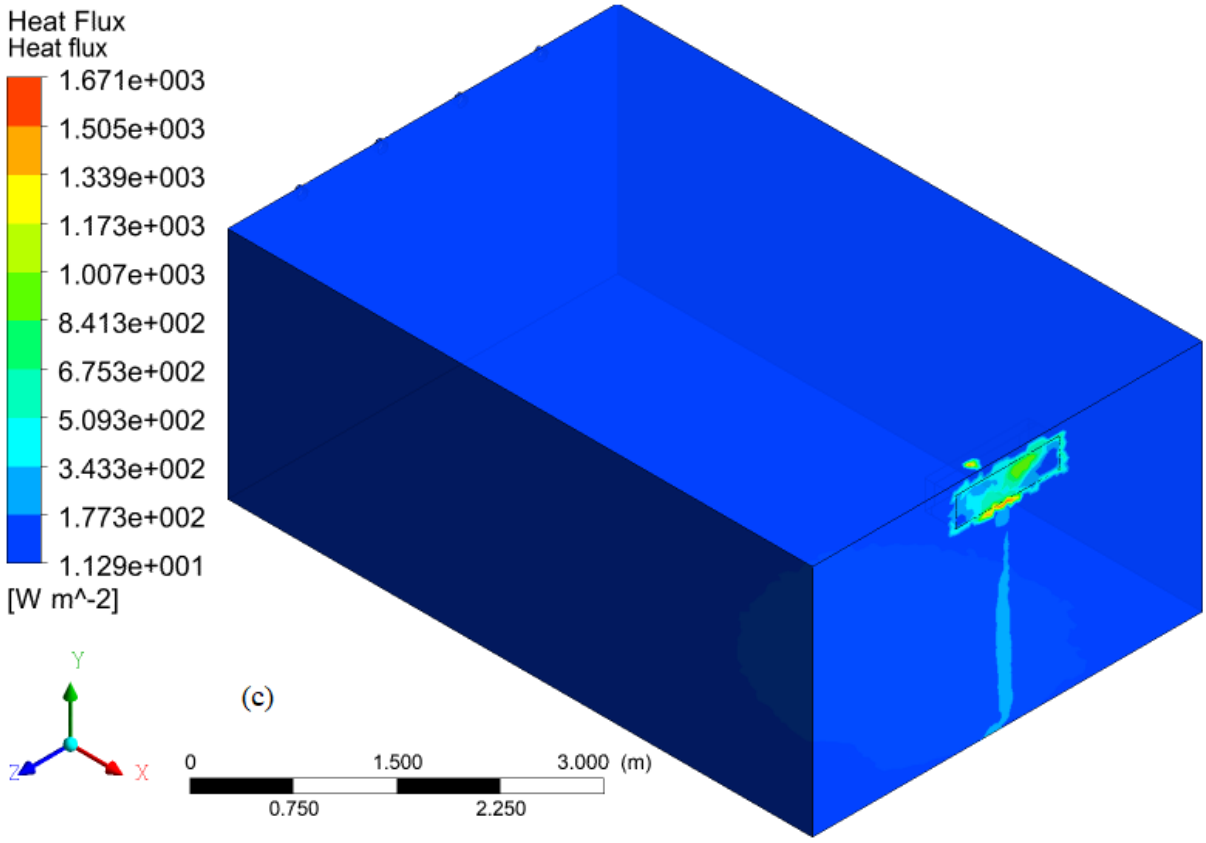

Figure 5.16 Air temperature contour and static enthalpy captured inside the CoolBot air conditioned cold storage chamber at vertical imaginary section plane at Z = 2 m from the wall of the room along a vertical symmetry plane where a) is air temperature contour, b) is static enthalpy and heat flux inside CBAC room (c)

5.2.3.3 Combined evaporative cooler and CoolBot-air-conditioner airflow characteristics

Figure 5.18 shows that the CFX model results, with the temperature and enthalpy contour along an imaginary plane section Y = 0.6 m in the combined evaporative cooler (EC) and CoolBot-air-c0nditioner cold room. Both the temperature and enthalpy were found to be uniform across the middle section of the plane (Figure 5.18 (a-b). The temperature and enthalpy inside the room were dominantly found to be 12-16ºC and -9.83 kJ.kg^{-1}, respectively. The temperature range obtained in this study, was found to be in the optimum temperature range for most of tropical fruit and vegetables (Thompson *et al.*, 2002). Homogeneous distribution of micro-climate inside a cold store was reported to be a critical aspect to be taken in to consideration for designing of the cold ventilated storage chambers (Datta, 2008; Dehghannya *et al.*, 2011). The results indicated that sufficient cooling can be achieved across the plane Y = 0.6 m high from the floor.

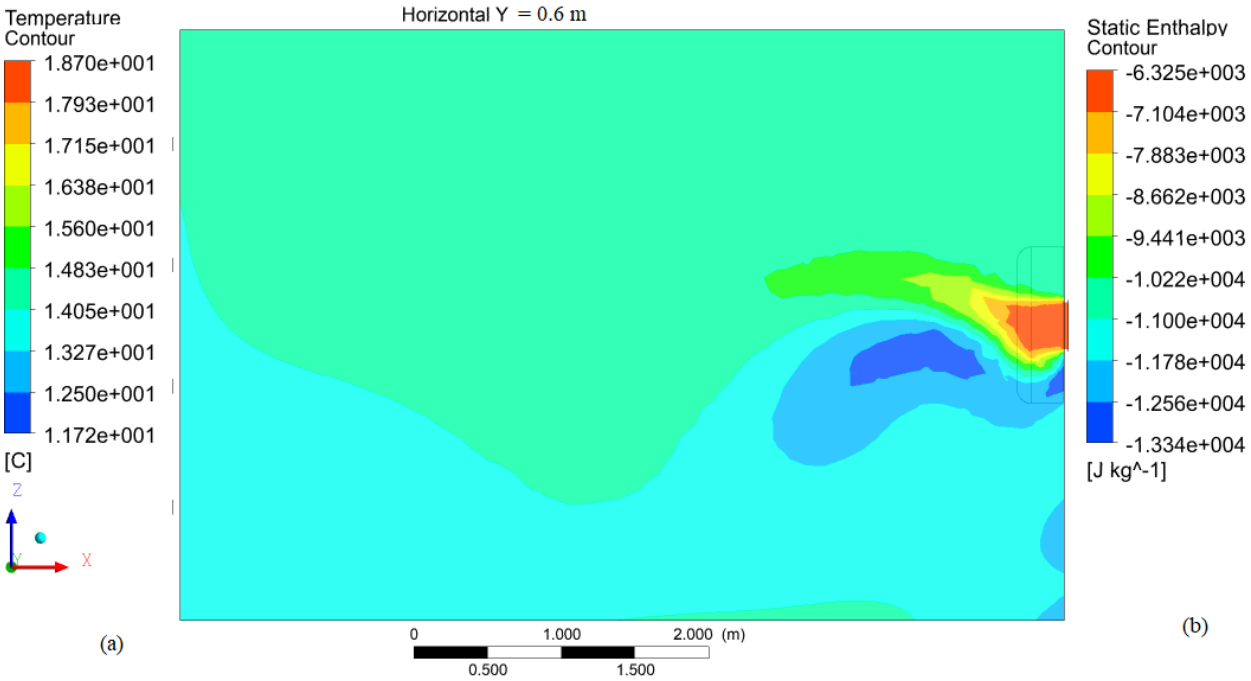

Figure 5.17 Air temperature contours inside the combined evaporatively cooled and CoolBot-air-conditioned cooled rooms (EC+CBAC) along different horizontal section planes Y-direction: a) is air temperature contour and b) is air static enthalpy at Y = 0.6 m high from the floor of the room

The temperature, enthalpy and heat flux contour along the vertical symmetry line is shown in Figure 5.19 (a-c). The results showed that the temperature and enthalpy were 13ºC and – 12.0 kJ.kg^{-1} and - 97.7 kJ.kg^{-1}, respectively, similar findings were reported by Peoun *et al.* (2015). On the other hand, the heat flux was found to be 10 kW.m^{-2}, inside the EC+CBAC (Figure 5.19 (c). When compared to EC and CBAC, the results demonstrated by EC+CBAC were the best, in terms of the changes in temperature and energy distribution.

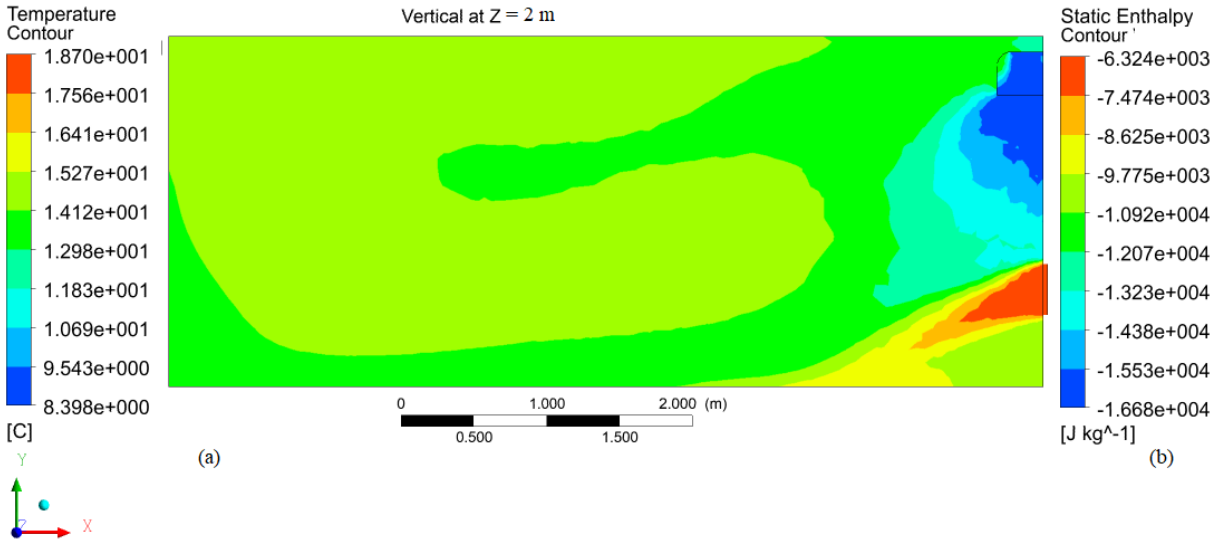

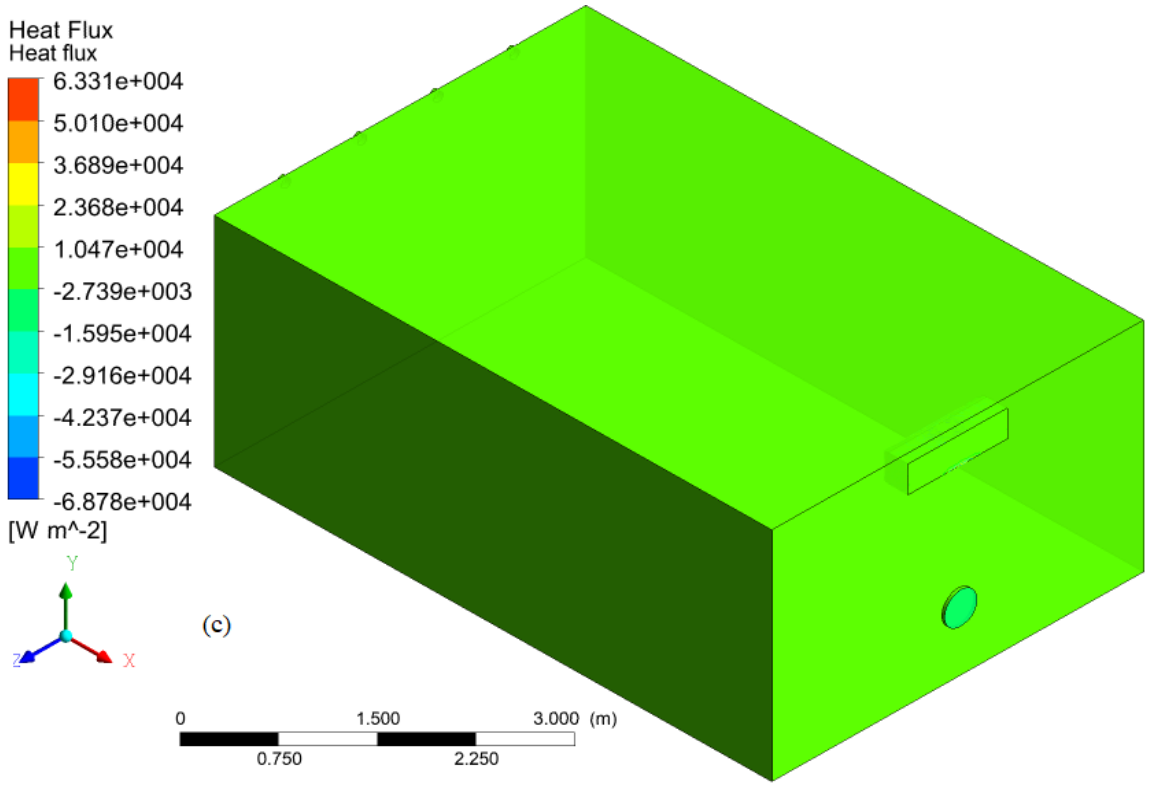

Figure 5.18 Air temperature contour inside the evaporatively and CoolBot-Air-Conditioned cooler at an imaginary vertical section plane at different positions along a symmetry line Z- = 2 m from the wall, where a) is air temperature contour, b) is air static enthalpy and c) heat flux inside CBAC room

5.2.3.4 Validation of the models

The validation of the numerical models was done by comparing the experimental (Exp) and computed temperatures at different positions inside the cold storage chambers (Nahor *et al.*, 2005; Zhang *et al.*, 2017). The results showed that the experimental temperatures at different locations fitted well into the simulation model.

Table 5.1 Experimental temperature (Exp. Temp.) and simulated temperature (Sim. Temp.) at different locations inside the EC, CBAC and EC+CBAC cold rooms for model validation

Cooler location	Exp. Temp. (ºC)	Sim. Temp. (ºC)	Error (%)
Outlet wall EC at 2.2 m high	24.15	24.0	0.62
Outlet wall CBAC at 0.5 m high	11.79	12.53	6.28
Outlet wall EC+CBAC at 2.2 m high	14.29	14.0	2.03

5.2.4 Conclusions

CFD model simulation is recommended to visualize and quantify the temperature and enthalpy of circulating air in cold storages. Transient state simulation, using CFD model, was performed, to quantify the temperature and enthalpy of air circulating inside the cold low-cost cold room. The validation of the models was done by comparing the experimental and computed air temperatures with those of the computed temperature, using CFD at different positions inside the store. The results showed that a dominant temperature value of 25-27ºC and 1.65 $kJ.kg^{-1}$ of enthalpy and 2.7 $W.m^{-2}$ and 40.0 $W.m^{-2}$ heat flux inside the evaporative cooler (EC) room was achieved at a total time of 1200 transient simulation. This is a high temperature for the storage of perishable commodities. Hence, a redesign of the psychrometric unit will be required to achieve a lower temperature range. Based on a similar simulation, the temperature, enthalpy and heat flux values achieved by the CoolBot-air-conditioner (CBAC) were 10-15ºC, -468.8 $J.kg^{-1}$ and 11 - 177 $W.m^{-2}$, respectively. Similarly, the combine operation (EC+CBAC) reduced the temperature, enthalpy and heat flux inside the room to 12 - 16ºC, – 12.0 to - 97.7 $kJ.kg^{-1}$ and 10 $kW.m^{-2}$, respectively. However, the experiment showed that no uniform air temperature, enthalpy and heat flux was found in all the storage chamber scenarios, in most cases. Moreover, further study of load of fresh produce is crucial for optimising the cooling capacity of the cold storage chambers.

5.2.5 Acknowledgements

We would like to warmly acknowledge the Federal Ministry of Education, Ethiopia. South African National Research Foundation (NRF – TWAS) and the host institute, University of Kwa-Zulu Natal.

5.2.6 References

Ambaw, A, Delele, MA, Defraeye, T, Ho, QT, Opara, LU, Nicolai, BM and Verboven, P. 2013. The use of CFD to characterize and design post-harvest storage facilities: Past, present and future. *Computers and Electronics in Agriculture,* 93**,** 184-194.

Arora, RC. 2010. *Refrigeration and air conditioning.* PHI Learning Pvt. Ltd., New Delhi, India.

Datta, AK. 2008. Status of Physics-Based Models in the Design of Food Products, Processes, and Equipment. *Comprehensive Reviews in Food Science and Food Safety,* 7**,** 121-129.

Defraeye, T. 2014. Advanced computational modelling for drying processes: a review. *Applied Energy,* 131**,** 323-344.

Dehghannya, J, Ngadi, M and Vigneault, C. 2011. Mathematical modeling of airflow and heat transfer during forced convection cooling of produce considering various package vent areas. *Food Control,* 22**,** 1393-1399.

Delele, MA, Ngcobo, MEK, Getahun, ST, Chen, L, Mellmann, J and Opara, UL. 2013. Studying airflow and heat transfer characteristics of a horticultural produce packaging system using a 3-D CFD model. Part II: Effect of package design. *Postharvest Biology and Technology,* 86**,** 546-555.

Duan, Z, Zhan, C, Zhao, X and Dong, X. 2016. Experimental study of a counter-flow regenerative evaporative cooler. *Building and Environment,* 104**,** 47-58.

Evans, JA, Hammond, EC, Gigiel, AJ, Fostera, AM, Reinholdt, L, Fikiin, K and Zilio, C. 2014. Assessment of methods to reduce the energy consumption of food cold stores. *Applied Thermal Engineering,* 62**,** 697-705.

Fang, L, Clausen, G and Fanger, PO. 1998. Impact of temperature and humidity on the perception of indoor air quality. *Indoor air,* 8**,** 80-90.

Foster, AM, Barrett, R, James, SJ and Swain, MJ. 2002. Measurement and prediction of air movement through doorways in refrigerated rooms. *International Journal of Refrigeration,* 25**,** 1102-1109.

Getahun, S, Ambaw, A, Delele, M, Meyer, CJ and Opara, UL. 2017. Analysis of airflow and heat transfer inside fruit packed refrigerated shipping container: Part II e Evaluation of apple packaging design and vertical flow resistance. *Journal of Food Engineering,* 203**,** 83-94.

Han, J, Badía-Melis, R, Yang, X, Ruiz-Garcia, L, Qian, J and Zhao, C. 2016. CFD Simulation of Airflow and Heat Transfer During Forced-Air Precooling of Apples. *Journal of Food Process Engineering,* 40**,** 1-11.

Ho, SH, Rosario, L and Rahman, MM. 2010. Numerical simulation of temperature and velocity in a refrigerated warehouse. *International Journal of Refrigeration-Revue Internationale Du Froid,* 33**,** 1015-1025.

Kolodziejczyk, M, Butrymowicz, D, Smierciew, K and Gagan, J. July 11-14, 2016 2016a. Numerical Modelling of Heat And Mass Transfer Processes In Chinese Cabbage Cold Storage Chamber. 16th International Refrigeration and Air Conditioning Conference 1-9. Purdue e-Pubs, Purdue University, USA.

Kolodziejczyk, M, Smierciew, K, Gagan, J and Butrymowicz, D. 2016b. Numerical Modelling of Heat and Mass Transfer in Vegetables Cold Storage. *Procedia Engineering,* 157**,** 279-284.

Nahor, HB, Hoang, ML, Verboven, P, Baelmans, M and Nicolai, BM. 2005. CFD model of the airflow, heat and mass transfer in cool stores. *International Journal of Refrigeration-Revue Internationale Du Froid,* 28**,** 368-380.

Peoun, P, Buntong, B, Yim, S, Vat, S, Acedo, AL, Easdown, W, Hughes, JA and Keatinge, JDH. 2015. Modified atmosphere packaging of leaf mustard during evaporative cooling and CoolBot cold storage. *In:* Acedo, AL, Buntong, B, Tong, S and G., Y, eds. III Southeast Asia Symposium on Quality Management in Postharvest Systems 1179, 173-176. Acta Horticulture, Siem Reap, Cambodia.

Sapounas, AA, Bartzanas, T, Nikita-Martzopoulou, C and Kittas, C. 2016. Aspects of CFD Modelling of a Fan and Pad Evaporative Cooling System in Greenhouses. *International Journal of Ventilation,* 6**,** 379-388.

Saran, S, Dubey, N, Mishra, V, Dwivedi, SK and Raman, NLM. 2013. Evaluation of coolbot cool room as a low cost storage system for marginal farmers. *Progressive Horticulture,* 45**,** 115-121.

Seng, M, Buntong, B, Acedo, AL, Easdown, W, Hughes, JA and Keatinge, JDH. 2015. Low-cost cold storage of tomato in modified atmosphere packaging. *In:* Acedo, AL, Buntong, B, Tong, S and Young, G, eds. III Southeast Asia Symposium on Quality Management in Postharvest Systems 1179, 197-200. Acta Horticulture, Siem Reap, Cambodia.

Thompson, JF, Mitchell, FG and Kasmire, RF. 2002. Cooling horticultural commodities. *In:* Kader, AA (ed.) *Postharvest technology of horticultural crops.* 3rd ed, Cha. 11, 97- 112. Agriculture and Natural Resources, University of California, USA.

Tolesa, GN and Workneh, TS. 2017. Influence of storage environment, maturity stage and pre-storage disinfection treatments on tomato fruit quality during winter in KwaZulu-Natal, South Africa. *Journal of Food Science and Technology,* 54**,** 3230-3242.

Versteeg, HK and Malalasekera, W. 2007. *An introduction to computational fluid dynamics: the finite volume method.* Pearson Education Limited, UK.

Workneh, TS. 2010. Feasibility and economic evaluation of low-cost evaporative cooling system in fruit and vegetables storage. *African Journal of Food, Agriculture, Nutrition and Development,* 10**,** 2984-2997.

Xie, J, Qu, XH, Shi, JY and Sun, DW. 2006. Effects of design parameters on flow and temperature fields of a cold store by CFD simulation. *Journal of Food Engineering,* 77**,** 355-363.

Zhang, X, Han, JW, Qian, JP, Wang, YZ, Wang, L and Yang, XT. 2017. Computational fluid dynamic study of thermal effects of open doors of refrigerated vehicles. *Journal of Food Process Engineering,* In Press.

Zou, Q, Opara, LU and Mckibbin, R. 2006a. A CFD modeling system for airflow and heat transfer in ventilated packaging for fresh foods: I Initial analysis and development of mathematical models. *Journal of Food Engineering,* 77**,** 1037-1047.

Zou, QA, Opara, LU and Mckibbin, R. 2006b. A CFD modeling system for airflow and heat transfer in ventilated packaging for fresh foods: II Computational solution, software development, and model testing. *Journal of Food Engineering,* 77**,** 1048-1058.

6. INVESTIGATING THE AIRFLOW INSIDE A SEMI-LOADED AND FULLY-LOADED COLD STORAGE CHAMBER OF A COMBINED EVAPORATIVE COOLING AND COOLBOT-AIR-CONDITIONER COOLING SYSTEM, USING THE CFD METHOD

Abstract

The airflow inside a cold storage chambers is critical for determining the heat and mass transfers during storage. This requires the establishment of a theoretical background in the design process. A numerical method, like computational fluid dynamics (CFD), can provide the qualitative visualization and quantitative analysis of the airflow distribution inside the storage chambers. The purpose of this study was: (1) to develop a detailed CFD model of horizontal airflow through stacked tomatoes that enables the estimation of the airflow resistance characteristics of the stack, (2) to develop a porous medium CFD model to simulate the airflow inside a fully-loaded, low-cost cold storage chambers, to determine the airflow characteristics. Therefore, the airflow inside the semi-loaded (half a pallet) combined low-cost evaporative cooler and CoolBot-air-conditioner (EC + CBAC) was simulated, using a detailed CFD model (Model 1). The Darcy-Forchhimer model was used to characterize the pressure drop resistances of the stacked tomatoes. The RMSE of the air velocity at the inlet and exit was found to be 0.175 $m.s^{-1}$ and 0.116 $m.s^{-1}$, respectively. The result of Model 1 showed that the air velocity at inlet, across the centre and at the exit of the stack are 1.5 $m.s^{-1}$, 0.1-0.6 $m.s^{-1}$ and 0.2-0.5 $m.s^{-1}$, respectively. The fully-loaded EC+CBAC store (Model 2) followed a similar trend to that of Model 1 *i.e.* the airflow at the center of the fully-stacked room and at near the outlet wall was found to be hard to cool in the cold room set-up. Therefore, the further modification of the air distribution devices is of paramount importance. The cooling kinetics and temperature distribution should be analyzed to completely evaluate the situation Moreover, a detailed study of the heat and mass transfer of the developed models is critically important for the further improvement of the cold rooms.

Keywords: Airflow distribution, CoolBot-air-conditioner, computational fluid dynamics models, combined evaporative cooling and CoolBot-air-conditioner, discrete model, fully-loaded tomatoes stacks, semi-loaded tomato stacks.

6.1 Introduction

Modelling the airflow, mass and heat transfer that takes place inside a cold storage, using the CFD tool, is the recent trend in food engineering (Ambaw *et al.*, 2013a; Defraeye, 2014). Maintaining the even and rapid cooling of fresh produce after harvest is the major challenge for postharvest handling (Duan *et al.*, 2016; Getahun *et al.*, 2017b). The unevenly distributed micro-climate inside cold storage might be due to the heterogeneous airflow distribution (Zou *et al.*, 2006a; Zou *et al.*, 2006b; Delele *et al.*, 2013). Only a few researchers have analysed the performance of evaporative cooling technologies for fresh produce pre-cooling and green house cooling, using CFD model (Sapounas *et al.*, 2008). Nahor *et al.* (2005) modeled the basics of airflow, heat and mass transfer inside an existing unloaded and loaded refrigerated room and characterized the cold air distribution. The authors validated the models by comparing the air velocity, temperature and weight loss of the pear fruit, measured experimentally, with that of the computation values.

The heat and mass transfer inside cold storage chamber is mainly affected by airflow dynamics (air velocity, air flow rate, temperature and relative humidity), fresh produce properties (*i.e.* geometry, thermo-physical and physiological), the packaging and stacking patterns of the produce and the packaging arrangements of the materials (Castro *et al.*, 2005; Ambaw *et al.*, 2013a; Zhao *et al.*, 2016). Hence, the detailed study of the airflow characteristics inside the cold storage chambers is fundamental for the further characterization of the storage performance determinations, in terms of the air velocity optimization, structural design modification and maintenance of the cold store (Han *et al.*, 2016).

Several pre-cooling low-cost technologies have been identified by previous researchers. These low-cost technologies are helpful for disadvantaged farmers, small-scale producers and emerging farmers. Technologies, such as evaporative cooler (EC) and CoolBot-Air-Conditioner (CBAC) (Workneh, 2010; Saran *et al.*, 2013), have been studied by many researchers. Sapounas *et al.* (2016) performed a CFD model simulation and reported that the ventilation rate of a green house is the most important factor for improving the efficiency of an evaporative cooling system. Though several CFD studies have been reported on the conventional cold storage handling of perishables in a standard precooling and cold storage facilities, similar studies on low-cost technologies are lacking. Hence, the main objective of the present study is to develop and experimentally validate a CFD model of an empty and semi-loaded, low-cost evaporative

cooler (EC), CoolBot-Air-Conditioner (CBAC) and combined operation EC+CBAC were, using the CFD model, to investigate the airflow distribution.

6.1.1 Theory of the evaporative cooler

The combination a direct and indirect evaporative cooler (EC) is recommended for arid and semi-arid climate regions, for the efficient pre-cooling of fruit and vegetables after harvest (Roy and Khardi, 1985; Roy and Pal, 1989, 1994; Yadav *et al.*, 2002; Roy, 2007; Tripathi and Lawande, 2010; Workneh, 2010). The temperature was reduced to approach the wet bulb temperature, while the relative humidity and absolute humidity increases after passing through the pads (Tripathi and Lawande, 2010; Xuan *et al.,* 2012). The cooling process accounted for the removal of latent heat of vaporization, from the surface of the wet pads to the environment (Pal *et al.*, 1997). Even though it is cheaper, there is limited research on the airflow pattern, heat, and mass transfer, inside the evaporatively cooled and conditioned cold room.

6.1.2 Theory of the CoolBot-air-conditioner

Boyette and Rohrbach (1993) developed the CoolBot-Air-Conditioner (CBAC) cooling system as a low cost, forced-air, portable modification of the domestic air conditioner, for fresh produce storage. The CBAC is an electronic device that overrides the room air conditioner to reduce the cooling temperature below the set point, for the preservation of fresh produce. It is easy to handle, install and maintain (Kitinoja, 2013; Saran *et al.*, 2013. However, there has been limited research on the airflow pattern, heat, and mass transfer inside the CBAC cold room.

Computational fluid dynamics (CFD) simulations of the airflow, mass and heat transfer process in cold storage has been shown to be a promising alternative for analysing the environmental conditions of the micro-climate and the postharvest equipment design optimization processes (Ambaw *et al.*, 2013a; Kolodziejczyk *et al.*, 2016). The physical parameters, such as air velocity, airflow patterns and temperature inside the cold storage chamber, are the determinant fundamental factors for heat and mass transfer modelling (Kolodziejczyk *et al.*, 2016). Therefore, airflow characteristics inside the empty storage chamber is a critical aspect that needs to be studied. The airflow inside the semi-loaded stores can be the basic characteristics before the precooling of fully-loaded fresh produce. Hence, the semi-loaded and fully-loaded cold room airflow may indirectly determine the shelf-life and quality of stored fresh produce.

In spite of the low-cost, in the case of EC, CBAC and EC+CBAC, there is no detailed study of airflow inside the partially- and fully-loaded storage chambers, using the CFD model. Hence, this study focused on the air velocity and distribution inside partially- and fully-loaded cold storage chambers, with the help of CFD models.

6.2 Materials and Methods

6.2.1 Fruit

Tomato fruit (*Lycopersicon esculentum Mill. cr Nemonetta*) samples were produced by the ZZ2 farm, Limpopo, South Africa, and collected for the experiment in February, 2017. The average weight of a single tomato box was 6 kg (40-48 tomatoes in each box) and the average diameter varied between a waist diameter of 65 mm and 68 mm. The tomatoes were transported overnight in refrigerated trucks and they were collected from the open wholesale market in Pietermaritzburg. They were immediately transported and stored inside the experimental cold storage chamber at the Ukulinga Research Farm of the University of KwaZulu-Natal, South Africa.

6.2.2 Packaging box

Tomato boxes, with the dimensions of 39 cm x 24.5 cm x 14 cm (LWH), were stacked, with 156 boxes in each stack (Figure 6.1 (a-b). The stacked boxes are shown in Figure 6.2 and one-third of the stacks were used for the experiments in the cold storage chambers.

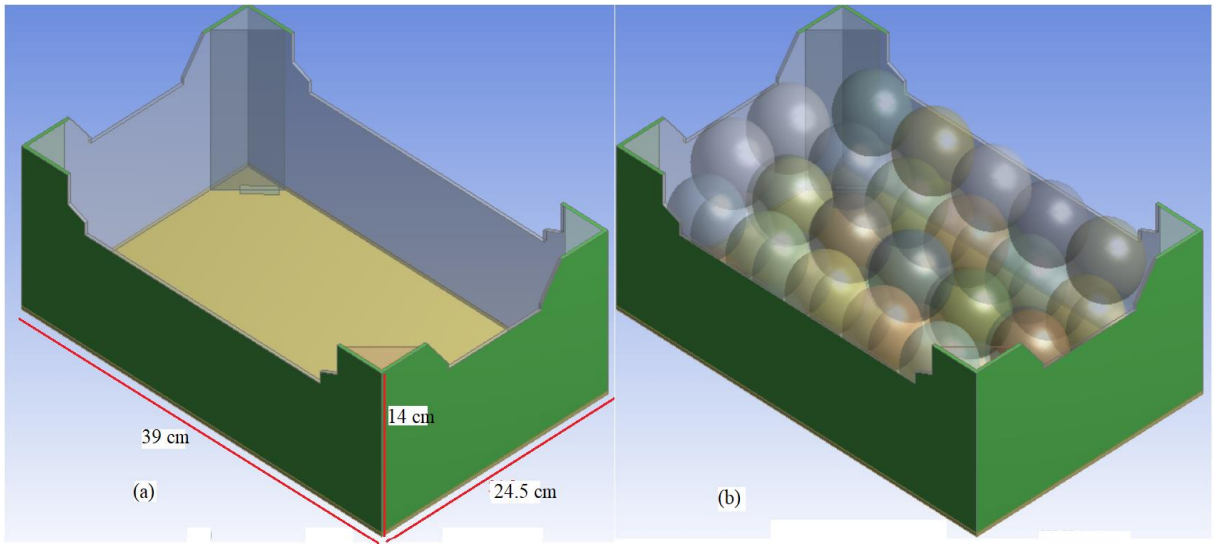

Figure 6.1 Sketch of tomato box (a) and the box filled with tomatoes for the model (b)

Figure 6.2 Tomato stack (a), empty box (b) and tomato loaded boxes (c)

6.2.3 Cold room set-up

An insulated experimental cold room was installed at the Ukulinga Research Farm, Pietermaritzburg, South Africa. The cold room consisted of an indirect heat exchanger, wet charcoal cooling pads and a CoolBot-air-conditioner air conditioning system (CBAC) (Figure 3.1). In the case of the evaporative cooler, the air was blown into the room by axial fan through the heat exchanger. All the walls of the room were insulated with polyurethane foam, in between 1 mm thick cast steel metal sheets. The floor of the store was made up of concrete. The following assumptions were made for CFD modelling: (1) the charcoal was continuously wet, (2) the whole operation was run under a normal atmospheric conditions (101.325 kPa), (3) it was assumed that there were no radiation effect, and (4) the conditions were performed at steady state. The reservoir volume was a 250 l plastic tank that was buried underground to keep the water reservoir cold all the time during the day and the night. The water pump capacity was 5 m x 2 l min^{-1}. Fan 2, which is the axial fan, was used to push the cold air into the cold room, which had a dimension of 350 mm external diameter with air ventilation rate capacity 0.218 $m^3.s^{-1}$ (Workneh *et al.*, 2012).

6.2.4 Cold store experiment

The air velocity and temperature were measured with a DS-2 sonic anemometer (Company, Decagon Devices, Inc., USA) at Fan 2 (0.6 m), the air conditioner inlet (Y = 2.2 m), 2 m from the inlet along the symmetry line at a height of 1.3 m, 4 m from the inlet along symmetry line at a height of 1.3 m, 6 m from the inlet along symmetry line at a height of 1.3 m ((Y = 1.3m) and at the exit holes (Y = 2.2 m).

6.2.5 Numerical modelling

6.2.5.1 Governing equations

The airflow in the domain was governed by the mass and momentum conservation equations, as given by Equations (6.1 and 6.2), respectively (Versteeg and Malalasekera, 1995). The density of the air was assumed to be constant, at the cooling air temperature of 272.65 K.

$$\nabla . \mathrm{V} = 0 \tag{6.1}$$

$$\frac{\partial \mathrm{V}}{\partial t} + \nabla \left(\mathrm{V} \otimes \mathrm{V} \right) - \nabla \left(\left(\frac{\mu + \mu_t}{\rho_a} \right) \nabla \mathrm{V} \right) - S_v + \frac{1}{\rho_a} \nabla P = 0 \tag{6.2}$$

Where:

V = the vector of the velocity ($m.s^{-1}$),

t = time (s),

ρ_a = the density of air ($kg.m^{-3}$),

P = the pressure (Pa), and

μ and μ_t = the dynamic and turbulent viscosity ($kg.m^{-1}.s^{-1}$), respectively.

In this study, the shear stress transport (SST) k-ω turbulence model was used to calculate the turbulent eddy viscosity. This turbulence model has been shown to perform better than the other turbulence models (Delele *et al.*, 2008a; Defraeye *et al.*, 2013b). The density and viscosity of air were 1.22 $kg.m^{-3}$ and 1.76×10^{-5} $kg.m^{-1}.s^{-1}$, respectively. In this study, the stacked produce inside the cold storage is modeled as a porous domain and its resistance characteristics were accounted for by S_V in Equation (6.2), which is a pressure loss term. This term is further described by the Darcy- Forchheimer equation (6.3).

$$S_{V,i} = K_{1i} v_i + K_{2i} \left| \mathrm{u} \right| u_i \quad (6.3)$$

Where *i* stands for the direction in the Cartesian coordinate system (*x*, *y* or *z*), $K_{1i} = \mu/k$ and $K_{2i} = \beta\rho$ are the viscous and inertial resistance coefficients, respectively. S_{Vi} is a pressure drop across the thickness of the obstacle (Pa.m^{-1}), μ [kg.m^{-1}.s^{-1}] is the dynamics viscosity of air (fluid), *k* (m^2) is the permeability of porous medium (stack), *u* is superficial velocity (m.s^{-1}) and β is Forchheimer coefficient [m^{-1}] (van der Sman, 2003; Verboven *et al.*, 2006; Rawangkul *et al.*, 2008). These coefficients were determined by using a detailed CFD model of the airflow across half a pallet of stacked tomatoes. This method of quantifying the flow resistance of stacked produce has been successfully used by Ambaw *et al.* (2013b).

6.2.5.2 Boundary and initial conditions

Two different types of CFD models were developed in this study: The first model (Model 1) is a detailed CFD model of the stack that is placed in a tunnel. This model is based on a detailed description of the stacked fruit and the actual shape and vent hole design of the package. In this model, the surface of the produce and the packaging boxes had no slip boundaries. At one end of the tunnel, a suction pressure was defined, while the other end of the tunnel was set as an open boundary, with a gauge pressure of 0 Pa. Hence, this arrangement was used to run a simulation at three different pressure differences, 10, 30 and 300 Pa, across the stack. The corresponding superficial velocities for each of the pressure differentials were obtained. The Curve-fitting of the pressure difference vs velocity data to the Darcy-Forchhimer equation (Equation 6.3) gives the inertial and viscous coefficients

The second model (Model 2) is a porous medium CFD model. Here, the stacked produce was modeled as a porous domain, based on the inertial and viscous coefficients, as obtained above. Inside these boundaries, we have the porous domain, consisting of tomato loaded boxes, the CBAC as Fluid Domain 1 and the remaining region, which is the free air stream, is defined as Fluid Domain 2. Accordingly, the fluid-fluid (between Fluid Domain 1 and Fluid Domain 2) and the fluid-porous (between the porous domain and Fluid Domain 2) interfaces were explicitly defined as a conservative flux interface boundary. The CBAC (Fluid Domain 2) was inside the cool store and it circulated the internal air only. To model this action, a momentum source term was added in Fluid Domain 2. The inlet and outlet of the CBAC were interfaced

with the room atmosphere, so that, the air is recirculated. The magnitude of the momentum was determined, based on the measured air velocity magnitudes at the inlet and outlet of the CBAC.

The EC was modeled by an inlet boundary on a circular cross-section, representing the inlet of the EC. All the walls, doors, floors, and ceilings of the store and the surface of the CBAC were no-slip walls (Nahor *et al.*, 2005).

6.2.5.3 Mesh generation, sensitivity analysis and simulation

The geometry of the model was developed by using the ANSYS® Design Modeler™ Release 17.0 (ANSYS, Canonsburg, PA, USA). The discretization of the computational domain was based on the flow characteristics, the structure of the geometry and the modelling approach. Fine mesh was used at the inlet and outlet of the CBAC and at the cross-section representing the EC of Model 2, as well as near the vent holes and between the tomato fruit in Model 1, since a large velocity gradient is expected in these locations. The discretization of the domain was on the ANSYS® Meshing™ Release 17.0 and the problem set-up and simulation was on the ANSYS® CFX™ Release 17.0 (ANSYS, Canonsburg, PA, USA).

A hybrid grid (tetrahedral and hexahedral elements) was used for the discretization of the computational domain, as this method of discretization is robust and appropriate for complex geometries in the postharvest cold handling system (Ambaw *et al.*, 2013a). The Richardson extrapolation method (Roache, 1994; Franke, 2007) was used to measure the level of grid independence in both models. Grids with four and three million cells were used for Models 1 and 2, respectively, with discretization errors of 3.2 and 5.0% in estimating mass fluxes through the boundaries.

The airflow in both models was solved, assuming a steady state condition. The transport equations were numerically solved, using the finite volume method in ANSYS-CFX-17 (ANSYS, Canonsburg, PA, USA). The advection scheme of the numerical solution uses the ANSYS-CFX high resolution method, which is a blend between central differencing and upwind differencing locally. Under the selected optimum solver format, a single full simulation took 10 to 15 hours on a 64-bit, Intel (R) Core (TM) 2 Quad CPU, 3 GHz, 8 GB RAM, Windows 7 PC.

6.2.5.4 Error calculation

The performance of the velocity prediction by the CFD simulations is evaluated by comparing simulated results to experimental data. For this, the root-mean-square error (RMSE) was calculated, as given by Equation (6.4) (Versteeg and Malalasekera, 1995).

$$RMSE = \sqrt{\frac{1}{N}\sum_{i=1}^{N}(U_{sim,i} - U_{Exp,i})^2} \quad (6.4)$$

Where:

$U_{Sim,i}$ and $U_{Exp,i}$ = the simulated and measured velocity magnitudes (m.s^{-1}), respectively.

6.3 Results and Discussion

6.3.1 Characterizing the flow resistances of the stacked tomatoes

The pressure drop across the half stack along two directions was simulated in Figure 6.3. (a–d) for flow along the +x and +z directions, respectively. Vertically, the boxes had no vent holes, hence there is no flow along the y direction. The direct CFD models helped to calculate and capture the anisotropic pressure losses effectively (Getahun *et al.*, 2017b). The air resistance characteristics along the short side of boxes (Figure 6.3 (a)) and long side (Figure 6.3 (b)) are detailed in Table 6.1.

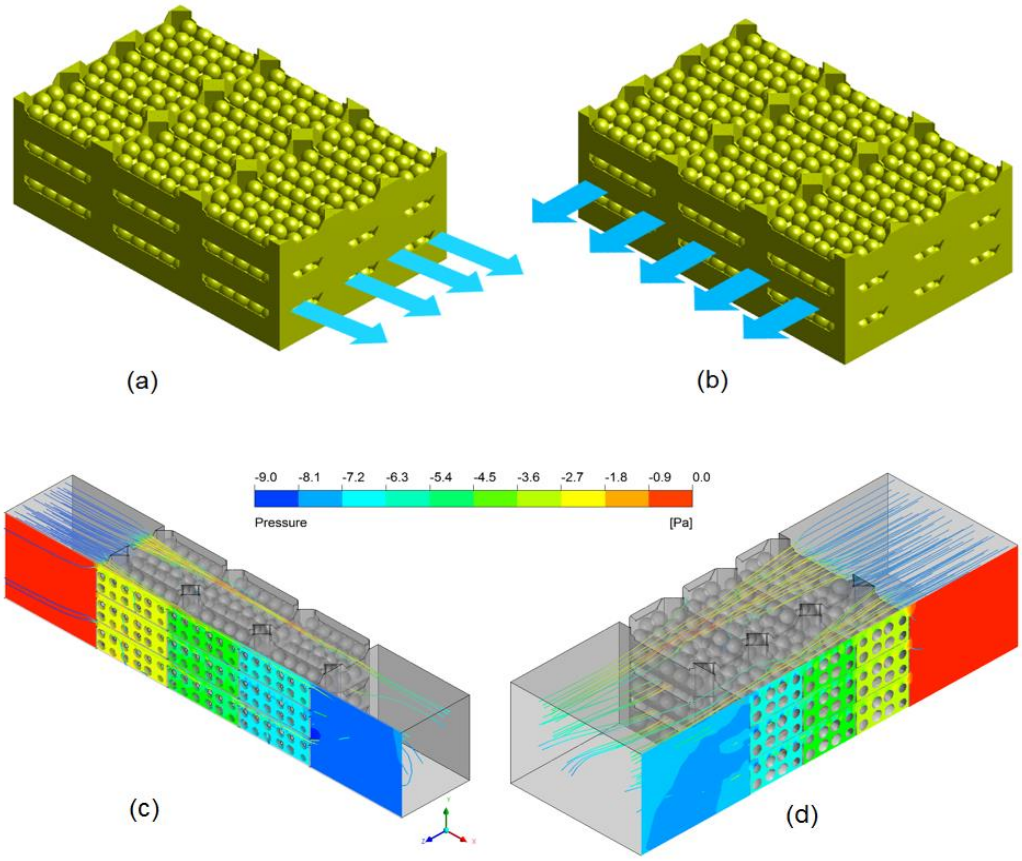

Figure 6.3 Schematics showing stacked tomatoes as placed in a wind tunnel. Horizontal airflow direction is perpendicular to the short side of the stack (a), to the long side of the stack (b), contours of pressure profiles obtained from the detailed CFD model for flow perpendicular to the short side (c) and the long side (d). Cartoons were loaded with 44 of spheres with a diameter of 65 mm representing 6 kg of tomato fruit

Figure 6.4 displays the pressure drop vs. the air velocity across the length (long side) and width (short side) of the pallet under horizontal flow conditions. Notice that the airflow resistance along the two horizontal conditions are different (Figure 6.4). The airflow resistance for flow, perpendicular the short side, is higher, due to the smaller vent hole proportion (Defraeye *et al.*, 2013a; Getahun *et al.*, 2017a). The vent hole proportion for smaller side and larger side of the box were found to be 8.7% and 15.1%, respectively. The results show that the flow direction along the short side stack may resist airflow along the stacks and, hence the flow along the long side facing to the airflow direction may be better.

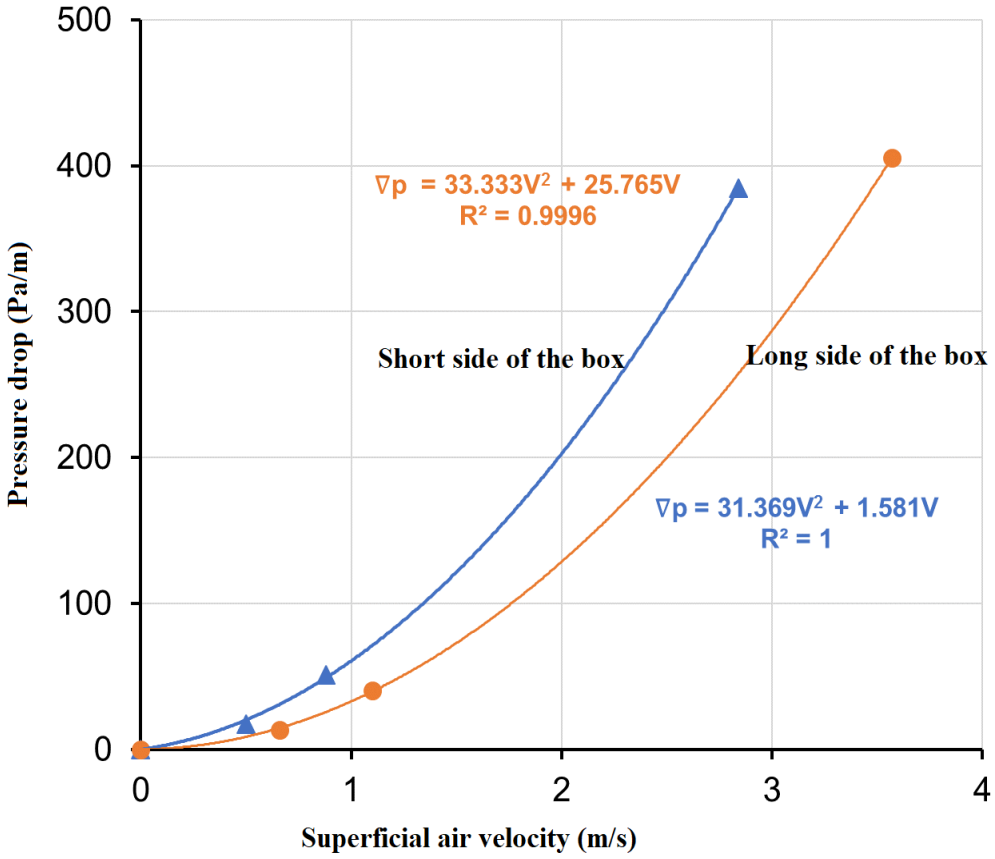

Figure 6.4 Graph of pressure vs superficial velocity of the airflow through the stacked tomatoes. Data is obtained from the CFD model

Table 6.1 gives the viscous and inertial coefficients obtained from fitting the simulated pressure vs. velocity data from the detailed CFD model. The pressure drop correlation determination of the experimental stack can be used for the high capacity load modelling of the cold storage chambers (Delele *et al.*, 2008b). The resistance coefficients along the two flow directions were used to model the stacked tomatoes as a porous domain. Therefore, the coefficients found can be used to further characterize the fully-loaded tomato storage chamber to model the further the storage capacity.

Table 6.1 Quantification of the inertial (Forchheimer) term (K1i = ρβ) and the viscous (Darcy) term (K2i = μ/K) of the Darcy- Forchheimer equation (Eqn. 6.3) of stacked tomato

Flow perpendicular to	Inertial term (kg m^{-4})	Viscous term (s^{-1})	R^2
Short side	33.33	25.76	1
Long side	31.37	1.58	1

6.3.2 Airflow characteristics inside the combined evaporative cooler and CoolBot-air-conditioned cold room

Figure 6.5 shows that air velocity streamlines inside the combined evaporative cooler and CoolBot-air-conditioner inside the cold room. The results show that the spatial distribution of the velocity magnitude varied from 0 $m.s^{-1}$ to 2 $m.s^{-1}$ inside the cold room. The air velocity magnitudes gradually decreased towards the outlet wall (nearly 0.5 $m.s^{-1}$). The air circulation, was established by the air conditioner, as well as the good distribution of the air velocities inside the storage chamber, may facilitate the turbulence and mixing of the air, to optimise heat and mass transfer (Ma *et al.*, 2011; Praneeth and Gowda, 2015). The uniformity of airflow distribution inside the cold storage chambers was affected by the position of the inlet fans, the number of inlets and the stacking orientation inside the cold storage chambers (Praneeth and Gowda, 2015). Similarly, the position and combination of the air conditioner and fan inlet might contribute to the uniformity of the airflow inside the EC+CBAC cold room that was tested.

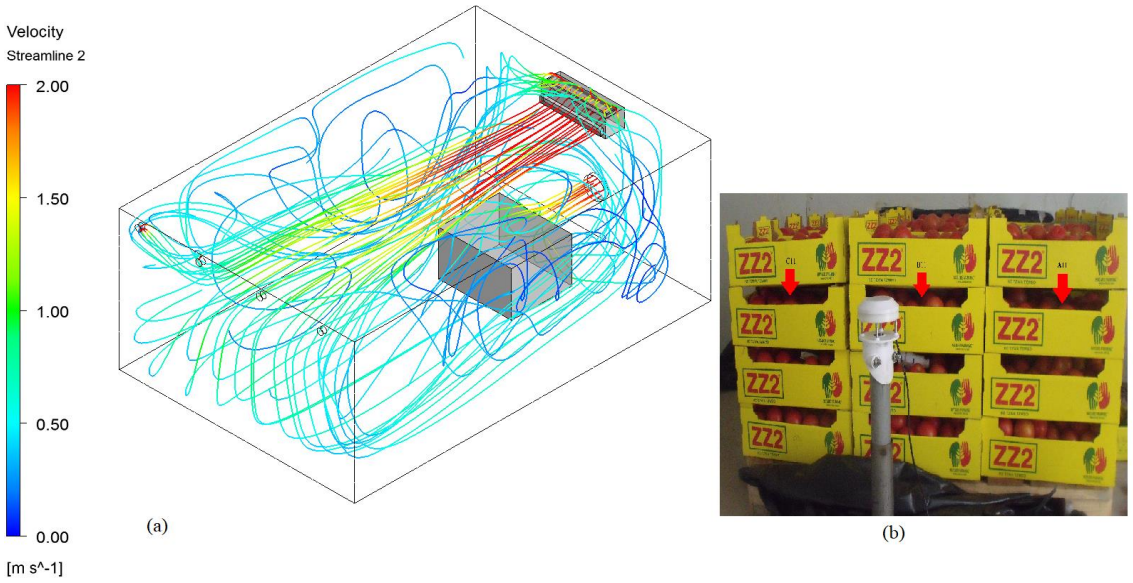

Figure 6.5 Simulated velocity stream line inside the cool room corresponding to the experimental setup (a). The grey box in the middle of the room is the porous domain representing a stack of cartoon containers each measuring 3×4×4 that are loaded with tomatoes (b)

6.3.3 Model validation

Figure 6.6 displayed contours of the air velocity on the symmetry plane passing through the pallet. During the experiment, the velocity meter was placed at three spots: to the left, middle and right of the stack, in the region in front of the stack, and at three spots, to the left, middle and right of the stack, in the region at the back (exit) of the stack. The sensor was placed 50 cm above the floor. The CFD model was used to predict the velocity magnitude corresponding to the sampling spots and the predicted and measured values were compared, for the validation. The model successfully captured the regions of high and low velocity magnitudes, with the RMSE of 0.12 $m.s^{-1}$ in the region in front of the stack and 0.18 $m.s^{-1}$ in the region at the back of the stack. Several researchers reported that, the RMSE value 0.15 $m.s^{-1}$ for apple stacks (Ambaw *et al.*, 2017). Nahor *et al.* (2005) reported that 20% of the air velocity magnitude accuracy was achieved inside loaded cold store, and a similar result was achieved in the current study.

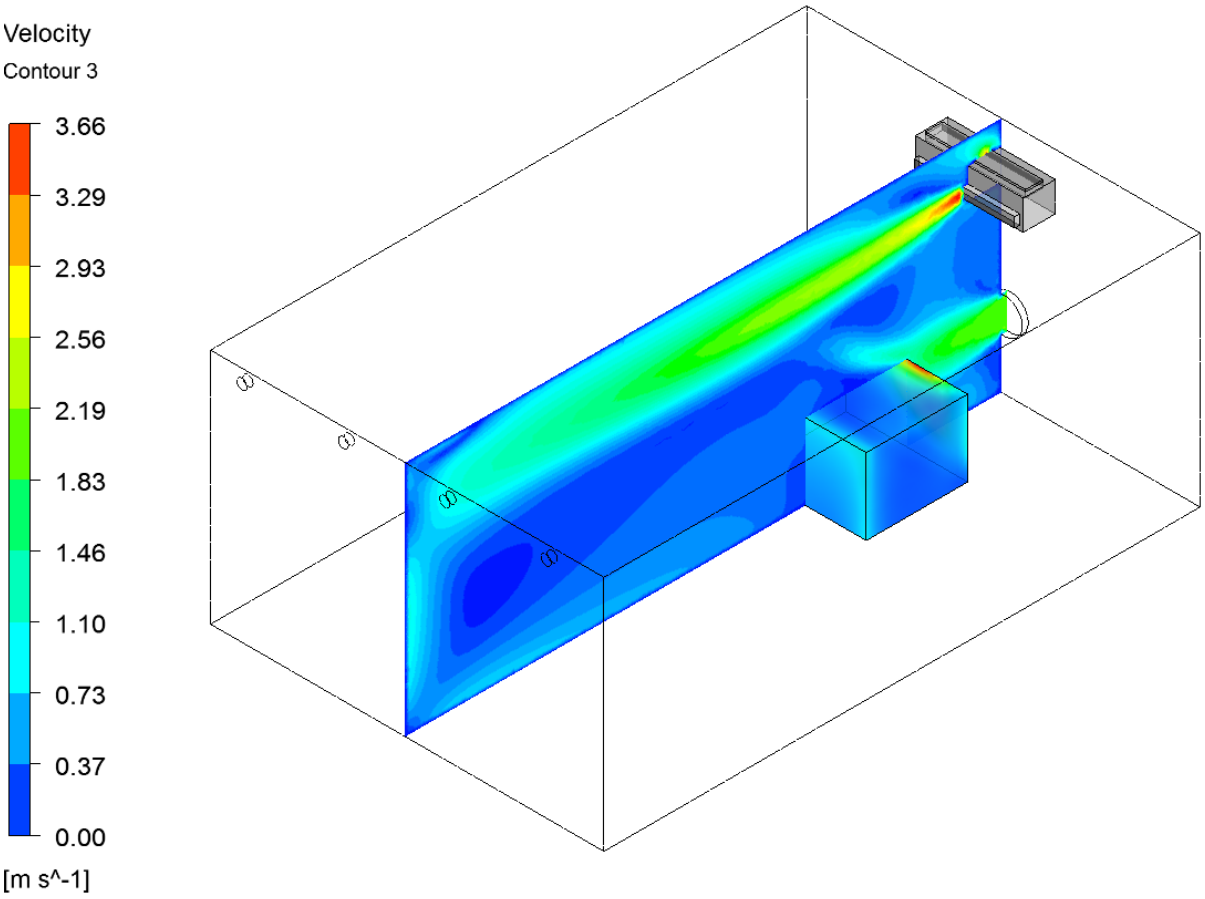

Figure 6.6 Contour of velocity magnitude on vertical plane bisecting the cool store and positions of the velocity meter across the experimental stack

Figure 6.7 shows the results of the horizontal airflow inside the combined evaporative cooler and CoolBot-air-conditioner (EC+CBAC) cold room, using a half pallet of the stored tomatoes. The results showed clear variations of airflow magnitudes at three plane sections *i.e.* across the inlet of the stack, at the middle cross-section of the stack and at the stack outlet cross-section planes. It is clearly demonstrated that the air velocity magnitude was found to be the highest in front of the inlet of the stack (1.5 $m.s^{-1}$) and decreased to the left and right of the inlet face of the stack (0.1 to 0.6 $m.s^{-1}$). On the other hand, across cross-section of the stack, the velocity vector, varied from 0.1 to 0.6 $m.s^{-1}$, while it varied from 0.2 to 0.4 $m.s^{-1}$ at the outlet of the stack. The magnitude of air velocity at the exit of the stack was found to be higher than the cross-section of the stack, which may have been contributed by the position of the air conditioner and the circulation the air inside the EC+CBAC room. Therefore, the orientations of the position of the inlet of the cold air (air conditioner or fan) clearly affected the air flow across the stack and along the inlet and exit (Figure 6.7). Hence, the optimization of the position of the inlets of the store is of paramount importance (Ma *et al.*, 2011; Praneeth and Gowda, 2015).

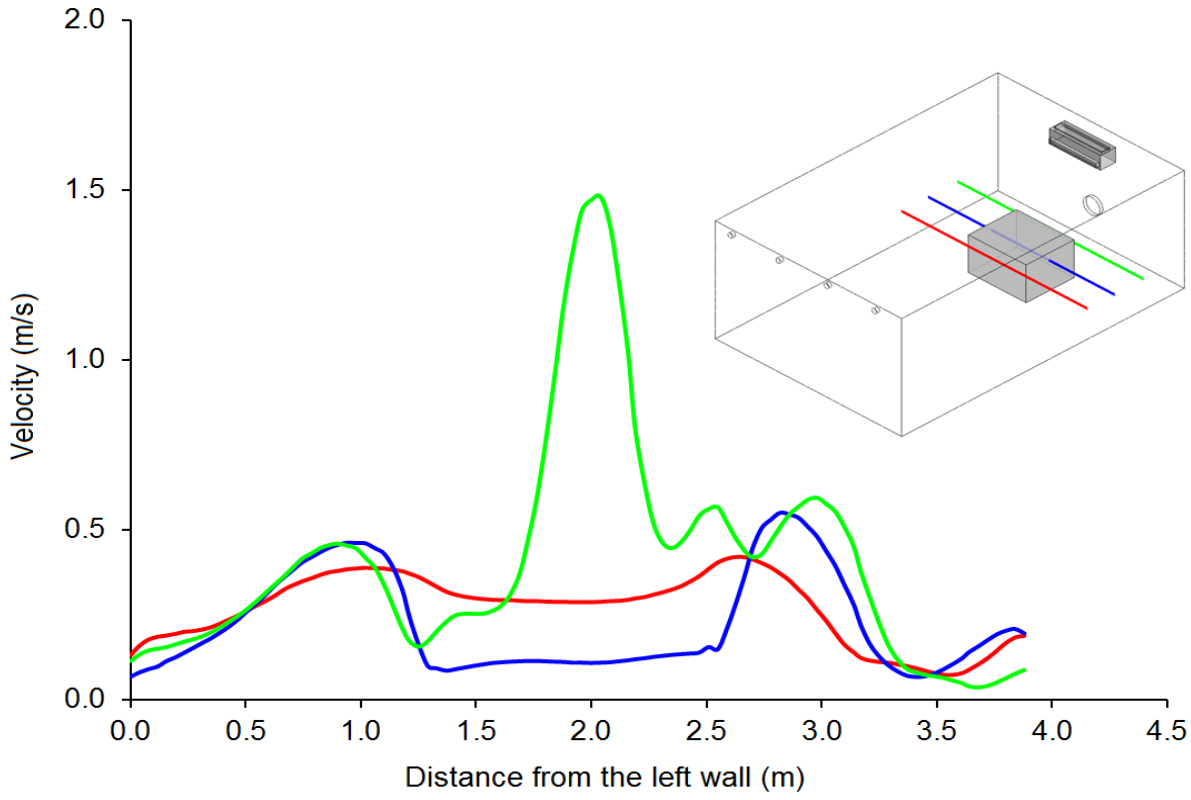

Figure 6.7 Velocity magnitudes along horizontal line passing through the inlet region of the stack (green), inside the stack (blue) and at the exit region of the stack (red), in the cold room operating under EC + CBAC

6.3.4 Investigating the airflow inside a fully-loaded cool store room

Using the validated CFD model, investigation has been made to evaluate and characterise the airflow inside a fully-loaded cool storage chamber (Figure 6.9). Loaded and unloaded cold storage chambers of fresh produce were modelled by the CFD and the air velocity for the two scenarios was predicted well by the model (Nahor *et al.*, 2005). The streamlines displayed by Figure 6.8 (a) and the air velocity contours (Figure 6.8 (b)) revealed that the level of airflow inside the stacks, located at the middle and near the back of the cool storage chamber, may be insufficient. The cooling kinetics and temperature distributions should be analyzed to completely evaluate the situation.

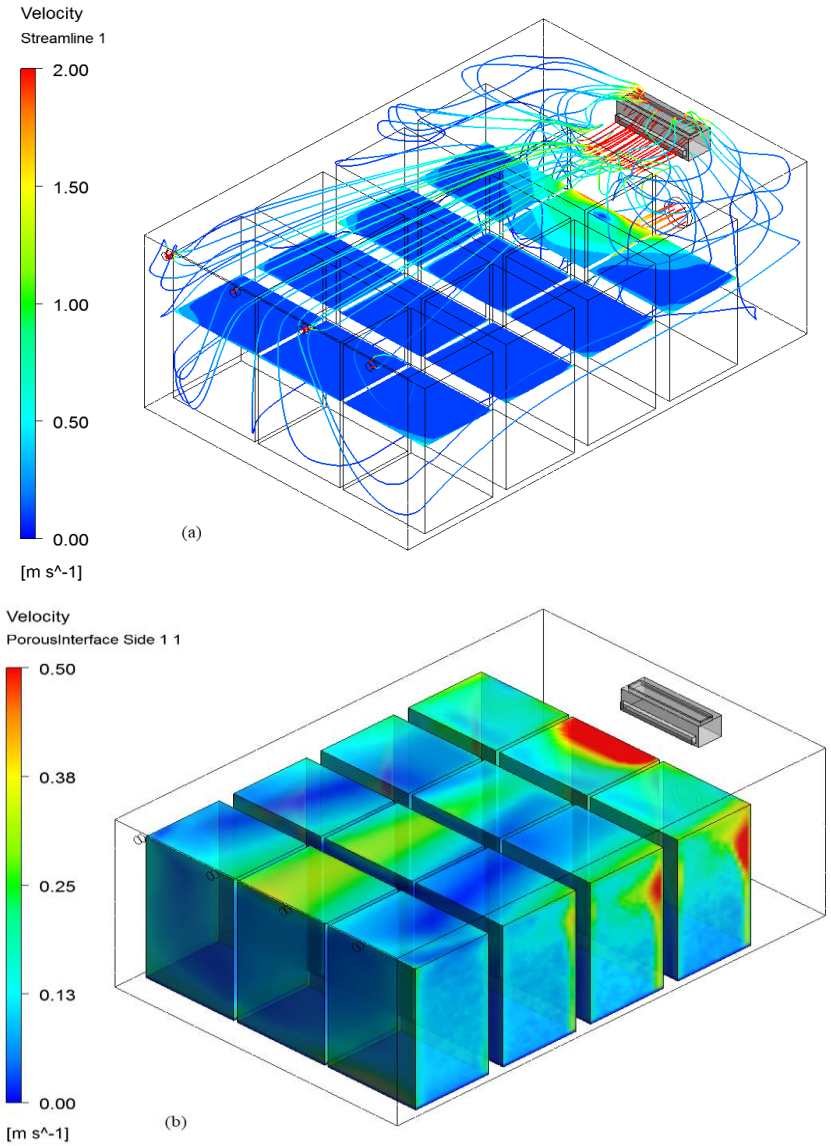

Figure 6.8 The airflow velocity streamlines (a) and contours of velocity magnitude crossing the porous boundary representing the stacked produce in a fully loaded room (b). Each pallet is 3×4×13 cartoons

6.4 Conclusions

Low-cost cooling technologies are an alternative for the small-scale and emerging farmers to store fresh produce, to extend days and to reduce postharvest losses. Cold storage chambers, such as the evaporative cooler, CoolBot-air-conditioner and the combination of the two, are promising technologies for the disadvantaged farmers. The following two airflow studies were performed, using CFD models: 1) the development of a model for the characterization of the resistance of the stack of tomato packages, and 2) the application of Model 1 to model different scenarios, for example, different cold rooms (EC, CBAC and EC+CBAC) and load size (fully loaded). Half a stack was used for Model 1 and pressure drop resistance coefficients were determined and further used to model the fully-loaded stack. Model 1 fitted well, with an RMSE air velocity of 0.18 $m.s^{-1}$ and 0.12 $m.s^{-1}$, across the inlet and outlet of the tomato stacks. The air velocity magnitudes at the inlet center of the stack was found to be 1.5 $m.s^{-1}$ and decreased towards left, right and exit sides of the stacked tomatoes. On the other hand, the airflow inside the stack varied between 0.1 $m.s^{-1}$ to 0.5 $m.s^{-1}$, which was found to be lower than the stack outlet side and which was probably created by the air conditioner and/or fan position circulating the air. Similarly, Model 2 followed the trends of the model 1 air flow characteristics, when fully-loaded. The air velocity magnitude was not distributed uniformly across the exit wall of the stacked pallets. The level of airflow inside the stacks, which was located at the middle and near the back of the cool store, may be insufficient. Hence, the CFD model clearly showed that the location is critical when considering the modification and maintenance of a cold room. Moreover, it is recommended that future studies should be undertaken on heat and mass transfer modelling. The cooling kinetics and temperature distribution should be analyzed, to completely evaluate the situation.

6.5 Acknowledgements

We would like to warmly acknowledge the Federal Ministry of Education, Ethiopia. South African National Research Foundation (NRF – TWAS); Tomato Producer Organization (TPO); Postharvest Innovation Program (PHI) for prevision of financial support; ZZ2 Tomato Farm for the prevision of the required sample tomatoes and the host institute, University of Kwa-Zulu Natal.

6.6 References

Ambaw, A, Dekeyser, D, Vanwalleghem, T, Van Hemelrijck, W, Nuyttens, D, Delele, MA, Ramon, H, Nicolai, B, Bylemans, D, Opara, UL and Verboven, P. 2017. Experimental and numerical analysis of the spray application on apple fruit in a bin for postharvest treatments. *Journal of Food Engineering,* 202**,** 34-45.

Ambaw, A, Delele, MA, Defraeye, T, Ho, QT, Opara, LU, Nicolai, BM and Verboven, P. 2013a. The use of CFD to characterize and design post-harvest storage facilities: Past, present and future. *Computers and Electronics in Agriculture,* 93**,** 184-194.

Ambaw, A, Verboven, P, Defraeye, T, Tijskens, E, Schenk, A, Opara, UL and Nicolai, BM. 2013b. Porous medium modeling and parameter sensitivity analysis of 1-MCP distribution in boxes with apple fruit. *Journal of Food Engineering,* 119**,** 13-21.

Boyette, MD and Rohrbach, RP. 1993. A low-cost, portable, forced-air pallet cooling system. *Applied engineering in agriculture,* 9**,** 97-104.

Castro, LR, Vigneault, C and Cortez, LaB. 2005. Cooling performance of horticultural produce in containers with peripheral openings. *Postharvest biology and technology,* 38**,** 254-261.

Defraeye, T. 2014. Advanced computational modelling for drying processes: a review. *Applied Energy,* 131**,** 323-344.

Defraeye, T, Lambrecht, R, Tsige, AA, Delele, MA, Opara, UL, Cronje, P, Verboven, P and Nicolai, B. 2013a. Forced-convective cooling of citrus fruit: Package design. *Journal of Food Engineering,* 118**,** 8-18.

Defraeye, T, Lambrecht, R, Tsige, AA, Opara, L, Delele, MA, Cronje, P, Verboven, P and Nicolai, B. 2013b. Intercomparison of package designs for cooling of citrus fruit by experimental and numerical analysis. 2nd IIR International Conference on Sustainability and the Cold Chain, 1-8. Division of Mechatronics, Biostatistics and Sensors (MeBioS), Paris.

Delele, MA, Ngcobo, MEK, Getahun, ST, Chen, L, Mellmann, J and Opara, UL. 2013. Studying airflow and heat transfer characteristics of a horticultural produce packaging system using a 3-D CFD model. Part II: Effect of package design. *Postharvest Biology and Technology,* 86**,** 546-555.

Delele, MA, Schenk, A, Tijskens, E, Ramon, H, Nicolaï, B and Verboven, P. 2008a. CFD modelling of humidification using presurized water atomizers in cold storage systems.

AgEng 2008. Division of Mechatronics, Biostatistics and Sensors (MeBioS), Crete, Greece.

Delele, MA, Tijskens, E, Atalay, YT, Ho, QT, Ramon, H, Nicolai, BM and Verboven, P. 2008b. Combined discrete element and CFD modelling of airflow through random stacking of horticultural products in vented boxes. *Journal of Food Engineering,* 89**,** 33-41.

Duan, Z, Zhan, C, Zhao, X and Dong, X. 2016. Experimental study of a counter-flow regenerative evaporative cooler. *Building and Environment,* 104**,** 47-58.

Franke, J. 2007. *Best practice guideline for the CFD simulation of flows in the urban environment.* COST Office, ISBN 3-00-018312-4, Brussels, Belgium.

Getahun, S, Ambaw, A, Delele, M, Meyer, CJ and Opara, UL. 2017a. Analysis of airflow and heat transfer inside fruit packed refrigerated shipping container: Part I–Model development and validation. *Journal of Food Engineering,* 203**,** 58-68.

Getahun, S, Ambaw, A, Delele, M, Meyer, CJ and Opara, UL. 2017b. Analysis of airflow and heat transfer inside fruit packed refrigerated shipping container: Part II e Evaluation of apple packaging design and vertical flow resistance. *Journal of Food Engineering,* 203**,** 83-94.

Han, J, Badía-Melis, R, Yang, X, Ruiz-Garcia, L, Qian, J and Zhao, C. 2016. CFD Simulation of Airflow and Heat Transfer During Forced-Air Precooling of Apples. *Journal of Food Process Engineering,* 40**,** 1-11.

Kitinoja, L. 2013. Innovative Small-scale Postharvest Technologies for reducing losses in Horticultural Crops. *Ethiop .J. Appl. Sci. Technol.* , Special Issue, 1**,** 9-15.

Kolodziejczyk, M, Butrymowicz, D, Smierciew, K and Gagan, J. July 11-14, 2016 2016. Numerical Modelling of Heat And Mass Transfer Processes In Chinese Cabbage Cold Storage Chamber. 16th International Refrigeration and Air Conditioning Conference 1-9. Purdue e-Pubs, Purdue University, USA.

Ma, J, Mathúna, SC, Hayes, M and Provan, G. 11 May 2016 2011. Model and visualise the relationship between energy consumption and temperature distribution in cold rooms. *In:* Carr, H and Grimstead, I, eds. 29th conference of theory and practice of computer graphics, 1-2. The Eurographics Association, EG, UK

Nahor, HB, Hoang, ML, Verboven, P, Baelmans, M and Nicolai, BM. 2005. CFD model of the airflow, heat and mass transfer in cool stores. *International Journal of Refrigeration-Revue Internationale Du Froid,* 28**,** 368-380.

Pal, RK, Roy, SK and Srivastava, S. 1997. Storage performance of kinnow mandarins in evaporative cool chamber and ambient condition. *Journal of food science and technology,* 34**,** 200-203.

Praneeth, HR and Gowda, BS. 2015. An analysis of cold store by CFD simulation. *International Journal of Innovations in Engineering Research and Technology,* 2**,** 1-14.

Rawangkul, R, Khedari, J, Hirunlabh, J and Zeghmati, B. 2008. Performance analysis of a new sustainable evaporative cooling pad made from coconut coir. *International Journal of Sustainable Engineering,* 1**,** 117-131.

Roache, PJ. 1994. Perspective: a method for uniform reporting of grid refinement studies. *Transactions-American Society of Mechanical Engineers Journal of Fluids Engineering,* 116**,** 405-405.

Roy, SK. 2007. *Low or no-cost cool chambers for fruits and vegetables.* National Horticulture Mission, India.

Roy, SK and Khardi, DS. 1985. Zero Energy Cool Chamber. *India Agricultural Research Institute: New Delhi, India. ,* Research Bulletin No.43: 23-30.

Roy, SK and Pal, RK. 1989. A low cost zero energy cool chamber for short term storage of mango. III International Mango Symposium 291, 519-524.

Roy, SK and Pal, RK. 1994. A low-cost cool chamber: an innovative technology for developing countries. *In:* Champ, BR, Highley, E and Johnson, GI, eds. Postharvest Handling of Tropical Fruits: ACIAR Proceedings, 393-395. Australian Centre for International Agricultural Research, Australia.

Sapounas, AA, Bartzanas, T, Nikita-Martzopoulou, C and Kittas, C. 2016. Aspects of CFD Modelling of a Fan and Pad Evaporative Cooling System in Greenhouses. *International Journal of Ventilation,* 6**,** 379-388.

Sapounas, AA, Nikita-Martzopoulou, C and Martzopoulos, G. 2008. Numerical and experimental study of fan and pad evaporative cooling system in a greenhouse with tomato crop. *In:* De Pascale, S, Mugnozza, GS, Maggio, A and Schettini, E, eds. International Symposium on High Technology for Greenhouse System Management: Greensys2007, 987-994. Acta Horticulture, Naples, Italy.

Saran, S, Dubey, N, Mishra, V, Dwivedi, SK and Raman, NLM. 2013. Evaluation of coolbot cool room as a low cost storage system for marginal farmers. *Progressive Horticulture,* 45**,** 115-121.

Tripathi, PC and Lawande, KE. 2010. Temperature-related changes in respiration and Q10 coefficient in different varieties of onion. *Progressive Horticulture,* 42**,** 88-90.

Van Der Sman, RGM. 2003. Simple model for estimating heat and mass transfer in regular-shaped foods. *Journal of food engineering,* 60**,** 383-390.

Verboven, P, Flick, D, Nicolai, BM and Alvarez, G. 2006. Modelling transport phenomena in refrigerated food bulks, packages and stacks: basics and advances. *International Journal of Refrigeration-Revue Internationale Du Froid,* 29**,** 985-997.

Versteeg, HK and Malalasekera, W. 1995. *An introduction to computational fluid dynamics* Essex, Longman Scientific & Technical and John Wiley & Sons Inc., USA.

Workneh, TS. 2010. Feasibility and economic evaluation of low-cost evaporative cooling system in fruit and vegetables storage. *African Journal of Food, Agriculture, Nutrition and Development,* 10**,** 2984-2997.

Workneh, TS, Ngejane, M, Thipe, EL, Larange, L and Smithers, JC. Nov. 25-28, 2012 2012. Design, construction and performance evaluation of a multistage pad evaporative cooler for extending the shelf life of fruit and vegetables. The 7th CIGR Section VI International Technical Symposium "Innovating the Food Value Chain" Postharvest Technology and AgriFood Processing, 1-20. CIGR, Stellenbosch, South Africa.

Xuan, YM, Xiao, F, Niu, XF, Huang, X and Wang, SW. 2012. Research and application of evaporative cooling in China: A review (I) - Research. *Renewable & Sustainable Energy Reviews,* 16**,** 3535-3546.

Yadav, VK, Singh, A and Chandra, P. 2002. Experimental Evaluation of the effect of Fan Pad Evaporative Cooling System parameters on Greenhouse Cooling. *Journal of Agricultural Engineering,* 39**,** 49-53.

Zhao, CJ, Han, JW, Yang, XT, Qian, JP and Fan, BL. 2016. A review of computational fluid dynamics for forced-air cooling process. *Applied Energy,* 168**,** 314-331.

Zou, Q, Opara, LU and Mckibbin, R. 2006a. A CFD modeling system for airflow and heat transfer in ventilated packaging for fresh foods: I Initial analysis and development of mathematical models. *Journal of Food Engineering,* 77**,** 1037-1047.

Zou, QA, Opara, LU and Mckibbin, R. 2006b. A CFD modeling system for airflow and heat transfer in ventilated packaging for fresh foods: II Computational solution, software development, and model testing. *Journal of Food Engineering,* 77**,** 1048-1058.

7. INFLUENCE OF STORAGE ENVIRONMENT, MATURITY STAGE AND PRE-STORAGE TREATMENTS ON TOMATO FRUIT QUALITY DURING WINTER IN KWAZULU-NATAL, SOUTH AFRICA

Abstract

The aim of this study was to explore influence of evaporative cooling (EC), pre-storage disinfection treatments and maturity stage at harvest on postharvest quality of tomato fruit. The tomato samples (*Lycopersicon esculentum* Mill. cv. Nemonetta) were harvested, stored for 28 days and data were collected every seven days. The pH, total titratable acidity (TA), total soluble solids (TSS), firmness, colour, weight loss (PWL) and marketability percentage were analysed. The temperature difference between ambient storage and EC at the fan varied between 4 and 7°C, the relative humidity (RH) varied between 31 to 86%, while at different locations inside the EC it varied between 2 - 3 °C and 5 - 8%, respectively. Maturity had significant ($p \leq 0.05$) influence on the overall quality of tomatoes. The pH value of green, pink and red tomato was varied between 4.86 and 5.03. The TA content, the TSS content significantly affected ($p \leq 0.05$) over the 14 days of storage. TSS:TA ratio was found to be in the range of 7.8 to 33.9. The EC storage shows a higher firmness and hue angle, when compared to the ambient conditions stored tomatoes. Compared to ambient storage, EC storage reduced the PWL by 7-10% over 30 days, while ambient storage took 15 days. Based on the above result, EC storage and pre-storage treatments improved the shelf-life and marketability of tomatoes. However, variation in temperature and RH inside EC could affect the storability of the produce.

Keywords: Evaporative cooler, Pre-storage disinfection treatments, Relative humidity distribution, Temperature distribution, Tomato quality.

7.1 Introduction

Fresh commodities should be available in good quality to meet consumer needs and hence an appropriate precooling and optimum desirable micro-climate inside storage facilities and packaging are required (Thompson, 2003). Cooling is employed to reduce chemical, biochemical and microbial changes, as well as respiration and water loss. Hence, this prolongs the shelf-life and enables the quality to be maintained (Ambaw *et al.*, 2013). Maintaining an optimum cooling temperature and relative humidity (RH) is very crucial to reduce postharvest losses. Different methods have been applied for the cooling fresh commodities, including mechanical refrigeration, hydro-cooling, natural convective cooling, vacuum cooling, room cooling, forced air cooling and evaporative (Kader, 1985; Xuan *et al.*, 2012; Ambaw *et al.*, 2013). Mechanical refrigeration is the most commonly applied technology, but it is expensive and requires a high initial investment cost and is associated with environmental impacts through direct and indirect greenhouse gas emissions (Tassou *et al.*, 2010). On the contrary, evaporative cooler (EC) was reported to have a lower costs in terms of installation and low energy requirements to run a fan and water pump, and hence it was reported to be affordable for small-scale farmers operating in arid and semi-arid regions (Saran *et al.*, 2010; Workneh, 2010; Xuan *et al.*, 2012; Kitinoja, 2013). For EC to be effective, the atmospheric air conditions should have a lower RH (65%) (Thompson, 2016). Several researchers reported that three basic methods of EC have been developed, including direct evaporative cooling (DEC), indirect evaporative cooling (IEC) and semi-indirect evaporative cooling (SIEC) (Dvizama, 2000; Sellers, 2004; Xuan *et al.*, 2012; Basediya *et al.*, 2013).. Several EC designs have been reported to be efficient for fruit and vegetable storage and preservation (Roy and Khardi, 1985; Roy and Pal, 1994; Pal *et al.*, 1997). The designs vary from a grass straw house to high technology designs, such as a wet wall, roof, charcoal, coconut straw, rice husk, cellulose pad, jute curtain, pot-in-pot EC and zero-energy EC (Liberty *et al.*, 2013). Therefore, it can be easily constructed from locally-available materials and is affordable for small-scale farmers.

For every 10°C temperature fluctuation, the respiration rate changes by two-to four-fold (Watada *et al.*, 1996) and the temperature is found to be the single most important factor that affects the shelf-life of fresh produce. Hence, optimal temperature management, which is attainable by using an EC system, is the most important operation for small-scale producers (Kader, 1985; Thompson *et al.*, 2002; Liberty *et al.*, 2013). Moreover, RH influences water loss and decay development, triggers physiological disorders and affects the ripening processes of

fresh produce (Kader, 1985). Therefore, a RH of between 85 to 95% was recommended for fruit and 90 to 98% for vegetables (Kader, 1985), which is attainable by EC. Temperature, RH, and ventilation management maintain the quality and longer shelf-life of fresh produce (Liberty *et al.*, 2013). Optimum storage temperatures for different tomato maturity stages are reported to be 12-20°C and 7-10°C, respectively, for the green and pink mature stage, within a period of four to seven days (Liberty *et al.*, 2013). Optimum storage RH was reported to be 85-90% for a shelf-life one to three weeks (Chinenye *et al.*, 2013; Liberty *et al.*, 2013). Even though EC reduces the temperature and RH, it is limited only for the pre-cooling of produce, with the main aim of removing the field heat. Therefore, several researchers recommended integrating postharvest treatments and the EC storage environment for best performance in shelf-life extension and maintaining the quality (Fallik *et al.*, 1996; Porat *et al.*, 2000; Workneh *et al.*, 2003; Workneh, 2010; Workneh *et al.*, 2012). Some pre-storage treatments, including anolyte water and chlorinated water disinfection (Workneh *et al.*, 2003), as well as dipping in hot water can be applied to fruit and vegetables as a pre-storage treatment for shelf-life extension (Fallik *et al.*, 1996). However, there is not much information available for the integration of these treatments with the EC storage environment system.

The quality indices that influence consumer acceptance and market success were reported to be colour, size, shape, texture, flavour, total soluble solids (TSS), titratable acidity and physiological weight loss (Kader, 1986; Barrett *et al.*, 2010). TSS varies from 3 to 15%, which is dependent on tomato variety and size (Beckles, 2012). The authors reported that both the temperature and the maturity stage at harvesting time have an influence on the texture and colour uniformity during postharvest handling. Hence, the main objectives of this study are to determine the temperature and RH distribution inside the EC chamber, as well as to investigate the cumulative effects of maturity stage, storage conditions, storage period, and pre-storage treatments on the quality and shelf-life of tomatoes.

7.2 Materials and Methods

7.2.1 Site description

The study was carried out at the Ukulinga Research Farm, Pietermaritzburg, South Africa, with a latitude of -29.668, a longitude of 30.406 and an altitude of 808.

7.2.2 Sample tomato production and preparation

Three maturity stages of tomato samples (green, pink and red) (*Lycopersicon esculentum* Mill. cv. Nemonetta), produced by the ZZ2 Farm, Limpopo, South Africa, were used for the study.

7.2.3 Evaporative cooler

A 4-ton capacity experimental scale multi-pad evaporative cooler (EC), with one indirect heat exchanger and three direct pads, was established at the Ukulinga Research Farm of the University of KwaZulu-Natal, South Africa (Figure 3.1). The dimensions of the EC is a length of 6 m, a width of 4 m and a height of 2.4 m. The wall thickness was 60 mm, of which 1 mm is plain carbon steel (mild steel) that is laminated to both the inner and outer wall sides, with 58 mm thick polyurethane foam insulation in between. An axial fan (OW354), with a blade size 340 mm (H)* 340 mm (W)* 260 mm (Φ), a power rating 0.12kw and a Gril code of OW395, was used to drive air into the EC storage chamber.

7.2.4 Experiential design

The experimental design consists of four factors, including three tomato maturity stages (green, pink and red), four treatments (AW, HotH_2O, Cl_2, and Control), two storage conditions (ambient and EC) and five storage periods with five replications. Five fruits per sample were used for the experiment (Figure 7.1).

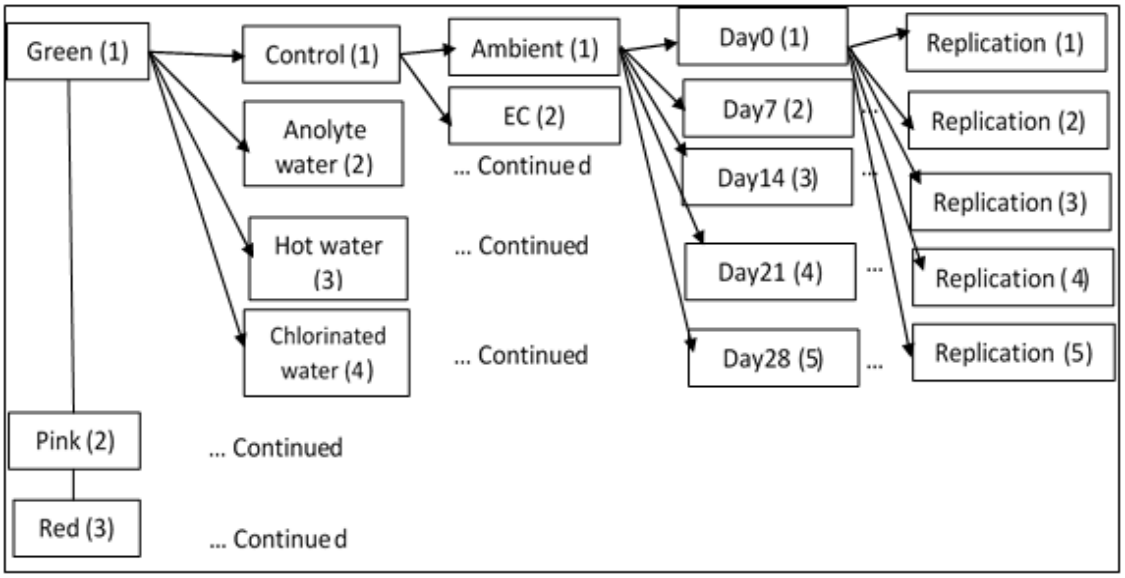

Figure 7.1 Experimental design set up used for the experimentations.

7.2.5 Data collection

7.2.5.1 Temperature and relative humidity measurements

Temperature and RH were recorded at different locations inside the cooler (Figure 3.1). The ambient air data was collected from ARC-AWS weather station, which is located at the Ukulinga Research Farm.

7.2.5.2 Disinfection pre-storage treatments

Different pre-storage treatments, including anolyte (AW), chlorination (Cl_2) water and hot water ($HotH_2O$), were applied to the sample. Sample tomatoes were dipped into an AW solution for 5 minutes (Workneh *et al.*, 2003; Workneh *et al.*, 2012) and air-dried, before being stored. The hot water treatment was done by dipping the sample into hot water at 42.5°C for 30 minutes (Itoh, 2003). Chlorine disinfection was done by dipping samples into a solution containing 100 µg. ml^{-1} total chlorine (Cl_2) for 20 minutes, which was prepared by dissolving standard grade sodium hypochlorite (5% NaOCl) in tap water (Workneh *et al.*, 2011). The control samples were dipped into cold water for 20 minutes. Five tomato fruits were randomly picked for the quality indices analysis every seven days for the 28 days of storage period. The measurements were replicated five times.

7.2.5.3 pH value

Five tomato samples from each maturity stage were taken and blended into a homogeneous pulp. This was then filtered, using Whatman filter paper No. 1, and 25 ml of the filtrate was then used to measure pH values with a pH meter (Orion Star, Model 210, Thermo Scientific Pty), according to the procedure used by AOAC (1995).

7.2.5.4 Total titratable acidity

A 25 ml filtrate of the pulped tomato was taken for total titratable acidity (TA) determination and was titrated with 0.1N NaOH, using a phenolphthalein indicator. The TA content was calculated, using the following Equation 7.1 (AOAC, 1995; Niño-Medina *et al.*, 2013):

$$\%TA = \frac{ml\ NaOH\ used * N * meq}{ml\ of\ tomato\ juice} * 100 \quad (7.1)$$

Where:

$\%TA$ = the total titratability percentage (%),

N = the normality of NaOH (N), and

meq = the milliequivalents of citric acid, which is 0.064.

7.2.5.5 Total soluble solids

The total soluble solid (TSS) content was determined, using a digital handheld refractometer (Pocket Refractometer, PAL-3, Japan). The tomato sample was pulped and filtered by Whatman filter paper No.1. The filtrate was used for the analysis (AOAC, 1995).

7.2.5.6 Total soluble solids to total titratable acidity ratio

The TSS to TA ratio of tomato slurry was calculated using Equation 7.2 (Moneruzzaman *et al.*, 2008):

$$TSS{:}TA\ ratio = \frac{\%\ TSS\ Content\ of\ Fruit\ Pulp}{\%\ TA\ of\ of\ the\ Fruit\ Pulp} \quad (7.2)$$

7.2.5.7 Firmness

The fruit firmness was determined by using the Intron Universal Testing Machine (Model No. 3345) with a 7.5 mm penetration depth, a 3.00 $m.min^{-1}$ speed, a 50 N maximum force and a 2 mm diameter probe, according to the procedure used by Pinheiro *et al.* (2013). Five fruits from each category of tomatoes, subjected to different treatments, were used for the analysis.

7.2.5.8 Colour

Tomato skin colour was measured along the waist diameter, using the digital Minolta Chromatic 400 method of the CIELAB colour space, according to the procedures of Batu (2004) and Messina *et al.* (2012). The instrument was calibrated against a white standard tile before each colour reading. The hue (h^o) value was measured and recorded.

7.2.5.9 Physiological weight loss

The physiological weight loss (PWL) was determined gravimetrically for change of weight of the samples every seven days of the storage period and converted to a percentage of the initial weight. The cumulative PWL (%) was expressed as a percentage with respect to storage period (Equation 7.3) (van Dijk *et al.*, 2006; Tefera *et al.*, 2007).

$$\%Weight\ loss = \frac{Weight_{(t=0)} - Weight_{(t=t)}}{Weight_{(t=0)}} * 100\% \quad (7.3)$$

Where:

%Weight loss = the percentage of with loss of sample tomato (%),

Weight $_{(t=0)}$ = the initial weight of sample tomato (kg), and

Weight $_{(t=t)}$ = the weight of sample tomato at time t (days of storage).

7.2.5.10 Percentage marketability

The marketability of the tomatoes was accessed subjectively, according to Mohammed *et al.* (1999). The visible shrivelling, smoothness, mould growth and shininess of the tomatoes were considered to select the sound and marketable fruit. The number of sound fruits was counted and the percentage was calculated with respect to the initial sample number every seven days over the 28 days period.

7.2.6 Data analysis

The data was subjected to a factorial analysis of variance (ANOVA). Duncan's multiple mean comparisons operated by the Least Significant Difference test (L.S.D.) was used to separate means. GenStat Version 17 was used for statistical analysis. The fresh produce kept in a multi-pad evaporative cooler and ambient storage environment for a 28-day period.

7.3 Results and Discussion

7.3.1.1 Temperature and relative humidity

The recorded ambient temperature ranged between 13 and 23ºC, while the temperature inside the EC varied between 11 and 18 ºC (Figure 7.2). Although the experiment was conducted in winter, a comprehensive lower temperature was achieved inside the EC storage chamber, due to the evaporative cooling effect resulting from the multi-pad cooling systems.

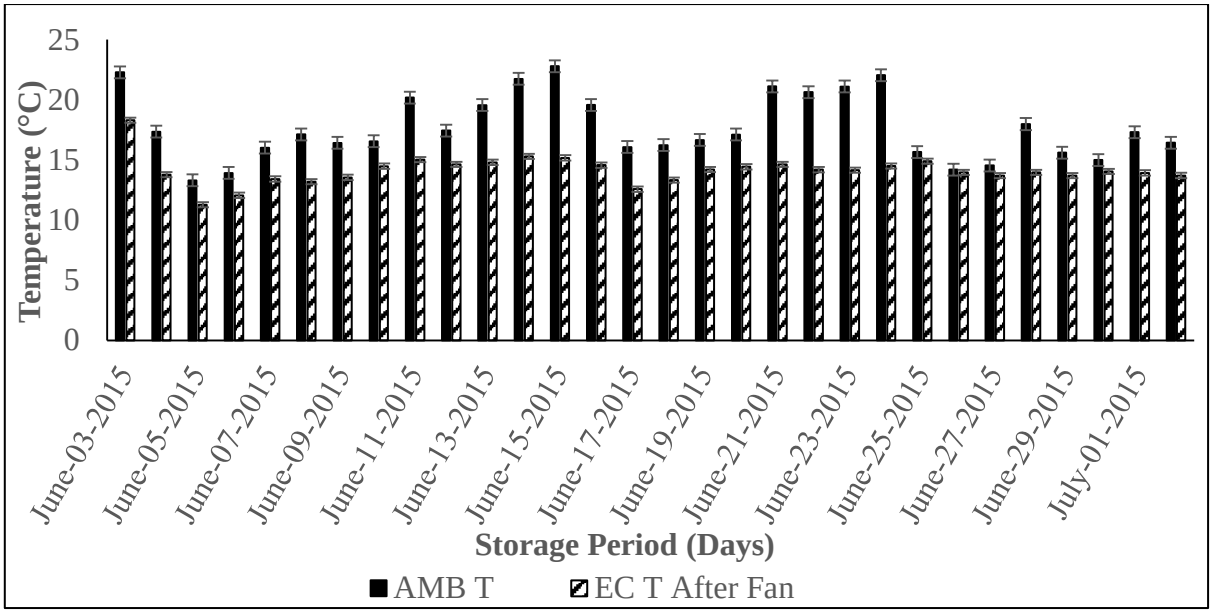

Figure 7.2 Temperature of outside (AMBT) and inside (ECT) evaporative cooler

The daily ambient RH and the relative humidity of air inside the EC varied from 16.8 - 67.8% to 69.3 - 90.4%, respectively (Figure 7.3). The result indicates that the ambient air RH was lower, compared to the RH of air inside the cooler chamber. The increase in RH was due to the humidification effect of the inlet air being forced through the direct cooling pads. Fresh commodities require low temperatures during storage. The maintenance of high RH is also important for keeping the freshness and for the reduction of moisture loss (Thompson et al., 2002). The data presented in this result display evidence demonstrating that the application of multi-pad EC reasonably reduces the inside temperature and increases the RH, which are both suitable for prolonging the shelf-life of fresh fruit and vegetables *(*Figure 7.3).

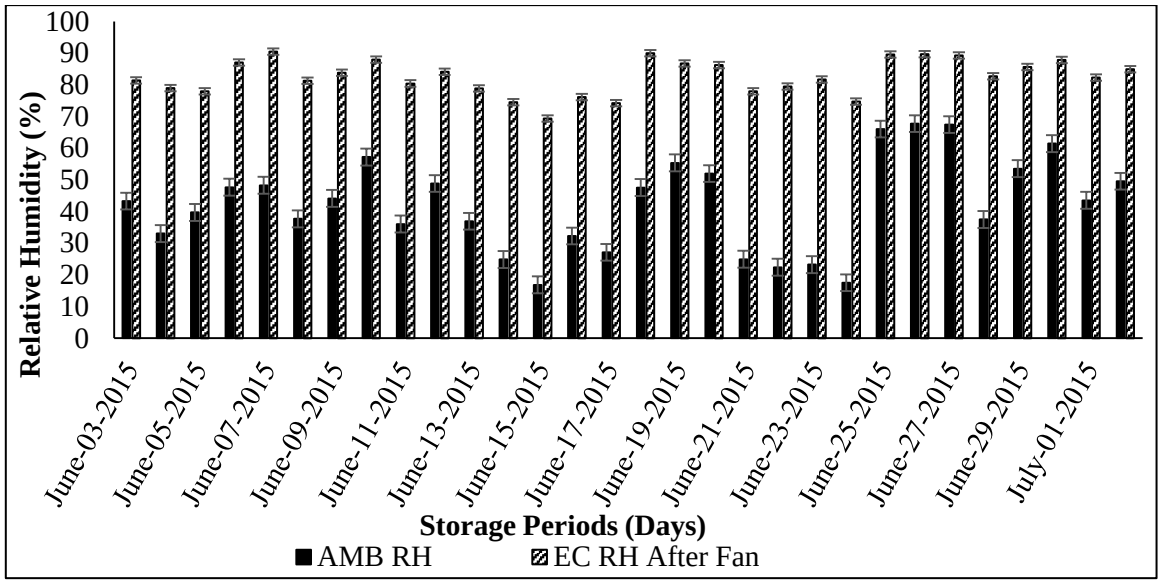

Figure 7.3 Relative humidity of the air outside (AMB) and inside (EC) of the EC

The maximum air temperature difference was found between 12 am and 5 pm, which is in agreement with the report of Anyanwu (2004) (Figure 7.4). Moreover, the maximum temperature difference between the outside and inside EC was attained during the same periods. These periods of the day are the time during which cooling is important for fruit and vegetables in order to maintain freshness (Anyanwu, 2004). This implies that the evaporative cooling technology is highly suitable for fresh produce pre-cooling and for short-term storage in arid and semi-arid regions (Workneh, 2010).

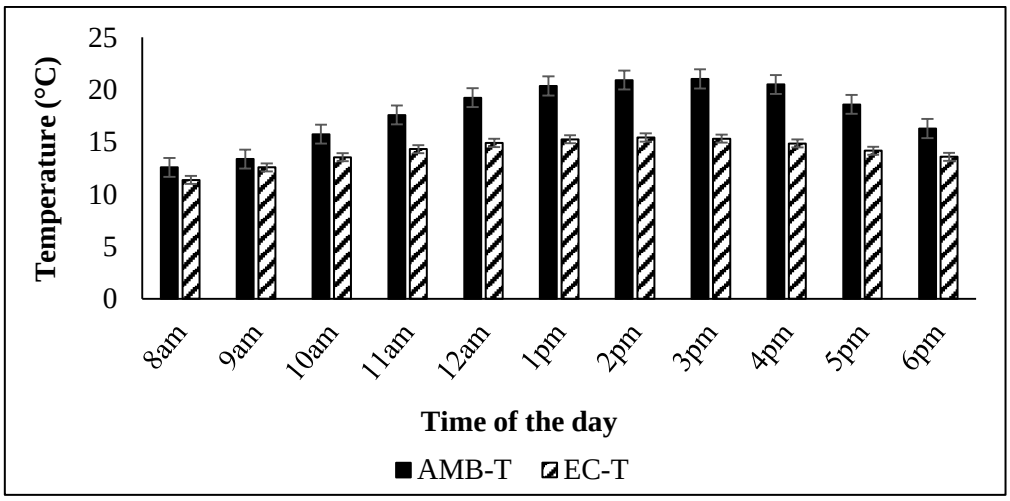

Figure 7.4 Hourly daytime temperature of the air outside (AMB-T) and inside the EC (EC-T)

The ambient RH was found to be very low at midday and towards the afternoon, while the RH inside EC was found to be high throughout the day (Figure 7.5). A low RH means that the air

is dry, hence removing much of the moisture from the wet surface of the fresh produce (Awole *et al.*, 2011). This implies that storage at ambient environmental conditions, from the midday to the late evening, will significantly influence the quality of fresh produce. On the other hand, the RH inside the EC was relatively high during the daytime, due to humidification and is suitable for extending the shelf-life of fruit and vegetables (Thompson, 2003). Low RH and high ambient dry bulb temperature are recommended for the effectiveness of the EC (Workneh, 2010; Xuan *et al.*, 2012). High temperatures and low RH were attained between 12 am to 5 pm, which is in agreement with the findings of Anyanwu (2004) and Getinet *et al.* (2011).

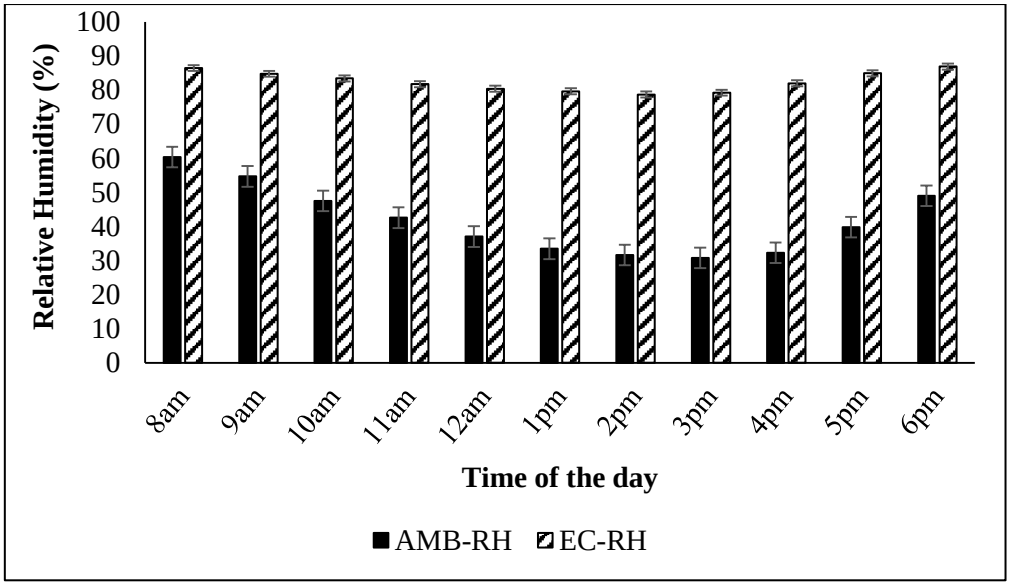

Figure 7.5 Hourly RH of ambient (AMB) and inside EC (EC) during the daytime.

The state of the ambient temperature and RH were found to be 22.8ºC and 31%, respectively (Figure 7.6). The difference in temperature between the ambient and inside EC was found to be 7.6ºC, while the RH increased by 55% during the hottest day. The air temperature and RH at different locations inside the EC were found to be 15.2ºC and 86%, respectively (Figure 7.6).

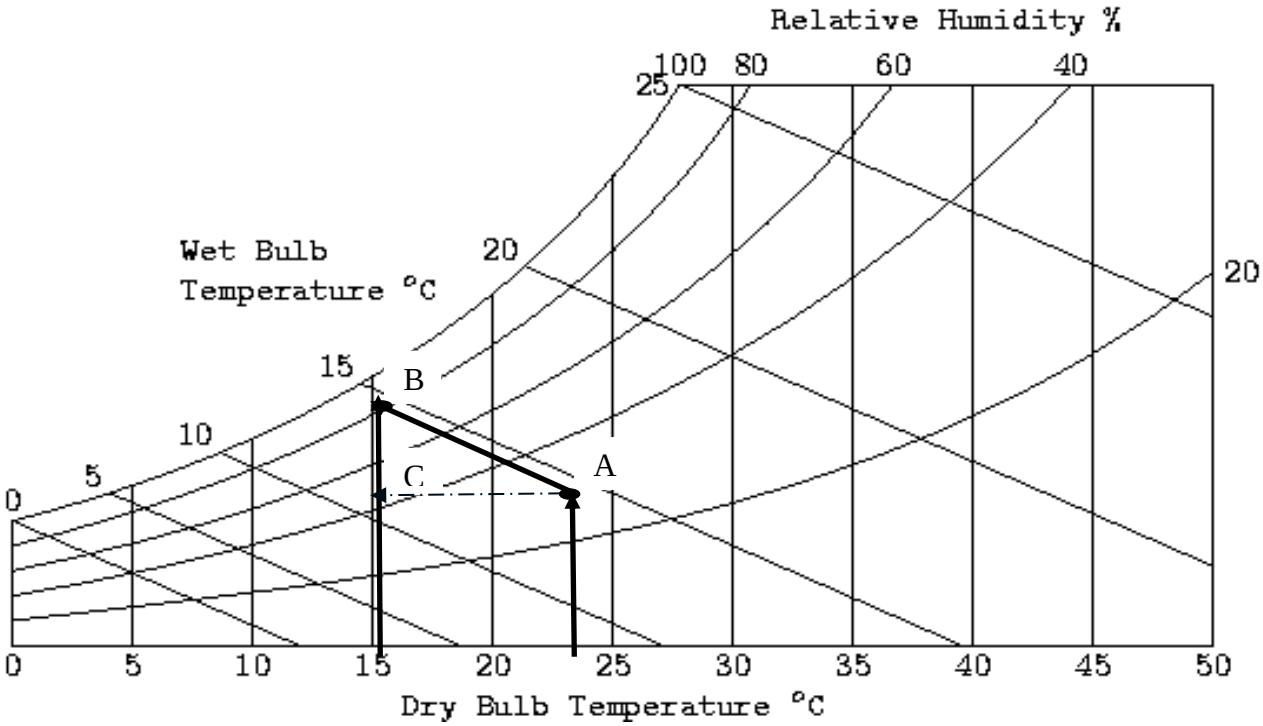

Figure 7.6 A psychrometric chart showing the evaporative cooling process during the daytime. A is the ambient air condition (22.8*ºC*, 31% of RH); B is the air condition after fan 2 (15.2ºC, 86% of RH); C is the change in temperature (7.6ºC) and RH (55%)

The result indicates that there were temperature variations between different sensor locations inside the EC (Figure 7.7). The temperature depression between the ambient and the EC at the fan location varied between 4 and 7ºC in this study when compared to 4 - 13ºC reported by Chinenye *et al.* (2013) and 5°C found by Getinet *et al.* (2008) during the hottest day of the storage periods. It is evident from the data obtained in this study that the RH was increased by 55%, when compared to the ambient air relative humidity. Getinet *et al.* (2008) reported that the RH was increased by 18%. The differences between the inlet and exit air temperatures and the relative humidity varied between 2 - 3°C and 5 - 8%, respectively. The coldest air was recorded near the inlet next to the axial fan, while the higher temperature was at the air exit of the EC storage. The difference in environmental conditions, with respect to the location inside the cooler chamber, might indicate their influence on the quality of fresh produce stored inside EC. Maintaining a uniform air distribution and the conditions inside the cooler chamber is preferable for keeping the proper physiology, quality and shelf-life extension of fresh produce throughout the cooler chamber space. Hence, more advanced studies might be required, using modelling tools such as Ansys for CFD.

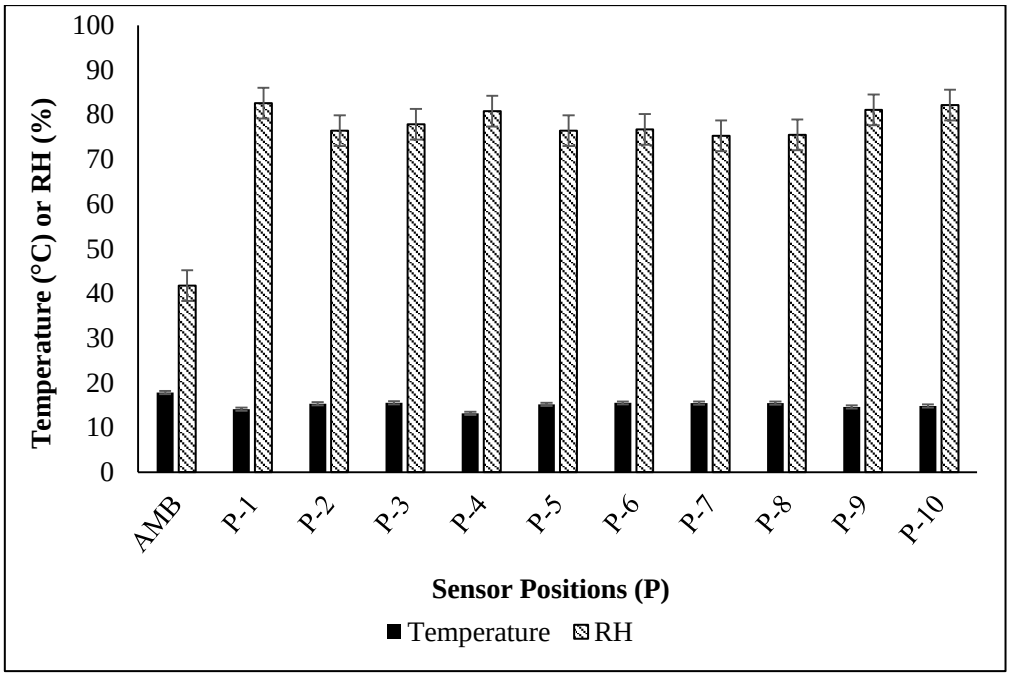

Figure 7.7 Temperature or RH distributions inside EC: where AMB is the ambient, Temperature-RH sensors: position-1 (P1), position-2 (P2), position-3 (P3), position-4 (P4), position-5 (P5), position-6 (P6), position-7 (P7), position-8 (P8), position-9 (P9), and position-10 (P10) (as described in Figure 3.1)

7.3.1.2 pH value

The pH value is one of the most essential processing features of tomatoes, hence remaining the main factor for the fruit industry (Paulson and Stevens, 1974; Moneruzzaman *et al.*, 2008). The pH value of tomatoes harvested at the green, pink and red mature stages was found to be 4.88, 5.05 and 4.96, respectively (Figure 7.8). The maturity stage had a significance ($p \leq 0.001$) influence in pH values of tomato samples (Table 7.1). The pH value of sample tomatoes increased with the storage period, which was in agreement with the findings of Moneruzzaman *et al.* (2008). This increase might be attributed to the enzymatic breakdown of pectin during the storage period (Anthon and Barrett, 2012). Both the ambient and EC storage conditions had no significant ($p \leq 0.05$) influence on the pH value. Pre-storage disinfection treatments and their interactions had a highly significant ($p \leq 0.001$) effect on the pH values of tomatoes. The slight increase in pH value in the maturity stage might be due to respiration, ripening and physiological changes, which might lead to a high susceptibility to deterioration. Moreover, tomato samples dipped in chlorinated water showed the lowest pH value. The control tomato samples and tomatoes subjected to hot water treatment had a relatively medium effect on the

changes in pH value. Anolyte water disinfection exhibited the highest pH value, but, Workneh *et al.* (2003) reported that it had no effect on the pH value of fresh carrots.

The effect of two-way interactions of all the maturity stage, storage condition, storage period and disinfection treatments exhibited a highly significant ($p \leq 0.001$) influence on the pH value (Table 7.1). The physiological changes of fruit components might contribute to the fluctuations in the pH value observed for all maturity stages of tomatoes (Pila *et al.*, 2010).

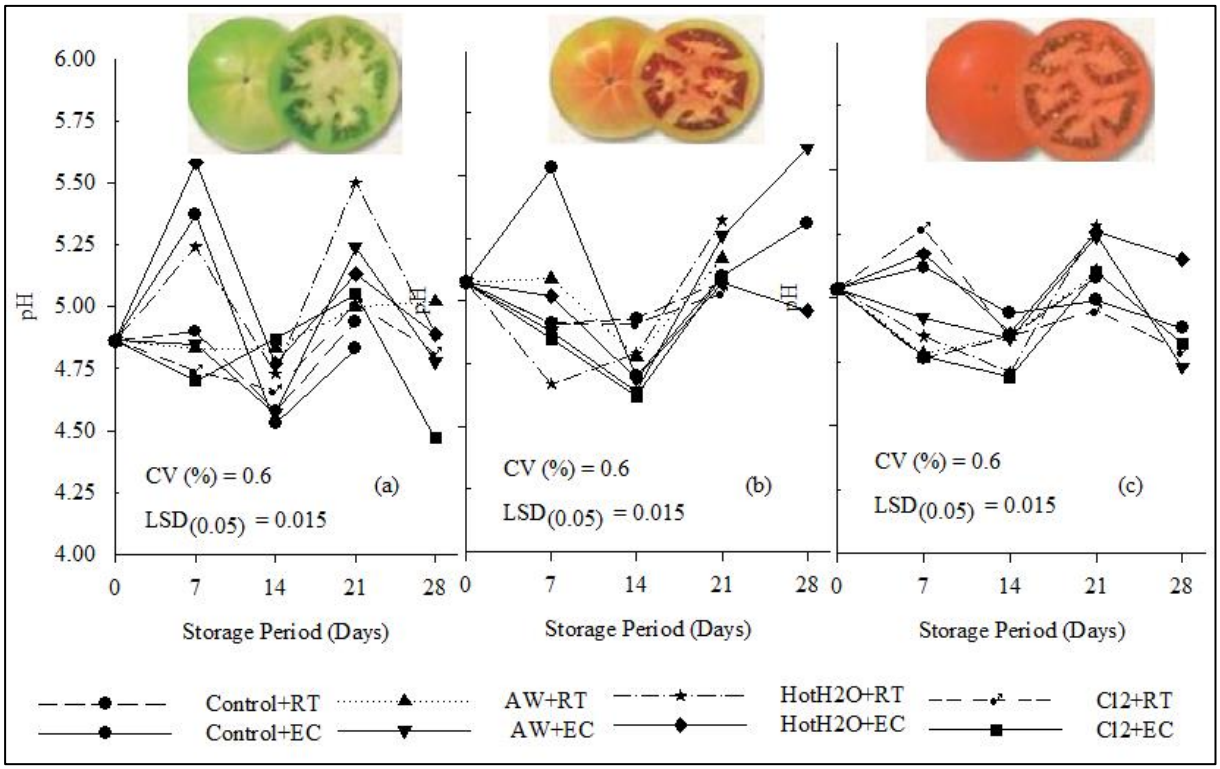

Figure 7.8 Changes in pH of tomatoes harvested at the green (a), pink (b) and red (c) maturity stage and subjected to pre-storage and storage environment treatments (n = 5). Where RT is room temperature, EC is evaporative cooling, AW is anolyte water, HotH2O is hot water and Cl2 is chlorinated water

7.3.1.3 Total titratable acidity content

TA content is one of quality indices directly related to the tomato processing industry (George *et al.*, 2004). The TA content of tomatoes was reported to be directly proportional to the ripening of tomatoes (Gautier *et al.*, 2008). It was suggested that a TA of 0.35 - 0.55% was recommended to be suitable for the tomato processing industry (Gould, 1992). The TA of

tomatoes decreased from 0.51 - 0.30%, 0.44 - 0.3% and 0.38 - 0.30% over the 14 days of storage, respectively, for green, pink and red stages (Figure 7.9). The decrease was reported to be due to the metabolic activity of the fruit itself, which reduces the organic acids (Bhattarai and Gautam, 2006; Pila *et al.*, 2010).

All individual factors, including maturity stage, storage conditions, storage period and pre-storage disinfection treatments, had a significant ($p \leq 0.001$) effect on the TA content of the tomato samples (Table 7.1). The TA content decreased with the ripening of tomatoes during the storage period, which is in agreement with the findings of Moneruzzaman *et al.* (2008). Hot water dipped samples exhibited the lowest TA, followed by chlorinated and anolyte water that was treated while the control sample showed the highest TA content.

All two-way interactions between the maturity stage, storage conditions, storage period, and disinfection treatments had a significant ($p \leq 0.001$) influence on the TA content of the tomato samples (Table 7.1). Compared to pink and red tomatoes, the green mature stage had the highest TA content, when stored under ambient conditions or in a EC storage environment in agreement with Bhattarai and Gautam (2006). The lowest TA content of tomatoes was exhibited by red tomatoes over a three-week period, while the largest shown was by green and pink over a short period, which was in agreement with Pila *et al.* (2010). Compared to the other treatments, the largest TA content was exhibited by the EC storage environment of tomato samples subjected to anolyte water disinfection. The result indicates that the combined effect of EC storage with anolyte water maintains the TA content and that the TA content decreases with storage period elongation (Bhattarai and Gautam, 2006; Pila *et al.*, 2010).

The three-way interaction effects of the maturity stage, storage conditions, storage periods and disinfection treatments had a significant ($p \leq 0.05$) effect on the changes in the TA contents, which is in agreement with the findings of Moneruzzaman *et al.* (2008). Tomatoes harvested at the green and pink stages and stored in an EC environment throughout the storage period, showed the highest TA content (Table 7.1). Compared to ambient storage, the EC storage conditions maintained the higher TA of tomato samples over the 14 days of the storage period. Anolyte and hot water dipped red tomatoes that were subjected to both outside and inside EC storage showed the lowest TA content, whereas the highest TA was shown by green tomatoes stored inside EC and subjected to all pre-storage disinfection treatments.

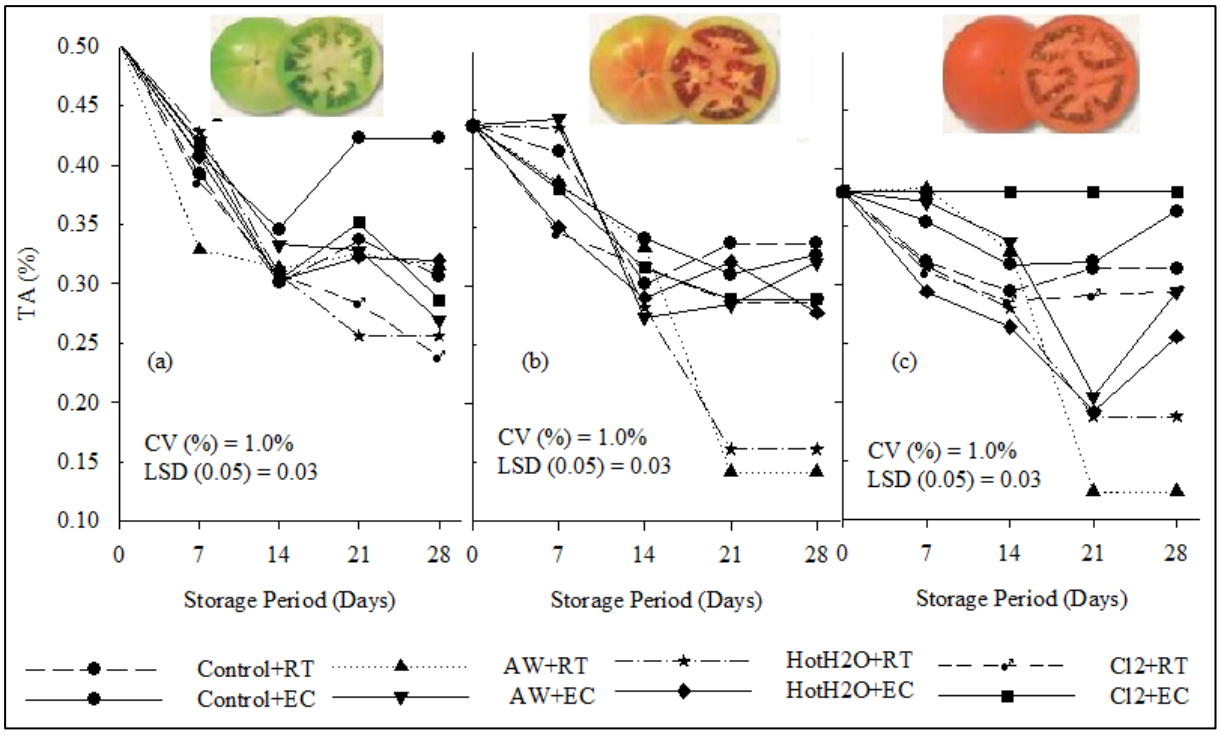

Figure 7.9 Changes in total titratable acidity (TA) of tomatoes harvested at the green (a), pink (b) and red (c) stages and subjected to pre-storage and storage environment treatments (n=5). Where RT is room temperature, EC is evaporative cooling, AW is anolyte water, HotH2O is hot water, and Cl2 is chlorinated water

7.3.1.4 Total soluble solids content

Total soluble solid (TSS) content is the refractometric index that indicates the percentage total soluble solids in a solution (Beckles, 2012) and it is one of tomato quality indices. It is the sum of fruit acids, sugars and other soluble components of the fruit pulp and is inversely proportional to fruit's size (Beckles, 2012). The TSS value from 5.5 - 8.5% is recommended to be suitable for the processing industry (Gould, 1992).

All individual factors, including the maturity stages, storage conditions, storage period and pre-storage treatments, had a significant ($p \leq 0.001$) effect on the TSS content of tomatoes (Figure 7.10). The TSS of tomatoes harvested at the green and pink mature stage increased from 3.9 - 4.2% to 3.7 - 4.5%, respectively, over a seven-day of storage period, followed by an increase over 14 days of storage, with a decreasing trend thereafter. This result was in agreement with Bhattarai and Gautam (2006) and Majidi *et al.* (2011). Compared to tomatoes stored under ambient condition, the TSS was higher for tomatoes stored under EC storage, which was in

agreement with the results reported by Getinet *et al.* (2008). The pre-storage disinfection treatment result proves that chlorination disinfection was the best of maintaining the TSS content, followed by anolyte and hot water dipping.

All the two-way interaction effects of the maturity stage, storage conditions, storage period and disinfection treatments had a significant ($p \leq 0.001$) effect on the TSS content of tomatoes (Table 7.1). Tomatoes harvested at the green maturity stage and stored inside an EC storage environment showed the lowest TSS content. This shows that EC storage qualifies in lowering the TSS, by reducing the physiological breakdown of the tomato constituents (Pila *et al.*, 2010). The lowest TSS content was found in the tomatoes that were harvested at the pink and green stages and dipped in anolyte and chlorinated water. On the other hand, green and red tomatoes dipped in anolyte water, and pink tomatoes subjected to hot water, showed the highest TSS content. Moreover, the interaction effects of anolyte water and chlorinated dipped samples subjected to EC storage had the lowest TSS content, which could be a good combination.

All individual three-way interactions between maturity stages, storage conditions, periods and disinfection treatments had a significant ($p \leq 0.001$) effect on the TSS content of tomatoes (Table 7.1). The EC storage environment maintained the low TSS content over two weeks of the storage period. Moreover, the lowest TSS content is shown by pink tomato samples that were dipped in anolyte or chlorinated water and stored in an EC environment. Low maturity stage tomatoes, combined with disinfection treatments and the EC environment, resulted in the lowest TSS content. Hence, the green maturity stage, a two-week storage period and an EC environment might be the best combination, to maintain the quality of tomatoes. Moreover, tomato samples dipped in anolyte water had the lowest TSS content over a two-week of storage period and stored in an EC environment.

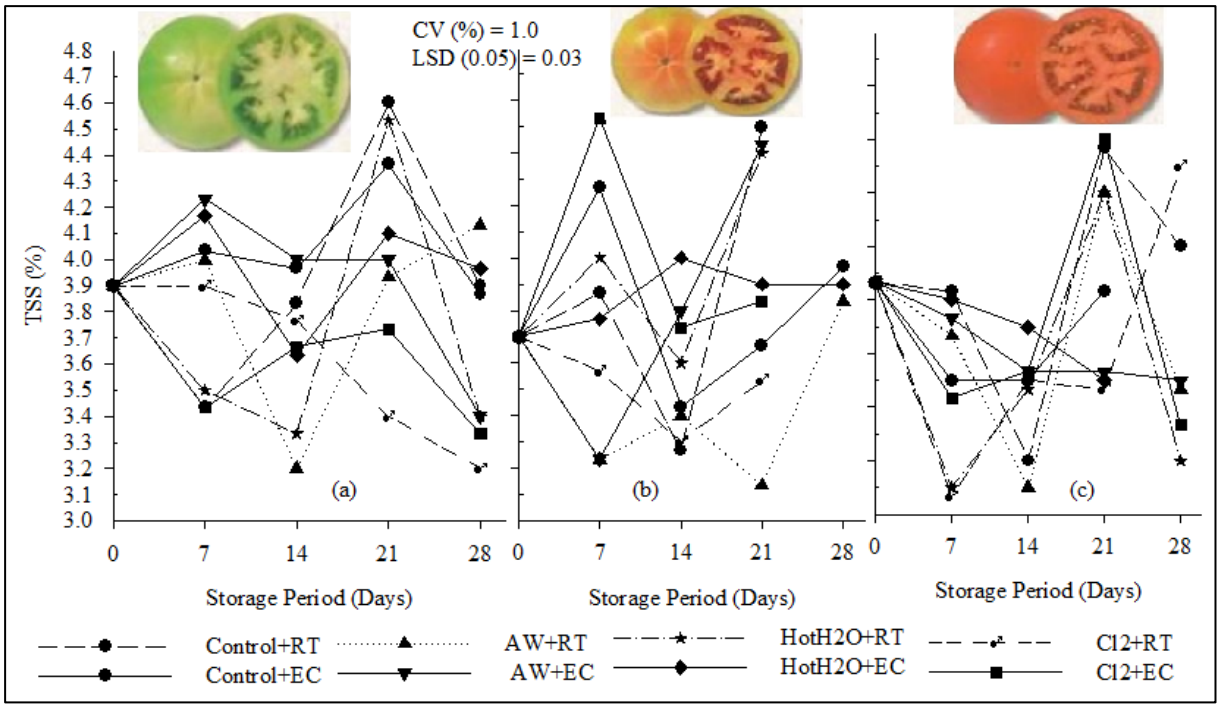

Figure 7.10 Effects of maturity stage, disinfection, and storage environment on the changes in total soluble solids of tomato fruits harvested at green (a), pink (b) and red (c) stage (n=5). Where RT is room temperature, EC is evaporative cooling, AW is anolyte water, HotH2O is hot water, and Cl2 is chlorinated water

7.3.1.5 Total soluble solids to total titratable acid ratio

The TSS to TA ratio (TSS:TA) is an important key indicator of the quality of fresh produce (Kader *et al.*, 1977; Kader *et al.*, 1978; Beckles, 2012). The TSS:TA is highly dependent on the maturity stage and growth conditions (Bertin *et al.*, 2000). In this study, the TSS:TA changed from 7.8 - 15.1, 6.7 - 27.3 to 8.8 - 33.9 for tomato samples harvested at the green, pink and red stages, respectively (Table 7.1). Several researchers reported that fruit size is dependent on the TSS:TA (Kader *et al.*, 1978). Thus, a TSS:TA content of 3-5%, 5-7% and 9-15% was identified for beefsteak (ideal for salsa processing), medium-sized and cherry tomatoes, respectively (Gautier *et al.*, 2005; Gautier *et al.*, 2008). As a result, the tomato samples used for this study are considered to be salad processing (large sized fruit) tomatoes.

7.3.1.6 Firmness

All individual factors, including the maturity stages, storage conditions, storage period and disinfection treatments, had a significant ($p \leq 0.05$) effect on the changes in firmness (Figure

7.11). Tomatoes harvested at the green maturity stage remained intact and were the firmest, followed by pink and red, respectively, which is in agreement with the report of Batu (2004). The tomatoes harvested at the green, pink and red maturity stages experienced a decrease in firmness from 29 to 10 N, 25 to 13 N, 20.5 to 10 N, respectively, over 21 days of the storage period. The decrease in firmness could be due to the physiological breakdown of the fruit cell wall during ripening (Batu, 2004; Viskelis *et al.*, 2008). Batu (2004) reported that a firmness greater than 8.76 N was very firm and very marketable in supermarkets, hence, the result of this experiment is in agreement with the author's report. Moreover, the tomatoes stored inside an EC environment had higher firmness, compared to those stored under ambient conditions, which is in agreement with the report of Luna-Guevara *et al.* (2014). The result indicates that EC storage kept the fruit structure intact and firm, which might contribute to the maintenance of tomato quality. Moreover, the effects of hot water treatment indicated the lowest firmness, as reported by Luna-Guevara *et al.* (2014), while anolyte water and chlorinated disinfected tomatoes maintained higher firmness.

All individual two-way interaction effects between the maturity stages, storage conditions, storage period and disinfection treatments, were found to be significant ($p \leq 0.05$) for the changes in the firmness of the tomatoes (Table 7.1). Compared to red and pink mature stage tomatoes, the green mature tomatoes that were subjected to EC storage conditions showed the highest firmness (Figure 7.11). The result indicates that a combination of less mature tomatoes and low temperature (EC) storage conditions gave the firmest tomatoes, which is in agreement with the research report of Lana *et al.* (2005). Moreover, tomatoes harvested at the red maturity stage and subjected to all disinfection treatments show the lowest firmness, while the green tomatoes display the highest firmness. On the other hand, the interaction of EC storage and chlorinated water dipping maintained the firmness better than the other treatments.

All the three-way interaction effects among the maturity stages, storage conditions, storage period and disinfection treatments, had a significant ($p \leq 0.05$) influence on the firmness of the tomatoes (Table 7.1). Tomatoes harvested at the green maturity stage, subjected to both ambient and EC conditions, had the largest firmness throughout storage period, but the red stage experienced the lowest firmness. Moreover, the results indicated that the combination of red maturity stage tomatoes, ambient storage and hot water treatment aggravated the firmness loss. However, the less mature stage tomatoes, subjected to EC storage and chlorination disinfection or hot water treatment, maintained their firmness. Similarly, a combination of less mature

tomatoes, subjected to short storage period and chlorinated or anolyte water disinfected, gave the highest firmness. However, Workneh *et al.* (2003) reported that dipping in anolyte water had no effect on the firmness of carrot.

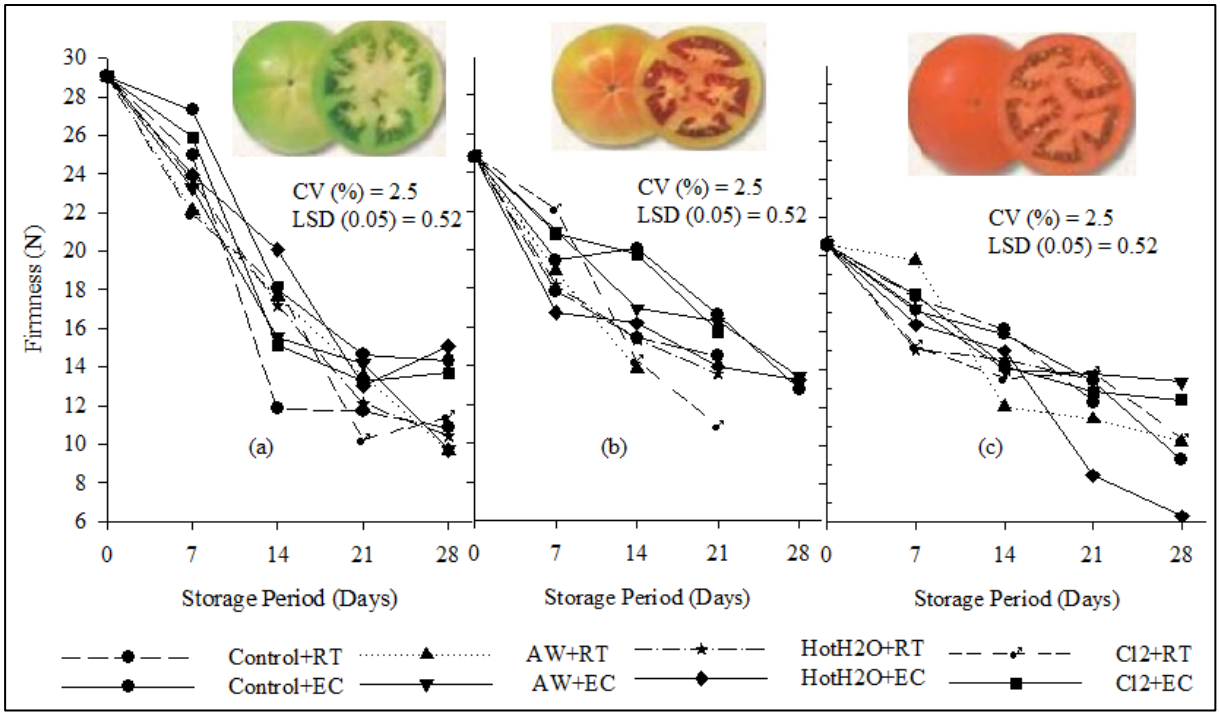

Figure 7.11 Changes in firmness (N) of tomatoes harvested at green (a), pink (b) and red (c) stage and subjected to pre-storage and storage environment treatments (n=5). Where RT is room temperature, EC is evaporative cooling, AW is anolyte water, HotH2O is hot water, and Cl2 is chlorinated water

7.3.1.7 Colour

Tomato colour is one of the most important factors that determines the consumer's acceptance and purchase (Camelo and Gómez, 2004). The higher hue angle of tomatoes indicates the lower physiological colour development. All individual factors, including maturity stage, storage period and disinfection treatments, had a significant ($p \leq 0.05$) influence on the changes in hue angle of the tomato fruit (Figure 7.12). The hue angle difference among the maturity stages could be acquired by the ripening of the fruit tissue. The hue angle was inversely proportional to the maturity stages, due to the ripening process (Viskelis *et al.*, 2008). The effects of storage conditions on the changes in hue angle were not found to be significant ($p > 0.05$), which is in agreement with the report of Luna-Guevara *et al.* (2014) (Table 7.1). Compared to ambient

storage, the EC storage environment slowed down the colour development of tomatoes harvested at three maturity stages. This indicates that the EC prolonged the shelf-life of the tomatoes by reducing physiological changes that lead to the colour development (Viskelis *et al.*, 2008). A prolonged storage period highly affected the hue angle, which might be due to a breakdown of the components and lycopene development (Viskelis *et al.*, 2008). In addition, hot water treatment maintained a high hue angle.

All individual two-way interaction effects between the maturity stages, storage condition, storage periods and disinfection treatments, had a significant ($p \leq 0.05$) effect on the hue angle of the tomato samples (Table 7.1). The tomato samples harvested at the green maturity stage experienced the largest hue angle, when stored under EC environment. Hence, combination of less maturity stage and EC storage environment, it was found to be significant for maintaining quality and freshness. Moreover, tomatoes harvested at the green and pink maturity stage and subjected to a short storage period experienced the highest hue angle. A hue angle of 103° to 45°, 73° to 45° and 60° to 45°, respectively, was demonstrated for tomatoes harvested at the green, pink and red maturity stages, over a 21-day storage period. Similar to the report of Radzevičius *et al.* (2009), the hue angle of the external tomato colour approached 40° to 45° for different maturity stages over 21-day storage period. A combination of the green maturity stage with all disinfection treatments, gave the largest hue angle. In addition, the results indicate that a combination of EC storage environment and hot water treatment maintained the firmness of tomatoes. Moreover, the results indicate that a short storage period and hot water or chlorine disinfection maintained the quality of the tomatoes.

All individual three-way interaction effects between the maturity stages, storage condition, storage period and disinfection treatments, had a significant ($p \leq 0.05$) influence on the hue angle (Table 7.1). The result showed that a combination of less ripe tomatoes and stored in an EC environment for short period, gave the best quality.

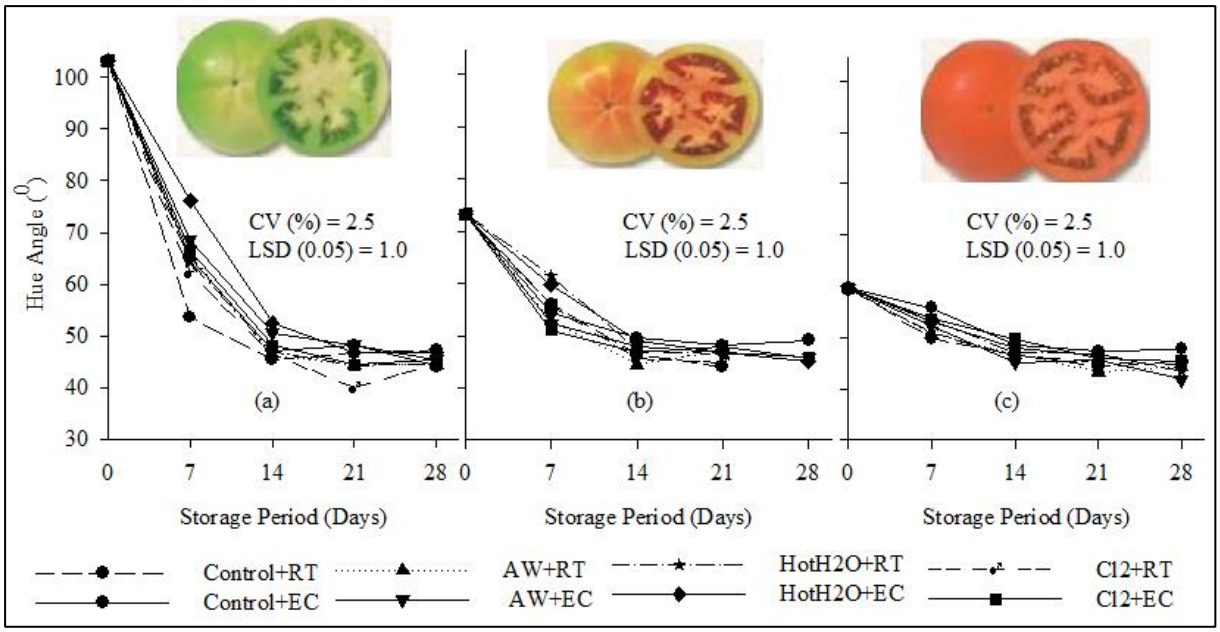

Figure 7.12 Changes in hue angle of tomatoes harvested at green (a), pink (b) and red (c) stage and subjected to pre-storage and storage environment treatments (n=5). Where RT is room temperature, EC is evaporative cooling, AW is anolyte water, HotH2O is hot water, and Cl2 is chlorinated water

7.3.1.8 Physiological weight loss

The cumulative physiological weight loss (PWL) of tomatoes harvested at the green, pink and red maturity stages and subjected to either an ambient or EC storage environment, is shown in Figure 7.13. The PWL of tomatoes harvested at the red maturity stage and subjected to an ambient storage environment was 12% over 15 days period, while that for tomatoes stored inside EC was 9.6% over a 29-day storage period. The PWL of tomatoes harvested at the pink maturity stage and subjected to ambient storage was found to be 10.7% over 15-day period, while the stored under the EC lost 7.2% weight during a 29-day storage period. Furthermore, the PWL of tomatoes harvested at the green maturity stage and subjected to ambient storage was 10.6% over a 20-day period, while inside EC it was 7% over a 29-day period. This implies that EC maintains the water content of the tomatoes by lowering the physiological respiration and removal of water from the fruit surface (Workneh *et al.*, 2003; Workneh *et al.*, 2011). Researchers report that about 10% of PWL is acceptable as a threshold for the quality of fresh produce (Acedo, 1997; Pal *et al.*, 1997). Islam *et al.* (2012) reported that tomatoes storage inside a zero energy evaporative cooling chamber resulted in only 2.6% PWL, compared to ambient storage (5.4%). The shelf-life of tomatoes stored inside EC had been extended by at least 14

days, when compared to tomatoes stored in an ambient storage environment, similar to that of Mogaji and Fapetu (2011). Moreover, the evaporative cooler can extend the shelf-life of carrots by three-week, compared to ambient storage (Babarinsa *et al.*, 1997). The result shows that storage under an EC environment over 30 days seems to be good enough to keep the PWL below the threshold level (10%).

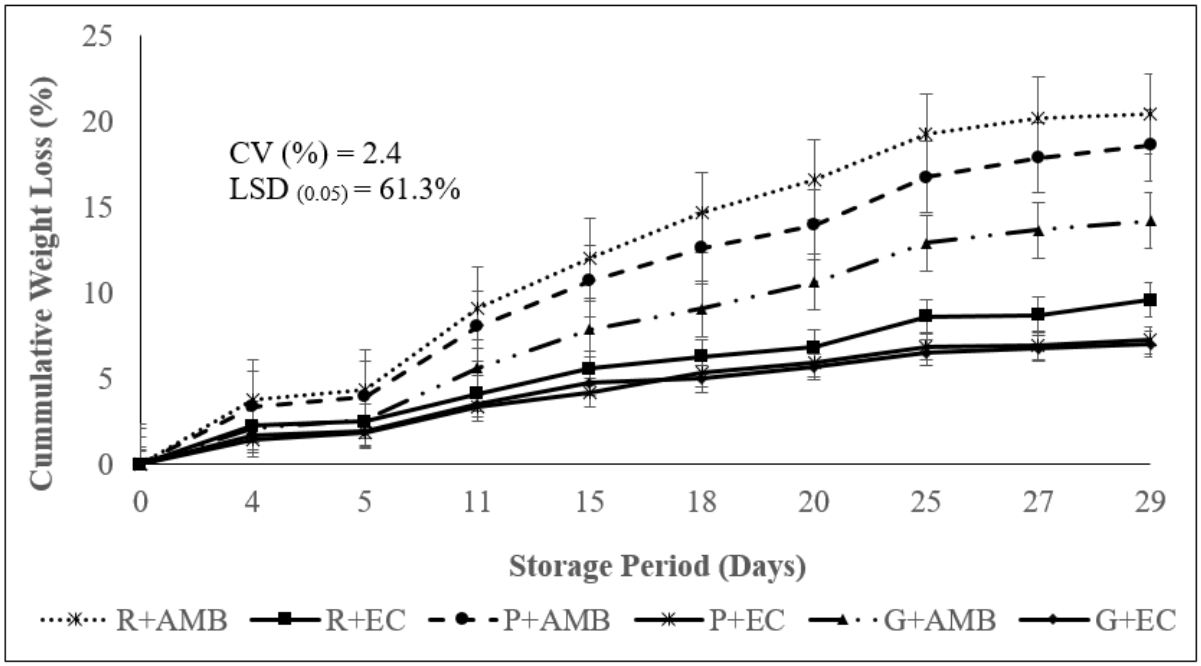

Figure 7.13 Change in cumulative percentage of physiological weight loss of three tomatoes maturity stages (Green (G), Pink (P) and Red (R)) at ambient temperature (AMB) of 21°C and evaporative cooler (EC)

7.3.1.9 Marketability

The percentage of marketable tomato fruits decreased during the storage period (Figure 7.14). The EC storage significantly ($p \leq 0.05$) improved the marketability of tomatoes harvested at all maturity stages (*i.e.* green, pink and red), in agreement to the report of Workneh *et al.* (2011). The control tomatoes dipped in hot water and stored in an ambient storage environment, showed a faster loss of marketability (80%) in the 14 days storage. However, tomato samples dipped in chlorinated water and stored under ambient conditions had a 40% loss in marketability. On the contrary, the control samples dipped in anolyte water displayed a small loss in marketability (10%) during the 14 days storage. Moreover, tomatoes dipped in anolyte and chlorinated water and stored in an EC environment had 80% marketability over the 21 days storage period. On

the contrary, the tomatoes treated with hot water and stored inside the EC were found to have 50% less marketability over the 14 days of storage.

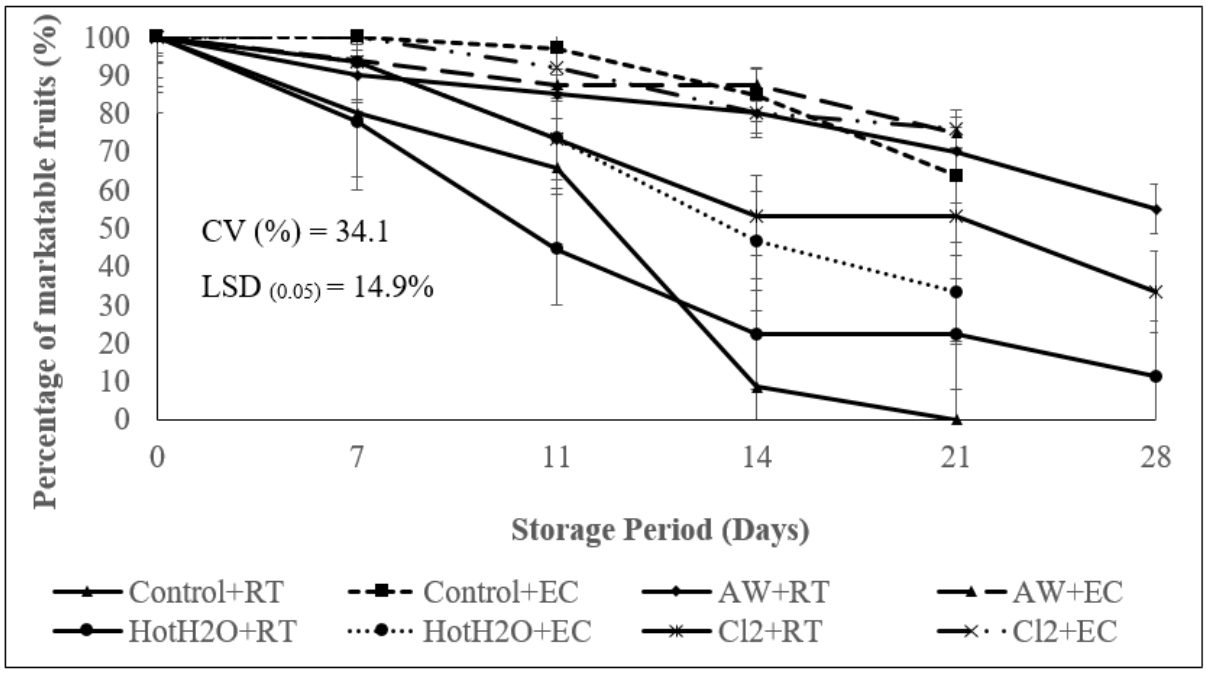

Figure 7.14 Change in cumulative percentage of marketability of tomatoes at room temperature of 20-23 °C and evaporative cooler (EC), where RT is room temperature, AW is anolyte water, HotH2O is hot water, and Cl2 is chlorinated water

7.4 Conclusions

This study shows that an evaporative cooler decreases the air temperature, while increasing the RH considerably. The midday to the late afternoon of the day is the hottest and, hence, reducing the temperature of the produce is highly important. The air temperature difference between the ambient and the EC environment ranged between 4 and 7ºC, while the RH increased by 55%. The reduced temperature can retard the physiological change and the RH increase can keep the tomatoes fresh. No uniform distribution of air temperature and RH found between the inlet and exit of EC. Integration between maturity stages, EC, pre-storage disinfection treatments significantly contribute to the maintenance of tomato quality. The pH value, TSS and TSS:TA of the tomatoes increased. But, the TA content showed a decline during the storage period of 14 days. All tomato samples experienced a decrease in firmness and hue angle over the storage period of 21 days. The EC storage maintained a higher firmness and hue angle, when compared to ambient condition. Tomatoes dipped in anolyte or chlorinated water and subjected to EC

storage maintained the percentage of marketability by two folds over a 21 days, when compared to tomatoes dipped in hot water and stored under similar conditions. Hence, the EC storage with pre-storage disinfection treatments improved the marketability of the fruit and, hence, extended the shelf-life of tomatoes. Moreover, the EC maintained the PWL 7 - 10% over the 30-day storage period, while the ambient storage was maintained at 10 - 12% for 15 days. Hence, integrated approaches of storage conditions and pre-storage disinfection treatments are important for extending the shelf-life and quality maintenance of fresh produce. However, further modelling studies of the micro-climate air dynamics might be of paramount important for the further modification of the design of the EC chamber, in order to attain further uniform air dynamics distribution.

7.5 Acknowledgments

The Federal Ministry of Education of Ethiopia is gratefully acknowledged for its research grant support. The South African National Research Fund (NRF-TWAS) is also greatly acknowledged for its scholarship grant (Reference No. SFH150902141138). The host institute, the University of KwaZulu-Natal, is warmly acknowledged for its support. Moreover, the ZZ2 and the tomato Postharvest Innovation Programme project is acknowledged for the provision of tomato samples.

Table 7.1 Changes in pH, total titratable acidity (TA) (%), total soluble solids (TSS) (%), TSS:TA ratio, of tomato fruits subjected to four treatments (anolyte water, chlorinated water, hot water and control), three maturity stages (green, pink and red) and two storage conditions [room temperature (RT) and evaporative cooling environment (EC)] and stored for 28-days of storage period

	pH content					Total titratable acidity (%)					Total soluble solid (%)					TSS:TA ratio				
Treatment	Day 1	Day 7	Day 14	Day 21	Day 28	Day 1	Day 7	Day 14	Day 21	Day 28	Day 1	Day 7	Day 14	Day 21	Day 28	Day 1	Day 7	Day 14	Day 21	Day 28
Evaporative cooler																				
G, Anolyte water	4.84^{uv}	4.85^{v}	4.57^{c}	5.24^{zq}	4.78^{qr}	0.50^{c}	0.42^{j}	0.33^{h}	0.33^{g}	0.27^{d}	3.88^{b}	5.24^{r}	4.00^{r}	4.00^{p}	3.42^{d}	7.68^{a}	12.38^{l}	12.01^{l}	12.01^{l}	12.85^{i}
G, Cl_2 water	4.84^{uv}	4.70^{m}	4.87^{vw}	5.05^{zk}	3.47^{a}	0.50^{c}	0.42j	0.30^{d}	0.30^{d}	0.29^{f}	3.98^{c}	3.44^{e}	3.66^{l}	3.660^{k}	3.30^{b}	7.88^{c}	8.23^{b}	12.11^{l}	12.11^{l}	11.63^{c}
G, Hot water	4.84^{uv}	5.58^{zt}	4.77^{op}	5.13^{zo}	4.89^{x}	0.50^{c}	0.41^{i}	0.30^{d}	0.30^{d}	0.32^{i}	3.98^{c}	4.12^{n}	3.64^{k}	3.64^{j}	3.96^{g}	7.88^{c}	10.12^{e}	11.98^{l}	11.98^{l}	12.47^{g}
G, Control	4.84^{uv}	5.87^{zv}	4.53^{b}	4.83^{u}	4.83^{u}	0.50^{c}	0.41^{i}	0.35^{j}	0.35^{j}	0.43^{m}	3.98^{c}	4.00^{m}	3.96^{r}	3.96^{p}	3.86^{g}	7.88^{c}	9.76^{d}	11.47^{i}	11.47^{i}	9.08^{a}
P, Anolyte	5.10^{zm}	5.09^{zm}	4.78^{qr}	5.87^{zv}	5.59^{zt}	0.43^{b}	0.39^{h}	0.33^{h}	0.33^{g}	0.35^{k}	3.70^{a}	3.30^{c}	3.42^{f}	3.42^{f}	4.44^{j}	8.74^{f}	8.54^{b}	10.27^{c}	10.27^{c}	15.24^{q}
P, Cl_2 water	5.10^{zm}	4.85^{v}	4.62^{e}	5.10^{zm}	4.68^{i}	0.44^{b}	0.38^{g}	0.32^{g}	0.32^{f}	0.27^{d}	3.72^{a}	4.48^{p}	3.74^{n}	3.74^{m}	3.35^{c}	8.54^{e}	11.75^{j}	11.87^{k}	11.87^{k}	13.66^{m}
P, Hot water	5.10^{zm}	5.02^{zi}	4.69^{ij}	5.07^{zk}	4.96^{ze}	0.44^{b}	0.35^{d}	0.29^{c}	0.29^{c}	0.28^{e}	3.72^{a}	3.76^{j}	4.00^{r}	4.00^{p}	3.92^{g}	8.54^{e}	10.81^{g}	13.83^{q}	13.83^{r}	14.20^{n}
P, Control	5.10^{zm}	5.53^{zt}	4.70^{m}	5.10^{zm}	-	0.44^{b}	0.39^{h}	0.34^{i}	0.34^{i}	-	3.72^{a}	4.26^{o}	3.44^{f}	3.44^{f}	-	8.54^{e}	10.90^{h}	10.13^{b}	10.13^{b}	-
R, Anolyte	5.05^{zk}	4.92^{yz}	4.84^{uv}	5.24^{zq}	4.73^{n}	0.38^{a}	0.37^{f}	0.34^{i}	0.34^{i}	0.29^{f}	3.92^{b}	3.74^{i}	3.56^{i}	3.56^{h}	3.50^{e}	10.27^{h}	10.09^{e}	10.53^{e}	10.53^{e}	12.11^{f}
R, Cl_2 water	5.05zk	4.77^{op}	4.69^{k}	5.10^{zm}	-	0.38^{a}	0.31^{b}	0.30^{d}	0.30^{d}	-	3.92^{b}	3.40^{d}	3.54^{h}	3.54^{h}	-	10.27^{h}	10.89^{h}	11.75^{j}	11.75^{j}	-
R, Hot water	5.05^{zk}	5.17^{zp}	4.86^{v}	5.26^{zq}	4.97^{zf}	0.38^{a}	0.25^{a}	0.27^{a}	0.27^{a}	0.30^{g}	3.92^{b}	3.78^{j}	3.70^{m}	3.70^{l}	3.96^{g}	10.27^{h}	12.83^{m}	13.92^{q}	13.92^{r}	11.86^{d}
R, Control	5.05^{zk}	5.12^{zn}	4.94^{za}	4.99^{zg}	4.88^{w}	0.38^{a}	0.36^{e}	0.32^{g}	0.32^{f}	0.36^{l}	3.92^{b}	3.48^{f}	3.50^{g}	3.50^{g}	3.92^{g}	10.27^{h}	9.78^{d}	11.04^{h}	11.04^{h}	9.06^{a}
Room temperature																				
G, Anolyte	4.85^{v}	4.83^{u}	4.83^{u}	5.00^{zh}	5.02^{zi}	0.50^{c}	0.33^{d}	0.31^{f}	0.31^{e}	0.31^{h}	3.88^{b}	4.02^{m}	3.20^{b}	3.20^{b}	4.14^{h}	7.74^{b}	12.33^{l}	10.21^{b}	10.21^{b}	13.19^{k}
G, Cl_2 water	4.84^{v}	4.74^{n}	4.66^{g}	5.01^{zi}	4.81^{s}	0.50^{c}	0.39^{h}	0.31^{f}	0.31^{e}	0.24^{a}	3.88^{b}	3.94^{l}	3.78^{o}	3.78^{n}	3.22^{a}	7.74^{b}	10.17^{f}	12.20^{m}	12.20^{m}	13.44^{l}
G, Hot water	4.85^{v}	5.24^{zq}	4.73^{n}	5.50^{zs}	4.89^{x}	0.50^{c}	0.43^{k}	0.31^{f}	0.31^{e}	0.26^{c}	3.88^{b}	3.48^{f}	3.36^{e}	3.36^{e}	3.42^{d}	7.74^{b}	8.12^{b}	10.93^{g}	10.93^{g}	13.35^{l}
G, Control	4.84^{v}	4.90^{xy}	4.58^{d}	4.94^{zb}	4.94^{zb}	0.50^{c}	0.39^{h}	0.30^{d}	0.30^{d}	0.31^{h}	3.98^{c}	3.40^{d}	3.82^{q}	3.82^{o}	3.92^{g}	7.94^{d}	8.63^{b}	12.66^{o}	12.66^{p}	12.71^{h}
P, Anolyte	5.04^{zj}	5.09^{zm}	4.78^{qr}	5.87^{zv}	-	0.43^{b}	0.39^{h}	0.33^{h}	0.33^{g}	-	3.70^{a}	3.30^{c}	3.42^{f}	3.42^{f}	-	8.74^{f}	8.54^{b}	10.27^{c}	10.27^{c}	-
P, Cl_2 water	5.04^{zj}	4.91^{y}	4.91^{y}	5.03^{zi}	-	0.43^{b}	0.34^{d}	0.32^{g}	0.32^{f}	-	3.70^{a}	3.58^{g}	3.32^{d}	3.32^{d}	-	8.74^{f}	10.38^{f}	10.45^{d}	10.45^{d}	-
P, Hot water	5.04^{zj}	4.67^{h}	4.79^{r}	5.32^{zr}	-	0.43^{b}	0.43^{k}	0.28^{b}	0.28^{b}	-	3.70^{a}	4.94^{q}	3.60^{j}	3.60^{i}	-	8.74^{f}	11.46^{i}	12.91^{p}	12.91^{q}	-
P, Control	5.04^{zj}	4.91^{y}	4.93^{z}	5.08^{zl}	-	0.43^{b}	0.41^{i}	0.30^{d}	0.30^{d}	-	3.70^{a}	3.86^{k}	3.26^{c}	3.26^{c}	-	8.74^{f}	9.36^{c}	10.77^{f}	10.77^{f}	-
R, Anolyte	5.00^{zh}	4.78^{qr}	4.85^{v}	6.10^{zw}	-	0.38^{a}	0.38^{g}	0.33^{h}	0.33^{g}	-	3.82^{b}	3.68^{h}	3.12^{a}	3.12^{a}	-	10.06^{g}	9.63^{d}	9.46^{a}	9.46^{a}	-
R, Cl_2 water	5.00^{zh}	5.27^{zq}	4.85^{v}	4.95^{zc}	-	0.38^{a}	0.31^{b}	0.28^{b}	0.28^{b}	-	3.82^{b}	3.10^{a}	3.50^{g}	3.50^{g}	-	10.06^{g}	10.05^{d}	12.31^{n}	12.31^{n}	-
R, Hot water	5.00^{zh}	4.85^{v}	4.71^{mn}	5.28^{zr}	-	0.38^{a}	0.32^{c}	0.28^{b}	0.28^{b}	-	3.82^{b}	3.08^{a}	3.48^{g}	3.48^{g}	-	10.06^{g}	9.72^{d}	12.66^{o}	12.66^{o}	-
R, Control	5.00^{zh}	4.76^{o}	4.85^{v}	5.08^{zl}	4.81^{s}	0.38^{a}	0.32^{c}	0.29^{c}	0.29^{c}	0.29^{f}	3.82^{b}	3.86^{k}	3.20^{b}	3.20^{b}	4.66^{k}	10.06^{g}	12.05^{k}	10.97^{g}	10.97^{g}	13.43^{l}
Significant level (P)																				
Storages (A)	<0.05					<0.001					<0.001					<0.001				
Maturity (B)	<0.001					<0.001					<0.001					<0.001				
Disinfection (C)	<0.001					<0.001					<0.001					<0.001				

Treatment	pH content					Total titratable acidity (%)					Total soluble solid (%)					TSS:TA ratio				
	Day 1	Day 7	Day 14	Day 21	Day 28	Day 1	Day 7	Day 14	Day 21	Day 28	Day 1	Day 7	Day 14	Day 21	Day 28	Day 1	Day 7	Day 14	Day 21	Day 28
Storage period (D)	<0.001					<0.001					<0.001					<0.001				
A x B	<0.001					<0.001					<0.001					<0.05				
A x C	<0.001					<0.001					<0.001					<0.001				
A x D	<0.001					<0.001					<0.001					<0.001				
B x C	<0.001					<0.001					<0.001					<0.001				
B x D	<0.001					<0.001					<0.001					<0.001				
C x D	<0.001					<0.001					<0.001					<0.001				
A x B x C	<0.001					<0.001					<0.001					<0.001				
A x B x D	<0.001					<0.001					<0.001					<0.001				
A x C x D	<0.001					<0.001					<0.001					<0.001				
B x C x D	<0.001					<0.001					<0.001					<0.001				
A x B x C x D	<0.001					<0.001					<0.001					<0.001				
	$LSD_{0.05}$ = 0.0907, CV (%) = 1.5, SE=0.0730					$LSD_{0.05}$ = 0.018, CV (%) = 4.3, SE = 0.0146					$LSD_{0.05}$ = 0.168, CV (%) = 3.6, SE = 0.135					$LSD_{0.05}$ = 0.8842, CV (%)=6.0, SE=0.712				

The means separation was carried out by the Duncan's multiple range test ($p<0.05$) and the column means with similar superscripted letter(s) are not significantly different. TSS:TA, total titratable acidity to total soluble solid ration; A, storage environments; B, maturity stages; C disinfection treatments; D, storage period; G, green mature tomatoes; P, pink tomatoes and R, red tomatoes.

7.6 References

Acedo, ALJ. 1997. Storage life of vegetables in simple evaporative coolers. *Tropical Science* 37**,** 169-175.

Ambaw, A, Delele, MA, Defraeye, T, Ho, QT, Opara, LU, Nicolai, BM and Verboven, P. 2013. The use of CFD to characterize and design post-harvest storage facilities: Past, present and future. *Computers and Electronics in Agriculture,* 93**,** 184-194.

Anthon, GE and Barrett, DM. 2012. Pectin methylesterase activity and other factors affecting pH and titratable acidity in processing tomatoes. *Food Chemistry,* 132**,** 915-920.

Anyanwu, EE. 2004. Design and measured performance of a porous evaporative cooler for preservation of fruits and vegetables. *Energy Conversion and Management,* 45**,** 2187-2195.

AOAC. 1995. *Official Methods of Analysis: Association of Official Analytical Chemists.* AOAC, Virginia, USA.

Awole, S, Woldetsadik, K and Workneh, TS. 2011. Yield and storability of green fruits from hot pepper cultivars (Capsicum spp.). *African Journal of Biotechnology,* 10**,** 12662-12670.

Babarinsa, FA, Williams, JO and Osanu, FC. 1997. Storage of carrots in a brick wall cooler under semi-arid conditions. *Tropical Science,* 37**,** 21-27.

Barrett, DM, Beaulieu, JC and Shewfelt, R. 2010. Color, flavor, texture, and nutritional quality of fresh-cut fruits and vegetables: desirable levels, instrumental and sensory measurement, and the effects of processing. *Critical Reviews in Food Science and Nutrition,* 50**,** 369-389.

Basediya, A, Samuel, DVK and Beera, V. 2013. Evaporative cooling system for storage of fruits and vegetables-a review. *Journal of Food Science and Technology,* 50**,** 429-442.

Batu, A. 2004. Determination of acceptable firmness and colour values of tomatoes. *Journal of Food Engineering,* 61**,** 471-475.

Beckles, DM. 2012. Factors affecting the postharvest soluble solids and sugar content of tomato (Solanum lycopersicum L.) fruit. *Postharvest Biology and Technology,* 63**,** 129-140.

Bertin, N, Guichard, S, Leonardi, C, Longuenesse, JJ, Langlois, D and Navez, B. 2000. Seasonal evolution of the quality of fresh glasshouse tomatoes under Mediterranean conditions, as affected by air vapour pressure deficit and plant fruit load. *Annals of Botany,* 85**,** 741-750.

Bhattarai, DR and Gautam, DM. 2006. Effect of harvesting method and calcium on post harvest physiology of tomato. *Nepal Agriculture Research Journal,* 7**,** 37-41.

Camelo, AFL and Gómez, PA. 2004. Comparison of color indexes for tomato ripening. *Horticultura Brasileira,* 22**,** 534-537.

Chinenye, NM, Manuwa, SI, Olukunle, OJ and Oluwalana, IB. 2013. Development of an active evaporative cooling system for short-term storage of fruits and vegetable in a tropical climate. *Agricultural Engineering International: CIGR Journal,* 15**,** 307-313.

Dvizama, AU. 2000. *Performance evaluation of an active cooling system for the storage of fruits and vegetables.* PhD, University of Ibadan, Nigeria.

Fallik, E, Grinberg, S, Alkalai, S and Lurie, S. 1996. The effectiveness of postharvest hot water dipping on the control of grey and black moulds in sweet red pepper (Capsicum annuum). *Plant Pathology,* 45**,** 644-649.

Gautier, H, Diakou-Verdin, V, Bénard, C, Reich, M, Buret, M, Bourgaud, F, Poëssel, JL, Caris-Veyrat, C and Génard, M. 2008. How does tomato quality (sugar, acid, and nutritional quality) vary with ripening stage, temperature, and irradiance? *Journal of Agricultural and Food Chemistry,* 56**,** 1241-1250.

Gautier, H, Rocci, A, Buret, M, Grasselly, D and Causse, M. 2005. Fruit load or fruit position alters response to temperature and subsequently cherry tomato quality. *Journal of the Science of Food and Agriculture,* 85**,** 1009-1016.

George, B, Kaur, C, Khurdiya, DS and Kapoor, HC. 2004. Antioxidants in tomato (Lycopersium esculentum) as a function of genotype. *Food Chemistry,* 84**,** 45-51.

Getinet, H, Seyoum, T and Woldetsadik, K. 2008. The effect of cultivar, maturity stage and storage environment on quality of tomatoes. *Journal of Food Engineering,* 87**,** 467-478.

Getinet, H, Workneh, TS and Woldetsadik, K. 2011. Effect of maturity stages, variety and storage environment on sugar content of tomato stored in multiple pads evaporative cooler. *African Journal of Biotechnology,* 10**,** 18481-18492.

Gould, WA. 1992. *Tomato production, processing and technology.* CTI Publications, Inc, USA.

Islam, MP, Morimoto, T and Hatou, K. 2012. Storage behavior of tomato inside a zero energy cool chamber. *Agricultural Engineering International: CIGR Journal,* 14**,** 209-217.

Itoh, K. 2003. Combined effects of hot water treatment (HWT) and modified atmosphere packaging (MAP) on quality of tomatoes. *Packaging Technology and Science,* 16**,** 171-178.

Kader, A, Stevens, M, Albright, M and Morris, L. 1978. Amino acid composition and flavor of fresh market tomatoes as influenced by fruit ripeness when harvested. *Journal of American Society for Horticultural Sciience,* 103**,** 541-544.

Kader, AA. 1985. Postharvest biology and technology: an overview. *In:* Kader, AA, Kasmire, RF, Mitchell, FG, Reid, MS, Sommer, NF and Thompson, JF, eds. Postharvest Technology of Horticultural Crops, 3-8. University of California, Division of agricultural and nutritional resource, CA, USA.

Kader, AA. 1986. Effects of postharvest handling procedures on tomato quality. *In:* El-Beltagy, AS and Persson, AR, eds. Acta Horticulture, 209-222. International Society for Horticultural Science (ISHS), Cairo, Egypt.

Kader, AA, Stevens, MA, Albright-Holton, M, Morris, LL and Algazi, M. 1977. Effect of fruit ripeness when picked on flavor and composition in fresh market tomatoes. *Journal of the American Society for Horticultural Science,* 102**,** 724-731.

Kitinoja, L. 2013. *Use of cold chains for reducing food losses in developing countries.* The Postharvest Education Foundation, University of California, La Pine, Oregon, USA.

Lana, MM, Tijskens, LMM and Van Kooten, O. 2005. Effects of storage temperature and fruit ripening on firmness of fresh cut tomatoes. *Postharvest Biology and Technology,* 35**,** 87-95.

Liberty, JT, Ugwuishiwua, BO, Pukumab, SA and Odo, CE. 2013. Principles and Application of Evaporative Cooling Systems for Fruits and Vegetables Preservation. *International Journal of Current Engineering and Technology,* 3**,** 1000-1006.

Luna-Guevara, ML, Jiménez-González, Ó, Luna-Guevara, JJ, Hernández-Carranza, P and Ochoa-Velasco, CE. 2014. Quality parameters and bioactive compounds of red tomatoes (Solanum lycopersicum L.) cv Roma VF at different postharvest conditions. *Journal of Food Research,* 3**,** 8-18.

Majidi, H, Minaei, S, Almasi, M and Mostofi, Y. 2011. Total soluble solids, titratable acidity and repining index of tomato in various storage conditions. *Australian Journal of Basic and Applied Sciences,* 5**,** 1723-1726.

Messina, V, Domínguez, PG, Sancho, AM, Walsöe, DRN, Carrari, F and Grigioni, G. 2012. Tomato quality during short-term storage assessed by colour and electronic nose. *International Journal of Electrochemistry,* 2012**,** 1-7.

Mogaji, TS and Fapetu, O. 2011. Development of an evaporative cooling system for the preservation of fresh vegetables. *African Journal of Food Science,* 5**,** 255-266.

Mohammed, M, Wilson, LA and Gomes, PI. 1999. Postharvest sensory and physiochemical attributes of processing and nonprocessing tomato cultivars. *Journal of Food Quality,* 22**,** 167-182.

Moneruzzaman, KM, Hossain, ABMS, Sani, W and Saifuddin, M. 2008. Effect of stages of maturity and ripening conditions on the biochemical characteristics of tomato. *American Journal of Biochemistry and Biotechnology,* 4**,** 329-335.

Niño-Medina, G, Rivera-Castro, JC, Vidales-Contreras, JA, Rodriguez-Fuentes, H and Luna-Maldonado, AI. 2013. Physicochemical Parameters for Obtaining Prediction Models in the Postharvest Quality of Tomatoes (Solanum Lycopersicum L.). *Transactions on Machine Learning and Data Mining,* 6**,** 81-91.

Pal, RK, Roy, SK and Srivastava, S. 1997. Storage performance of kinnow mandarins in evaporative cool chamber and ambient condition. *Journal of food science and technology,* 34**,** 200-203.

Paulson, KN and Stevens, MA. 1974. Relationships among titratable acidity, pH and buffer composition of tomato fruits. *Journal of Food Science,* 39**,** 354-357.

Pila, N, Gol, NB and Rao, TVR. 2010. Effect of post harvest treatments on physicochemical characteristics and shelf life of tomato (Lycopersicon esculentum Mill.) fruits during storage. *American-Eurasian J Agric Environ Sci,* 9**,** 470-479.

Pinheiro, J, Alegria, C, Abreu, M, Gonçalves, EM and Silva, CLM. 2013. Kinetics of changes in the physical quality parameters of fresh tomato fruits (Solanum lycopersicum, cv. 'Zinac') during storage. *Journal of Food Engineering,* 114**,** 338-345.

Porat, R, Daus, A, Weiss, B, Cohen, L, Fallik, E and Droby, S. 2000. Reduction of postharvest decay in organic citrus fruit by a short hot water brushing treatment. *Postharvest Biology and Technology,* 18**,** 151-157.

Radzevičius, A, Karkleliene, R, Viškelis, P, Bobinas, C, Bobinaite, R, Sakalauskiene, S and Metspalu, L. 2009. Tomato (Lycopersicon esculentum Mill.) fruit quality and physiological parameters at different ripening stages of Lithuanian cultivars. *Agronomy research,* 7**,** 712-718.

Roy, SK and Khardi, DS. 1985. Zero Energy Cool Chamber. *India Agricultural Research Institute: New Delhi, India. ,* Research Bulletin No.43: 23-30.

Roy, SK and Pal, RK. 1994. A low-cost cool chamber: an innovative technology for developing countries. *In:* Champ, BR, Highley, E and Johnson, GI, eds. Postharvest Handling of Tropical Fruits: ACIAR Proceedings, 393-395. Australian Centre for International Agricultural Research, Australia.

Saran, S, Roy, SK and Kitinoja, L. 2010. Appropriate postharvest technologies for small scale horticultural farmers and marketers in Sub-Saharan Africa and South Asia-Part 2. Field trial results and identification of research needs for selected crops. *In:* Cantwell, MI and Almeida, DPF, eds. XXVIII International Horticultural Congress on Science and Horticulture for People (IHC2010): International Symposium 41-52. Acta Horticulture, Lisbon, Portugal.

Sellers, DA. 2004. Evaporative Cooling: Design Considerations. *HPAC Engineering,* 76**,** 10-19.

Tassou, SA, Lewis, JS, Ge, YT, Hadawey, A and Chaer, I. 2010. A review of emerging technologies for food refrigeration applications. *Applied Thermal Engineering,* 30**,** 263-276.

Tefera, A, Seyoum, T and Woldetsadik, K. 2007. Effect of disinfection, packaging, and storage environment on the shelf life of mango. *Biosystems Engineering,* 96**,** 201-212.

Thompson, JF. 2016. Pre-cooling and storage facilities. *The Commercial Storage of Fruits, Vegetables, and Florist and Nursery Stocks: Agriculture handbook, No. 66.* Cha. 2, 11-18. USDA, ARS, Beltsville, USA.

Thompson, JF, Mitchell, FG and Kasmire, RF. 2002. Cooling horticultural commodities. *In:* Kader, AA (ed.) *Postharvest technology of horticultural crops.* 3rd ed, Cha. 11, 97- 112. Agriculture and Natural Resources, University of California, USA.

Thompson, K. 2003. *Fruit and vegetables: harvesting, handling and storage.* Blackwell Publishing LTD, UK.

Van Dijk, C, Boeriu, C, Stolle-Smits, T and Tijskens, LMM. 2006. The firmness of stored tomatoes (cv. Tradiro). 1. Kinetic and near infrared models to describe firmness and moisture loss. *J. Food Eng,* 77**,** 575-584.

Viskelis, P, Jankauskiene, J and Bobinaite, R. 2008. Content of carotenoids and physical properties of tomatoes harvested at different ripening stages. *In:* Ciprovica, I, Karklina, D, Venskutonis, PR, Vokk, R, Verhe, R, Lucke, FK, Kuka, P, Rukshan, L and Shleikin, A, eds. Foodbalt, 3rd Baltic Conference on Food Science and Technology, 166-170. Jelgava, Latvia.

Watada, AE, Ko, NP and Minott, DA. 1996. Factors affecting quality of fresh-cut horticultural products. *Postharvest Biology and Technology,* 9**,** 115-125.

Workneh, TS. 2010. Feasibility and economic evaluation of low-cost evaporative cooling system in fruit and vegetables storage. *African Journal of Food, Agriculture, Nutrition and Development,* 10**,** 2984-2997.

Workneh, TS, Osthoff, G, Pretorius, J and Hugo, C. 2003. Comparison of anolyte and chlorinated water as a disinfecting dipping treatment for stored carrots. *Journal of food quality,* 26**,** 463-474.

Workneh, TS, Osthoff, G and Steyn, M. 2012. Effects of preharvest treatment, disinfections, packaging and storage environment on quality of tomato. *Journal of food science and technology,* 49**,** 685-694.

Workneh, TS, Osthoff, G and Steyn, MS. 2011. Influence of preharvest and postharvest treatments on stored tomato quality. *African Journal of Agricultural Research,* 6**,** 2725-2736.

Xuan, YM, Xiao, F, Niu, XF, Huang, X and Wang, SW. 2012. Research and application of evaporative cooling in China: A review (I) - Research. *Renewable & Sustainable Energy Reviews,* 16**,** 3535-3546.

8. MODELS FOR EVALUATION OF THE QUALITY OF TOMATO FRUIT AS AFFECTED BY THE LOW-COST COOLING TECHNOLOGIES

8.1 Logistic Regression Analysis of Marketability of Tomato Fruit Harvested at Different Maturity Stages and Subjected to Disinfection, Storage Condition and Storage Period Treatments

Abstract

This study was conducted to apply the logistic regression analysis to study the combined effects of continuous and categorical variables on the probability of marketability of tomato. Tomato fruits harvested at three maturity stages (green, pink, red) after pre-storage disinfections treatments (control, anolyte water, hot water, chlorinated water) were stored under evaporative cooler and ambient conditions for 28 days. Changes in the quality characteristics of the tomatoes were assessed every 7 days. Significant relationships were observed (p<0.001) between the variables and probability of marketability of tomato. Nevertheless, some of the variables were not significant (p>0.05) for the multiple logistic regression models. Combination of chlorinated water (Tr4), anolyte water (Tr2), green tomato (MS1) and evaporative cooler (SC2) showed high odds ratios. For instance, the odds of marketability of tomato for Tr4 was 27.501 times that of control (Tr1), for Tr2 it was 17.971 times that of Tr1, for MS1 it was 15.792 times that of red tomato (MS3) and for SC2 it was 3.271 times that of ambient storage over 28-day. This showed that Tr4 and Tr2 extended the marketability over a longer period, when compared to that of Tr1. The probability of marketability of tomatoes was higher for tomatoes stored in the evaporative cooling environment. The model developed can be applied by farmer and processor just by measuring any of the convenient physical/chemical parameters (pH, TA, TSS, colour, texture) and apply the models developed to predict the marketability level for different storage periods.

Keywords: Disinfection treatments; evaporative cooler; logistic regression modeling; probability of marketability; storage period; tomato quality indices

8.1.1 Introduction

Tomato (*Lycopersicon esculentum* Mill. cv Nemonetta) is one of the most important vegetable crops, globally (Sibomana *et al.*, 2017). The physiological, physical and biochemical changes of tomato fruit continue during postharvest and even at cold storage (Laguerre *et al.*, 2013). Sloof *et al.* (1996) reported that consumers and producers are considering fresh produce quality as one of the most important market factors. The most important quality characteristics that influence consumer acceptance and market success were reported to be firmness, colour, pH, total titratable acidity (TA), total soluble solids (TSS), TSS : TA ratio and physiological weight loss (Kader, 1984; Batu, 2004; Barrett *et al.*, 2010; Beckles, 2012; Pinheiro *et al.*, 2013). These indices are highly dependent on tomato variety, size, storage conditions, maturity stage and postharvest treatments (Beckles, 2012).

Evaporative cooling of fresh fruits was reported to have a lower cost in terms of installation and requires low energy for the preservation of fruit and vegetables. This cooling technology was found to be affordable for small and medium scale farmers operating in arid and semi-arid regions (Saran *et al.*, 2010; Workneh, 2010; Xuan *et al.*, 2012; Kitinoja, 2013). Unlike the optimally controlled micro-climate (*i.e.* mechanical refrigeration), the effectiveness of evaporative cooling is highly dependent on the atmospheric air conditions (*i.e.* temperature and relative humidity (RH) fluctuations) (Thompson, 2016). However, several researchers recommended the integration of postharvest treatments with the evaporative cooling storage for optimum performance in terms of shelf-life extension and preservation of the quality of fresh produce (Fallik *et al.*, 1996; Porat *et al.*, 2000; Workneh *et al.*, 2003; Workneh, 2010; Workneh *et al.*, 2012). Some pre-storage treatments, including anolyte water and chlorinated water disinfection (Workneh *et al.*, 2003), as well as dipping in hot water, can be applied to fruit and vegetables as a pre-storage disinfection treatment for shelf-life extension of the fresh produce in evaporatively cold stores (Fallik *et al.*, 1996). Although the effectiveness of this low-cost cooling technology for shelf life extension of fresh produces have been well established, the modeling aspects of quality changes require study.

There are no studies on the development of models that can be used to predict the probability of marketability of fresh produces stored under evaporatively cooled conditions by measuring quality parameters that require less complex techniques and instrumentation. The conventional laboratory analyses of fresh produce need sophisticated experimental equipment, requires high

technical knowledge to interpret the outcome and are also time-consuming (Melesse *et al.*, 2016). In addition, the empirical quality indices are subjected to analysis of variance for interpretation for quality evaluation on an individual basis (Melesse *et al.*, 2016). Hence, a simple approach to determine the probability of marketability of fresh produce could have paramount importance in the supply chain of fresh produce and a model to predict the probability of marketability of fresh produce could have practical application for fruit and vegetable producers and processors (Melesse *et al.*, 2016). Consequently, recently several approaches such as principal component analysis, discriminant analysis, log-linear analysis, logistic analysis have been used to develop models that predict the quality of fresh produce (Melesse *et al.*, 2016). Logistic regression modeling is advantageous since it accommodates both categorical and continuous fresh produce quality variables (Melesse *et al.*, 2016).

Therefore, the model developed can replace the laboratory work and make it easy to detect quality subjectively in terms of marketability. A previous study (Melesse *et al.*, 2016). reported modelling of changes in quality of tomatoes subjected to storage treatment in mechanical refrigerated store. In the study reported here, the effects of postharvest disinfection treatments such as low-cost evaporative cooling (technologies suitable for small-scale or newly established farmers) on the changes in the firmness, hue-angle and maturity stages of sample tomato fruit were considered. Low-cost and environmentally friendly evaporative cooling technology was proven to be effective in extending the shelf-life of several fruit and vegetables (Workneh *et al.*, 2003; Workneh, 2010; Workneh *et al.*, 2012).

However, no models have been developed for fruit and vegetables, including tomato, based on quality data obtained during evaporatively cooled storage. Moreover, no model has been developed to understand the effects of anolyte water treatment (which is environmentally friendly) and/or hot water treatment with evaporative cooling for fruit and vegetables including tomato quality data, which can be preferred for safety and for their environmentally friendly features. Hence, the model to be developed can help to understand the combined effect of anolyte or hot water with evaporative cooling. Moreover, no multiple parameter data have been used to develop a model for fresh agricultural produce that has been subjected to a combination of harvesting stage, pre-storage disinfection treatments and storage under the evaporative cooling conditions.

Under varying micro-climatic conditions of an evaporative cooler, where temperature and relative humidity is dependent on atmospheric climate conditions, it is crucial to predict the quality of fresh produce using empirical equations. Accordingly, the logistic model can be applied to determine the probability of marketability of tomato fruit as a shelf life indicator based on pH, TA, TSS, TSS:TA ratio, firmness, and skin color. Therefore, the aim of this study was to develop the logistic model, screen and apply the best fit for the prediction of the probability of marketability of tomatoes stored under evaporatively cooled storage micro-climate conditions.

8.1.1.1 The fundamentals of logistic regression

Logistic regression is one of the statistical modeling techniques applied to study the relationship between the probability of an event with a binary outcome and a set of explanatory variables (Lammertyn *et al.*, 2000; Melesse *et al.*, 2016). Likewise, the event marketable or non-marketable can be modeled as a function of independent (predictor) variables (Hosmer *et al.*, 2013; Melesse *et al.*, 2016). Hence, the logistic regression model was designed to designate a probability (0 to 1) of marketable (1) or non-marketable (0) tomato fruit (Melesse *et al.*, 2016). This study described the probability of the tomato fruit sample to be marketable or non-marketable. For one predictor *X*, for example, tomato firmness and a binomial outcome variable *Y*, the marketability of the fruit, the model predicts the logit of the probability of the outcome variable (*Y*) from predictor variable *X*. The simplest form of the logistic model with only one predictor variable is indicated in Equation 8.1 (Melesse *et al.*, 2016).

$$logit\big(\pi(x)\big) = \ln\left(\frac{\pi(x)}{1-\pi(x)}\right) = \ln(odds) = \alpha + \beta x \tag{8.1}$$

The alternative form of this simplest logistic model is as follows (Equation 8.2):

$$\pi(x) = P\ (Y\ is\ probability\ of\ marketablity, given\ that, X = x) = \frac{e^{\alpha+\beta x}}{1+e^{\alpha+\beta x}} \tag{8.2}$$

Where:

$\pi(x)$ = the chance of the tomato to be marketable,

X = the firmness replaced the x amount that either continuous or categorical variable,

α = the intercept parameter, and

β = the slope coefficient.

The model indicated in Equation 8.1 shows that the log odds of marketability is a linear function of the predictor. This simple linear model can be extended to the model with multiple independent variables (Melesse *et al.*, 2016). This approach relates the single dichotomous outcome to multiple independent variables in a multiple logistic regression as indicated in Equations 8.3 and 8.4.

$$lgit\big(\pi(X)\big) = \ln\left(\frac{\pi(X)}{1-\pi(X)}\right) = \alpha + \sum_{i=1}^{k}\beta_i x_i \tag{8.3}$$

$$\pi(x) = \frac{e^{(\alpha+\sum_{i=1}^{k}\beta_i x_i)}}{1+e^{(\alpha+\sum_{i=1}^{k}\beta_i x_i)}} \tag{8.4}$$

Where*:*

$\pi(x)$ = probability of tomato to be marketable,

α = the intercept,

β_i = the slope parameters, and

x_i = the independent or explanatory variables for the model.

Logistic regression is aimed at estimating the unknown parameters of the model expressed in Equation 8.3 (Melesse *et al.*, 2016). Therefore, the maximum likelihood (ML) approach was applied to achieve the estimations of model parameters. The maximum likelihood estimation (MLE) approach is a method of estimating parameters of the model by finding the value the parameter that maximises the likelihood function (SAS Institute Inc., 2015; IBM SPSS Cor, 2016). The ML computation is a complex analysis, but the statistical packages made it simple (Agresti, 1996).

8.1.2 Materials and methods

8.1.2.1 Sample tomato production and preparation

Three maturity stages of tomato samples (green (MS1), pink (MS2) and red (MS3)), produced by ZZ2 farm, Limpopo, South Africa, were used for the study. The samples of tomatoes had been produced using Natuurboerdery® (nature farming) protocols, which are protocols for farming without causing damage to environment and human health (Taurayi, 2011). This farming system is neither organic nor conventional farming, and uses both organic and inorganic inputs that are compatible for sustainable faming of tomato in Limpopo Region, South

Africa. Inorganic fertilisers and organic soil sediments were used as plant nutrition and for the maintenance of soil health during the production of tomato. Fermented plant extracts and compost teas were used as plant nutrition while biological control agents were used as plant protection during the production (Taurayi, 2011). The tomato samples were stored at ambient storage environment (SC1) and inside an experimental scale multi-pad evaporative cooler (EC) (SC2). The EC was with one indirect heat exchanger and three direct pads were established at the Ukulinga Research Station of the University of KwaZulu-Natal, South Africa (24°24′E, 30°24′S). The dimensions of the EC were 6 m length, 4 m width and 2.4 m height. The wall thickness was 60 mm of which 1 mm is plain carbon steel (mild steel) and laminated to both inner and outer wall side with 58 mm thick polyurethane foam insulation in between. An axial fan (OW354) with the blade size of 340 mm (H) x 340 mm (W) x 260 mm (Φ), the power rating of 0.12kw, and Gril code of OW395 was used to drive air into EC storage chamber (Figure 3.1).

8.1.2.2 Experimental design

The factorial experimental design was employed with four factors including three tomato maturity stages (green, pink and red), four disinfection pre-storage treatments (control, anolyte water, hot water and chlorinated water), two storage conditions (ambient and evaporative cooler) and five storage periods, with five replications. Five fruits per sample were used for the experiment in a randomized complete block design for each sampling.

8.1.2.3 Data collection

Disinfection pre-storage treatments

Different pre-storage disinfection treatments, including control with no treatment (Tr1), anolyte water (Tr2), hot water (Tr3) and chlorinated (Tr4) water were applied to the sample. Sample tomatoes were dipped into an anolyte water (AW) for five min (Workneh *et al.*, 2003; Workneh *et al.*, 2012; Kassim *et al.*, 2017; Sibomana *et al.*, 2017) and air-dried, before being stored. The hot water treatment was done by dipping the sample into hot water at 42.5°C for 30 min (Itoh, 2003; Kassim *et al.*, 2017). Chlorine disinfection was done by dipping samples into a solution containing 100 µg. mL^{-1} total chlorine (Cl_2) for 20 min, which was prepared by dissolving sodium hypochlorite (5% NaOCl) in tap water (Workneh *et al.*, 2011). The control samples were dipped into cold water for 20 min. Five tomato fruits were randomly picked for quality

analysis at every 7 day for the 28-day storage period. The measurements were replicated five times.

pH value

Five tomato samples from each maturity stage were taken and blended into a homogeneous pulp. This was then filtered, using Whatman filter paper No. 1, and 25 mL of the filtrate was then used to measure pH values with a pH meter (Orion Star, Model 210, Thermo Scientific Pty, Wilmington, USA), according to the procedure described in AOAC AOAC (1995).

Titratable acidity

A 25 mL filtrate of the pulped tomato was taken for total titratable acidity (TA) determination and was titrated with 0.1N NaOH, using a phenolphthalein indicator (see Equation 7.1).

Total soluble solids

The total soluble solid (TSS) content was measured a digital handheld refractometer (Pocket Refractometer, PAL-3, Japan). The tomato sample was pulped and filtered through Whatman filter paper No.1. The filtrate was used for the analysis (AOAC, 1995).

Total soluble solids to total titratable acidity ratio

The TSS to TA ratio of tomato slurry was determined using Equation 7.2 (Moneruzzaman *et al.*, 2008).

Firmness

The fruit firmness (N) was determined by using the Intron Universal Testing Machine (Model No. 3345, assembled in USA) with a 7.5 mm penetration depth, a 3.00 $mm.s^{-1}$ speed, a 50 N maximum force and a 2 mm diameter probe as described by Pinheiro *et al.* (2013). Five fruits from each category of tomatoes, subjected to different treatments, were used for the analysis.

Colour

Tomato skin colour was measured along the diameter *b* as indicated in Sharifi *et al.* (2007) and Kassim *et al.* (2017), using the digital Minolta Chromatic 400 method of the CIELAB colour space, according to procedures by Batu (2004). The instrument was calibrated against a white standard tile before each color reading. The hue (h^o) value was measured and recorded.

Percentage marketability

The marketability of the tomatoes was assessed subjectively, according to Mohammed *et al.* (1999). The visible shriveling, smoothness, mold growth and shininess of the tomatoes were considered. The number of marketable fruits was counted and the percentage was calculated with respect to the initial sample number every 7 day over the 28-day period (Equation 7.3).

8.1.2.4 Data analysis

SPSS Version 24 and SAS Version 9.4 were used for the logistic regression analysis and model validation parameter generation (SAS Institute Inc., 2015; IBM SPSS Cor, 2016). The fresh tomatoes stored in a multi-pad evaporative cooler (EC) and ambient storage environment for a 28 day period and the data generated every 7 day (at 0, 7, 14, 21 and 28 days) from the laboratory assessments were analysed statistically.

8.1.3 Results and discussion

8.1.3.1 Marketability probability of tomato fruit depending on categorical variable

Different predictor variables (maturity stages, treatments, storage conditions, days of storages, pH, TA, TSS, TSS:TA ratio, firmness and hue angle) were used separately to fit the simple logistic regression model (Table 8.1). The detailed analysis was given for firmness of tomato fruit stored for a 28-day period. The firmness was found to be a significant ($p \leq 0.001$) predictor by the model with the odds ratio of 1.276. This indicated that firmness had a strong influence on the probability of tomato marketability. The probability of marketability was judged as the global tomato quality changes that were affected by the maturity stage, storage environments, pre-storage disinfection treatments and storage period to which the fruit was exposed at the

postharvest stage. The fitted simple logistic model between the probability of marketability and firmness of tomato indicated that there was a positive relationship. The positive relationship between firmness and the probability of marketability of tomato fruit was observed (Equation 8.5).

$$\pi(x) = \frac{Exp^{-2.243+0.244x}}{1+Exp^{-2.243+0.244x}} \quad (8.5)$$

Where*:*

$\pi(x)$ = probability of tomato marketability when x is a particular firmness value.

At a particular value of firmness, the probability of tomato marketability can be predicted (Figure 8.1). For example, when the firmness of the tomato sample was 25.5 N, the probability of marketability was 0.9817. But, when the firmness decreased to 10.5 N, the probability of the marketability of tomatoes reduced to 0.5785. The probability of marketability was increased as the firmness of tomato increased. The less mature tomatoes demonstrated the higher probability of marketability. The probability increased from 0.5 to 0.9 for the firmness range between 10 to 25 N. The odds ratio (Exp (β)) of 1.276 the tomato firmness showed that for a 1 N increase of firmness, the odds of marketability increases by (1.276-1) x 100 = 27.6%.

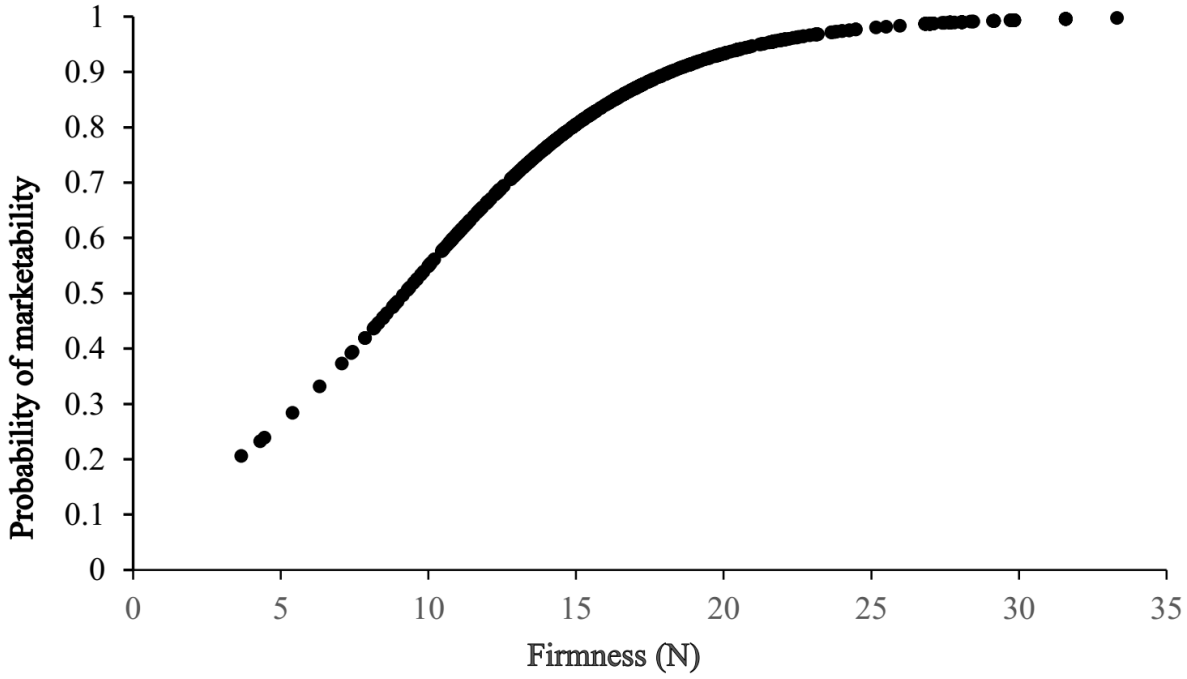

Figure 8.1 Probability of tomato marketability of the tomato fruits as influenced by firmness (N) over 28 days of storage

The outputs of all individual variables are shown in Table 8.1. The maturity stages (MS), total titratable acidity (TA), firmness and hue angle indicate positive regression parameter estimates (coefficients). The values indicated a positive relationship with the chance of tomato fruit marketability. On the other hand, the negative coefficient of days of storage (DOS), pH, TSS, TSS:TA ratio indicated that the prospective negative relationship with the probability of tomato fruit marketability. This relationship indicated that the chance of marketability decreased with increases in these factors. The Exp(β)-coefficients manipulated for chlorinated water (Tr4) (4.386), green maturity stage (MS1) (3.808), anolyte water (Tr2) (3.289), evaporative cooler (SC2) (2.187) and hot water (Tr3) (1.930). The result showed that there was evidence that the pre-storage disinfection treatments affected the probability of marketability of the tomatoes.

Table 8.1 Output of simple (single variable response to marketability) logistic model using both continuous and categorical variables

Variables	Regression coefficients	Wald X^2	Odds ratio (Exp(β))	95% Cl for Exp(β)	
				Lower	Higher
MS		21.953			
MS1	1.337	21.953	3.808	2.177	6.661
MS2	0.428	3.166	1.534	0.957	2.457
Constant	0.860	28.598	2.364		
Tr		28.068			
Tr2	1.191	16.016	3.289	1.836	5.894
Tr3	0.657	5.925	1.930	1.137	3.277
Tr4	1.478	5.756	4.386	2.323	8.282
Constant	0.642	13.496	1.900		
SC2	0.783	12.988	2.187	1.429	3.348
Constant	1.030	58.585	2.800		
DOS	-0.207	103.642	0.813	0.781	0.846
Constant	5.095	128.974	163.176		
pH	-0.376	1.053	0.687	0.335	1.408
Constants	3.436	3.526	31.064		
TA	9.223	33.810	10131.956	452.354	22938.26
Constant	-1.45	8.114	0.235		
TSS	-1.363	26.985	0.256	0.153	0.428
Constant	6.982	44.441	1076.613		
TSS:TA ratio	-0.143	33.764	0.867	0.826	0.910
Constant	3.475	103.112	32.302		
Firmness	0.244	59.636	1.276	1.199	1.357
Constant	-2.243	24.058	0.106		
Hue angle	0.193	38.715	1.212	1.141	1.288
Constant	-7.934	29.830	0.000		

Note: MS is red maturity stage tomato, MS1 is green maturity stage tomato, MS2 is pink maturity stage tomato, Tr is control treatment, Tr2 is anolyte water, Tr3 is hot water dipping, Tr24 is chlorinated water dipping, SC2 is evaporative cooling condition, DOS is days of storage, TA is titratable acidity, TSS is total soluble solids.

8.1.3.2 Probability of marketability depending on categorical and continuous variables

The probability of marketability was higher for tomatoes in the evaporative cooler tomatoes than for those stored in ambient conditions (Figure 8.2). The result showed that the evaporative cooler maintained higher marketability of the tomatoes throughout the storage period. Moreover, the probability of marketability decreased after seven days storage under both ambient and evaporative cooler conditions.

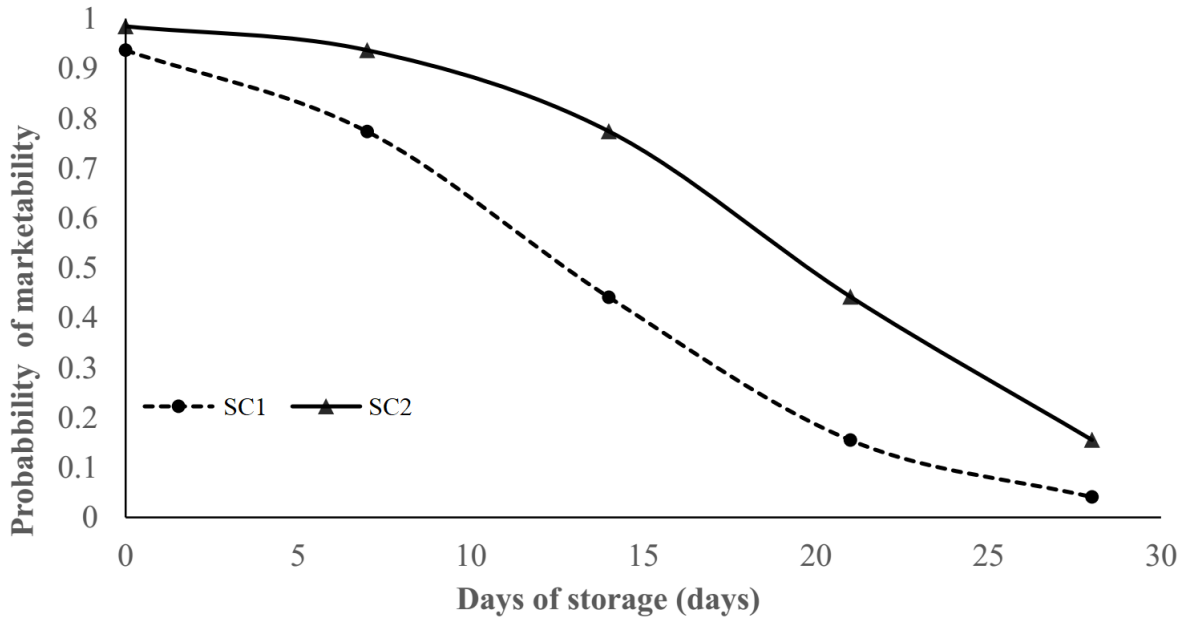

Figure 8.2 Forecasted chance of tomato marketability as a function of storage conditions (SC1 is ambient storage environment and SC2 is evaporative cooler storage environment)

Firmness based probability of marketability is shown in Figure 8.3. The tomatoes stored in the evaporative cooler storage had higher probability of marketability than those stored in an ambient storage environment. The result indicated that the evaporative cooling storage condition improved the probability of marketability.

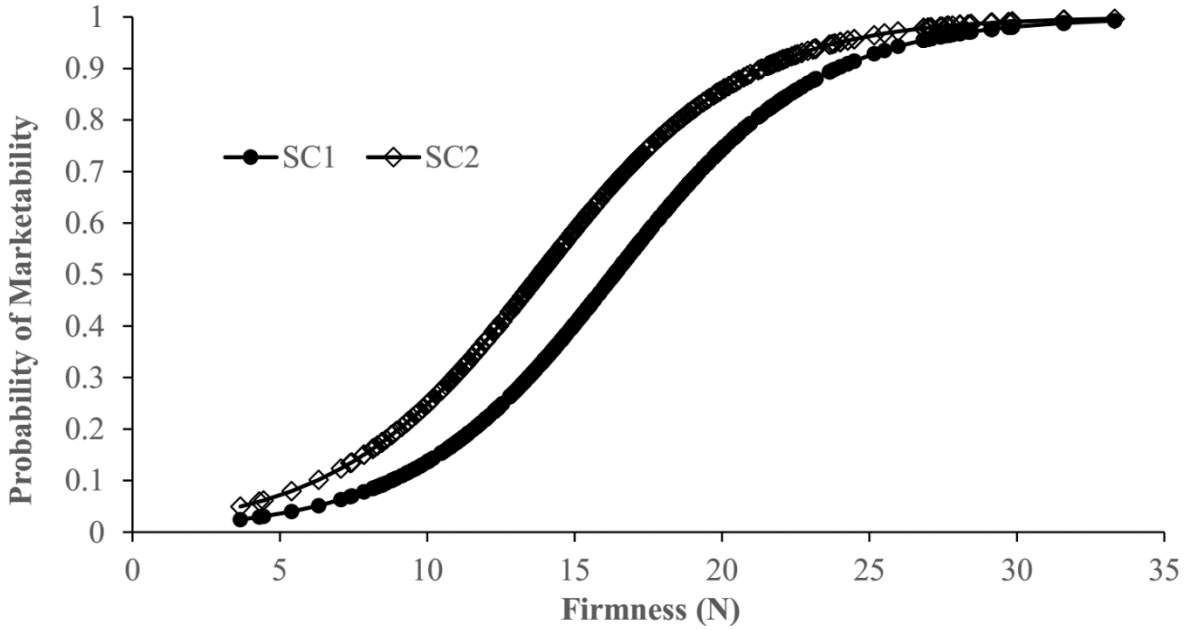

Figure 8.3 Probability of marketability based on the firmness as affected by storage conditions (SC1 is ambient storage environment and SC2 is evaporative cooler storage environment)

The probability of marketability of tomato fruit depending on maturity stage and firmness is displayed in Figure 8.4. Maturity stage 1 (green) showed a higher chance of marketability depending on firmness. Both pink and red tomatoes experienced similar marketability tendency.

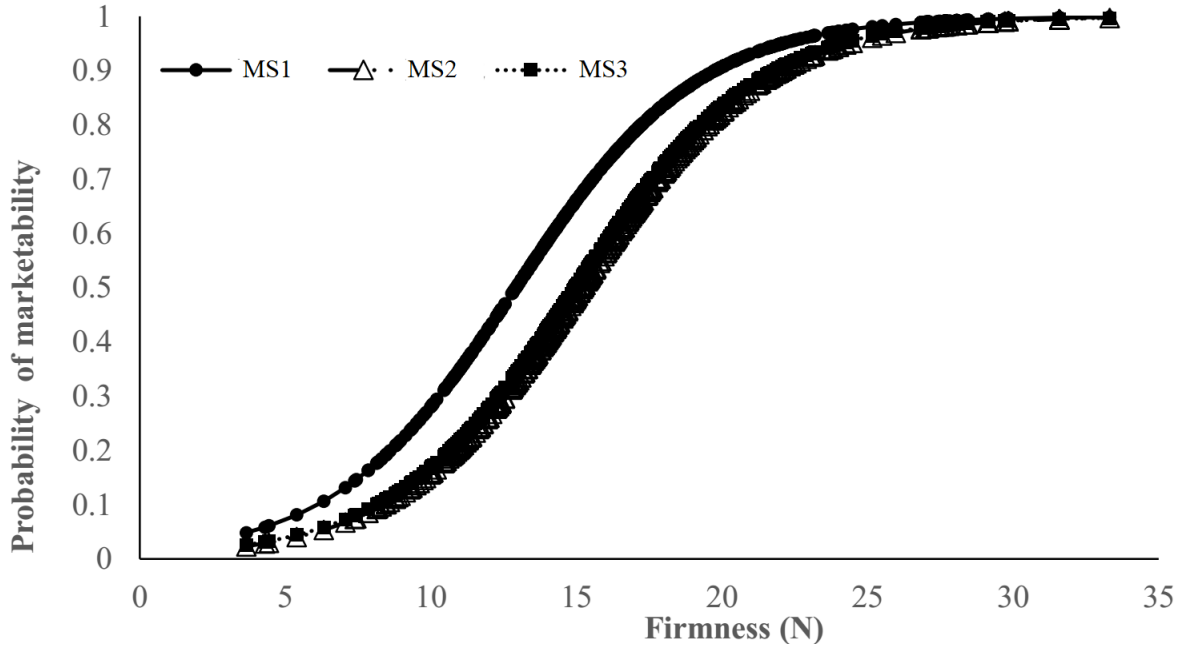

Figure 8.4 Probability of marketability based on the firmness as affected by maturity stage where MS1 is maturity stage 1 (green), MS2 is maturity stage two (pink) and MS3 is maturity stage three (red)

8.1.3.3 Multiple logistic regression model fitting based on several explanatory variables

Most of the independent variables were fitted to multiple logistic regression models and some of them were not statistically significant in predicting the chance of tomato marketability. The categorical variables included in the multiple logistic models were maturity stage (MS1, MS2, MS3), pre-storage disinfection treatments (Tr1, Tr2, Tr3, Tr4) and storage conditions (SC1, SC2). The remaining variables considered in the model were continuous variables (see Table 8.2). Due to the high correlative effect of days of storage (DOS) and many another dependent variables, the inclusion of the DOS resulted in non-significant effects on the other dependent variables. Hence, the overall multiple logistic models was fitted with the exclusion of the DOS (Table 8.2). This will not have affected the logistic regression model, as firmness and days of storage were highly correlated and one can be replaced by the other. The hot water treatment (Tr3), pink tomato maturity stage (MS2), total titratable acidity (TA) and total soluble solids to titratable acidity ratio (TSS:TA) did not significantly ($p > 0.05$) affect the tomato fruits probability of marketability.

The odds ratio is the ratio of the odds of an event happening in one group to the odds of the same event happening in another group (Melesse *et al.*, 2016). The variables SC1, MS3 and Tr1 were not included in Table 8.2. These variables were treated as references by the multiple logistic regression modeling. For instance, the odds ratio of SC2 at 3.271 showed that the odds of marketability of tomato for SC2 was 3.271 times that of SC1, keeping all other factors at fixed level. The odds ratio of chlorinated water dipping (Tr4) was the highest, at 27.501, followed by anolyte water dipping (Tr2) with an odds ratio of 17.971. The odds of being marketable for tomatoes under Tr4 was 27.501 times the odds of being marketable when tomatoes were in the control (no treatment = Tr1) (Table 8.2).

Table 8.2 Parameter estimates for multiple logistic regression model

Variables	Regression coefficient	Wald X^2	p	Odds ratio (Exp(β))	95% Cl for Exp(β)	
					Lower	Higher
SC2	1.185	11.892	0.001	3.271	1.668	6.415
MS1	2.760	30.446	<0.001	15.792	5.926	42.087
MS2	0.628	2.389	0.122	1.873	0.845	4.154
Tr2	2.889	26.992	<0.001	17.971	6.043	53.440
Tr3	1.226	8.499	0.004	3.406	1.494	7.765
Tr4	3.314	30.925	0.001	27.501	8.552	88.436
pH	2.832	16.775	<0.001	16.978	4.379	65.830
TSS	-2.701	40.665	<0.001	0.067	0.029	0.154
Firmness	0.238	18.819	<0.001	1.269	1.139	1.413
Hue angle	0.269	33.018	<0.001	1.309	1.194	1.435
Constant	-21.437	24.423				

Note: MS1 is green maturity stage tomato, MS2 is pink maturity stage tomato, Tr2 is anolyte water, Tr3 is hot water dipping, Tr24 is chlorinated water dipping, SC2 is evaporative cooling condition, TSS is total soluble solids.

Figure 8.5 shows the combined effect of maturity stage (MS) and storage conditions (SC) for different values of firmness variables on the chance of marketability of tomato fruits. The combination effect of green maturity stage (MS1) and evaporative cooler storage condition (SC2) exhibited the highest probability of marketability as a function of firmness, while the pink maturity stage (MS2) and ambient storage (SC1) showed the lowest chance of marketability of the tomatoes.

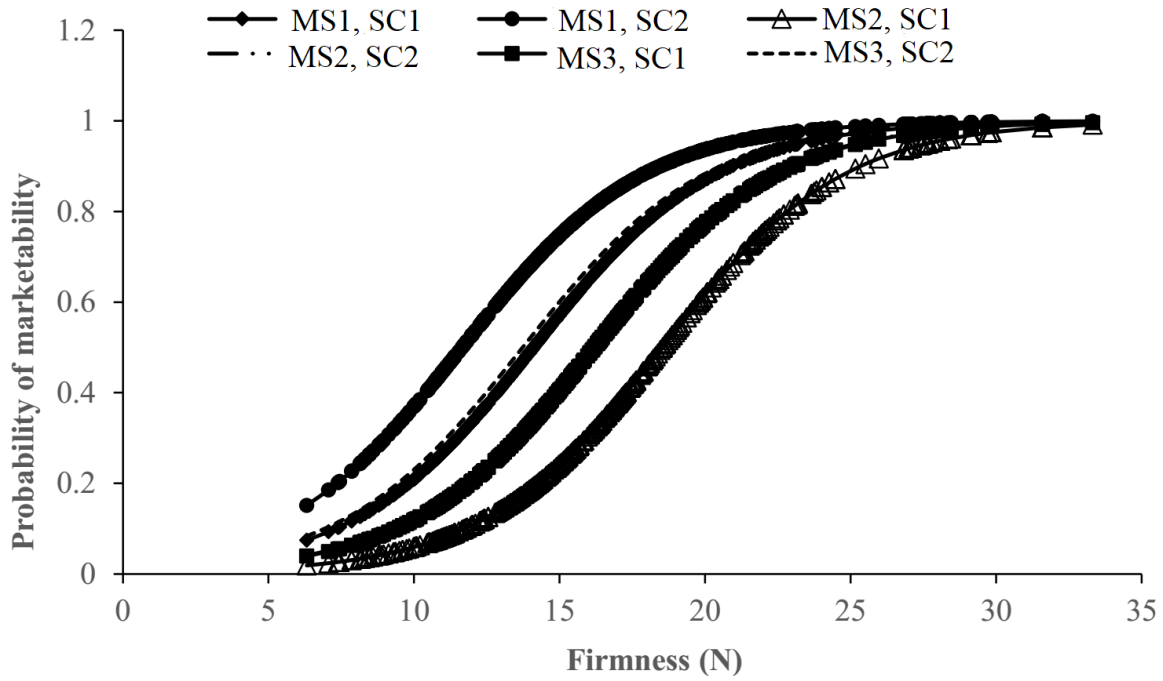

Figure 8.5 Probability of marketability based on firmness as affected by the maturity stage (MS) and storage condition (SC) where MS1 is maturity stage 1 (green), MS2 is maturity stage two (pink) MS3 is maturity stage three (red) and SC1 is ambient storage environment and SC2 is evaporative cooler storage environment

Figure 8.6 shows the combined effect of maturity stage (MS) and storage conditions (SC) for different storage periods (DOS) variables on the probability of marketability of tomato fruits. The combination effect of green maturity stage (MS1) and evaporative cooler storage condition (SC2) exhibited the highest chance to be marketable depending on DOS, while the red maturity stage (MS3) and ambient storage (SC1) showed the lowest chance for marketability during the storage period.

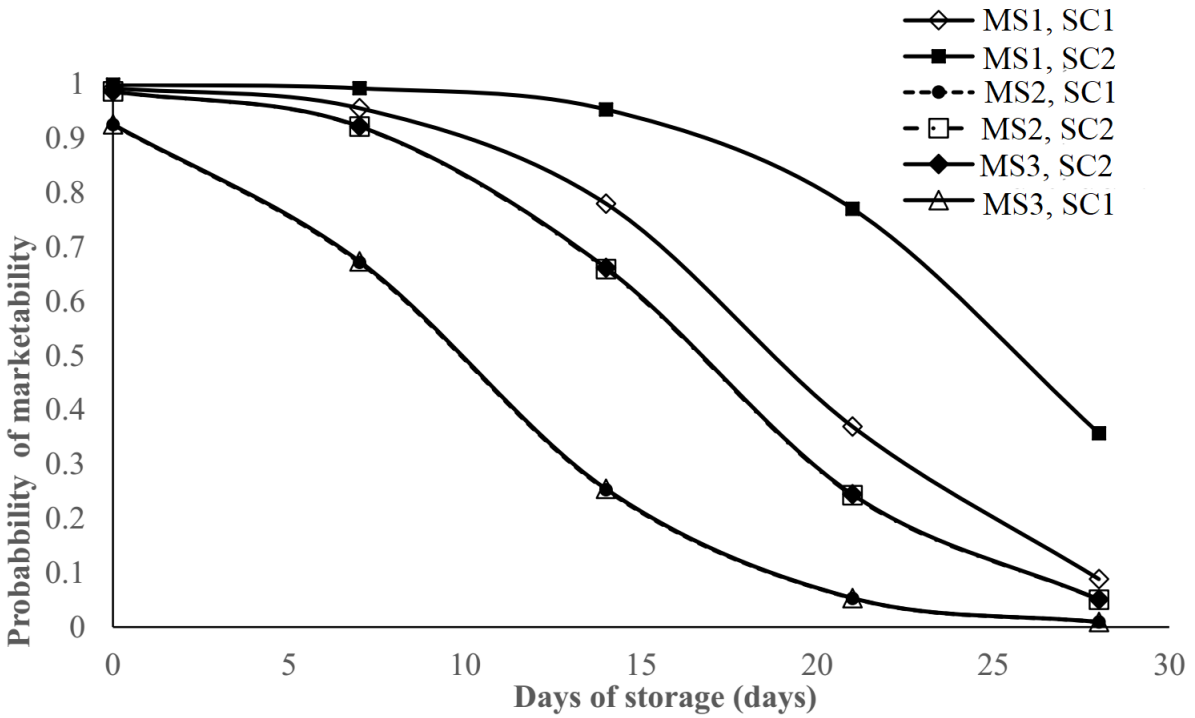

Figure 8.6 Predicted probability of marketability based on the maturity stage (MS) and storage condition (SC) where MS1 is maturity stage 1 (green), MS2 is maturity stage two (pink) MS3 is maturity stage three (red) and SC1 is ambient storage environment and SC2 is evaporative cooler storage environment

Hence, the core concept of this paper lies in predicting the probability of marketability for a combination of maturity stage, pre-storage disinfection treatments, storage conditions and storage period, through the application of multiple logistic regression modeling. The approach can filter out the most important variables from both categorical and continuous variables which can affect the dependent tomato quality indices that predict the tomato marketability.

8.1.3.4 Model validation

The overall significance ($p < 0.001$) level of likelihood ratio test statistics of the final model was 233.65 (Table 8.3). The results indicated that the overall multiple logistic models fitted were significant. Individual regression coefficients were analyzed for statistical significance by using the *Wald* χ^2 statistic (Melesse *et al.*, 2016). The parameter is the square of the ratio of the estimated slope parameter over its standard error. The Pearson χ^2 statistic ($p = 0.9980$) and deviance based ($p = 0.9977$) goodness fit were applied to test the sufficiency of the logistic model to explain the data. Moreover, the Hosmer and Lemeshow goodness of the model fit test

with the value of 5.5644 and $p = 0.6959$ supported the evidence that the logistic model fitted the data very well (Table 8.3).

The validation of predicted probability should also be checked for multiple logistic modeling (Melesse *et al.*, 2016). The classification table with a limit of 0.5 was used to analyse the extent of agreement between the predicted and the actual probabilities of marketability. The actual sensitivity test resulted in 85.97% compared to specificity value of 76.58%. The sensitivity is the proportion of correctly classified output marketability, while specificity is the proportion of correctly non-marketable (Melesse *et al.*, 2016). On the other hand, the positive predictive and the negative predictive values were 14.25% and 23.04%, respectively. The positive predictive values measure the rate of proportions of observations misclassified as marketability over all the actual classified as a marketable fruit. The negative predictive values are measures of the proportions of observations misclassified as non-marketable overall the actual classified as a not marketable fruit. The overall prediction of the model for dependent variables was about 85.75%. The measures of association were used for evaluation of the predicted and observed probability values. The Goodman Krushkal Gamma statistic value was 0.874, the Somer's *D* statistic was 0.874, and the *c*- statistic value was 0.937. The values of these statistics were close to 1, which supported that there was a strong association between the observed and predicted probabilities of the marketability of the tomato fruit.

Researchers have applied logistic regression analysis to analyse the changes in postharvest quality of tomato fruit during the combined pre-harvest applications, washing disinfections, packaging and cold temperature storage (Melesse *et al.*, 2016). Lammertyn *et al.* (2000) applied logistic regression analysis for modeling the factors influencing core breakdown in conference pears. The occurrence of discoloration disorder of chicory leaves head was investigated by multiple logistic regression analysis (Vanstreels *et al.*, 2002). The researchers found that anolyte water and cold storage at 13ºC showed the highest odds ratio. In this paper, a similar approach was applied to analyze the tomato maturity stage, pre-storage disinfection treatments, storage conditions and storage period. The multiple logistic regression result showed that chlorinated water treatment showed the highest odds ratio of 27.501, followed by anolyte water with an odds ratio of 17.971, green maturity stage tomato with an odds ratio of 15.792 and evaporative cooling environment odds ratio 3.271 ($p < 0.001$).

Table 8.3 Overall model evaluation

Model evaluation parameter	Wald X^2	DF	p
Overall significance			
Likelihood ratio test	233.6457	12	<0.0001
Score test	153.0777	12	<0.0001
Wald test	81.2246	12	<0.0001
Goodness of fit test			
Hosmer and Lemeshow	5.5644	8	0.6959
Pearson X^2	279.0878	527	0.9980
Deviance X^2	236.5276	527	0.9977
Association of predicted probabilities and observed response			
Somer's D	0.874		
Goodman Kruskal Gamma	0.874		
c-Statistic	0.937		

8.1.4 Conclusions

This study showed that the multiple logistic regression modeling was a good approach for the manipulation of the probability of marketability of tomatoes, harvested at different maturity stages and subjected to different pre-storage disinfection treatments, storage conditions and storage periods. The models were developed to fit probability of marketability of tomato fruits as a function of independent variables (quality indices). Most of the simple logistic models showed highly significant associations between the probability of tomato marketability and the predictor variables. However, in the multiple logistic regression models, some of the predictors were found to be non-significant. This could be due to the strong correlation among some predictors considered in the model. By multiple logistic models, most of the variables were significant and used to predict the probability of tomato marketability. The results indicated that firmness, hue angle, TSS and DOS were the most important determinants of tomato marketability. The chlorinated water dipping, anolyte water dipping, green maturity stage and evaporative cooler storage environment treatments showed highly significant ($p < 0.001$) effects compared with the other combinations. The disinfection pre-storage treatments, including anolyte water dipping, are appropriate for organic and environmentally friendly production systems and are currently recommended to partly, or fully, replace the use of other

chemical treatments. The use of evaporative cooling conditions for storage is also environmentally friendly and is safe for the produce, for the environment and for human health. The probability model will therefore provide a useful tool to predict the probability of tomato marketability for different storage conditions, pre-storage treatments and maturity stage for a range of environmentally-friendly production systems.

8.1.5 Acknowledgements

The Federal Ministry of Education of Ethiopia is gratefully acknowledged for its research grant support. The South African National Research Fund (NRF-TWAS) is also greatly acknowledged for its scholarship grant (Reference No. SFH150902141138). The host institute, the University of KwaZulu-Natal, is warmly acknowledged for its support. Moreover, the ZZ2 Farm and PHI Tomato Project under Grant 7/2015 are highly acknowledged for the tomato sample provision.

8.1.6 References

Agresti, A. 1996. *An introduction to categorical data analysis.* Wiley Interscience, A John Wiley & Sons, Inc., Publication, New York, USA.

AOAC. 1995. *Official Methods of Analysis: Association of Official Analytical Chemists.* AOAC, Virginia, USA.

Barrett, DM, Beaulieu, JC and Shewfelt, R. 2010. Color, flavor, texture, and nutritional quality of fresh-cut fruits and vegetables: desirable levels, instrumental and sensory measurement, and the effects of processing. *Critical Reviews in Food Science and Nutrition,* 50**,** 369-389.

Batu, A. 2004. Determination of acceptable firmness and colour values of tomatoes. *Journal of Food Engineering,* 61**,** 471-475.

Beckles, DM. 2012. Factors affecting the postharvest soluble solids and sugar content of tomato (Solanum lycopersicum L.) fruit. *Postharvest Biology and Technology,* 63**,** 129-140.

Fallik, E, Grinberg, S, Alkalai, S and Lurie, S. 1996. The effectiveness of postharvest hot water dipping on the control of grey and black moulds in sweet red pepper (Capsicum annuum). *Plant Pathology,* 45**,** 644-649.

Hosmer, DW, Lemeshow, S and Sturdivant, RX. 2013. *Applied logistic regression.* John Wiley & Sons, USA.

IBM SPSS Cor. 2016. *IBM SPSS statistics for windows, Version 24.0.* IBM Coreporation, Armonk, New York, USA.

Itoh, K. 2003. Combined effects of hot water treatment (HWT) and modified atmosphere packaging (MAP) on quality of tomatoes. *Packaging Technology and Science,* 16**,** 171-178.

Kader, AA. 1984. Effects of postharvest handling procedures on tomato quality. Symposium on Tomato Production on Arid Land 190, 209-222.

Kassim, A, Workneh, TS and Laing, MD. 2017. Development and Evaluation of a Small-scale In-field Integrated Postharvest Citrus Treatment Unit–Part 1. *International Journal of Food Engineering***,** pp.- Retrieved 28 Jun. 2017, from doi:10.1515/ijfe-2016-0192.

Kitinoja, L. 2013. *Use of cold chains for reducing food losses in developing countries.* The Postharvest Education Foundation, University of California, La Pine, Oregon, USA.

Laguerre, O, Hoang, HM and Flick, D. 2013. Experimental investigation and modelling in the food cold chain: Thermal and quality evolution. *Trends in Food Science & Technology,* 29**,** 87-97.

Lammertyn, J, Aerts, M, Verlinden, BE, Schotsmans, W and Nicolaï, BM. 2000. Logistic regression analysis of factors influencing core breakdown in 'Conference'pears. *Postharvest Biology and Technology,* 20**,** 25-37.

Melesse, S, Sobratee, N and Workneh, TS. 2016. Application of logistic regression statistical technique to evaluate tomato quality subjected to different pre-and post-harvest treatments. *Biological Agriculture & Horticulture,* 32**,** 277-287.

Mohammed, M, Wilson, LA and Gomes, PI. 1999. Postharvest sensory and physiochemical attributes of processing and nonprocessing tomato cultivars. *Journal of Food Quality,* 22**,** 167-182.

Moneruzzaman, KM, Hossain, ABMS, Sani, W and Saifuddin, M. 2008. Effect of stages of maturity and ripening conditions on the biochemical characteristics of tomato. *American Journal of Biochemistry and Biotechnology,* 4**,** 329-335.

Pinheiro, J, Alegria, C, Abreu, M, Gonçalves, EM and Silva, CLM. 2013. Kinetics of changes in the physical quality parameters of fresh tomato fruits (Solanum lycopersicum, cv. 'Zinac') during storage. *Journal of Food Engineering,* 114**,** 338-345.

Porat, R, Daus, A, Weiss, B, Cohen, L, Fallik, E and Droby, S. 2000. Reduction of postharvest decay in organic citrus fruit by a short hot water brushing treatment. *Postharvest Biology and Technology,* 18**,** 151-157.

Saran, S, Roy, SK and Kitinoja, L. 2010. Appropriate postharvest technologies for small scale horticultural farmers and marketers in Sub-Saharan Africa and South Asia-Part 2. Field trial results and identification of research needs for selected crops. *In:* Cantwell, MI and Almeida, DPF, eds. XXVIII International Horticultural Congress on Science and Horticulture for People (IHC2010): International Symposium 41-52. Acta Horticulture, Lisbon, Portugal.

SAS Institute Inc. 2015. *SAS Version 9. 4 Procedures Guide: Statistical Procedures.* SAS Institute, Cary, NC, USA.

Sharifi, M, Rafiee, S, Keyhani, A, Jafari, A, Mobli, H, Rajabipour, A and Akram, A. 2007. Some physical properties of orange (var. Tompson). *International Agrophysics,* 21**,** 391.

Sibomana, MS, Ziena, LW, Schmidt, S and Workneh, TS. 2017. Influence of transportation conditions and postharvest disinfection treatments on microbiological quality of fresh market tomatoes (cv. Nemo-Netta) in a South African supply chain. *Journal of Food Protection,* 80**,** 345-354.

Sloof, M, Tijskens, LMM and Wilkinson, EC. 1996. Concepts for modelling the quality of perishable products. *Trends in Food Science & Technology,* 7**,** 165-171.

Taurayi, S. 2011. *An investigation of natuurboerdery (natural farming) approach: a ZZ2 case study.* M.Sc., University of Stellenbosch, South Africa.

Thompson, JF. 2016. Pre-cooling and storage facilities. *The Commercial Storage of Fruits, Vegetables, and Florist and Nursery Stocks: Agriculture handbook, No. 66.* Cha. 2, 11-18. USDA, ARS, Beltsville, USA.

Vanstreels, E, Lammertyn, J, Verlinden, BE, Gillis, N, Schenk, A and Nicolaı, BM. 2002. Red discoloration of chicory under controlled atmosphere conditions. *Postharvest biology and technology,* 26**,** 313-322.

Workneh, TS. 2010. Feasibility and economic evaluation of low-cost evaporative cooling system in fruit and vegetables storage. *African Journal of Food, Agriculture, Nutrition and Development,* 10**,** 2984-2997.

Workneh, TS, Osthoff, G, Pretorius, J and Hugo, C. 2003. Comparison of anolyte and chlorinated water as a disinfecting dipping treatment for stored carrots. *Journal of food quality,* 26**,** 463-474.

Workneh, TS, Osthoff, G and Steyn, M. 2012. Effects of preharvest treatment, disinfections, packaging and storage environment on quality of tomato. *Journal of food science and technology,* 49**,** 685-694.

Workneh, TS, Osthoff, G and Steyn, MS. 2011. Influence of preharvest and postharvest treatments on stored tomato quality. *African Journal of Agricultural Research,* 6**,** 2725-2736.

Xuan, YM, Xiao, F, Niu, XF, Huang, X and Wang, SW. 2012. Research and application of evaporative cooling in China: A review (I) - Research. *Renewable & Sustainable Energy Reviews,* 16**,** 3535-3546.

8.2 Modelling the Effects of Pre-Storage Treatments, Maturity Stage, Low-Cost Storage Technology Environment and Storage Period on the Quality of Tomato Fruit

Abstract

The aim of this study was to develop a model for prediction of the quality of tomato during storage. Two storage conditions (evaporatively cooled and ambient), four disinfection treatments (tap, anolyte, hot and chlorinated water) and three maturity stages (green, pink and red) were employed in this experiment. Using multivariate analysis, the principal components (PC) (PC1, PC2) were analysed. Non-linear fractional and polynomial models were fitted to the experimental data to screen the best models. The PC1 and PC2 contributed 47.9% and 26.0% of total variation, respectively. Maturity stages and the disinfection treatments had significant ($P<0.05$) influence on PC1 and PC2. Hue angle, firmness, total titratable acidity (TA) and total soluble solid: TA demonstrated non-linear relationship with days of storage. TA, hue angle and firmness of tomatoes fitted well to the models developed. The models are recommended for use by tomato farmers to predict changes in the quality parameters.

Keywords: Models for quality prediction; multivariate analysis; postharvest; pre-storage disinfection treatments; principal component analysis; tomato quality

8.2.1 Introduction

A huge postharvest loss of fruit and vegetables including tomato fruit is a bottleneck for agricultural sector industry development. To maintain postharvest quality and freshness of tomatoes, a number of studies have been conducted to maintain the quality and thereby extend shelf-life (López and Gómez, 2004; Gharezi *et al.*, 2012; García-García *et al.*, 2013; Schouten *et al.*, 2014). Quality determination is a critical operation for the ease of processing and storability for stakeholders involved in the fresh produce industry. Measurement of quality-related attributes is the tool that can help to investigate and quality control of fresh produce at postharvest handling (Abbott, 1999; Schouten *et al.*, 2007; Schouten *et al.*, 2014; Pinheiro *et al.*, 2016).

Alimi *et al.* (2014) reported that the final quality is dependent on the interaction effects of the different treatments. Building multiple factors statistical analysis to study the effects of continuous and categorical variables and covariates is vital for the determination of tomato quality (Binder *et al.*, 2013; Sobratee and Workneh, 2015). A multivariable regression model development is dependent on the selection of covariates that related to the response of interests and searching for an appropriate efficient model for continuous covariates (Binder *et al.*, 2013). These data analysis methods can be used to model factors and responses and search for the relationship that exists between all factors and responses and can allow the extraction of useful information from multivariate quality data (Var, 1998; Harrell, 2015). Facts extracted from multivariate data are very helpful in understanding the characteristics of systems and processes and are useful in solving problems encountered by multiple factors (Var, 1998). The multivariate models can be principal component (PC) analysis, factor analysis, cluster analysis and discriminant analysis (Var, 1998; Harrell, 2015). The variable clustering approach such as oblique-rotation PC analysis was used for categorization of the variables (Alimi *et al.*, 2014; Alimi *et al.*, 2016). This approach can be used to reduce the number of continuous variables to put in the representative group by identifying patterns in a data set and help to eliminate the repetition in a univariate analysis (Iezzoni and Pritts, 1991; Martens and Martens, 2001). The PC is the linear combination of variables that has maximum variance subject to normalization constraints on the coefficients (eigenvectors) (Harrell, 2015) and the total variance created by each PC evaluated as eigenvalue (Iezzoni and Pritts, 1991; Martens and Martens, 2001; Sobratee and Workneh, 2015).

The non-linear dependence on some quality measures and time (days of storage (DOS)) were captured by applying fractional polynomials models. These models have the form $\alpha_0 + \alpha_1 t^p + \alpha_2 t^q$ for $p \neq q$ and $\alpha_0 + \alpha_1 t^p + \alpha_2 t^p \ln t$ for $p = q$. The powers p and q are chosen from among −2, −1, −0.5, 0, 0.5, 2, 3 (Melesse and Zewotir, 2017). The power factor terms were explored by several researchers to express categorical or continuous variables in fruit and vegetable postharvest management (Long and Ryoo, 2010; Binder *et al.*, 2013). Multivariate methods of analysis can identify important variables and functional continuous variables (Binder *et al.*, 2013). Alimi *et al.* (2016) analysed the effects of some pre- and postharvest treatments effect on the quality of tomatoes that stored inside refrigerated storage. The authors didn't account for the effects of firmness, hue angle and maturity stages (MSs) of tomato fruit. Moreover, the cooling approach was not evaporative cooler. The authors rather used mechanical refrigerated cooling system for the study of tomato storability. However, there is no research on model development for the fresh tomato harvested at different MSs, stored under evaporative cooler, treated with environmentally friendly pre-storage disinfection treatments and stored for a period of time. This study, therefore, applied analysis of variance (analysis of covariance (ANCOVA)), multivariate analysis (multivariate analysis of variance (MANOVA)) and the factorial polynomial models to reveal the multifactorial effects of MS harvest, postharvest pre-storage disinfection treatments and low-cost evaporative cooling technology on the quality of tomato fruit during the storage period. The common quality attributes that can be affected includes tomato skin colour, firmness, total soluble solids (TSSs), total titratable acidity (TA) and TSSs to TA ratio.

8.2.2 Materials and methods

8.2.2.1 Sample collection and pre-storage treatments

The study took place at the Ukulinga Research Station of the University of KwaZulu-Natal, South Africa. The tomato samples harvested at different MS (*i.e.* green, pink and red) (*Lycopersicon esculentum Mill. cv. Nemonetta*) were harvested and transported from ZZ2 firm, Limpopo, South Africa, and transported during the night time by the truck to Pietermaritzburg market station, South Africa, and collected for this experiment. The tomato sample was treated with pre-storage disinfection treatments and stored under two different storage conditions (SC)

(*i.e.* ambient environment 22.8ºC and RH of 31% and inside the experimental forced ventilation multi-pad evaporatively cooled store EC 15.2 ºC and RH of 86%).

Different pre-storage disinfection treatments (Tr) including control (tap water) treatment (Tr1), anolyte (Tr2), hot water (Tr3) and chlorinated water (Tr4) were applied to the sample. Sample tomatoes were dipped into an anolyte water solution for 5 min (Workneh *et al.*, 2003; Workneh *et al.*, 2012) and surface air dried, before storage in the EC and under ambient conditions (Temperature and RH). The hot water treatment was done by dipping the sample into hot water at 42.5°C for 30 min (Itoh, 2003). Chlorine disinfection was done by dipping samples into a solution containing 100 $\mu g.mL^{-1}$ total chlorine (Cl_2) for 20 min, which was prepared by dissolving standard grade sodium hypochlorite (5% NaOCl) in tap water (Workneh *et al.*, 2011). The control samples were dipped into cold water for 20 min.

8.2.2.2 Quality attributes analysis

pH value

Five tomato samples from each MS were taken and blended into a homogeneous pulp. This was then filtered, using Whatman filter paper No. 1, and 25 mL of the filtrate was then used to measure pH values with a pH meter (Orion Star, Model 210, Thermo Scientific Pty), according to the procedure (AOAC, 1995). The pH meter was buffered in to buffer solution for the calibration.

Total titratable acidity

A 25 ml filtrate of the pulped tomato was taken for total titratable acidity (TA) determination and was titrated with 0.1N NaOH, using a phenolphthalein indicator (Equation 7.1).

Total soluble solids

The TSS content was measured a digital handheld refractometer (Pocket Refractometer, PAL-3, Japan). The tomato sample was pulped and filtered by Whatman filter paper No.1. The filtrate was used for the analysis (AOAC, 1995). The refractometer prism was cleaned with distilled

water and dried by lint-free tissue paper. After every measurement it was calibrated to zero with distilled water.

TSS to TA ratio

The TSS to TA ratio of tomato slurry was determined using Equation 7.2.

Firmness

The fruit firmness was determined by using the Intron Universal Testing Machine (Model No. 3345) with a 7.5 mm penetration depth, a 3.00 $mm.s^{-1}$ speed, a 50 N maximum force and a 2 mm diameter probe, according to the procedure used by Pinheiro *et al.* (2013). Five fruits from each category of tomatoes, subjected to different treatments, were used for the analysis. The plate of the instrument, on which tomato sample was placed is a bowl type to fix the spherical tomato fruit in place during penetration. It has a hole at the centre of the plate for safety reason.

Colour

Tomato skin colour was measured three times for single fruit along the equatorial diameter, using the digital Minolta Chromatic 400 method of the CIELAB colour space, according to the procedures of Batu (2004). The instrument was calibrated against a white standard tile before each color reading. The L, a*, b* and hue angle (^{o}h) values were measured and recorded. The hue angle (^{o}h) was used for the analysis of tomato colour skin.

8.2.2.3 Experimental design

A three factor experiment, three maturities (green, pink and red), four pre-storage treatments (control, anolyte water, hot water and chlorinated water), two SCs (ambient and evaporative cooler) and five replications for each measurements. The data were collected on 0, 7, 14, 21 and 28 DOS at evaporative cooler and ambient environment. The experimental design was arranged in a factorial type of randomized complete block design, with five fruits per sample were randomly picked for the experiment and quality data measurement.

8.2.2.4 Data analysis

Statistical analysis was performed using statistical packages for social sciences (SPSS) 24.0 (SPSS Inc.) SAS version 9.4, R ver. 3.32 and MATLAB version 2013a. The descriptive statistics in combination with univariate and multivariate analysis was performed. The significance of the interactions of quality indices in MANOVA was performed by using Wilks' lambda (λ) test statistics. In addition, ANCOVA was performed.

The PC analysis was performed to evaluate the relationship among the quality indices analysed. The PCs were extracted using Varmix rotation approach (Iezzoni and Pritts, 1991; David and Jacobs, 2014), which was based on the eigenvalue >1.0 (Iezzoni and Pritts, 1991; Shlens, 2014). The variances are calculated based on eigenvalues of the correlation values (Iezzoni and Pritts, 1991). The PCs can be used in multiple regression analysis to determine the relationship among correlated groups of predictor and individual outcome variables (Iezzoni and Pritts, 1991; Alonso-Gutierrez *et al.*, 2015; Jolliffe and Cadima, 2016). The univariate extraction was followed by the multivariate component analysis for ANOVA. The quality of the models was tested by using some graphical methods including a plot of residuals versus fitted values, residuals homogeneity and normal probability plot. Fractional polynomials can help to handle the presence of curvature in the relationship among variables. The Royston and Altman (1994) and Ambler and Royston (2001) approach to fractional polynomial were adopted to investigate the relationship between DOS and all dependent variables. The details procedure on fractional polynomials can be found on Royston and Altman (1994), Ambler and Royston (2001) and Long and Ryoo (2010).

8.2.3 Results and discussions

Several statistical methods were applied to determine the effects of covariates (*i.e.* MSs, SCs and disinfection treatments Tr) on different quality variables (pH, TA, TSS, TSS:TA ratio, firmness and hue angle). Both univariate ANOVA and MANOVA approaches were used to study the effect of these covariates on the quality measurement variables. An attempt to fit the MANOVA model was made. In that, all the quality attributes were considered as a response vector and the covariates as factors affecting the response vector. Four test statistics are usually applied to test for the significance of interactions among covariates used in MANOVA. Pillai's trace, Wilks' lambda (λ), Hotelling's trace and Roy's largest root were used to study the

significance of interaction covariate variables. Wilks' lambda is more commonly used when the factor variable has more than two categories (Rencher, 2003; Royston and Sauerbrei, 2003; Alimi *et al.*, 2016). In this study, both treatment and MSs have more than two categories. Therefore, Wilks' lambda test statistic is used. The significance of ($p \leq 0.05$) of the three-way interaction test showed the presence of significant interactions of the factors on some, or all, of the dependent variables. Based on this result, the significance interaction for each quality parameter was tested separately using univariate analysis of variance tests.

In the univariate ANOVA tests, in addition to the p-values, the partial eta-squared statistic was employed. Eta squared (η^2) measures the ratio of the total variance explained in a dependent variable which was associated with the membership of different groups defined by an independent variable (Richardson, 2011). On the other hand, partial eta squared value is a similar measure by which the effects of other independent variables and interactions are separately singled out (Richardson, 2011). That means partial eta squared was used as a measure of effect size or magnitude of variability in the dependent variable that was due to the independent variable.

pH value

The interactions of MS, Tr and SC had no significant effect on the pH of stored tomato (Table 8.4). Of the two-way interaction terms analysed, only MS x Tr and SC x Tr were found to be highly significant ($p \leq 0.001$, $p \leq 0.01$ and $p \leq 0.05$) on the pH value of tomatoes and responsible for 4.5% and 4.5% variances, respectively. MS x SC interaction had no significant effect. The main factors, MS and Tr, had a significant ($p \leq 0.001$, $p \leq 0.01$ and $p \leq 0.05$) effect on the pH of the stored tomato and responsible for the variation of 4.6% and 4.7%, respectively (Table 8.4). The factor SC has no significant effect on the pH of stored tomato. However, its interaction with Tr has a significant effect. Therefore, SC will remain in the ANOVA model since its higher order interaction is significant.

The result verifies report of Moneruzzaman *et al.* (2008) that the pH increased with storage time and influenced by postharvest pre-storage disinfection treatments. In this study, application of multifactorial analysis, the result showed that some of the individual treatments and two-way interactions had an effect on the pH of tomato during the storage, while the three-way interaction had no effect on the pH value.

The partial etta-squared (η^2) analysis, variability level in the dependent factors, which are related to and accounted for by the independent variable, was 0.045 and 0.047, respectively for the one-way interaction of Tr or MS and two-way interaction MS x SC, respectively (Table 8.4). This indicates that the one-way interaction was accountable for the variance of more 4.7% than the two-way interaction in pH value.

Titratable acidity

The two- and three-way interaction between MS, SC and Tr terms analysed had no significance on the TA value (Table 8.4). The main effects MS, SC and Tr had a significant ($p \leq 0.001$, $p \leq 0.01$ and $p \leq 0.05$) effect on the TA of the stored tomato and, hence, responsible for their variations (partial etta squared) in variances of 7.7%, 1.6% and 3.8%, respectively. The result shows that the MS is the most responsible factor to affect the variance, followed by Tr and SC on the TA of the stored tomatoes. The result supports the Moneruzzaman *et al.* (2008) report that TA increased with storage time and also affected by postharvest treatments.

Total soluble solid

The three-way interactions of MS, Tr and SC had significant ($p \leq 0.01$ and $p \leq 0.05$) effect on the TSS content of the stored tomatoes and responsible for the variances of 3.5% (Table 8.4). Moreover, of the two-way interaction terms analysed, only MS x Tr and SC x Tr were significant ($p \leq 0.001$, $p \leq 0.01$ and $p \leq 0.05$) on the TSS content. The effect sizes of these two-way interactions are 6.9% and 2.3%, respectively. The main factors (SC and Tr) had a significant ($p \leq 0.001$, $p \leq 0.01$ and $p \leq 0.05$) effect on the TSS content of the stored tomato and accounted for the effect sizes of 2.4% and 2.3%, respectively. However, MS had a significant ($p \leq 0.01$) effect on TSS and responsible for 1.3% of the variation in the dependent variable, TSS. The result shows that two-way (MS x Tr) is the most important factor that affects TSS with higher effect sizes (6.6%) than the three-way interaction (3.5%). That means interaction effect of MS by Tr had more influence on the TSS content than the three-way interaction.

TSS to TA ratio

Both the two- and three-way interaction terms analysed had no significant effect on the TSS:TA ratios (Table 8.4). Individually, the main effects MS and Tr had a significant ($p \leq 0.001$, $p \leq 0.01$

and p≤0.05) effect on the TSS:TA ratio of the stored tomato, while the SC had a significant (p≤0.05) effect on the TSS:TA ratio of the stored tomato. The effects size of MS, Tr and SC was found to be 3.3%, 6.3% and 1.2%, respectively. This shows that Tr is the most prominent independent factor that affects the variances of the TSS:TA ratio followed by MS and SC during the storage period. The result is similar to that of Moneruzzaman *et al.* (2008) report that TSS:TA ratio increased with storage time and affected by postharvest treatments. Therefore, the quality changes of tomato fruit can be maintained in terms of TSS:TA ratio by applying selective postharvest handling (Tr, MS and SC).

Firmness

The two-and three-way interaction terms analysed had no significant effect on the firmness value (Table 8.4). Among the main effects only MS had a highly significant (p≤0.01) effect on the firmness (N) value of the stored tomatoes and accounted 6.0% to the total variations in firmness. The result shows that the sole factor that is responsible for firmness is MS of the tomatoes, which can play a great role in the study of fresh tomato fruit texture dynamics and structure. Kader (1986) reported a similar result that firmness decreased with storage time and affected by postharvest treatments. Therefore, the less mature (green and pink) tomato quality can maintain more quality. It could be due to less physiological disorders in less mature and ripe tomato fruit.

Hue angle

The two-and three-way interaction terms analysed had no significant effect on the hue angle value (Table 8.4). Among the main effects, only MS had a highly significant (p≤0.01) effect on the hue angle (^{o}h) value of the stored tomato and responsible for 7.1% of the variances in Hue angle. The result shows that MS is the most important factor that affects the colour of the stored tomatoes. It can play a role in science and technology of colour changes in tomato fruit for quality determination. The result is in support of Kader (1986) report that hue angle decreased with storage time and affected by postharvest treatments. The changes in physiological respiration might contribute to the colour change effect, which can affect the tomato quality during the storage period.

Table 8.4 The main and interactive effect of independent variables on some tomato quality indices, where TA is total titratable acidity, TSS denotes total soluble solids, TSS:TA ratio represent the fraction of total soluble solids to titratable acidity

Variables	pH		TA		TSS		TSS:TA ratio		Firmness		Hue Angle	
	p-value	Partial-η^2	p-value	Partial-η^2	p-value	Partial-η^2	p-value	Partial-η^2	p-value	Partial-η^2	p-value	Partial-η^2
MS	0.000^{**}	0.046	0.000^{**}	0.077^{*}	0.036^{**}	0.013^{**}	0.000^{**}	0.033^{**}	0.000^{**}	0.060^{*}	0.000^{**}	0.071^{*}
SC	0.285^{*}	0.002^{**}	0.004^{**}	0.016^{**}	0.000^{**}	0.024^{**}	0.011^{**}	0.012^{**}	0.098^{*}	0.005^{**}	0.445^{*}	0.001^{**}
Tr	0.000^{**}	0.047	0.000^{**}	0.038^{**}	0.007^{**}	0.023^{**}	0.000^{**}	0.063^{*}	0.757^{*}	0.002^{**}	0.903^{*}	0.001^{**}
MS x SC	0.953^{*}	0.000^{**}	0.293^{*}	00.005^{**}	0.91^{*}	0.000^{**}	0.948^{*}	0.000^{**}	0.707^{*}	0.001^{**}	0.753^{*}	0.001^{**}
MS x Tr	0.001^{**}	0.042^{**}	0.784^{*}	0.006^{**}	0.000^{**}	0.069^{*}	0.157^{*}	0.018^{**}	0.649^{*}	0.008^{**}	0.999^{*}	0.001^{**}
SC x Tr	0.000	0.045^{**}	0.930^{*}	0.001^{**}	0.001^{**}	0.023^{**}	0.354^{*}	0.006^{**}	0.536^{*}	0.004^{**}	0.974^{*}	0.000^{**}
MS x SC x Tr	0.313^{*}	0.014^{**}	0.599^{*}	0.009^{**}	0.005^{**}	0.035^{**}	0.302^{*}	0.014^{**}	0.865^{*}	0.005^{**}	0.998^{*}	0.001^{**}

* indicates non-significant ($p \geq 0.05$) and ** indicates significant ($p \leq 0.05$)

8.2.3.1 PC analysis

The PC analysis is one of the multivariate analysis methods by which the quantitative dependent variable data observations that are inter-correlated are analysed (Abdi and Williams, 2010). The model validity for PC analysis validity is dependent on Kaiser Meyer Olkin (KMO) statistical coefficient, of which the minimum requirement was 0.5 to be appropriate (Alimi *et al.*, 2016). The calculated value of KMO is 0.514 which is above the minimum requirement of 0.5. The approximated value of chi-square for Bartlett's test is 2155.75 with a $p \leq 0.0001$. This indicates that the data are well suited for PC analysis. Two PCs (PC1 and PC2) were extracted, which were responsible for 47.92% and 25.97% of current data variances, respectively. Varimax rotation was used in data reduction process. The result showed that four variables (TA, TSS:TA ratio, firmness and Hue Angle) contributed more to PC1 and the pH and TSS contributed more to PC2 (Table 8.5).

Parameters that fall under the same PC were reported to have similar characteristic (Shittu *et al.*, 2007; Alimi *et al.*, 2016). Accordingly, TA (92.9%) and Firmness (87.9%) were the most contributing positive components to PC1, while hue angle (-88.7%) and TSS:TA ratio (-65.9%) had shown the most negative component effect on PC1. The result shows that the positive PC1 percentage value shows a positive relationship between TA and firmness, while hue angle and TSS:TA ratio had a negative percentage values and, hence, reverse relationship. Moreover, TSS (75.7%) and pH (71.5%) showed high load effect on PC2 and the result reveals that TSS and pH are related positively and had a similar effect on tomato quality during the DOS, which is similar to the report of Kader (1986).

Table 8.5 Rotated principal components of factor loading for some of the quality attributes of tomato fruit

	Principal components	
Quality parameter	PC1	PC2
pH	-0.072	0.715
TA	0.929	-0.182
TSS	0.116	0.757
TSS:TA ratio	-0.659	0.655
Firmness	0.879	0.028
Hue Angle	-0.887	0.104
Percent of total (%)	47.922	25.966

Table 8.6 shows that the output of the univariate factorial ANOVA used to study the treatment factors on the two extracted PCs. The result can help to identify the relative importance of the treatments to the individual PCs as a group of tomato quality parameters. Moreover, it allows predicting the effects of treatments on the group, rather on the individual quality measurements. All the two-way and three-way interactions between the factors had no significant effect on PC1.The three-way interaction, MS x SC x Tr, had a significant ($p \leq 0.05$) effect on PC2. Among the two-way interactions, only MS x Tr had shown significant ($p \leq 0.05$) effect on PC2. MS had a significant ($p \leq 0.001$) effect and SC had a significant ($p \leq 0.05$) effect on PC1. The result shows that the MS is responsible for 8.2% of the overall variances, while SC contributed 1.2% of the variations in PC1. The Tr is accountable for 5.6% variation, MS x Tr for 2.8% variations and MS x SC x Tr for 2.6% of the total variances of PC2. As a result, of all treatment factors, MS and TR had shown an important contribution on the quality of stored tomatoes.

Table 8.6 Interactive and main effect of treatments on the extracted principal components summarized ANOVA table

Quality parameter	Principal component 1		Principal component 2	
	p-value	Partial-η^2	p-value	Partial-η^2
MS	0.000	0.082	0.533	0.002
SC	0.012	0.012	0.533	0.001
Tr	0.105	0.012	0.000	0.056
MS x SC	0.610	0.002	0.977	0.000
MS x Tr	0.929	0.004	0.023	0.028
SC x Tr	0.956	0.001	0.804	0.002
MS x SC x Tr	0.846	0.005	0.033	0.026

8.2.3.2 Regression model analysis

The analysis of variance applied in the previous section (PCs) can only consider categorical predictor (Jolliffe and Cadima, 2016). However, in this study, the data have also continuous covariate (DOS) that might affect the quality variables used in this study. In ANCOVA analysis, it is possible to consider both categorical and continuous predictors simultaneously (Huitema, 2011). Therefore, attempts to fit ANCOVA models for each of the response variables (pH, TSS, TSS:TA ratio, firmness and hue angle) on DOS and three categorical covariates (MS, Tr and

SC) together with all possible interactions were performed. At the beginning, TSS was fitted as a function of these covariates (MS, Tr and SC). DOS has no significant effect on TSS. On the other hand, the three-way interaction of categorical predictors (MS x SC x Tr) is significant at 5% level ($p \leq 0.05$).Therefore no further model reduction step is necessary (Huitema, 2011) A similar model was fitted using pH as the response variable of interest. DOS has no significant effect on pH value. Similarly, the three-way interaction of MS*Tr* SC term was not significant. Therefore, a simpler model with only two-way interactions between MS x Tr, MS x SC, Tr x SC terms were considered. The two-way interaction between MS and SC was not significant. ANCOVA model of the response variable, TA as a function of DOS and the three categorical covariates, together with their all possible interactions, were fitted to the model. DOS has a highly significant ($p \leq 0.001$) effect on TA. The three-way interaction was not significant. Moreover, the two-way interaction MS x Tr, MS x SC, Tr x SC terms were found to be not significant. Therefore, a model without any interaction term is selected as the final model (Huitema, 2011; Egbewale *et al.*, 2014).

A similar analysis was made for the response variable TSS:TA ratio. None of the interaction terms were found significant. The results for the response variables (TA, TSS:TA ratio, Firmness and Hue Angel) are presented in Table 8.7. The output indicates that the fitted values of Firmness (Table 8.7c) and TSS:TA ratio (Table 8.7b) are respectively given by equations 8.6 and 8.7:

$$\text{Firmness} = 25.461 + 1.1335\text{SC2} - 1.8373\text{MS2} - 4.531\text{MS3} - 0.5075\text{DOS} \quad (8.6)$$

$$\text{TSS: TA ratio} = 7.04 + 1.871\text{Tr2} + 2.262\text{Tr3} + 0.1857\text{Tr4} + 1.281\text{MS2} + 2.367\text{MS3} - 1.022\text{SC2} + 0.2473\text{DOS} \quad (8.7)$$

Where:

SC2 = an evaporative cooler condition,
MS2 and MS3 = the pink and red MSs,
DOS = the days of storage (days),
Tr2 = an anolyte water dipping,
Tr3 = the hot water dipping, and
Tr4 = chlorinated water dipping.

Each of the categorical covariates is binary variable which have a value either 0 or 1. In each case the first category of each of the categorical covariates was used as reference category and it did not appear in the fitted model. That means for treatment level 1 (Tr2=0, Tr3=0, Tr4=0), first MS (MS2=0, MS3=0) and first SC (SC=0), then the value TA will be (Equation 8.8):

$$\text{TSS: TA tatio} = 7.04 + 0.2473\text{DOS} \tag{8.8}$$

Most of the coefficients are negative for TA while most of them are positive for TSS:TA ratio (Table 8.7a). TA was negatively related to anolyte and chlorinated water and all MSs. Moreover, as the DOS increases, the value of TA decreases. On the other hand, TSS:TA ratio is positively related to both treatment and MSs. It appears that SC2 has a positive contribution towards TA but a negative contribution towards TSS:TA ratio. There is a positive relationship between TSS:TA ratio and DOS (Table 8.7b). DOS is negatively related to TA, Firmness and Hue Angel. Firmness decreases with the DOS (Figure 8.7). The level of firmness is highest for the MS1 and SC1.

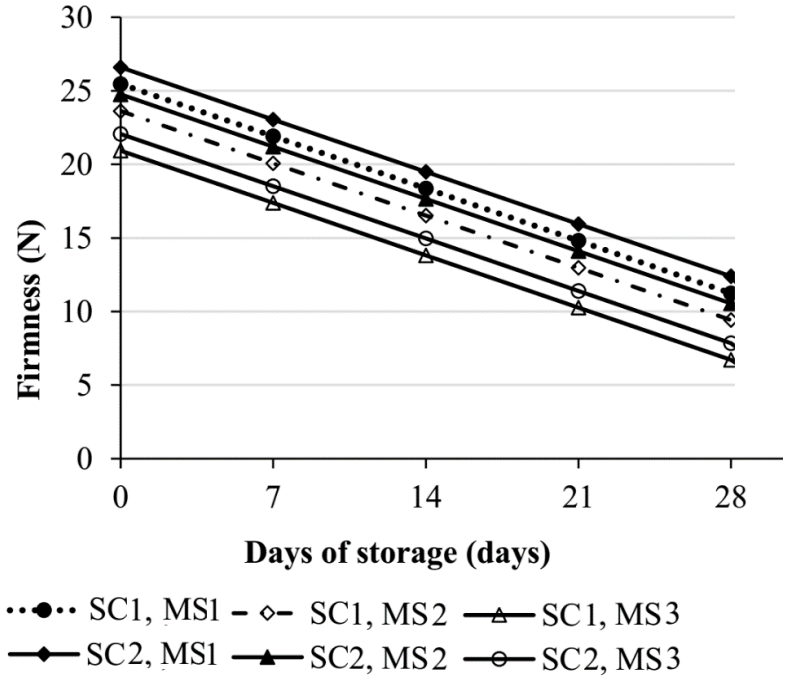

Figure 8.7 The typical level of firmness as the function of days of storage (DOS) (n = 5)

Table 8.7 Parameter estimates of the analysis of covariance models for different response variables

(a) Response variable TA				
Factors	Estimate	Standard error	t-	p-value
Intercept	0.4680	0.0063	74.621	< 0.001 ***
Tr 2	-0.0258	0.0059	-4.361	<0.001 ***
Tr 3	0.0416	0.0059	-7.034	<0.001 ***
Tr 4	-0.0200	0.0059	-3.383	<0.001 ***
MS2	-0.0368	0.0051	-7.218	<0.001 ***
MS3	-0.0682	0.0051	-13.357	<0.001 ***
SC2	0.0237	0.0042	5.647	<0.001 ***
DOS	-0.0064	0.0002	-28.088	<0.001 ***
(b) Response variable TSS:TA ratio				
Intercept	7.0440	0.4304	16.368	<0.001 ***
Tr 2	1.8707	0.4061	4.606	<0.001 ***
Tr 3	2.2616	0.4059	5.572	<0.001 ***
Tr 4	0.1857	0.4063	0.457	>0.05*
MS2	1.2813	0.3503	3.658	<0.001 ***
MS3	2.3671	0.3502	6.760	<0.001 ***
SC2	-1.0215	0.2875	-3.553	<0.001 ***
DOS	0.2473	0.0157	15.716	<0.001 ***
(c) Response variable firmness				
Intercept	25.4614	0.3427	74.297	<0.001 ***
SC2	1.1335	0.2812	4.031	<0.001 ***
MS2	-1.8373	0.3427	-5.362	<0.001 ***
MS3	-4.5310	0.3425	-13.228	<0.001 ***
DOS	-0.5075	0.0154	-32.962	<0.001 ***
(d) Response variable hue angel				
Intercept	78.7527	1.1393	69.125	<0.001 ***
SC2	1.9275	0.9347	2.062	<0.05 **
MS2	-9.6537	1.13913	-8.475	<0.001 ***
MS3	-13.9098	1.1387	-12.216	<0.001 ***
DOS	-1.30281	0.0512	-25.452	<0.001 ***

* Denotes non-significant (p>0.05), ** significant (P<0.05) and *** shows highly significant (P<0.001), Tr2: anolyte water, Tr3: hot water), Tr4: chlorinated water, MS2: pink tomato, MS3: red tomato, SC2: evaporative cooler storage, DOS: days of storage.

8.2.3.3 Model validation

The validity of the fitted models was checked using graphical methods (Harrell, 2015). For all models considered, it appears that the assumptions needed for fitting the models are not violated. For instance, the plot of residuals versus fitted values, MS and SC presented in Figure 8.8 (A, B, C) for the model that considers firmness as the response variable. As can be seen from Figure 8.8, the assumption of constant variance is not violated and implies the fitted model is valid. The residual population is distributed around 0 - axis, which is usually the sign of the fact that the model assumptions are met. Moreover, the residuals are homogeneously distributed with respect of the covariates in the model. The normal probability plot of residuals was also used to check the assumption of normality. The assumption normality is plausible. For other models, also none of the graphs indicates any violation of the underlying assumptions.

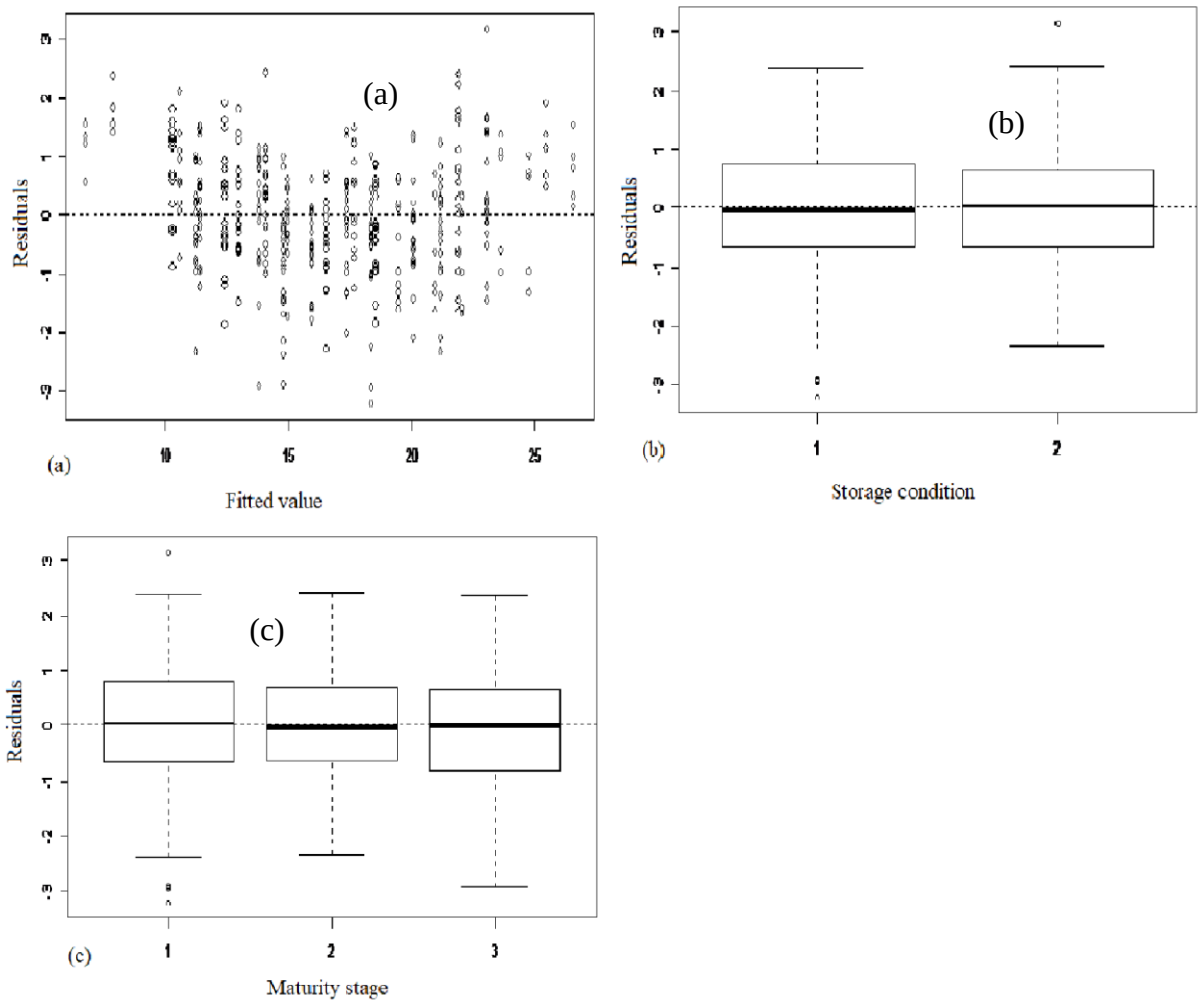

Figure 8.8 a) residuals plotted versus fitted values, b) residuals plotted versus maturity stage and c) residuals plotted versus storage condition

8.2.3.4 Fitted fractional and polynomial model

In the application of ANCOVA model, it was found that there is no significant effect of storage period on TSS content of tomatoes and pH values. Even when DOS has a significant ($p \leq 0.05$) effect, the value of multiple R^2 ranges from 0.4 to 0.69. These suggest that the relationship between DOS and the tomato quality attributes may be not linear and this implies that it could be curvilinear. Based on this analysis, fractional polynomial model analysis was performed.

An attempt to model non-linear relationship between DOS and tomato quality measures was performed. The fractional and polynomial models were used to investigate the nonlinear relationship. Neither TSS nor pH was found to have a significant ($p > 0.05$) relationship with DOS. This proves that the result obtained using ANCOVA model which can explain that both pH and TSS are not changed through the storage period. The other quality measures (TA, TSS:TA ratio, firmness and hue angle) appear to have a curvilinear relationship with DOS.

8.2.3.5 Models for green mature tomatoes

The fractional and polynomial models fit for green tomatoes and shown in Figure 8.9. The models are presented in equations 8.9-8.11. The result showed that the models for green maturity stage tomato were fitted well.

$$\text{TA} = 0.000381 * \text{DOS}^2 - 0.01755 * \text{DOS} + 0.5015 \quad (8.9)$$

$$\text{Firmness} = 0.001112 * \text{DOS}^3 - 0.03145 * \text{DOS}^2 - 0.6122 * \text{DOS} + 29.11 \quad (8.10)$$

$$\text{Hue angle} = -0.005046 * \text{DOS}^3 + 0.3478 * \text{DOS}^2 - 7.872 * \text{DOS} + 104 \quad (8.11)$$

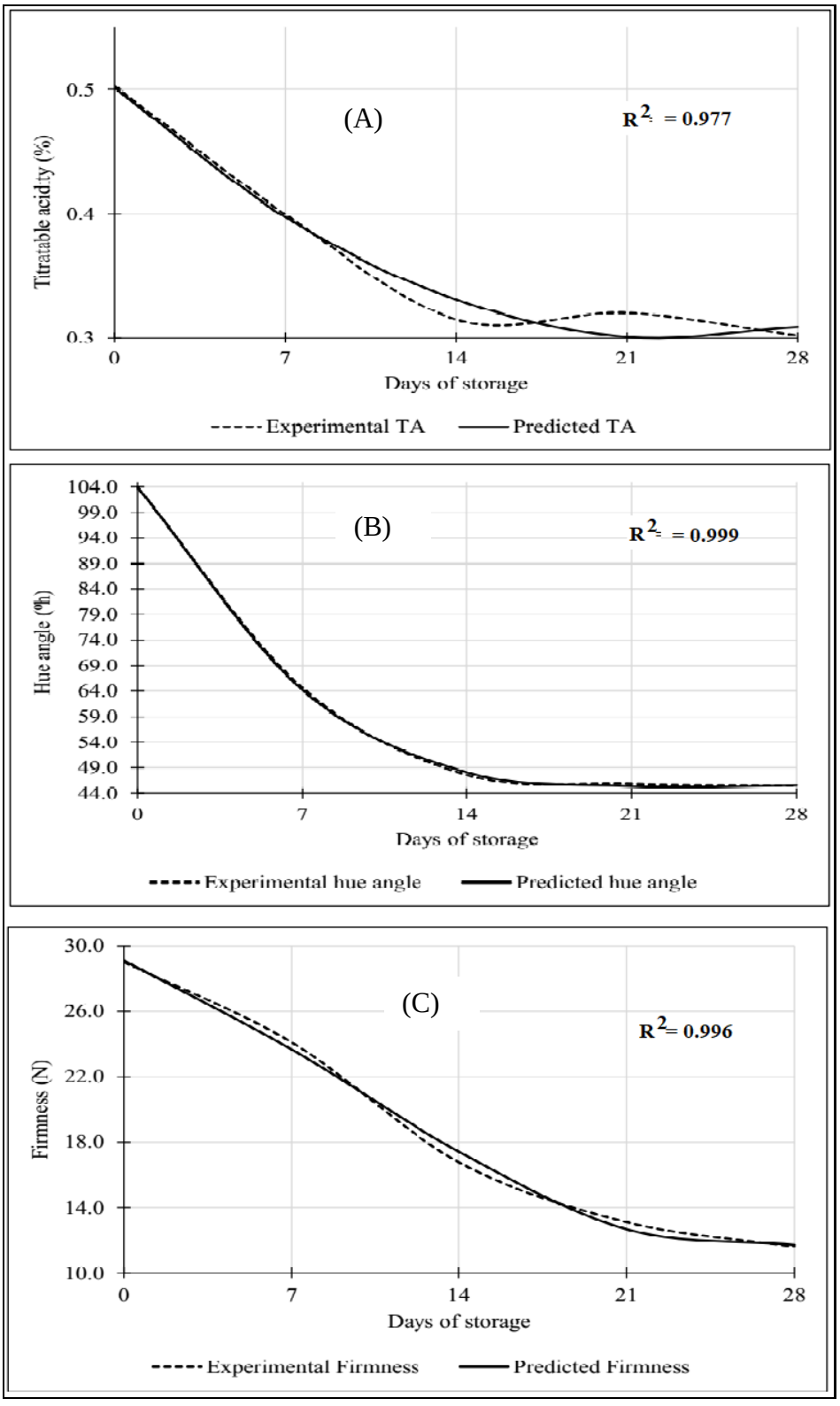

Figure 8.9 Factorial polynomial models predicted and experimental data fitted for the nonlinearly related green tomato quality indices with respect to days of storage (DOS), TA versus DOS (A), hue angle versus DOS (B) & firmness versus DOS (C)

8.2.3.6 Models for pink mature tomatoes

The models fitted for the pink tomatoes are displayed in Figure 8.10 and Equations 8.12 – 8.14 models odels fitted well to the experimental data.

$$\text{TA} = 3.354\text{e} - 05 \ * \text{DOS}^3 - 0.001112 * \text{DOS}^2 + 0.0003359 * \text{DOS} + 0.4337 \quad (8.12)$$

$$\text{Hue angle} = 0.0483 \ * \text{DOS}^2 - 2.188 * \text{DOS} + 70.25 \quad (8.13)$$

$$\text{Firmness} = -0.0002831 * \text{DOS}^3 + 0.02501 * \text{DOS}^2 + -0.9021 * \text{DOS} + 24.79 \quad (8.14)$$

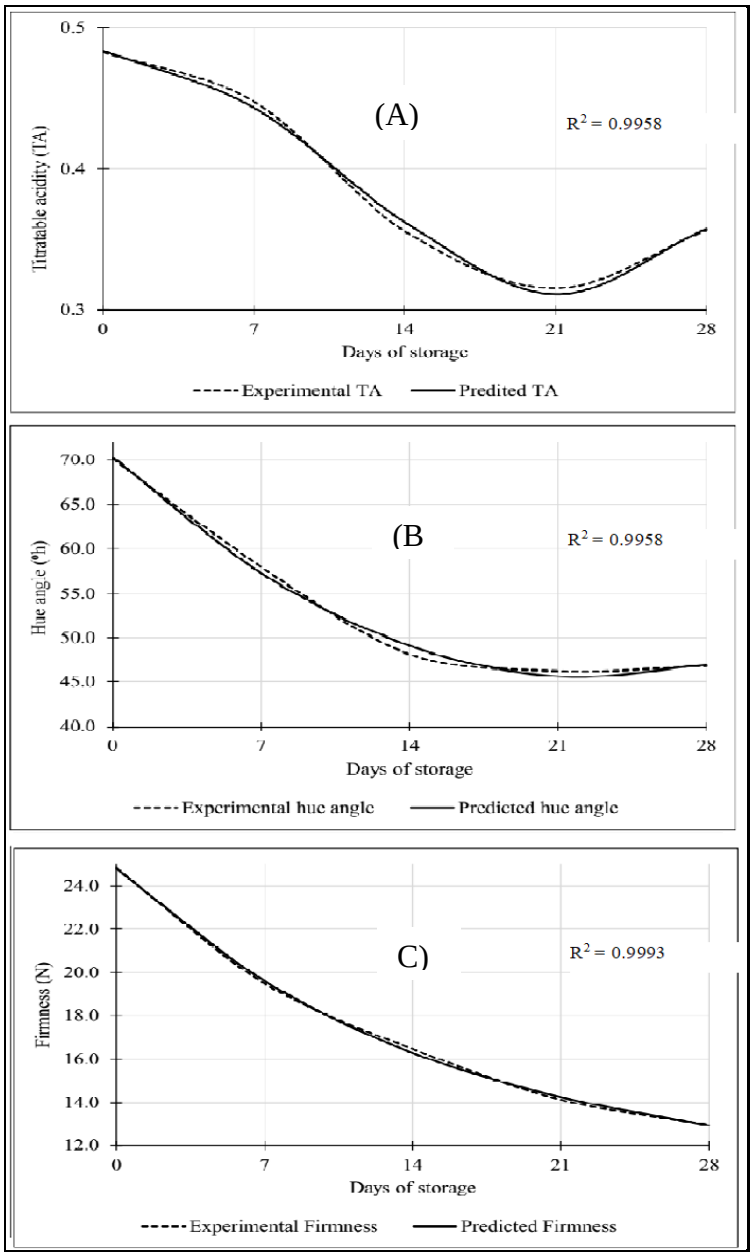

Figure 8.10 Factorial polynomial models predicted and experimental data fitted for the nonlinearly related pink tomato quality indices with respect to days of storage (DOS), TA versus DOS (A), hue angle versus DOS (B) & firmness versus DOS (C)

8.2.3.7 Models for red mature tomatoes

Models for red tomatoes shown in Figure 8-11 and by Equations 8.15 - 8.17 and the models observed to fit well to the experimental data.

$$\text{TA} = 2.22e-05 * \text{DOS}^{3} - 0.0006415 * \text{DOS}^{2} - 0.001862 * \text{DOS} + 0.3785 \quad (8.15)$$

$$\text{Hue angle} = 0.02562 * \text{DOS}^{2} - 1.212 * \text{DOS} + 59.47 \quad (8.16)$$

$$\text{Firmness} = 0.0006301 * \text{DOS}^{3} - 0.0199 * \text{DOS}^{2} - 0.1969 * \text{DOS} + 19.41 \quad (8.17)$$

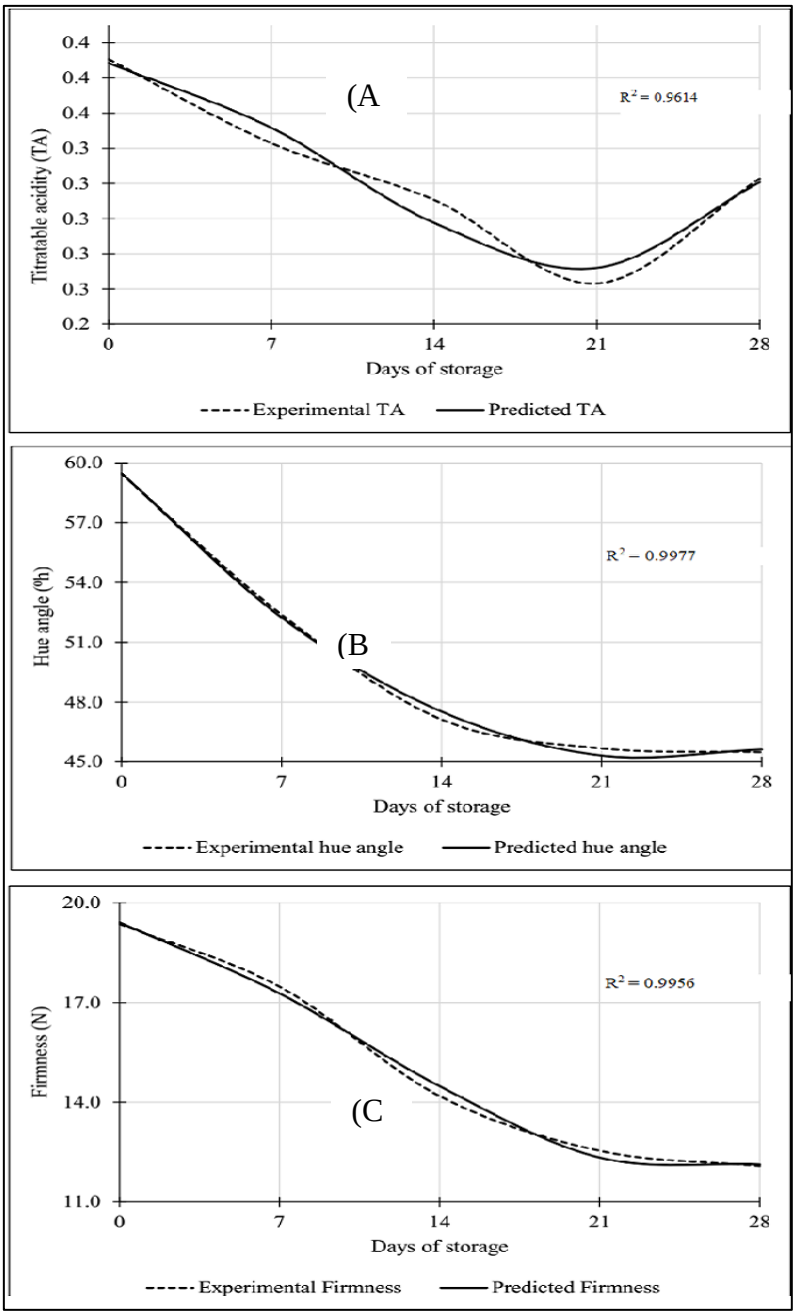

Figure 8.11 Factorial polynomial models predicted and experimental data fitted for the nonlinearly related red tomato quality indices with respect to days of storage (DOS), TA versus DOS (A), hue angle versus DOS (B) and firmness versus DOS (C)

8.2.3.8 Models for averaged quality data

The fractional and polynomial models were used to investigate the nonlinear relationship. Accordingly, TSS and pH were not found to have a significant (P>0.05) relationship with DOS. This proves that the result obtained using ANCOVA model which can explain that both pH and TSS were not changed through the storage period. The other quality measures (TA, hue angle, firmness and TSS:TA ratio) appear to have a curvilinear relationship with DOS (Equations 8.18 – 8.20). The results of fractional and polynomial models for these quality measures are given below.

$$\text{TA} = \frac{(0.00065*\text{DOS}^3 - 0.0243*\text{DOS}^2 + 0.4323*\text{DOS})}{(\text{DOS}+9.264)} \quad (8.18)$$

$$\text{Firmness} = 0.0110 * \text{DOS}^2 - 0.7644 * \text{DOS} + 24.62 \quad (8.19)$$

$$\text{Hue angle} = \frac{(1.982*\text{DOS}^2 - 45.45*\text{DOS} + 24448)}{(\text{DOS}+31.42)} \quad (8.20)$$

The plots of the fitted fractional polynomial models for the response variables of the individual tomato quality indices (TA, hue angle and firmness) are presented in Figure 8.12. The findings of this analysis showed that the relationship between the quality measures and DOS is not strictly linear. The relationship is rather curvilinear. The non-linearity relationship might be due to the combination effects of the MS, Tr and SC. The TA model showed a slow decline throughout the storage period, which indicates that the acidity level is reducing during DOS and the model fit with the R^2 value of 0.998 (Figure 8.12A).

The fractional polynomial model for the hue angle with fit R^2 value of 0.999 (Figure 8.12B). The plot showed a steep decline during the first week and slow decrease thereafter indicates that the hue angle level has decreased during DOS. The result is similar to the findings of by Khairi *et al.* (2015) that has shown a decrease in the hue angle during storage period. The result might be caused by breakdown of the tomato fruit cell wall and the lycopene development was intensified during storage (Khairi *et al.*, 2015). The result can help to study the tomato colour kinetics affected by storage period.

The polynomial model was fitted for the firmness of tomato samples with the goodness of fit R^2 value of 0.996 (Figure 8.12C). The plot showed a steep decline during the storage period. A

decrease in the firmness during storage period, which caused by breakdown of the tomato fruit cell structure (Schouten *et al.*, 2007). Oliveira *et al.* (2015) reported that the firmness of tomato fruit can vary from 34.68 to 21.24 N, while the result from this paper shows which was between 45 and 10 N during storage time. The decrease of tomato firmness during storage period was reported by several researchers (Schouten *et al.*, 2007; Schouten *et al.*, 2014; Oliveira *et al.*, 2015). The result of this paper can help to study the structural hardness of tomato fruit during the storage period.

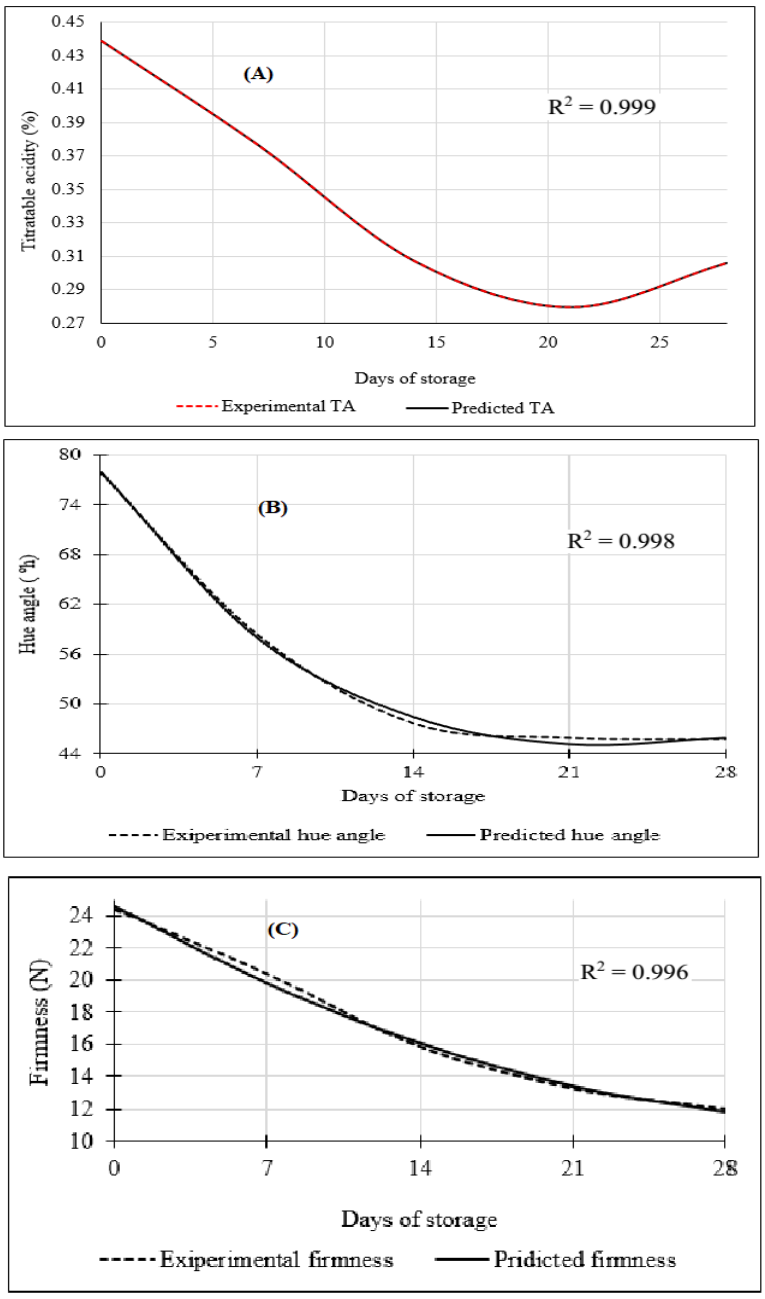

Figure 8.12 Factorial polynomial models predicted and experimental data fitted for the nonlinearly related tomato average quality indices with respect to days of storage (DOS): TA vs DOS (A), hue angle vs DOS (B) and firmness vs DOS (C)

Overall, the fractional polynomial models predicted well the changes in TA and hue angle (colour of tomatoes), while polynomial model was found to be the best equation that described well the firmness of tomatoes during the storage period (Figure 7.12). The tomato quality data calculated using the fractional polynomial models and the corresponding experimental tomato quality values are presented in Table 8.8. This study, therefore, demonstrated that the developed models (Equations 8.18 and 8.19) can be used to predict the changes in the selected tomato quality attributes during storage period by destructive approach (Figure 8.12 (a, c)) or by non-destructive approach (Equation 8.20) (Figure 8.12 (b)). In general, the TA of tomatoes was found to be the best tomato quality change indicator during storage under evaporative cooling and ambient storage environments, which was followed by the tomato hue angle and firmness.

Table 8.8 The predicted and experimental data of the fractional polynomial model for the nonlinear responsive variables of tomato sample

Storage days	Experimental quality data			Predicted quality data		
	TA (%)	Hue angle (°h)	Firmness (N)	TA (%)	Hue angle (°h)	Firmness (N)
0	0.4388	77.8259	24.3964	0.4388	77.912	24.6200
7	0.3766	58.3353	20.3527	0.3766	57.9638	19.8101
14	0.3071	47.6180	15.8113	0.3071	48.4406	16.0822
21	0.2794	45.8774	13.2610	0.2794	45.1662	13.4362
28	0.3057	45.6939	12.0098	0.3058	45.9321	11.8722

The experimental data are the overall average of all the three maturity stages and replications of the tomato samples.

8.2.4 Conclusions

The purpose of this study was to investigate and model the effects of MS, pre-storage treatments and cold storage treatments on tomato quality during the storage period. Different modelling and model screening steps were applied. The multivariate (PCs) analysis was one of the methods employed. The multivariate statistical analysis applied in order to consider the simultaneous observation and analysis of more than one outcome variable. Interaction effect indicates that the relative importance of the independent variables on the fruit quality during the storage period. Accordingly, the MS (*i.e.* mature green, pink and red), SC (*i.e.* evaporative

cooler store and ambient environment) and Tr (disinfection treatments) (*i.e.* control treatment, anolyte water dipping, hot water dipping and chlorinated water dipping) were the most important factors that affected the tomato quality during storage period inside EC and ambient conditions. The combinations of MS, SC and Tr treatments had positive significant ($P < 0.05$) influence on the changes in the quality of sample tomato fruit during the storage period. In conclusion, integrating postharvest treatments such as chlorinated water, anolyte water dipping, evaporative cooling SC and harvesting at green or pink MS are recommended to maintain the quality of tomatoes during storage and thereby to extend their shelf-life. Among the fractional and polynomial models developed, the models for TA were found to be the best fit to the experimental quality data. The model developed using hue angle and firmness experimental data also predicted the quality of tomatoes during storage periods well. The models are recommended for use by tomato postharvest handlers to predict changes in these quality attributes during storage of tomatoes subjected to pre-storage disinfection treatments and stored under EC and ambient storage.

8.2.5 Acknowledgements

We would like to warmly acknowledge the Federal Ministry of Education of Ethiopia, South African National Research Foundation (NRF – TWAS); Tomato Producer Organization (TPO); Postharvest Innovation Program (PHI) for prevision of financial support; ZZ2 Tomato Farm for the prevision of the required sample tomatoes and the host institute, University of Kwa-Zulu Natal.

8.2.6 References

Abbott, JA. 1999. Quality measurement of fruits and vegetables. *Postharvest Biology and Technology,* 15**,** 207-225.

Abdi, H and Williams, LJ. 2010. Principal component analysis. *Wiley interdisciplinary reviews: computational statistics,* 2**,** 433-459.

Alimi, BA, Melesse, SF and Workneh, TS. 2016. Multifactorial analysis of the effects of pre and postharvest treatments on the quality of stored tomato. *CyTA-Journal of Food,* 14**,** 206-212.

Alimi, BA, Shittu, TA and Sanni, LO. 2014. Effect of hydrocolloids and egg content on sensory quality of coated fried yam chips. *Journal of Culinary Science & Technology,* 12**,** 168-180.

Alonso-Gutierrez, J, Kim, EM, Batth, TS, Cho, N, Hu, Q, Chan, LJG, Petzold, CJ, Hillson, NJ, Adams, PD, Keasling, JD, Garcia, MH and Lee, TS. 2015. Principal component analysis of proteomics (PCAP) as a tool to direct metabolic engineering. *Metabolic Engineering,* 28**,** 123-133.

Ambler, G and Royston, P. 2001. Fractional polynomial model selection procedures: investigation of Type I error rate. *Journal of Statistical Computation and Simulation,* 69**,** 89-108.

AOAC. 1995. *Official Methods of Analysis: Association of Official Analytical Chemists.* AOAC, Virginia, USA.

Batu, A. 2004. Determination of acceptable firmness and colour values of tomatoes. *Journal of Food Engineering,* 61**,** 471-475.

Binder, H, Sauerbrei, W and Royston, P. 2013. Comparison between splines and fractional polynomials for multivariable model building with continuous covariates: a simulation study with continuous response. *Statistics in Medicine,* 32**,** 2262-2277.

David, CC and Jacobs, DJ. 2014. Principal component analysis: a method for determining the essential dynamics of proteins. *In:* Dennis, RL (ed.) *Protein Dynamics: Methods and Protocols.* 11, 193-226.

Egbewale, BE, Lewis, M and Sim, J. 2014. Bias, precision and statistical power of analysis of covariance in the analysis of randomized trials with baseline imbalance: a simulation study. *BMC medical research methodology,* 14**,** 1-12.

García-García, I, Taboada-Rodríguez, A, López-Gomez, A and Marín-Iniesta, F. 2013. Active packaging of cardboard to extend the shelf life of tomatoes. *Food and Bioprocess Technology,* 6**,** 754-761.

Gharezi, M, Joshi, N and Sadeghian, E. 2012. Effect of Post Harvest Treatment on Stored Cherry Tomatoes. *J. Nutr. Food Sci,* 2**,** 157-167.

Harrell, FE. 2015. *Regression modeling strategies: with applications to linear models, logistic and ordinal regression, and survival analysis.* Springer, USA.

Huitema, B. 2011. *The analysis of covariance and alternatives: Statistical methods for experiments, quasi-experiments, and single-case studies.* John Wiley & Sons, Inc. Publication, USA.

Iezzoni, AF and Pritts, MP. 1991. Applications of principal component analysis to horticultural research. *HortScience,* 26**,** 334-338.

Itoh, K. 2003. Combined effects of hot water treatment (HWT) and modified atmosphere packaging (MAP) on quality of tomatoes. *Packaging Technology and Science,* 16**,** 171-178.

Jolliffe, IT and Cadima, J. 2016. Principal component analysis: a review and recent developments. *Philisophical Transactions of the Royal Society A,* 374**,** 1-16.

Kader, AA. 1986. Effects of postharvest handling procedures on tomato quality. *In:* El-Beltagy, AS and Persson, AR, eds. Acta Horticulture, 209-222. International Society for Horticultural Science (ISHS), Cairo, Egypt.

Khairi, AN, Falah, MaF, Suyantohadi, A, Takahashi, N and Nishina, H. 2015. Effect of Storage Temperatures on Color of Tomato Fruit (Solanum Lycopersicum Mill.) Cultivated under Moderate Water Stress Treatment. *Agriculture and Agricultural Science Procedia,* 3**,** 178-183.

Long, J and Ryoo, J. 2010. Using fractional polynomials to model non-linear trends in longitudinal data. *British Journal of Mathematical and Statistical Psychology,* 63**,** 177-203.

López, CaF and Gómez, PA. 2004. Comparison of color indexes for tomato ripening. *Horticultura Brasileira,* 22**,** 534-537.

Martens, H and Martens, M. 2001. *Multivariate analysis of quality. An introduction.* John Wiley and Sons, Chichester, UK.

Melesse, SF and Zewotir, T. 2017. Variation in growth potential between hybrid clones of Eucalyptus trees in eastern South Africa. *Journal of Forestry Research,* 28**,** 1157-1167.

Moneruzzaman, KM, Hossain, ABMS, Sani, W and Saifuddin, M. 2008. Effect of stages of maturity and ripening conditions on the biochemical characteristics of tomato. *American Journal of Biochemistry and Biotechnology,* 4**,** 329-335.

Oliveira, GHH, Corrêa, PC, Botelho, FM and Oliveira, APLR. 2015. Mechanical Properties of Tomatoes Subjected to an Induced Compression during Storage. *Journal of Texture Studies,* 46**,** 293-301.

Pinheiro, J, Alegria, C, Abreu, M, Gonçalves, EM and Silva, CLM. 2013. Kinetics of changes in the physical quality parameters of fresh tomato fruits (Solanum lycopersicum, cv. 'Zinac') during storage. *Journal of Food Engineering,* 114**,** 338-345.

Pinheiro, JC, Alegria, CSM, Abreu, MMMN, Gonçalves, EM and Silva, CLM. 2016. Evaluation of Alternative Preservation Treatments (Water Heat Treatment, Ultrasounds,

Thermosonication and UV-C Radiation) to Improve Safety and Quality of Whole Tomato. *Food and Bioprocess Technology,* 9**,** 924-935.

Rencher, AC. 2003. *Methods of multivariate analysis.* John Wiley & Sons, USA.

Richardson, JT. 2011. Eta squared and partial eta squared as measures of effect size in educational research. *Educational Research Review,* 6**,** 135-147.

Royston, P and Altman, DG. 1994. Regression using fractional polynomials of continuous covariates: parsimonious parametric modelling. *Applied statistics,* 43**,** 429-467.

Royston, P and Sauerbrei, W. 2003. Stability of multivariable fractional polynomial models with selection of variables and transformations: a bootstrap investigation. *Statistics in medicine,* 22**,** 639-659.

Schouten, RE, Farneti, B, Tijskens, LMM, Alarcón, AA and Woltering, EJ. 2014. Quantifying lycopene synthesis and chlorophyll breakdown in tomato fruit using remittance VIS spectroscopy. *Postharvest Biology and Technology,* 96**,** 53-63.

Schouten, RE, Huijben, TPM, Tijskens, LMM and Van Kooten, O. 2007. Modelling quality attributes of truss tomatoes: Linking colour and firmness maturity. *Postharvest Biology and Technology,* 45**,** 298-306.

Shittu, TA, Sanni, LO, Awonorin, SO, Maziya-Dixon, B and Dixon, A. 2007. Use of multivariate techniques in studying the flour making properties of some CMD resistant cassava clones. *Food Chemistry,* 101**,** 1606-1615.

Shlens, J. 2014. A tutorial on principal component analysis. *arXiv preprint arXiv:1404.1100.*

Sobratee, N and Workneh, TS. 2015. Evaluation of chemical, biochemical and microbiological quality in tomato using multivariate analysis. *International Journal of Food Engineering,* 11**,** 173-184.

Var, I. 1998. Multivariate data analysis. *vectors,* 8**,** 125-136.

Workneh, TS, Osthoff, G, Pretorius, J and Hugo, C. 2003. Comparison of anolyte and chlorinated water as a disinfecting dipping treatment for stored carrots. *Journal of food quality,* 26**,** 463-474.

Workneh, TS, Osthoff, G and Steyn, M. 2012. Effects of preharvest treatment, disinfections, packaging and storage environment on quality of tomato. *Journal of food science and technology,* 49**,** 685-694.

Workneh, TS, Osthoff, G and Steyn, MS. 2011. Influence of preharvest and postharvest treatments on stored tomato quality. *African Journal of Agricultural Research,* 6**,** 2725-2736.

9. CONCLUSIONS AND RECOMMENDATIONS

As the result of the high investment and initial costs, the mechanical refrigeration cooling system, which is the most common cooling method used for agricultural produce, was found to unaffordable for small- and medium-scale, as well as emerging farmers. Most of the fresh produce is lost after harvest during postharvest handling. Therefore, low-cost and affordable cooling technologies are of paramount importance for reducing postharvest losses of perishable commodities, particularly for farmers in arid and semi-arid climate regions. Consequently, low-cost cooling technologies, such as the evaporative cooler (EC), the CoolBot-air-conditioner (CBAC) and the combinations cooling systems (*i.e.* EC+CBAC), were recommended by several researchers for farmers in arid and semi-arid climatic regions, as well as for the short-term storage of fruit and vegetables by small-scale producers.

This thesis aimed at investigating the effects of low-cost cooling technologies on the airflow and temperature distribution in selected fruit and vegetables technologies. Moreover, several models were developed to study the effects of the cooling technologies and different pre-storage disinfecting treatments on the quality of the tomato fruit during storage, using the selected cooling technologies. The second chapter, based on a literature review, investigated the impact of computational fluid dynamics (CFD) models on low-cost cooling technologies for the modelling of airflow, temperature, heat and mass transfer. Moreover, models for tomato fruit that was subjected to cooling and different pre-storage disinfection treatments (anolyte water, hot water and chlorinated water) were reviewed in detail.

The characteristics (*i.e.* temperature, relative humidity and air velocity) of the cold air inside the unloaded EC, CBAC and EC+CBAC cold storage chambers were studied experimentally and reported in Chapter Three. In this study, the air velocity, temperature and relative humidity distribution inside the unloaded cold rooms were studied. The EC maintained a higher the relative humidity, although it did not achieve the required lowest temperature for the short-term storage of tomatoes, while EC+CBAC maintained both optimum temperatures, which is suitable for the short-term storage of tomatoes and the relative humidity required for the fresh tomato fruit. On the other hand, the CBAC system alone can maintain the temperature, while the RH was found to be slightly higher than the RH that tomatoes require during storage, which is sufficient for the short-term storage of tomatoes, without significant deterioration. This

comparative study is the first of its kind and part of this study provided a set of useful data that are basic for future selections among the low-cost cooling technologies and future design optimization. Further investigation, in terms of the characterization or visualisation of fluid dynamics inside the coolers, which are either loaded or unloaded, taking into account the heat generation and airflow resistances that are required for the optimization of the cooling processes of the technologies.

In the next study, the focus was to characterise the inflow air numerically, in terms of airflow, air temperature and air enthalpy, through the psychrometric unit, using the computational fluid dynamics (CFD) model (see Chapter Four). Some attempts have been made in the past to characterise the airflow resistance for non-charcoal cooling pads. Nevertheless, the results presented in this section differed from previous the studies in that it was comprised of an indirect heat exchanger and wet charcoal multi-pads. What is important, is the combination of the indirect heat exchanger and of the wet multi-pads. Since the experimental results in Chapter Three demonstrated that, there was no significant effect on the air characteristics, after passing through Pads 2 and 3, except an increase in the RH, it was decided that the IHE+Pad 1 was enough to cool the air. The air velocity vector after IHE+Pad 1 was found to be 1.0 $m.s^{-1}$ and there was a small temperature change between the inlet and the outlet (0.6ºC). The static enthalpy of the air at the exit of the psychrometric unit was found to be 86 $kJ.kg^{-1}$. A critical analysis of the results showed that the air velocity optimization at the inlet was more pronounced and reduced the temperature of the air to at least the wet-bulb temperature of the ambient air. The CFD models clearly showed that to solve the problem of the psychrometric unit, the airflow, and, hence the temperature distribution across the unit, must be optimised. The results of this study can be used in the development of an optimised psychrometric unit, in terms of the airflow and temperature distribution.

The systematic analysis airflow, temperature and heat distribution inside unloaded low-cost cold storage chambers (*i.e.* EC, CBAC and EC+CBAC), using CFD models (Chapter Five), was desirable to help in the effective design and optimization of the cold storage chambers for removing heat from the inside *i.e.* since airflow governs the heat and mass transfer inside the cold store. The research results showed that the airflow distribution was not uniform inside the stores in all the three cooling methods. However, the EC+CBAC was found to be the best, in terms of relatively uniformity, air distribution and air velocity. The validation of the models was performed by comparing the experimental air velocity with the computed air velocity at

different positions inside the cold storage chambers and good agreement shown. Whereas research on the CFD simulation of the low-cost cooling systems is limited in literature, this study presented the detailed airflow inside the cold storage chambers, which can help as a data base for the future design optimization of the cold stores. This study clearly showed that CFD modelling is a novel way of identifying airflow inside cold storage chambers and, hence, it was found to be an appropriate tool for not only advanced design technology, but also for low-cost technology design. The results imply that the cold storage chambers require further modifications, to improve the uniformity of airflow. Since all the storage air dynamics are fundamentally dependent on the airflow, the airflow aspect of the low-cost cold storage chambers is the new aspect of this particular study.

Using a similar approach to airflow analysis, the air temperature and energy distribution inside unloaded low-cost cooling technologies was studied using the CFD model. The results shown in this study revealed that the temperature and energy parameters followed a similar trend to that of airflow inside the cold storage chambers. In most cases, no uniform air temperature, enthalpy and heat flux inside the stores were observed from the CFD mode visualization and quantification. The air temperature and energy indicator analysis is also the first of its kind for unloaded low-cost cooling technologies, using the CFD models and, hence, the result can be used as a database for further design modifications of the cold storage chambers. The innovative application of the CFD model is important for the improvement of the storage chambers. The CFD clearly visualized the intensity of the temperature, enthalpy and heat flux inside the unloaded storage chambers, which can be used to identify the importance of the modification of the storage chambers. A further study of the airflow characterization of loaded storage chambers is the key to understanding the detailed airflow with obstacles (stacked tomato fruits), and this data can be used to evaluate the airflow resistance and to model different scenarios of low-cost storage.

The semi- and fully-loaded airflow characteristics (*i.e.* air velocity, pressure drop, flow resistance) of the EC+CBAC was studied, using the CFD models (Chapter Six), as a fundamental analysis for heat and mass transfer inside the cold storage chambers and for further design considerations. The EC+CBAC demonstrated a good uniform airflow and temperature distribution (Chapter Three and Five). The study developed the quantification of horizontal airflow through the long and short sides of stacked tomato boxes, using the CFD models, which enables the estimation of the airflow resistance characteristics of the stack inside the low-cost

cold store (EC+CBAC). The results led to the development of a porous medium CFD model to simulate the airflow inside a fully-loaded cold storage chambers. The results showed that the air velocity at the inlet at the centre of tomato stack was found to be the highest, followed by the air velocity across the exit and the centre of the stack, 1.5 $m.s^{-1}$, 0.1-0.6 $m.s^{-1}$ and 0.2-0.5 $m.s^{-1}$, respectively. Inside the fully-loaded EC+CBAC the airflow at the centre of the fully stacked room and at near the outlet wall was also difficult to cool. The study showed that modifications to the air distributing devices are critically important. The study was the first of its kind for low-cost the EC+CBAC and can be used as a data base for the further characterization of tomato cold storage chambers. The cooling kinetics and temperature distribution should be analysed in order to completely evaluate the loaded situation. Furthermore, a detailed study of the heat and mass transfer of the models is critically important for a further understanding of the cold room micro-environment dynamics, with the additional generation of heat from the tomato stacks.

An analysis of the integrated effects of low-cost cooling technologies (EC), tomatoes harvested at different maturity stage, pre-storage disinfection treatments and storage periods on the quality and marketability of fresh tomato fruit, were reported in Chapter Seven. The study was performed to screen the best combinations for maintaining the quality and marketability of tomatoes during the storage period. Several researchers have studied the effects of integrated effect of mechanically refrigerated stores and pre- and postharvest treatments on the quality of different fresh produces. The aim of the current study was different from the previous work, since it integrates the study of low-cost cooling technology and the application of pre-storage disinfection technologies (*i.e.* anolyte, chlorinated and hot water), as well as the maturity stage of the tomato fruit on the quality during the storage period. The findings of this study showed that all green, pink and red tomatoes experienced a decrease in firmness and hue angle over 21 days. The EC storage shows a higher firmness and hue angle, when compared to the ambient conditions of the stored tomatoes. Compared to ambient storage, EC storage reduced the PWL by 7-10% over 30 days, while ambient storage took 15 days. The green maturity stage, EC storage and pre-storage treatments (*i.e.* chlorinated and anolyte water) conclusively improved the shelf-life and marketability of tomatoes. Therefore, a farmer can use a combination of tomatoes harvested at the green stage, those that have been cooled by evaloratively-cooled storage and those have been treated with anolyte water or chlorinated water, to maintain a better quality of tomatoes and to extend their shelf-life. The variation in temperature and relative humidity observed inside the EC could affect the storability of the produce and, hence, the

further modification of the cold storage chamber, to improve the temperature and relative humidity, is important.

Finally, further studies were undertaken to investigate the effects of low-cost storage technology and pre-storage disinfection treatments on the quality of fresh tomato fruit (Chapter Eight) and different models *i.e.* logistic regression model, fractional-polynomial models and polynomial models were developed and presented. The logistic regression analysis model was used to show the marketability of the tomato fruit harvested at different maturity stages, and they were subjected to disinfection, different storage conditions and storage period treatments (Chapter 8.1). The results showed that the chances of the marketability of tomatoes was higher for tomatoes stored in evaporatevely-cooled. Several researchers used logistic models to model changes in quality of fresh produce stored inside mechanically refrigerated storage chamber after subjecting the produces to pre-and post-harvest treatments. However, the present study is also focused on the investigation of effects of low-cost cooling technology and post-harvest disinfection treatments and, hence, the original models developed using data obtained in this research can be used for predicting probability of marketability and changes in quality of fresh tomatoes subjected to low-cost cooling technologies (*i.e.* EC, CBAC, EC+CBAC). Therefore, the logistic model can be used by farmers and processors just by measuring any of the convenient physico-chemical parameters *i.e.* pH, TA, TSS, colour and texture and inserting it into the developed model, to predict the marketability level during the storage period.

Moreover, fractional polynomial, polynomial, and multivariate models were developed to analyse the effects of the pre-storage treatments, the maturity stage, the low-cost storage technology environment and the storage period on the quality of the tomato fruit (Chapter 8.2). In this study, the development of a simple, appropriate and applicable model was attempted to determine tomato quality indices. Several studies were performed for the modelling of fruit and vegetables that were stored inside mechanically refrigerated storage chamber and subjected to both pre- and post-harvest treatments. This study was peculiar in that it focused on develop models for tomatoes stored inside low-cost cold storage chambers. The study found that the maturity stages (green, pink and red), the storage conditions (ambient and evaporative cooler) and the pre-storage disinfection treatments (anolyte-, chlorinated- and blanched-water) were the most important controlling for maintaining the quality of the tomato fruit during the storage period. The relationship between the storage period and most of the tomato quality parameters, such as colour and firmness, were found to be curvilinear (fractional polynomial, polynomial

and multivariate). The farmers can pick, for instance, the colour model to evaluate the quality of tomatoes during the storage period and can predict the freshness of the stored fruits. The developed models appear to be complex, and hence, the development of a model that is simpler, is recommended, so that farmers (any layman) can utilize it.

The work presented in this thesis is important because there is a scarcity of both quantitative and qualitative information on airflow characteristics of low-cost cooling technologies, as well as combined effects of cold storage and different pre-storage disinfection on the quality of the tomato fruit, which can be used by small-scale and emerging farmers' cooperatives. This work has also contributed to improve the understanding of the effect of low-cost cooling technologies on the quality characteristics of fresh tomato fruit and screening the models that fit best for predicting tomato quality subjected to these technologies.

Recommendations

(a) The further air velocity optimization of the psychrometric unit will be important to screen the best air flow velocity.
(b) The optimization of the inlet locations for three cooling scenarios is critically recommended for further improvement in order to optimise the design of the cold storage chambers.
(c) A suction fan is recommended for forced air cooling, to make the cold air flow through the stored stacks or packed fresh produce. The fan used for the evaporative psychrometric unit was an axial fan, the application of which was not found to be sufficient to push the air through the established indirect heat exchanger and charcoal Pad 1, and hence, further fan modification is critical.
(d) The psychrometric unit tunnel was not tight enough to protect air leakage and to force the air through the pads by Fan 1, and hence, there is no optimum capacity evaporative cooling of the air ensured at charcoal pads.
(e) The installed one and three charcoal pads were found to be an extra expense for Pads 2 and 3. Hence, we recommend that only one indirect heat exchanger and one charcoal cooling pad (Pad 1) will be enough to achieve the required optimum temperature reduction.

(f) The openings affected the efficiency of the CBAC and EC+CBAC; therefore, the exhaust opening modifications are recommended, to achieve lower temperature inside the cold storage chambers.